Multimodal Mapping of the Hippocampus across the lifespan and in dementia

Inaugural dissertation

for the attainment of the title of doctor
in the Faculty of Mathematics and Natural Sciences
at the Heinrich Heine University Düsseldorf

presented by

Anna Plachti
from Krasnoarmejsk, Kazakhstan

Düsseldorf, August 2020

From the institute of Neuroscience and Medicine (INM-7)
At the Forschungszentrum Jülich

Published by permission of the
Faculty of Mathematics and Natural Sciences at
Heinrich Heine University Düsseldorf

Supervisor: Prof. Dr. Simon B. Eickhoff
Co-supervisor: Prof. Dr. Christian Bellebaum

Date of the oral examination:

Declaration of Authorship:

I hereby certify that this thesis has been composed by me and is based on my own work, unless stated otherwise. No other person's work has been used without due acknowledgment. All references have been quoted and all sources of information have been specifically acknowledged.

Date: Signature:

Abbreviations

ALE	Activation Likelihood Estimation
BOLD	Blood Oxygen Level Dependent
CBP	Connectivity-Based Parcellation
CA	Cornu Ammonis
DG	Dentate Gyrus
fMRI	functional Magnetic Resonance Imaging
MACM	Meta-analytical connectivity modeling
MNI	Montreal Neurological Institute
MP RAGE	Magnetization-Prepared, Rapid Acquisiton Gradient Echo
MRI	Magnetic Resonance Imaging
MTL	Medial Temporal Lobe
PET	Positron Emission Tomography
RSFC	Resting-state functional connectivity
SC	Structural covariance
VBM	Voxel-Based Morphometry

Table of Contents

Zusammenfassung

Der Hippocampus wird mit Verhaltensweisen wie Gedächtnis und Navigation in Verbindung gebracht, und ist eine der ersten Gehirnregionen, die bei Erkrankungen wie Alzheimer, Depression und Angststörungen betroffen ist. Personen, die sich einer hippocampalen Resektion unterziehen mussten, erleben große Schwierigkeiten im Alltag und leiden an anterograder und retrograder Amnesie. Zu verstehen, wie der Hippocampus aufgebaut ist und welche Verhaltensweisen mit ihm zusammenhängen, ist daher von größter Bedeutung. Allerdings ist bis jetzt die Kartierung des Hippocampus, nämlich die Beschreibung des Aufbaus, auf die zelluläre Ebene beschränkt. Es fehlt eine Beschreibung der Organisation des Hippocampus auf der Ebene der Netzwerkkonnektivität, die für Rückschlüsse auf Verhalten möglicherweise wichtiger ist, als die zelluläre Ebene.

Mit der Nutzung bildgebender Verfahren und der Methode der „Konnektivitäts-Basierten-Parzellierung“ ist es möglich *in-vivo* Karten vom Hippocampus über eine Vielzahl von Personen hinweg zu erstellen. Die Methode der Konnektivitäts-Basierten Parzellierung unterteilt den Hippocampus in Subregionen, die sich in ihren Konnektivitätsprofilen besonders stark voneinander unterscheiden und deshalb ein bestimmtes Differenzierungsmuster aufweisen.

Die vorliegende Arbeit zielte somit darauf ab, den Hippocampus auf der Basis von funktionaler Konnektivität und struktureller Kovarianz, zu kartieren. Funktionale Konnektivität wurde entweder meta-analytisch über Aufgaben hinweg publizierter funktionaler Studien errechnet oder unter Ruhebedingung mit dem Magnetresonanztomographen gemessen. Strukturelle Kovarianz stellt eine relativ junge Messgröße dar, die die Ko-Variationen in der Intensität der grauen Substanz über Personen hinweg misst, und damit Ko-Plastizität und Ko-Atrophie abbildet, wenn Gehirnregionen zusammen wachsen oder degenerieren.

Neben der Kartierung des Hippocampus war ich ebenfalls stark daran interessiert zu untersuchen, ob sich Differenzierungsmuster innerhalb des Hippocampus im Laufe des Lebens und bei der Demenzerkrankung verändern und voneinander unterscheiden lassen. Hierbei wurden Veränderungen im Hippocampus basierend auf Veränderungen in den strukturellen Kovarianz-Netzwerken betrachtet.

Die Untersuchungen wurden an hunderten von funktionalen und strukturellen bildgebenden Daten frei zugänglicher Datenbanken durchgeführt. Hierbei zeigte sich, dass im Gegensatz zur zytoarchitektonischen Organisation, die Organisation des Hippocampus basierend auf

funktionaler Konnektivität eine Differenzierung entlang der anterior-posterior Achse aufwies mit einer Unterteilung in eine anteriore, mittlere, und posteriore Subregion. Die Organisation basierend auf struktureller Kovarianz hingegen zeigte vornehmlich eine medial-laterale Differenzierung in eine anteriore, mediale und laterale Subregion, die der Differenzierung in Cornu ammonis und Subiculum ähnelte.

Altersbedingte Veränderungen waren vor allem im posterioren Bereich des Hippocampus zu finden, wo die laterale Subregion schrumpfte. In der Demenz ähnelte die hippocampale Organisation allerdings stark einer funktionalen Unterteilung entlang der anterior-posterior Achse, da die laterale Subregion sich stark in die mediale Richtung ausbreitete und fast den gesamten hippocampalen Körper bedeckte. Diese Veränderungen wurden als möglicher Hinweis darauf interpretiert, dass bei Demenz vor allem funktionale Netzwerke von der Ausbreitung von Pathogenen wie ‚neurofibrillary tangles' und ‚amyloid beta plaques' betroffen sind und sich dies längerfristig auf die Ko-atrophie des Hippocampus auswirkt.

Um zu verstehen, in welche Verhaltensweisen der Hippocampus involviert ist, charakterisierte ich sowohl die Subregionen als auch die assoziierten Netzwerke behavioral unter Verwendung von Datenbanken, die tausende von Aktivierungsstudien archievieren. Die Ergebnisse legten nahe, dass der anteriore Hippocampus eher in Selbst-zentrierter Informationsverarbeitung und der posteriore Hippocampus eher in Welt-zentrierter Informationsverarbeitung involviert ist. Zusätzlich ist zu vermuten, dass basierend auf den Netzwerken der strukturellen Kovarianz, die mediale Subregion etwas mit der visuell-motorischen Verarbeitung zu tun hat.

Die vorliegende Arbeit zeigte demnach auf, dass der Hippocampus sowohl eine anterior-posterior als auch eine medial-laterale Organisation in Abhängigkeit von der Art der Netzwerke (funktionale oder strukturelle) aufweist. Strukturelle Netzwerke sind nicht stabil über die Lebensspanne, sondern verändern sich im Alter und in der Demenzerkrankung und spiegeln somit unterschiedliche zugrundeliegende Mechanismen wieder.

Abstract

The hippocampus is associated with behaviors such as memory and navigation, and is one of the first brain regions to be affected in diseases such as Alzheimer's dementia, depression and anxiety disorders. Patients who have undergone hippocampal resection experience great difficulties in everyday life and suffer from anterograde and retrograde amnesia. Understanding how the hippocampus is organized and what behaviors are associated with it, is therefore of utmost importance. The mapping of the hippocampus, i.e. the description of its organization, has so far been limited to the cellular level. However, a description of the organization of the hippocampus at the level of large-scale networks is missing, which may be more important for drawing conclusions about behavior than the cellular organization.

With the use of imaging techniques and the method of "Connectivity-Based Parcellation", it is possible to create *in-vivo* maps of the hippocampus across a large number of participants. The method of Connectivity-Based Parcellation divides the hippocampus into subregions that differ particularly strongly in their connectivity profiles and display therefore a specific differentiation pattern. The present work thus aimed at mapping the hippocampus on the basis of functional connectivity and structural covariance. Functional connectivity was either calculated meta-analytically across tasks of published functional studies or measured under resting state conditions with the magnetic resonance tomography. Structural covariance is a relatively new measure that estimates the co-variation in grey matter intensities across individuals and thus maps co-plasticity and co-atrophy as brain regions grow or degenerate together.

In addition to mapping the hippocampus, I was also strongly interested in investigating whether differentiation patterns within the hippocampus change over the course of life and in dementia and whether they can be distinguished from each other. Therefore changes in hippocampal organization based on alterations in structural covariance networks were studied. The investigations were carried out on hundreds of functional and structural imaging data from open accessible databases. In contrast to the cytoarchitectonic organization, the organization of the hippocampus based on functional connectivity showed a differentiation along the anterior-posterior axis with a subdivision into an anterior, middle and posterior subregion. In contrast, the organization based on structural covariance showed a medial-lateral differentiation into an anterior, medial and lateral subregion similar to the differentiation into cornu ammonis and subiculum.

Age-related changes were mainly found in the posterior region of the hippocampus, where the lateral subregion decreased. However, the hippocampal differentiation pattern in dementia closely resembled a functional division along the anterior-posterior axis, as the lateral subregion extended strongly in the medial direction and covered almost the entire hippocampal body. These changes were interpreted as a possible indication that in dementia functional networks are particularly affected by the spread of pathogens such as neurofibrillary tangles and amyloid beta plaques and have therefore a long-term effect on the co-atrophy of the hippocampus.

To understand in which behaviors the hippocampus is involved, I characterized both the subregions and the associated networks behaviorally using databases that archive thousands of activation studies. The results suggested that the anterior hippocampus is more involved in self-centric information processing and the posterior hippocampus more involved in world-centeric information processing. In addition, it can be assumed that based on the networks of structural covariance, the medial subregion has something to do with visual-motor processing.

The present work therefore showed that the hippocampus has both an anterior-posterior and a medial-lateral organization, depending on the type of networks, whether functional or structural. Structural networks are not stable over the lifespan but change with age and dementia mirroring different underlying processes.

1 Introduction

Clive Wearing (Wilson, Baddeley, & Kapur, 1995), Henry Molaison (Scoville & Milner, 1957) and Kent Cochrane (Gao et al., 2020) experienced the same symptoms. All three were unable to store new information and could not built new memories, a symptom described as anterograde amnesia. Furthermore, they also had difficulty remembering past events, manifesting a form of retrograde amnesia. All these symptoms were due to damage to or a resection of a small subcortical brain region, namely the hippocampus.

These men and their clinical history exemplify how important the hippocampus is for human life. Without this subcortical brain region we would not be able to remember, perceive and regulate our emotions, or to navigate our environment. Every day would be the same, with us being stuck in the present, without a past and without a vision of the future. The hippocampus

did not only attract clinicians working with amnestic patients, but also neuroanatomists and early neuroscientists interested in its organization and its relationship to behavior.

The work leading up to this thesis was especially designed from the perspective of the last ones tracking hippocampus' organization and linking it to human behavior. The aim was to investigate hippocampus' organization based on different magnet resonance imaging (MRI) measures and to follow changes in organization patterns across the lifespan and in dementia populations.

A growing interest in the architecture of the brain and its involvement in human behavior has guided research for more than 100 years now. The discovery that brain tissue is not homogenous, but displays micro-anatomical differences, heralded the era of brain mapping, in which Campbell, Brodmann, Ecomono, Koskinas and the couple Vogt published atlases and maps of the brain (Katrin Amunts & Zilles, 2015; Catani, Dell'acqua, & Thiebaut de Schotten, 2013). Their two-dimensional drawings helped to understand how the architecture of the brain looks like and which areas of the brain share a common cellular anatomy.

With the development and introduction of automatic and computerized technology, as well as the possibilities provided by widespread applications of MRI, brain mapping achieved a new momentum. Very quickly it turned from *ex-vivo* histological mapping established on the brains of a few human beings, to *in-vivo* mapping of the brains of hundreds of participants.

Today, the architecture of the brain is investigated from different perspectives, at different resolution levels. Atlases are established on a broad range of markers such as task-based or task-independent functional connectivity[1] (E. M. Gordon et al., 2014; Schaefer et al., 2017; Yeo et al., 2011), functional and anatomical connections represented together (Fan et al., 2016), or based on white matter tractography (Catani & Thiebaut de Schotten, 2008) exemplifying a wide range of features.

In line with these developments, I applied multimodal *in-vivo* mapping to the hippocampus, which, as mentioned above, plays an enormous role in human life and whose organization is primarily known from traditional histological mapping. In this research work, I circumvented two previous problems. On the one hand, *in-vivo* brain atlases do not provide a fine-grained differentiation pattern for individual regions and are additionally mostly lacking for subcortical brain regions as the hippocampus. On the other hand, even though cytoarchitectonic differentiation patterns are detailed as they are derived at the spatial

[1] Functional connectivity refers to the synchronous blood oxygenation level dependent (BOLD) signal measured with functional MRI (fMRI) either during the execution of a task or at rest (Biswal, Yetkin, Haughton, & Hyde, 1995). It is not restricted to the neighborhood of spatial related brain regions, but rather descries a correlational connection between those networks and brain areas that functionally act together.

[2] The stratum granulosum of the dentate gyrus is characterized by densely packed granular neurons, which somata is small and round. Stratum moleculare is thick, contains interneurons, receives fibers from the perforant pathway and also contains commissural and septal fibers. The polymorphic layer contains few interneurons and axons of granular neurons, which are crossing the layer (Duvernoy, 2013) (p.17).

resolution of micrometers, they are at the same time, established on micro-anatomical features of cells (e.g. morphology, density etc.) mirroring within hippocampal architecture. But focusing on a different feature, such as extra-hippocampal connectivity would, however, complement our current understanding of hippocampus' organization based on cyto- and receptor-architecture (K. Amunts et al., 2005; Palomero-Gallagher, Kedo, Mohlberg, Zilles, & Amunts, 2020) (Fig. 1).

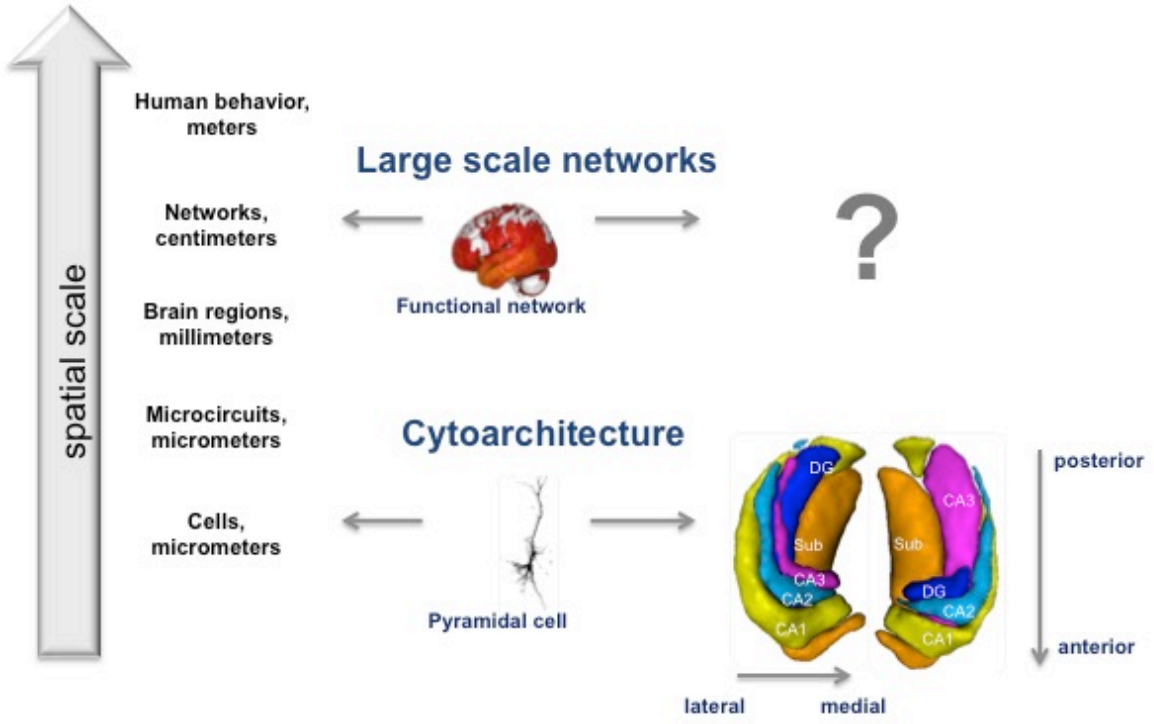

Figure 1. Hippocampus' organization at different spatial scales and different features.

The first aim was therefore to reveal hippocampal organization based on hippocampal connectivity represented in macro-scale networks assessed with different MRI measures such as functional connectivity and structural co-variation of grey matter intensity. Such an approach would not only help us to understand how the hippocampus is organized at a higher spatial scale based on networks, but it would also reveal, which brain regions are related to the hippocampus.

Since the hippocampus as a brain region displays high plasticity and high vulnerability at the same time, the second aim was to track changes in the organization of the hippocampus over the entire lifespan and in dementia pathology reflecting age-related co-plasticity and disease-related co-atrophy. Since previous histological maps were established on *ex-vivo* brains, this would be the first attempt to create 'non-static' maps capturing changes of organization.

A third aim was to bridge the gap between the organization of the hippocampus and its involvement in specific behavior. Apart from a few exceptions, the investigation of brain's biological tissue organization (e.g. mapping using microscopy) and brain's function (utilizing e.g. functional MRI while performing a task) remained mostly separate for the last decades. In this work, we characterized meta-analytically across hundred of studies archived in the databases of BrainMap (http://www.brainmap.org/) and NeuroSynth (https://neurosynth.org/) hippocampal differentiation pattern based on functional connectivity on the one hand, and the associated grey matter co-variation networks on the other hand. Performing such an extensive behavioral profiling can accelerate our understanding about hippocampus' behavioral involvement in healthy and diseased conditions of human life.

The outcomes of this work will enhance our understanding about hippocampal organization at the macro-scale level as an additional layer to histological mapping. The resulted hippocampal maps can be used in clinical environment to predict healthy and deviant hippocampal differentiation patterns, but also in the context of artificial intelligence and data mining. Using maps that combine voxels containing the same information instead of using all voxels of the hippocampus can reduce computing resources to simulate hippocampal organization and functionality. Overall, an in-vivo mapping of the hippocampus based on large-scale networks would not only complement our understanding but also help the user to navigate in hippocampal organization and its associated behavior.
To achieve the aims, the method of Connectivity-Based Parcellation (CBP) was applied in this thesis. It is introduced and explained in the next section, followed by an introduction of the hippocampus and its accompanying processes and alterations during aging and dementia.

1.1 In-vivo hippocampal mapping and behavioral profiling

The aforementioned aims were accomplished in two studies using CBP, which subdivides (i.e. parcellates) a region of interest (here the hippocampus as seed region) into subregions. CBP uses unsupervised learning (i.e. a clustering algorithm) to identify objects (e.g. voxels within the seed region) that share a common feature and group them either in the same or a different cluster (e.g. subregion) (S. B. Eickhoff, Thirion, Varoquaux, & Bzdok, 2015). In contrary to traditional histological mapping, which captures differences in intra-hippocampal tissue properties, the feature of interest was here extra-hippocampal connectivity, which was defined statistically using Pearson's correlation. Connectivity was computed for each voxel in

the seed region (i.e. hippocampus) to every voxel in the target region (i.e. whole brain grey matter voxels) characterizing each seed voxel by a unique connectivity profile. Depending on the (dis)similarity of seed voxels' connectivity profiles, voxels within the hippocampus were either clustered together or apart from each other resulting in a certain differentiation pattern (i.e. parcellations, clustering) (S. B. Eickhoff et al., 2015).

In order to probe multimodality of hippocampal mapping, three different MRI measures (i.e. modalities) were applied to reveal hippocampal organization from different perspectives. One of the modalities was task-based meta-analytical connectivity modeling (MACM), which represents task-dependent functional connectivity. Connectivity was meta-analytically computed across functional activation studies of the BrainMap database by correlating activation peaks between seed and target voxels across activation studies. The second functional modality was task-independent resting-state functional connectivity (RSFC). For each participant in our sample, connectivity was assessed by correlating the time-series of the BOLD signal between seed and target voxels, which was recorded while participants were at rest in the MR-scanner. In contrast to the both functional measures, structural co-variation of grey matter intensity was derived from anatomical T1 MRI images and measured using structural covariance. Structural covariance as a proxy for co-plasticity was computed at the group-level by correlating seed voxel's grey matter intensity with target voxel's grey matter intensity.

The second study exclusively focused on structural covariance to capture co-plasticity mirroring lifespan changes in healthy populations, whereas in mild cognitive impairment (MCI) and dementia it represents more likely co-atrophy due to a stronger degeneration during pathology. Structural covariance represents an interesting and a challenging modality, partly capturing cell density being able to reflect tissue changes (DeKraker, Ferko, Lau, Kohler, & Khan, 2018), and partly function related changes (Maguire, Woollett, & Spiers, 2006; Seeley, Crawford, Zhou, Miller, & Greicius, 2009). In either case, it complements our view on the hippocampus.

In order to bridge the long-lasting gap between organization and behavior, hippocampal subregions were behaviorally characterized using the databases of BrainMap and NeuroSynth in study 1. In study 2, however, the associated structural covariance networks of subregions were characterized to reveal a behavioral profile of underlying large-scale networks. The advantage of using databases that archive thousands of activation studies instead of conducting a single experiment, is to combine the knowledge of the last years and thus to study a broad spectrum of behaviors meta-analytically. Such a broad-based meta-analytical

analysis is urgently needed, since previous behavioral characterizations have referred to individual experiments, thus only revealing partial aspects of behavioral involvement of the hippocampus.

Taken together, studying hippocampus' organization at the macro-level using multimodal MRI measures is a promising alternative to micro-anatomical *ex-vivo* brain mapping based on cytoarchitecture. CBP is a data-driven *in-vivo* mapping approach, which reveals an additional level of organization of the hippocampus yielding its networks. On top, it is possible to track lifespan changes and pathological alterations, hence, providing non-static maps, which is not possible with *ex-vivo* mapping. By revealing hippocampal organization and its associated networks we can learn which brain regions are associated with the hippocampus, how does the hippocampus change during healthy aging and which networks and subregions of the hippocampus are affected most in dementia. This again provides new knowledge about hippocampus' associated behavior and new assumptions for future investigations.

1.2 Hippocampus

The hippocampus is one of the evolutionary oldest and most complex brain regions, which topography is defined at different levels such as macro-anatomy, strata, cells, receptors, connectivity, genes and function. The hippocampus is involved in a wide range of behavior ranging from episodic memory to navigation, and if affected in disease its consequences are tremendous for human life. However, most of our knowledge about the hippocampus is derived from investigations in rodents, whose hippocampus might substantially differ from human hippocampus in terms of cellular morphology, connectivity, and receptor- or chemical topography (Andersen et al., 2007). Therefore, our understanding about rodents' hippocampus is well established whereas it is scarce for human hippocampus. As far as neuroanatomical tracing techniques are not applicable to the human brain *in-vivo*, our understanding in terms of hippocampal connectivity and function is limited to the techniques of *ex-vivo* cartography.
In order to give an insight into the complexity of hippocampal organization I report the already known differentiation patterns of the hippocampus at the macro-anatomy-, strata-, cytoarchitecture and behavioral level along the medial-lateral and anterior-posterior dimensions.

1.3 Medial-lateral differentiation of the hippocampus

In the last decades, hippocampus' morphology was mainly examined with the traditional approach of microscopy of histological stained sections. To do so, the brain was cut along the horizontal plane in thin 2D coronal slices, which were stained and histologically delineated into subfields and strata along the medial-lateral and dorsal (superior) –ventral (inferior) dimensions. The following sections summarize the results and insights that were achieved about hippocampus' architecture using the traditional approach of microscopy.

Hippocampal segmentation based on strata and cytoarchitecture

The shape of the hippocampus reminded early neuroanatomists of a sea horse naming this brain region 'hippocampus', which is the Greek word for sea horse. Structurally, the hippocampus is bilaminar, consisting of the Cornu Ammonis (CA) and dentate gyrus. Both are separated by the hippocampal sulcus, which usually disappears with development so that CA and dentate gyrus fuse together being folded into each other (Duvernoy, 2013) (p.15ff), which reminds of a Swiss role.

Depending on neurons' morphology and distribution, CA is further divided into CA1-4 (Fig. 2 and 3A). CA1 is characterized by pyramidal neurons' somata, which are triangular and small, whereas CA2's pyramidal cells' somata is ovoid, large and densely packed. The pyramidal cells of CA3 are similar to those of CA2 but they are less densely packed and characterized by fine, nonmyelinated fibers, the mossy fibers. CA4, on the other hand, contains few ovoid, large and scattered somata as well as myelinated fibers (Duvernoy, 2013)(p.15ff).

Some researchers consider CA4 subfield as part of the dentate gyrus, which has a simpler structure compared to CA consisting of three layers[2]: stratum moleculare, stratum granulosum and polymorphic layer. The dentate gyrus with Fascia dentata (stratum granulosum) is a densely packed band of granular cells and is therefore identifiable as a separated structure from the CA subfields (K. Amunts et al., 2005).

In addition to cytoarchitectonic differentiation, the CA is also divided into layers or strata, which are the alveus, stratum oriens, stratum pyramidale, stratum radiatum, stratum

[2] The stratum granulosum of the dentate gyrus is characterized by densely packed granular neurons, which somata is small and round. Stratum moleculare is thick, contains interneurons, receives fibers from the perforant pathway and also contains commissural and septal fibers. The polymorphic layer contains few interneurons and axons of granular neurons, which are crossing the layer (Duvernoy, 2013) (p.17).

lacunosum and stratum moleculare (Fig. 2 and 3; more details are summarized in the footnote[3]) (Duvernoy, 2013) (p.15ff).

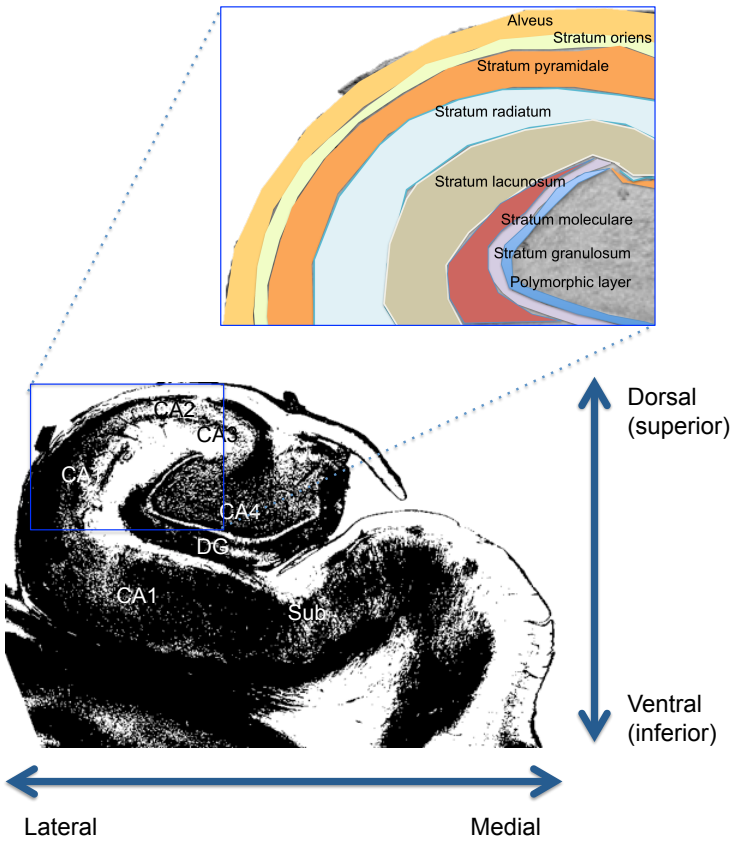

Figure 2. Schematic oversimplified representation of hippocampal strata.

Next to the CA1-4 and dentate gyrus, the subiculum is also considered to be part of the hippocampal formation since the hippocampus is prolonged by the subiculum considered as part of the parahippocampal gyrus (Duvernoy, 2013) (p.17). Several studies divide the subiculum into prosubiculum, presubiculum and parasubiculum (Ricardo Insausti, Muñoz-

[3] The alveus of the CA subfields is composed of axons of neurons of the CA and subiculum and represents the efferent pathway of these structures (Duvernoy, 2013)(p.15). It enters the fimbria, which again enters the fornix projecting to the limbic structures and being the main output pathway of the hippocampus (Fig. 3 and 4a).
The stratum oriens contains basket cells whereas the stratum pyramidale consists of pyramidal neurons, which partly reach the contralateral hippocampus. The axons of the pyramidal neurons project back to the stratum radiatum and reach other pyramidal neurons (Duvernoy, 2013) (p.15ff). The stratum radiatum contains the apical dendrites of pyramidal neurons and receives information through Schaffer collaterals, from fibers of the septal nuclei and commissural fibers. The stratum lacunosum consists of axons of the perforant fibers and Schaffer collaterals. The stratum moleculare contains the branches of apical dendrites of pyramidal neurons, which reach all layers of the CA (Duvernoy, 2013) (p.15ff).
In the dentate gyrus the stratum granulosum consists of somata of granular neurons. One part of the stratum moleculare receives fibers from the perforant pathway and another part is overlaid with commissural and septal fibers. The polymorphic layer contains few interneurons, and combines granular layer with CA4 and axons of granular neurons pass by (Duvernoy, 2013)(p.15ff).

López, Insausti, & Artacho-Pérula, 2017) and propose to add those to the hippocampal formation (Kedo et al., 2016). The subiculum, which pyramidal axons were perceived as output of the hippocampus and which receives input from entorhinal cortex and CA1, has been treated rather poorly in the past (Naber & Witter, 1998) so that further investigations are needed.

All in all, the most likely differentiation pattern, that is used in the literature to study the hippocampus, is the differentiation into CA1-4, dentate gyrus and subiculum (K. Amunts et al., 2005; Ding & Van Hoesen, 2015). In contrast to this histological differentiation pattern along the medial-lateral and ventral-dorsal dimension a distinction along the anterior-posterior dimension was suggested and is introduced in the next section.

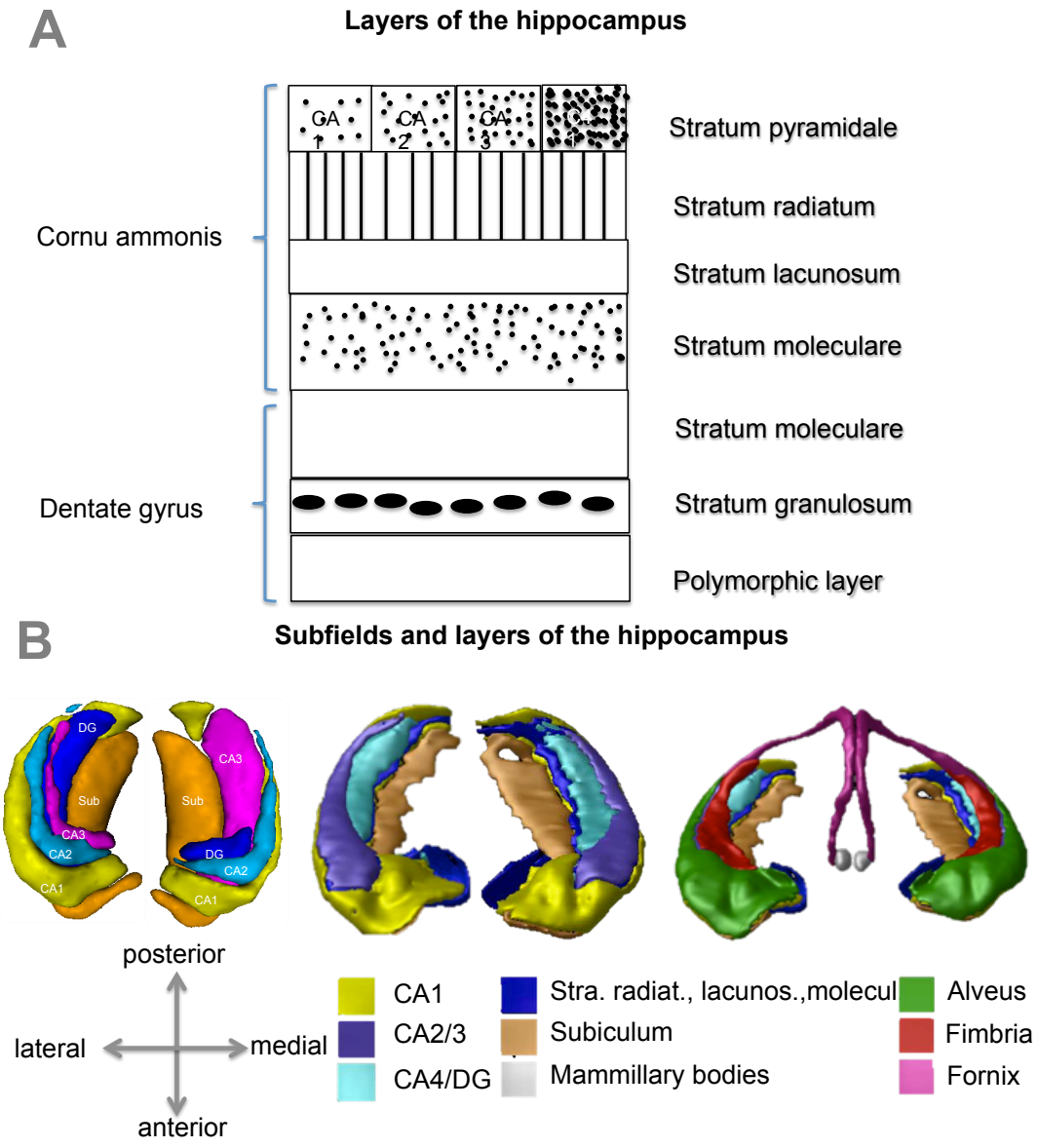

Figure 3. Hippocampus organization based on layers and cytoarchitecture in 2D and 3D. GD = dentate gyrus, CA=cornu ammonis. A) Reproduced based on Duvernoy (2013) B) Adapted from R. S. C. Amaral et al. (2018) with the permission from Elsevier.

1.4 Anterior-posterior differentiation of the hippocampus

In addition to histological mapping, increasing advancements in electroencephalography as well as MRI promoted an additional differentiation pattern of the hippocampus along the longitudinal axis. However, this organization pattern has been insufficiently researched to date, so that I briefly discuss the scientific basis on which an assumption about longitudinal differentiation pattern in the hippocampus can be made.

1.4.1 Segmentation based on macro-anatomy

The hippocampus is curved around the mesencephalon, and can be broadly divided into three segments, which are the head (anterior) with digitations, body (middle) and tail (posterior) subregions (Fig. 4) (Duvernoy, 2013)(p. 6). However, no standard convention for this division exists, but segmentation is mostly performed according to subjective evaluation. Poppenk, Evensmoen, Moscovitch, and Nadel (2013) proposed to use the uncal apex (y = -21 mm in MNI) as a standard landmark to delineate head from body. But no clear anatomical landmark to identify unambiguously the border between body and tail was proposed so far.

Other procedures simply segment the hippocampus into three parts of equal size, whereas others use a more refined schemes, for example 35% as head, 45% as body, and 25% as tail (Poppenk et al., 2013). In sum, rather vague and subjective segmentations were performed to divide the hippocampus macro-anatomically into head, body and tail. Independent of macro-anatomy, it was also suggested that head-body-tail subregions are supported by divergent connectivity profiles and behavioral meaning, which is discussed in the next section.

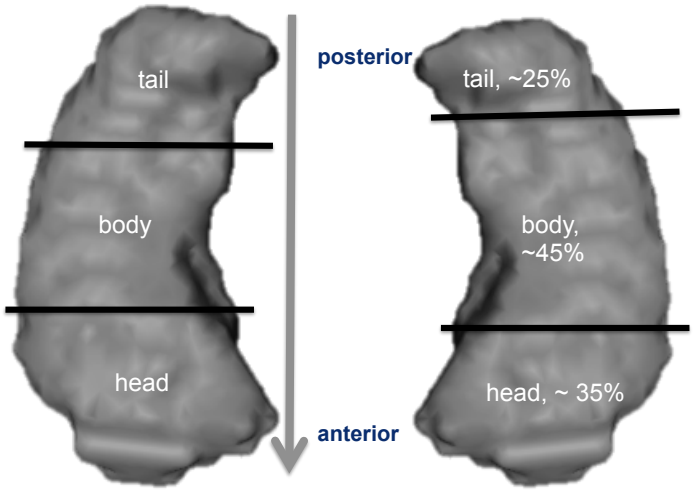

Figure 4. Head-body-tail segmentation of the hippocampus.

1.4.2 Connectivity along the longitudinal axis of the hippocampus

The hippocampus is suggested to be subdivided into head, body and tail because of divergent extra-hippocampal connectivity underlying those subregions.

Resting state functional and structural connectivity indicated that the anterior hippocampus is connected to the perirhinal cortex, amygdala, nucleus accumbens, hypothalamus, anterior cingulate cortex, temporal pole, anterior medial temporal lobe, orbitofrontal cortex and ventromedial prefrontal cortex. In contrast, the posterior hippocampus is suggested to be connected to parahippocampal cortex, retrosplenial and posterior cingulate cortices, medial and lateral parietal cortex, brainstem with raphe nuclei, as well as mammillary bodies (Adnan et al., 2016; Boedhoe et al., 2017; Fanselow & Dong, 2010; Kahn, Andrews-Hanna, Vincent, Snyder, & Buckner, 2008; Libby, Ekstrom, Ragland, & Ranganath, 2012; Poppenk & Moscovitch, 2011; Wagner et al., 2016). The intermediate subregion of the hippocampus remains poorly characterized and shares a connectivity pattern partly similar to the posterior and partly to the anterior hippocampal subregion's profiles (Qin et al., 2016).

Moreover, increasing evidence from studies even highlights the possibility that connectivity is organized in a gradient like fashion along the anterior-posterior axis in non-human primates (R. Insausti & Munoz, 2001) and in humans (Beaujoin et al., 2018; Qin et al., 2016).

But not only extra-hippocampal connectivity but also intra-hippocampal connectivity within the hippocampus seems to follow the same gradient along the longitudinal axis. Subfields in the anterior subregion are more likely to be connected to each other than to subfields in the posterior subregion, found in both functional and anatomical connectivity (Beaujoin et al., 2018; Dalton, McCormick, & Maguire, 2019).

All these findings propose that hippocampal organization into anterior-middle-posterior subregions are supported by extra-hippocampal connectivity organized along the anterior-posterior dimension.

1.4.3 Behavioral differentiation of the hippocampus along the longitudinal axis

The hippocampus is considered to be functionally heterogeneous along the longitudinal axis. Accordingly, it was suggested that the anterior and posterior hippocampus are involved in different behavior because of divergent connectivity profiles underlying these subregions along the longitudinal axis.

M. B. Moser and Moser (1998) suggested a functional differentiation of the rodent hippocampus into ventral, middle and dorsal subregions (equivalent to the anterior-head, middle-body and posterior-tail subregions[4] in humans) similar to the macro-anatomical segmentation. While the dorsal (i.e. posterior) subregion was suggested to process sensory information and is involved in navigation, the ventral (i.e. anterior) subregion is less behaviorally characterized except for its involvement in emotion processing (Fanselow & Dong, 2010; M. B. Moser & Moser, 1998).

In humans a similar tripartite organization pattern into head, body and tail, was found along the longitudinal axis suggesting divergent behavioral involvement (Fanselow & Dong, 2010; Poppenk et al., 2013; Poppenk & Moscovitch, 2011). Single experiment studies proposed several theories to capture the specificity of behavior along the **anterior**-*posterior* dimension:

- **vestibular**-*visual* (Hufner et al., 2011),
- **imagination**-*perception* (Zeidman & Maguire, 2016),
- **context coding**-*spatial behavior* (Nadel, Hoscheidt, & Ryan, 2013),
- **novelty**-*familiarity* (Zeidman & Maguire, 2016),
- **recent (vividness)** - *remote memories* (Gilboa, Winocur, Grady, Hevenor, & Moscovitch, 2004),
- **episodic memory**-*navigation* (Kühn & Gallinat, 2014),
- episodic memory: **multi-event narratives** (anterior), comprehensive (middle) *detailed* (posterior) (Collin, Milivojevic, & Doeller, 2015),
- **abstraction**-*individual* memory (Bowman & Zeithamova, 2018; Morton, Sherrill, & Preston, 2017; Schlichting, Mumford, & Preston, 2015),

[4] Referred in this study as the functional tripartite model.

- **emotion**-*cognition* (M. B. Moser & Moser, 1998),
- **encoding**-*retrieval* (H. Kim, 2015; Lepage, Habib, & Tulving, 1998),
- **pattern integration** – *pattern separation* (Morton et al., 2017; Zeidman & Maguire, 2016).

All these descriptions have in common that they were derived from individual experiments testing specific hypotheses. What is rather missing is an overarching view on the hippocampus and its behavioral involvement supported by a broad range of experiments. Robinson, Salibi, and Deshpande (2016) made such an attempt and created a behavioral map of the hippocampus along the longitudinal axis using the behavioral domains of BrainMap. According to their results, both, the anterior and posterior hippocampus, are involved in a wide range of behavior such as action, cognition, emotion, interoception and perception. While this characterization stresses hippocampus' functional diversity, it also shows a low functional specificity so far, which might be related to BrainMap's categorization system using broad behavioral domains.
All in all, these studies indicate behavioral heterogeneity along the anterior-posterior axis of the hippocampus in animals and humans. But they also raise the question, whether a more fine-grained behavioral characterization is evident for humans' hippocampus along the longitudinal axis derived from meta-analytical analyses rather than single experiments.

In addition to behavioral characterization, previous maps were not able to demonstrate changes in hippocampal maps due to aging and dementia. Since the hippocampus undergoes a variety of alterations during these processes, the question whether hippocampal maps stay stable or not was never addressed before. The next sections therefore describe changes that were associated with the hippocampus during aging and dementia, and summarize briefly the results of previous studies.

1.5 Hippocampal changes in aging and dementia

During aging, the hippocampus undergoes changes in synaptic plasticity, neurovasculature, neuroinflammation, protein folding and aggregation (Bettio, Rajendran, & Gil-Mohapel, 2017). On top, hippocampus' volume declines and cortical thinning in the temporal lobe can be detected (C. Chang et al., 2018; Fjell, McEvoy, Holland, Dale, & Walhovd, 2014; Fraser, Shaw, & Cherbuin, 2015; Sowell et al., 2003; Yang et al., 2016; Yao et al., 2012). The origins

and the underlying mechanisms of volume loss are still unclear but are generally attributed to reduced neurogenesis and neuronal regression as fewer new cells emerge and consequently fewer cells mature into neurons (Bettio et al., 2017; Lazic, 2012). A decrease in the number of dendritic spines and synapses was also discussed as potentially responsible influence on atrophy (Adams et al., 2008; Bettio et al., 2017).

Some processes accompanying aging are so severe that it is assumed to be a risk factor for Alzheimer's disease. Aging causes metabolic modifications in the amyloid precursor protein, which leads to an accumulation of amyloid-beta plaques, which again triggers the accumulation of neurofibrillary tangles resulting in a loss of synapses, neurons and axons (Metzler-Baddeley et al., 2019). Another scenario assumes that during aging, damage of neuroglia occurs and impairs myelination and microglia-mediated clearance so that neuroinflammation is triggered. Independent of which scenario is true, abnormal metabolism leads to neuronal death (Metzler-Baddeley et al., 2019).

In dementia and Alzheimer's disease the distribution of amyloid plaques and tau neurofibrillary tangles[5], which are assumed to be responsible for neuronal loss in entorhinal cortex and the hippocampus (Franko & Joly, 2013), is very prominent and characteristic for the disease (Braak & Braak, 1991; Franzmeier et al., 2019). Amyloid plaques are predominantly distributed in the temporal (medial) lobe (Thal et al., 2000) whereas tau pathology starts in the locus coeruleus and entorhinal cortex spreading to the hippocampus, anterior frontal and posterior parietal cortex before afflicting the whole brain (Franzmeier et al., 2019). Studies show that soluble amyloid-beta and less the amyloid plaques influence the dendritic spine, synaptic and neuronal loss determining cognitive dysfunction (Jack et al., 2008; Montembeault, Rouleau, Provost, & Brambati, 2016; J. C. Morris et al., 2009; Walsh & Selkoe, 2007).

Interestingly, not only dementia patients, but also clinically normal elderly accumulate amyloid-beta and tau pathologies, which, if phosphorylated, misfolds and aggregates forming neurofibrillary tangles, in the hippocampus and entorhinal cortex (Sperling et al., 2019; Ziontz et al., 2019). Higher amyloid-beta is associated with higher tau pathology, and both are associated with higher memory decline (Sperling et al., 2019). However, cognitive decline is not always present even in a profound distribution of neurofibrillary tangles as shown in individuals above 70 years (Ziontz et al., 2019), questioning a direct relationship between cognitive decline and the accumulation of pathogens.

[5] Amyloid plaques and tau neurofibrillary tangles are proteins, which accumulate outside and inside of neurons during aging and Alzheimer's disease.

All these processes seem to lead to the prominent effect of atrophy, which was extensively studied in the hippocampus in aging and dementia populations using either the subfield model (CA1-4, dentate gyrus, subiculum) or the functional tripartite model (head-body-tail), which I summarized in Table 1 and 2.

It is noteworthy that the functional tripartite model is underrepresented in dementia research, so that no clear conclusion can be derived about volume reduction along the longitudinal axis. By visual inspection, Table 1 and 2 indicate that overall, studies demonstrate high inconsistencies in localization of highest atrophy in the hippocampus. In MCI and dementia, CA1 and subiculum seem to be more atrophied compared to other subfields. But the same pattern of results was also found in aging, which casts doubt on the specificity of atrophy related to dementia. Additionally, CA1 and subiculum are the largest subfields, which might have facilitated to find atrophy there with the technique of low resolution MRI compared to smaller subfields.

In this thesis, however, no assumptions about any hippocampus models were made meaning that differentiation patterns were derived with the data driven approach of CBP. In addition, I did not measure the absolute atrophy of the hippocampus but used the MRI modality of structural covariance assessing the co-variation of hippocampal grey matter intensity with the whole brain in a sample. Therefore structural covariance was an indirect measure of co-atrophy in the group of MCI and dementia patients since mutual degradation of the hippocampus with other brain regions is more prominent in pathological conditions than in the group of healthy elderly. In contrary, we assumed that structural covariance in aging would more likely mirror co-plasticity on top of co-atrophy as healthy aged brains are more preserved.

Table 1. Volume reduction of hippocampus' subfields and subregions in aging

study	subfields	subregions
(Raz, Ghisletta, Rodrigue, Kennedy, & Lindenberger, 2010)	hippocampus (not specified)	/
(Raz et al., 2005)	Hippocampus (not specified)	/
(S. G. Mueller & Weiner, 2009)	CA1, CA3&DG	/
(La Joie et al., 2010)	subiculum	/
(Frisoni et al., 2008)	CA1, presubiculum	head, tail, body

(Chen, Chuah, Sim, & Chee, 2010)	/	head
(Rajah, Kromas, Han, & Pruessner, 2010)	/	head, body
(Ta et al., 2012)	/	anterior and posterior (body and tail)
(Driscoll et al., 2003)	/	posterior
(Kalpouzos et al., 2009)	/	posterior
(Malykhin, Bouchard, Camicioli, & Coupland, 2008)	/	head> body>tail
(B. A. Gordon, Blazey, Benzinger, & Head, 2013)	/	head, body
(Lowe et al., 2019)	/	posterior
(Pruessner, Collins, Pruessner, & Evans, 2001)	/	head, tail
(Malykhin, Huang, Hrybouski, & Olsen, 2017)	Dentate gyrus, subiculum	body
(Lupien et al., 2007)	No difference in whole hippocampus	/
(Sullivan, Marsh, & Pfefferbaum, 2005)	No age effects on volume	/
(Schuff et al., 1999)	Whole hippocampus (not differentiated)	/
(Sullivan, Marsh, Mathalon, Lim, & Pfefferbaum, 1995)	No age effects on volume	/
(Daugherty, Bender, Raz, & Ofen, 2016)	CA1-2	/
(S. G. Mueller et al., 2007)	CA1	/
(Pereira et al., 2014)	CA2-3, CA4-DG	/

Table 2. Volume reduction of hippocampus' subfields and subregions in MCI and dementia

study	subfields	subregions
(Pievani et al., 2011)	CA1, subiculum	/
(West, Coleman, Flood, &	CA1, subiculum	/

Troncoso, 1994)		
(Price et al., 2001)	CA1	/
(Fouquet et al., 2012)	CA1	/
(S. G. Mueller & Weiner, 2009)	CA1, CA1-2, subiculum	/
(Susanne G. Mueller et al., 2010)	CA1, CA1-2, subiculum	/
(La Joie et al., 2013)	CA1	/
(L. G. Apostolova et al., 2006)	CA1, CA2, CA3	/
(Apostolova et al., 2010)	CA1, subiculum, CA2-3	/
(L. Wang et al., 2006)	CA1, subiculum	/
(Chetelat et al., 2008)	hippocampus (not specified)	/
(Yassa et al., 2010)	CA1, CA3/DG	/
(Atienza et al., 2011)	CA1-3, DG	/
(Frisoni et al., 2006)	CA1, subiculum	/
(Frisoni et al., 2008)	CA1	body, tail, head
(Gemmell et al., 2012)	CA1	/
(Hanseeuw et al., 2011)	CA2-3, subiculum	/
(Lindberg et al., 2012)	CA1, subiculum	/
(Pluta, Yushkevich, Das, & Wolk, 2012)	CA1	head, tail
(Rossler, Zarski, Bohl, & Ohm, 2002)	CA1, subiculum (neuronal loss)	/
(Shi, Liu, Zhou, Yu, & Jiang, 2009)	hippocampus (not specified)	/
(L. Wang et al., 2003)	subiculum	head, lateral body (shape analysis)
(West et al., 1994)	CA1 (neuronal loss)	/
(Bobinski et al., 1995)	CA1-3, subiculum	/
(Bobinski et al., 1997)	CA1, subiculum (neuronal loss)	/
(Csernansky et al., 2000)	CA1	/
(Csernansky et al., 2005)	CA1	/

(Adachi et al., 2003)	CA1, subiculum	/
(Hyman, Van Hoesen, Damasio, & Barnes, 1984)	subiculum	/
(Jack et al., 1997)	Hippocampus (not specified)	/
(B. A. Gordon et al., 2013)	/	head
(Kesslak, Nalcioglu, & Cotman, 1991)	Hippocampus (not specified)	/
(Laakso, Lehtovirta, Partanen, Riekkinen, & Soininen, 2000)	Hippocampus (not specified)	/
(S. G. Mueller et al., 2007)	CA1, subiculum	/

1.6 Aims

In this thesis three overarching questions were addressed in two studies. First, how is the hippocampus organized based on large-scale networks assessed with different MRI measures? Second, does the differentiation pattern within the hippocampus change across the lifespan, in MCI and in dementia pathology? Third, which behavior is associated with the hippocampus and its associated networks?

Study 1: While most hippocampal differentiation schemas were derived from histology revealing a differentiation pattern along the medial-lateral dimension, a hippocampal map based on large-scale networks was lacking. To fill this gap and to reveal hippocampal organization from different perspectives, multimodal MRI measures such as task-(un)related functional connectivity and structural covariance as complementary windows into hippocampal organization were used. Since previous studies on functional measures indicated a differentiation pattern along the longitudinal axis, we hypothesized to find a similar organization along the anterior-posterior axis on the basis of functional connectivity in the human hippocampus. Moreover, we expected higher convergence between maps of both functional connectivity measures (i.e. MACM and RSFC) compared to structural covariance. The first study therefore served to explore and to describe convergent and divergent hippocampal maps derived from heterogeneous MRI measures. On top, hippocampal organization was linked to human behavior by analyzing meta-analytically the association between hippocampal subregions revealed in the first step and behavioral concepts across activation studies of the databases of BrainMap and NeuroSynth.

Study 2: The second study was devoted to investigate whether hippocampal differentiation patterns change in aging and dementia. The question was whether hippocampal maps stay stable or not. The study was performed on one modality namely structural covariance, which was disregarded so far in the scientific field. Structural covariance is supposed to reflect both co-plasticity in healthy and co-atrophy in pathological conditions as it measures the co-variation of grey matter intensities between brain regions mirroring both mutual co-preservation in aging and co-degeneration in dementia. As structural covariance reflects co-dependencies between brain regions it might be more sensitive to subtle changes, which would not be captured by measuring solely atrophy. To follow up on the behavioral characterization of the first study, the age and disease dependent underlying networks of hippocampal subregions were behaviorally characterized with NeuroSynth in order to infer from networks to behavior.

2 Study1: Multimodal parcellations and extensive behavioral profiling tackling the hippocampus gradient

Anna Plachti[1,2], Simon B. Eickhoff[1,2], Felix Hoffstaedter[1,2], Kaustubh R. Patil[1,2], Angela R. Laird[4], Peter T. Fox[5], Katrin Amunts[2,3] & Sarah Genon[1,2,6]

1 Institute of Systems Neuroscience, Heinrich Heine University Düsseldorf, Düsseldorf, Germany;

2 Institute of Neuroscience and Medicine (INM-1, INM-7), Research Centre Jülich, Jülich, Germany;

3 C. & O. Vogt Institute for Brain Research, Heinrich Heine University, Düsseldorf. Germany;

4 Department of Physics, Florida International University, Miami, FL, USA;

5 Research Imaging Institute, University of Texas Health Science Center at San Antonio, TX, USA;

6 GIGA-CRC In vivo Imaging, University of Liege, Liege, Belgium.

contact: Telefon: +49 2461 61-1409

Fax: +49 2461 61-1880

E-Mail: a.plachti@fz-juelich.de

Cerebral Cortex (2019)
Doi:10.1093/cercor/bhy336
Impact Factor (2018/2019): 5.21

Own contributions	Conception and design of study
	Reviewing and adapting analysis code
	Statistical data analysis
	Interpretation of results
	Preparing figures
	Writing paper
	Total contribution 80%

Abstract: The hippocampus displays a complex organization and function that is perturbed in many neuropathologies. Histological work revealed a complex arrangement of subfields along the medial-lateral and the ventral-dorsal dimension, which contrasts with the anterior-posterior functional differentiation. The variety of maps has raised the need for an integrative multimodal view. We applied connectivity-based parcellation to 1) intrinsic connectivity 2) task-based connectivity and 3) structural covariance, as complementary windows into structural and functional differentiation of the hippocampus. Strikingly, while functional properties (i.e., intrinsic and task-based) revealed similar partitions dominated by an anterior-posterior organization, structural covariance exhibited a hybrid pattern reflecting both functional and cytoarchitectonic subdivision. Capitalizing on the consistency of functional parcellations, we defined robust functional maps at different levels of partitions, which are openly available for the scientific community. Our functional maps demonstrated a head-body and tail partition, subdivided along the anterior-posterior and medial-lateral axis. Behavioral profiling of these fine partitions based on activation data indicated an emotion-cognition gradient along the anterior-posterior axis and additionally suggested a self-world centric gradient supporting the role of the hippocampus in the construction of abstract representations for spatial navigation and episodic memory.

Keywords: anterior-posterior, gradient, medial temporal lobe, structural covariance, map.

1 Introduction

The hippocampus is involved in a variety of tasks ranging from memory, learning, navigation and emotion (Fanselow & Dong, 2010; M. B. Moser & Moser, 1998; Poppenk et al., 2013; Prince, Daselaar, & Cabeza, 2005; Strange, Witter, Lein, & Moser, 2014). However, an integrative conceptual framework is currently lacking to account for this diversity of behavioral findings. To progress in that direction, first, a better understanding of the hippocampus' organization and function is crucially needed to shed light on its role in a range of behavioral aspects and second, a common generic map would be highly useful to further support cross-studies comparison and integration.

As far, two opposing organizational patterns were introduced in the past. The first mapping based on cytoarchitecture has evidenced a subdivision into subfields (CA1-4, dentate gyrus, subiculum) along the medial-lateral and ventro-dorsal axes as illustrated in **Figure 1**, Amunts et al. 2005). In parallel to this organization, an organization into subregions (head, body, tail) along the anterior-posterior (longitudinal) axis (Moser & Moser 1998; Lepage et al. 1998; Fanselow & Dong 2010; Poppenk et al. 2013; Strange, et al. 2014) commonly emerged across a variety of in-vivo approaches such as electrophysiology (Komorowski et al. 2013) and connectivity-based parcellation (CBP) (see **Figure 1**,(K. Amunts et al., 2005; Chase et al., 2015; Robinson et al., 2015)).

In line with the histological work and despite evidence of functional anterior-posterior differences, many *in-vivo* and *ex-vivo* studies in the human hippocampus used *a-priori* segmentation into subfields based on either an automated or a manually delineation in the anatomical MRI scans (see **Figure 1**, (Adler et al., 2014; Adler et al., 2018; de Flores, La Joie, & Chetelat, 2015). Such segmentation into subfields has the advantage of using the histological "ground truth" as an a-priori representation, but has the disadvantage of neglecting higher order features, such as the rich long-range connectivity of the hippocampus, which contributes to its functional organization. Thus, the knowledge from this one-sided perspective should be complemented by a CBP approach, which now allows the combination of different MRI measurements within the whole hippocampus hence potentially probing different aspects of its organization.

CBP is an *in-vivo* brain-mapping method that characterizes the organization of the brain based on connectivity estimates, usually derived from MRI (S. B. Eickhoff, Yeo, T., Genon, S., in press). CBP can be applied on any estimates of connectivity from MRI data (functional or structural) with different types of connectivity measurements being usually referred to as

different CBP-modalities. Across the previous years, evidence have been brought that CBP can capture organizational aspects that were previously revealed by tracing studies, as well as by histological work (Behrens et al., 2003; Lambert, Simon, Colman, & Barrick, 2017). Additionally, CBP was shown to be sensitive to functional distinction, for example, replicating the supplementary motor area (SMA) and pre-SMA differentiation evidenced by functional signal during task (Johansen-Berg et al., 2004). Hence this approach appears to identify regional differentiation supported by local microarchitecture, connectivity and local functional signal to some extent.

In the present study, we focused on the functional connectivity between hippocampus' voxels and all grey matter voxels. In other words, we examined long-range (whole brain) connectivity by computing for every hippocampal voxel its individual connectivity fingerprint with all other grey matter voxels. Based on the (dis-)similarity of connectivity fingerprints the voxels were clustered into either same or different partitions. CBP has the advantage to be model-free and unsupervised hence offering maps that optimally represent the data at hand. It has already been used in previous studies to examine hippocampal organization. Nevertheless, previous work focused mainly on a single CBP modality, either structural connectivity (Adnan et al., 2016) or meta-analytic connectivity modeling (MACM) (Chase et al., 2015; Robinson et al., 2015; Robinson et al., 2016). Examining structural connectivity, Adnan et al. (2016) proposed a bipartite anterior-posterior subdivision of the hippocampus, which contrasted with MACM parcellations revealing a more detailed architecture. This latter modality yielded a three-part organization for the left hippocampus and a 5-partite structure for the right hippocampus along the anterior-posterior axis (Robinson et al., 2015; Robinson et al., 2016), while the subiculum subfield was subdivided into five modules (Chase et al., 2015). In sum, uni-modal CBP has thus far provided evidence for an anterior-posterior organization of the hippocampus, but at different levels of partition across studies and even across hemispheres. This variety of partition schemes hinders a deep investigation of the functional relevance of the anterior-posterior differentiation, and also complicates the study of hippocampus dysfunction in brain pathology.

In this latter perspective, a common set of maps of the hippocampus for MRI investigation would be highly useful. Across the previous years, one major avenue of neuroimaging research of brain pathology has developed from phenotype (such as cognitive performance or symptoms) prediction approaches based on multivariate pattern analyses applied to large-scale clinical datasets (Zhang et al., 2016). In this promising avenue of research, individual voxels have to be compressed into homogeneous subregions in which the measurements (e.g.

fMRI signal) can be summarized. This compression is most of the time required not only for computational purposes, but also for post-hoc investigations of subregions contributing to the predictions. In this framework, the compression should be based on robustly defined maps that would represent a universal framework for comparison and integration of results across studies.

In this study, we investigated hippocampal functional organization using a multimodal CBP approach to generate robust functional hippocampal maps based on hippocampus - whole-brain connectivity profiles (S. B. Eickhoff et al., 2015; S. B. Eickhoff, Yeo, T., Genon, S., in press). To do so, we focused on two purely functional modalities: MACM-CBP and resting-state functional connectivity (RSFC-CBP). Despite showing convergence (Reid et al., 2016) and being conceptually related, these two modalities are based on very different types of data and methods. MACM reflects functional organization during task and is computed from whole-brain co-activation peaks in activation databases such as BrainMap. For each hippocampal voxel we obtained a whole-brain co-activation profile. RSFC, on the other hand, reflects the functional connectivity estimated in the unconstrained function of the brain and is computed at the subject-level. For each individual hippocampal voxel we obtained its functional connectivity profile to all the other grey matter voxels in the brain. RSFC is based on resting state functional MRI (RS-fMRI), which is known to be prone to noise due to various artifacts (Power, Schlaggar, & Petersen, 2015; Satterthwaite et al., 2017; Satterthwaite et al., 2013; Van Dijk, Sabuncu, & Buckner, 2012), but the choice of an optimal denoising strategy has remained relatively unexplored in the particular framework of CBP. For that reason, as a preliminary step in the present study, we performed a systematic evaluation of different denoising methods in order to favor stable partitions with high biological validity for RSFC-CBP. We aimed to generate a functional subdivision of the hippocampus that would be stable across subjects and CBP modalities offering a representation that would be optimal for any type of functional signal (such as task-based fMRI activations, RS-fMRI or PET).

Nevertheless, to complement this purely functional parcellation and to start building a scientific bridge with previous structural mapping modalities, we additionally examined the subdivision of the hippocampus based on structural covariance (SC-CBP), which represents on group-level the co-variation of hippocampal voxels with all the other brain voxels. SC stands at an ambiguous place in the mapping approaches. On one hand, it is assumed to reflect functional dependencies between regions through synchronous firing of neurons reflecting functional neuroplasticity (Alexander-Bloch, Raznahan, Bullmore, & Giedd, 2013; Evans, 2013). Accordingly, SC and RSFC are conceptually related to each other (Kotkowski, Price,

Mickle Fox, Vanasse, & Fox, 2018), as indicated by structural changes through function (Seeley et al., 2009) although both are technically two distinct modalities. However, on the other hand, SC is based on structural changes (Alexander-Bloch et al., 2013; Mechelli, Friston, Frackowiak, & Price, 2005) and thus should be influenced by the underlying structural organization like gene expression during neurodevelopment and direct structural connectivity through monosynaptic connection as indicated in a recent rodent study (Yee et al., 2017). In sum, SC is assumed to reflect common influences of certain factors on microstructure be it synaptogenesis based on functional synchronous firing, connectivity as direct monosynaptic connection, or gene expression in synapses development. Therefore, we expected that SC-CBP would to some extent confirm functional organization, and additionally, provide anatomical information conveyed in brain structure to complement our understanding of the hippocampal functional topography and provide an alternative map for studies capitalizing on structural MRI data.

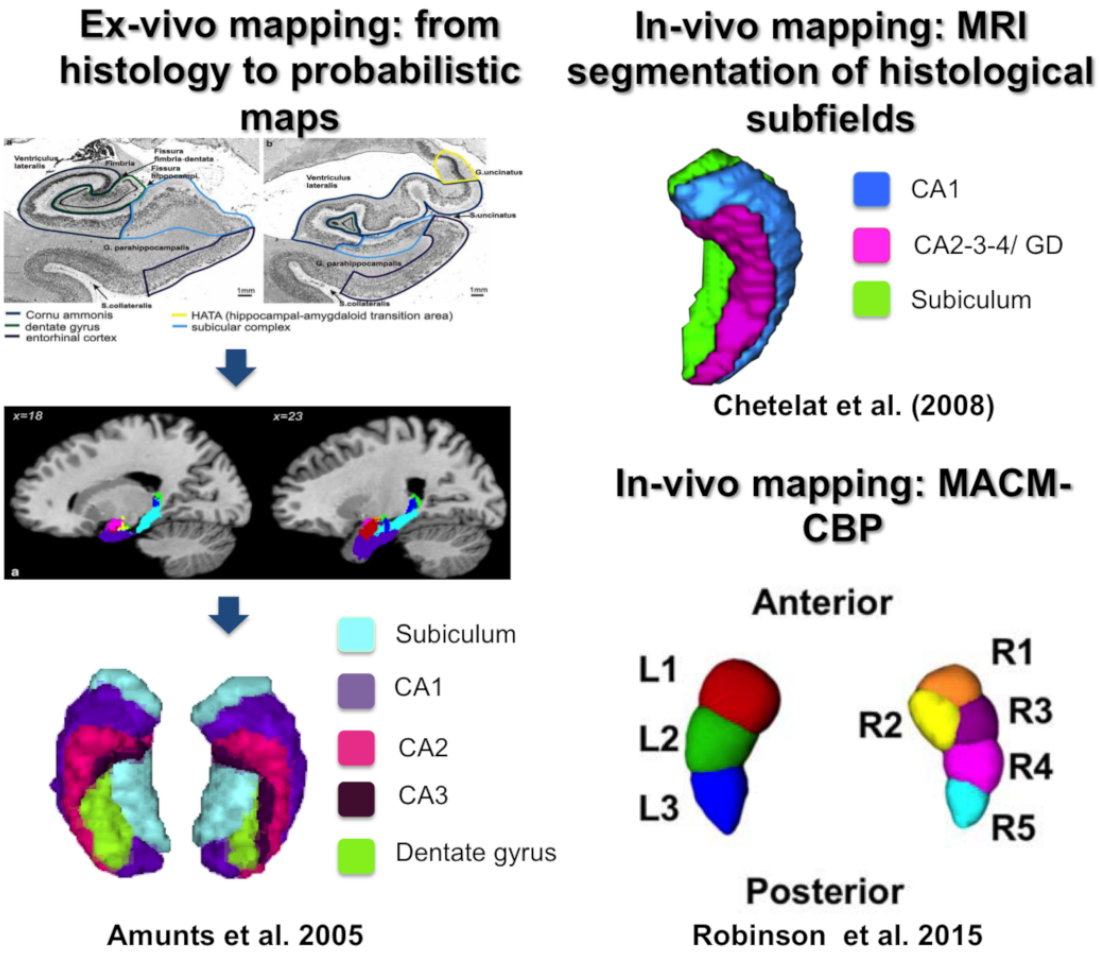

Figure 1. Hippocampal mapping based on histology, structural MRI segmentation, and CBP method. (Images reproduced with permission from publishers.)

Our final objective was to characterize the obtained cross-modal functional maps in terms of associated behavioral functions via a quantitative approach of activation studies (e.g., using the BrainMap or NeuroSynth databases). Importantly, our conceptual objective here was not to identify specific behavioral functions segregated into different subregions of the hippocampus, but rather to assess the functional relevance and integration of the organization pattern in terms of cognitive information processing. Several hypotheses have been proposed in the past to describe the anterior-posterior differentiation in terms of psychological functions. But these hypotheses usually pertain to a specific psychological or neuroscientific research domain and hence could not account for pluripotency of the engagement of the hippocampus across psychological domains. As far, two main hypotheses derived from psychological ontologies have been proposed in that regard: an emotional-cognitive dimension (M. B. Moser & Moser, 1998) and an encoding-retrieval dimension (H. Kim, 2015; Lepage et al., 1998; Prince et al., 2005). Further investigations have proposed a novelty-familiarity (Strange, Fletcher, Henson, Friston, & Dolan, 1999) and an imagination-perception differentiation along the anterior-posterior axis (Zeidman & Maguire, 2016). However, a common framework accounting for the relevance of the organization of the hippocampus across domains of human behavior is still lacking. The current study aimed to fill this gap by performing behavioral profiling (Genon, Reid, Langner, Amunts, & Eickhoff, 2018b) of hippocampus subregions using thousands of activation studies collected across two different databases using different behavioral taxonomies. Such a quantitative approach offers an overview, which can be used as a starting point to build an integrative theory.

Thus, the objectives of the present study were two-fold 1) a conceptual objective of understanding hippocampal organization as revealed across different neurobiological properties and its relevance in terms of cognitive information processing, and 2) a mapping objective to provide robust and fine-grained partitions of the hippocampus. While current high-level parcellations (M. F. Glasser et al., 2016; Schaefer et al., 2017) have focused on the cerebral cortex they neglected crucial subcortical structures. A consensual robust map of the bilateral hippocampus is still missing which in turn can help to study its structure and function across the lifespan as well as in disease. Our study was designed to offer such partitions and their patterns of associations with behavioral functions. These resources are openly available to the scientific community via ANIMA database (http://anima.fz-juelich.de/).

2 Materials and Methods

The bilateral hippocampi were parcellated using different connectivity modalities. Task-based connectivity was examined with MACM performed on reported activation peaks across paradigms in the BrainMap database. RSFC-CBP was performed at the subject level for a sample of participants from the Human Connectome Project (HCP) while SC-CBP was performed at the group level using the structural MRI data of the same HCP sample (Smith et al., 2013; Ugurbil et al., 2013). The main methodological differences between these two CBP modalities are illustrated in Supplemental Material Methods I.5.

After computing parcellations for each modality, we established a functional map of the hippocampus by merging the functional parcellations (i.e. RSFC and MACM, that showed the highest convergence) into one hippocampal map, hence representing a cross-modal consensus map. Finally, we characterized our cross-modal consensus map at high granularity with regards to behavioral functions using BrainMap and NeuroSynth databases.

2.1 Volume of interest

We defined our VOI as a consortium of the cytoarchitectonic maps, available in the SPM Anatomy Toolbox 2.0 (S. B. Eickhoff et al., 2005), and the macro anatomically-defined Harvard-Oxford Structural Probability Atlas (http://neuro.imm.dtu.dk/wiki/Harvard-Oxford_Atlas) (Desikan et al., 2006). The hippocampal formation included the following subfields: CA1-3, dentate gyrus and subiculum. The total number of voxels in a 2 mm x 2 mm x 2 mm space in the right hippocampus was 865 (6920 mm^3) and that of the left hippocampus was 831 (6648 mm^3) voxels.

2.2 Sample

The sample was obtained from the longitudinal study of the Human Connectome Project (Van Essen & Ugurbil, 2012) representing one of the best openly accessible MRI datasets. We included unrelated participants in order to avoid heritability effects. The sample consisted of n = 323 young adults (age: 22-37 years, mean age: 28.2 years, 50.7% females). All participants gave their written statement of agreement, and the analyses of the data were approved by the ethical committee of the Heinrich Heine University Düsseldorf.

2.3 MRI measurements

Structural MRI. All scans were acquired on a 3T MRI scanner of Siemens Skyra (Siemens AG, Erlangen, Germany) with a 32-channel coil (Van Essen & Ugurbil, 2012). The 3D structural T1-weighted MRI scans were performed with a MPRAGE sequence (256 sagittal slices in a single slab, *TR* = 2400 ms, *TE* = 2.14 ms, TI = 1000 ms, FoV = 224 x 224 mm, flip angle = 8◦, voxel size = 0.7 x 0.7 x 0.7 mm^3). Preprocessing of the MRI data was performed with SPM8 (Statistical Parametric Mapping) and the VBM8 toolbox, running on Matlab R2014a. Structural images were normalized with the DARTEL algorithm to the ICBM-152 template using both affine and non-linear spatial normalization. Images were bias-field corrected and segmented into grey matter, white matter, and cerebrospinal fluid tissues. The grey matter segments were then modulated for non-linear transformations only and subsequently smoothed with an isotropic Gaussian kernel (full-width-half-maximum = 8).

Resting-state functional MRI. The acquisition of resting state fMRI with opposite phase encoding directions (L/R and R/L) was performed with an EPI sequence for a duration of 30 min (eyes open and fixated on a hair cross), 72 slices covering the whole brain (*TR* = 720 ms, using a multiband factor of 8, *TE* = 33 ms, FoV = 208 x 180 mm, flip angle = 52◦, voxel resolution = 2 x 2 x 2 mm^3 (Smith et al., 2013; Ugurbil et al., 2013). During pre-processing we corrected for movements by affine two-pass registration and aligned the images to the first volume and to the mean of the volumes. Variance explained by six motion parameters from the realignment and their first derivatives were regressed out. Spatial normalization to the Montreal Neurological Institute (MNI) was carried out for the average EPI scans for each subject using the unified segmentation approach (Ashburner & Friston, 2005). We applied a band-pass filter with the cut-off frequencies of 0.01 and 0.08 Hz. The images were smoothed with the isotropic Gaussian Kernel (full-width-half-maximum = 5).

2.4 Connectivity-based parcellation

2.4.1 Parcellation based on structural covariance (SC-CBP)

For each subject, structural covariance was measured by computing the Pearson's correlation coefficient between grey matter volume values of the hippocampus' VOI voxels (seed voxels)

and all other brain grey matter voxels across the whole sample. This procedure yielded a seed voxels by target voxels connectivity matrix at the group level that was then used for clustering (see Supplemental material I.5 Fig.4).

2.4.2 Parcellation based on resting-state functional connectivity (RSFC-CBP)

Resting state functional connectivity between two brain regions was estimated by computing Pearson's correlation between time series of blood oxygen level-dependent signal (BOLD) at the subject level (Biswal et al., 1995; Buckner, Krienen, & Yeo, 2013). For each seed voxel in the VOI we calculated the correlation with every other grey matter voxel of the brain (see Supplemental material I.5 Fig.4). Correlation values were then standardized using the Fisher's Z-transformation.

2.4.2.1 Temporal MRI preprocessing

The goal of denoising is to remove or at least to reduce the contribution of any artifacts and confounds that contaminate neurally generated BOLD-signal. Noise in RSFC can result from scanner artifacts (Ojemann et al., 1997), subject movement (Power et al., 2014; Satterthwaite et al., 2013; Van Dijk et al., 2012) and physiological processes (Birn, Diamond, Smith, & Bandettini, 2006). Standard denoising approaches aim to regress out variance that is driven by noise in the measured BOLD signal. One simple approach to do so relies on the calculation of global signal or/and signal in two specific non-grey matter tissues (i.e., white matter and cerebrospinal fluid), which are assumed to reflect artifacts. An alternative approach capitalizes on machine-learning techniques (e.g., FIX) to automatically identify potential noise in the data. With these approaches, the part of variance related to noise is typically first estimated and then regressed out from time-series. Several variants have been developed over the previous years and we described below the most commonly used strategies.

2.4.2.2 Global signal regression

In global signal regression (GSR), the mean fMRI signal across all brain voxels is regressed out (Desjardins, Kiehl, & Liddle, 2001; Macey, Macey, Kumar, & Harper, 2004). The underlying axiom is that any fluctuations that are measured globally are not attributable to neural activity but have physiological or mechanical origin (Bianciardi et al., 2009; Birn et al.,

2006; Caballero-Gaudes & Reynolds, 2017; Wise, Ide, Poulin, & Tracey, 2004). Although it is unclear what exactly is reflected in the global signal and to what extent signal or nuisance is regressed out, it is still widely used. In this context of scientific uncertainty, the consequences of GSR on RSFC should be considered.

2.4.2.3 White matter-, cerebrospinal fluid signal regression

Another alternative is to estimate nuisance regressors from white matter (WM) and cerebrospinal fluid signal (CSF) (Anderson et al., 2011; Hallquist, Hwang, & Luna, 2013; Jo et al., 2013; Jo, Saad, Simmons, Milbury, & Cox, 2010; Power, Barnes, Snyder, Schlaggar, & Petersen, 2012; Weissenbacher et al., 2009; Yan et al., 2013). The signal's fluctuations in these parts of the brain are assumed to reflect drifts mainly caused by cardiac and respiratory effects (Dagli, Ingeholm, & Haxby, 1999; de Munck et al., 2008; Van Dijk et al., 2010; Windischberger et al., 2002). To measure the mean signal across these regions, we created subject-specific masks by co-registering the WM and CSF templates to each individuals' space and subsequently, regressed out the mean signal computed within these masks. Note that the subject-specific templates were eroded in order to remove voxels on the edge of the mask that relate to grey matter and do not contain pure WM/CSF tissue (Caballero-Gaudes & Reynolds, 2017; Jo et al., 2010).

2.4.2.4 FMRIB's ICA-based X-noiseifier

FMRIB's ICA-based X-noiseifier (FIX) is based on a machine learning approach, in which RS-fMRI signal has been decomposed into components of neural and non-neural sources by applying an independent component analysis (ICA) method (Beckmann & Smith, 2004; Cole, Smith, & Beckmann, 2010; Salimi-Khorshidi et al., 2014). FIX classifies the ICA components into relevant signal and noise-related components (Cole et al., 2010; Salimi-Khorshidi et al., 2014). We used the default classifier trained on a standard fMRI dataset, which has been shown to achieve 95% accuracy (Salimi-Khorshidi et al., 2014). For each participant spatial ICA was performed using FSL's MELODIC toolbox (Beckmann & Smith, 2004) and subsequently noise-variance components were regressed out.

In this study, we evaluated the denoising techniques both individually or in combination as recently suggested by Burgess et al. (2016) (see Supplemental material I.4 methods).

We investigated six different strategies:

(1) Standard motion regression with 24 regressors without additional explicit denoising, termed as "no denoising" emphasizing no additional transformations.
(2) Regression of the averaged fMRI signal across all voxels of the brain (GSR).
(3) Regression of white matter and cerebro-spinal fluid-related variance (WM/CSF).
(4) Neutralization of 'bad' components of fMRI signal decomposed by ICA (FIX).
(5) A combination of FIX and GSR regression (FIX+GSR).
(6) A combination of FIX and WM/CSF regression (FIX+WM/CSF).

2.4.3 Parcellation based on meta-analytic connectivity modeling (MACM-CBP)

From a computational point of view, MACM substantially differs from the aforementioned approaches since connectivity is not computed from collected MRI data as done for RSFC and SC but meta-analytically across activation foci of neuroimaging studies and paradigms archived in the BrainMap database (Laird et al., 2011) (http://www.brainmap.org). All experiments in BrainMap that were associated with each seed voxel or in the immediate vicinity of activation were considered. To account for spatial uncertainty, a spatial filter was systematically varied by including the closest 20 to 200 experiments in steps of 5 (for more details, see (Clos, Amunts, Laird, Fox, & Eickhoff, 2013; Clos, Rottschy, Laird, Fox, & Eickhoff, 2014; Genon et al., 2017; Genon, Reid, Li, et al., 2018). For each seed voxel, a meta-analytical co-activation likelihood profile for every other brain voxel given each of the 25 filter sizes was computed (with revised ALE algorithm (S. B. Eickhoff, Bzdok, Laird, Kurth, & Fox, 2012). The final CBP analysis was performed in the filter range of 100 to 148 experiments for the right hippocampus and in the filter range of 82 to 130 for the left hippocampus. An optimal filter range was defined based on the consistency of each voxels' cluster assignment across all the filter sizes (see Clos et al. 2013; (Chase et al., 2015; Clos et al., 2013; Genon et al., 2017) (see in Supplementary Methods I.3).

2.6 Clustering method

In line with previous studies, we used k-means (using MATLAB software 2014a) clustering, which showed good agreement with spectral clustering and outperformed hierarchical clustering (Arslan et al., 2018). The repetition number was set to 500, which almost doubled the recommended number of 256 repetitions (Nanetti, Cerliani, Gazzola, Renken, & Keysers,

2009), and the iteration number was set to 255. We examined six levels of granularity (levels of partitions) ranging from *k= 2* to *k=7* since previous work has reported stable cluster solutions at different level of partitions (2,3 and 5 (Adnan et al., 2016; Chase et al., 2015; Robinson et al., 2015; Robinson et al., 2016)). The clustering was performed at the subject-level for RSFC and at the experiments range (filter range) for MACM while it was performed at the group-level with average across bootstrap resampling for SC. Modality-specific and group-specific parcellations were achieved by assigning the hippocampal voxels to its most frequent cluster's label (i.e. by using the mode) across subjects, filter sizes and bootstrapping samples.

2.7 Measurement of stability and consistency of parcellations

In this work, we estimated stability and consistency of the partitions yielded by RSFC-CBP since this modality is particularly challenging in terms of its sensitivity to noise, inter-individual variability (S. Mueller et al., 2013) and its dynamic nature (Hutchison, Womelsdorf, Gati, Everling, & Menon, 2013). We examined both criteria in this CBP framework, but emphasized consistency over stability, as we aimed for biological validity in addition to stability by capturing convergent organizational characteristics across CBP modalities. In line with previous study (Varikuti et al., 2017), we considered the possibility that high stability within RSFC could be influenced by 'structured noise', which when regressed out might result in apparently lower stability but preserving biological relevance or even enhancing it.

We used two procedures in order to cross-validate our findings: (1) split-half (LaConte et al., 2003; Strother et al., 2002) to estimate the stability within a CBP modality (i.e. RSFC) and (2) bootstrap resampling with replacement to assess consistency between CBP modalities (i.e. RFSC vs MACM) (Bellec, Rosa-Neto, Lyttelton, Benali, & Evans, 2010; Efron, 1979).

In contrast to previous studies, we here assumed that multiple partitions at different granularities might be valid representations of the hippocampus organization, but at different levels. Accordingly, we focused on split-half and bootstrap resampling instead of internal validity criteria such as the silhouette value or the percentage of misclassified voxels as these latter metrics probe optimal data representation within the specific modality at hand, while we here aimed for stability within and reproducibility across modalities. Stability was estimated by splitting the sample into halves 10,000 times. The similarity between the two halves was examined by computing the Adjusted Rand Index (ARI) between the two split partitions. To

assess consistency, we generated 10,000 bootstrap samples for each modality and compared these samples between CBP modalities using the ARI (RSFC vs MACM, RSFC vs SC, MACM vs SC). An ARI value of 1 indicates that the clusterings are identical and a value of 0 suggests that the clusterings are not similar to each other, whereas negative values indicate a dissimilarity of clusterings higher than chance (see Supplemental material I.6 methods for detailed information).

2.8 Evaluating denoising performance

To better understand the actual effect of denoising strategies on the stability and consistency of RSFC-CBP partitions, we investigated the effect of denoising on seed voxels' time-course similarity and on connectivity profile dissimilarity. We assumed that structured noise influences the BOLD-response in the measured time-series in such a way that the voxels become more artificially similar (higher time-series similarity) and show higher similarity in their connectivity profiles. Accordingly, we can expect that a denoising method, which reduced structured noise successfully, will decrease time-series similarity and increase dissimilarity of the connectivity fingerprint. Since this latter marker directly drives the clustering pattern, its sensitivity to denoising is crucially relevant in the CBP application perspective. We could indeed expect that efficient denoising would to some degree enhance voxels dissimilarity facilitating the assignment of voxels to clusters. We therefore first examined voxels similarity regarding their time-series as measured by correlations of the time-series (Pearson's correlation), but we also examined the dissimilarity of the seed voxels regarding their pattern of connectivity with all other brain grey matter voxels by computing the Euclidean distance between seed voxels' connectivity fingerprint.

2.9 *Consensus clustering*

In order to create a cross-modal and stable map of the hippocampus from functional modalities, we used the bootstrap resampling method (Bellec et al., 2010). The basic idea was to simulate the replication process of parcellation a large number of times to preserve stable features and to reduce the occurrence of unlikely or unstable individual patterns (Bellec et al., 2010). After having created 10,000 bootstrap samples containing a matrix with all seed voxels and their cluster' labels (assigning each voxel to a cluster for each modality), we pooled these samples. After pooling we identified for each seed voxel the most frequent assignment to a

cluster by computing the mode. This procedure allowed each modality to be represented in the same regard independent of group or filter size, but only the most stable partition across both modalities was retained. Accordingly, if one modality provides unstable partitions, which is particularly likely for RSFC-CBP, the stable partitions from the other modality (here MACM) will determine the final clustering. Thus, this procedure promotes a final general parcellation, which is both, functionally cross-modal, and stable.

2.10 Cluster characterization with BrainMap and NeuroSynth databases

To characterize the clusters of our cross-modal consensus parcellation behaviorally we used two different databases, BrainMap (http://www.brainmap.org/) and NeuroSynth (http://neurosynth.org/). Both databases are complementary so that we expect their combination to provide novel insights into the behavioral association and the profile of a brain region (Genon, Reid, Langner, Amunts, & Eickhoff, 2018a). Furthermore, using both databases circumvents a circularity limitation (see Supplementary methods I.2). In the BrainMap protocol, each activation peak has been individually labeled according to a predefined taxonomy of behavioral domains such as cognition.memory.working (see (Genon et al., 2017). Behavioral profiling was performed with a reverse inference approach (Genon, Reid, et al., 2018a), which identifies the posterior probability P(Task|Activation), that is the probability of task given activation in that cluster.

In contrast, studies in NeuroSynth were labeled according to terms occurrence in the paper by using a text-mining approach so that behavioral associations were determined by the terms used in the corresponding article text (Yarkoni, Poldrack, Nichols, Van Essen, & Wager, 2011). This automated strategy resulted in the inclusion of 11406 studies (tripled the number of archived studies in BrainMap), but can suffer from a lack of behavioral precision. We also used the reverse inference approach with NeuroSynth i.e. P(Term|Activation). The decoding with BrainMap was region of interest (ROI)-based whereas it was coordinate-based with NeuroSynth requiring the usage of centroid coordinates of each cluster in MNI152 space (see Supplementary Methods I.7, Table 1). The lexical meta-analysis approach of NeuroSynth required decision criteria for selecting functional associated terms so that we excluded all non-content words (e.g., “addressed”, “abstract”, or “reliable”) and all brain terms that did not refer to function (e.g., “hippocampus”, “middle temporal lobe”). Additionally, we pooled terms with the same phonological root (e.g. ‘memory’ was used as a generic term for ‘memories’). All terms that reached a z-score higher than zero were included.

3 Results

To optimize first the reliability of RSFC-CBP, we examined the stability of its yielded partitions dependent on the application of different denoising strategies. After having identified the most reliable denoising method for RSFC, we investigated hippocampal organization across CBP modalities to determine consistency between modalities and levels of partition in order to establish a stable cross-modal functional map, which we characterized behaviorally in the last step.

3.1 Stable RSFC parcellations as a function of denoising

We measured stability within RSFC-CBP with split-half cross-validation and computed a two-way ANOVA with denoising as one factor (no denoising, GSR, WM/CSF, FIX, FIX+GSR vs FIX+WM/CSF), levels of partition as a second factor (k=2-7), and ARI as a dependent variable.

The analysis showed that the most robust RSFC parcellation was achieved when using FIX+WM/CSF (M = 0.82 ARI, SE = 0.03), GSR (M = 0.82 ARI, SE = 0.03) or WM/CSF regression (M = 0.81 ARI, SE = 0.04). The least stable parcellation was achieved when using FIX only (M = .76 ARI, SE = .005); main effect denoising F (5, 719999) = 60220, $p < .0001$] (see **Figure 2a**).

The main effect of partition levels was also significant [F (5, 719999) = 7377.6, $p < .0001$] demonstrating highest stability for 6 clusters (M = .81 ARI, SE = .03), followed by 7 clusters (M = .81 ARI, SE = .03). The ANOVA yielded also a significant interaction effect between denoising and levels of partition, [F (25, 719999) = 6812.48, $p < .0001$] (see **Figure 2d**). All comparisons between denoising methods and between levels of partition were significant according to a *post-hoc* Bonferroni-corrected analysis ($p < 0.001$).

However, the small magnitude of the differences between denoising approaches suggested that, overall, they all offered high stability. In the following section, we further investigated the effect of denoising at the voxel level to better understand how different methods influence voxels' properties and thereby the stability of the clustering.

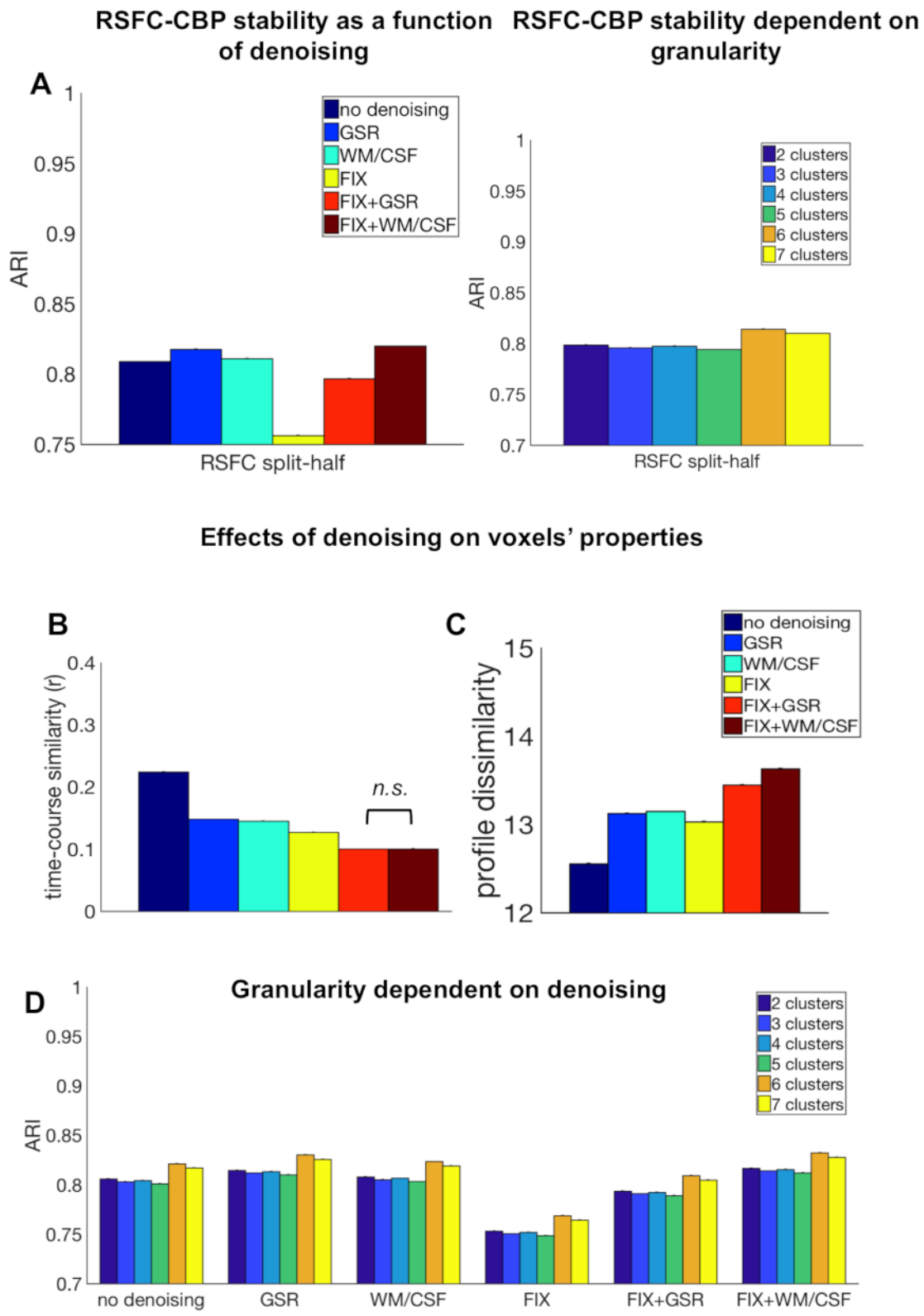

Figure 2. The effect of denoising on RSFC-CBP and on voxel functional properties. A) Most stable hippocampal parcellations across all levels of partition (k =2-7) were obtained with FIX+WM/CSF, GSR and WM/CSF regression as denoising approaches. Bars indicate mean ARI (±standard errors). Independent of denoising technique the highest stability was acquired for six clusters. All comparisons were statistically significant. B) Seed voxels' time-

course similarity was reduced after the application of denoising. No significant difference was observed between FIX+GSR and FIX+WM/CSF whereas all the other comparisons were significant. C) Denoising resulted in an increase of seed voxels' dissimilarity in comparison to uncleaned data. FIX-related strategies demonstrated the strongest effect of connectivity profile dissimilarity. D) FIX+WM/CSF showed the highest stability across all levels of partition (k=2-7) compared to other denoising techniques. Mean ARI (±standard errors). All comparisons were statistically significant.

3.2 Effects of denoising on voxels' time-course similarity and connectivity profile dissimilarity

We computed two separated ANOVAs in order to examine the effect of variance regression performed with denoising on each type of voxel measure separately: voxels' time-course similarity and voxels' connectivity profile dissimilarity.

The ANOVA with averaged seed voxels' time-course similarity as dependent variable revealed a significant main effect denoising [F (5, 4311269) = 78078.56, $p < .0001$], demonstrating a decrease in time-course similarity for denoised data. *Post hoc* Bonferroni-corrected multiple comparisons revealed no significant difference between FIX+GSR and FIX+WM/CSF regression ($p = .40$), but all the other comparisons were significant ($p < .0001$). The combination of a model-based (FIX) and model-free (GSR, WM/CSF) denoising strategy resulted in highly reduced seed voxels' time-course similarity compared to other techniques (**Figure 2b**).

The second ANOVA with averaged seed voxels' connectivity profile dissimilarity as dependent variable revealed an increase in dissimilarity of seed voxels with every additional denoising technique [significant main effect denoising: F (5, 4311269) = 113132.16, $p < .0001$] (**Figure 2c**). Our results showed that following denoising, seed voxels' connectivity profiles were more discriminable and especially, FIX+WM/CSF led to the highest dissimilarity between seed voxels' connectivity profiles. All *post hoc* Bonferroni-corrected comparisons were significant ($p < .0001$).

Thus, overall our analyses supported the use of FIX+WM/CSF as a denoising strategy and accordingly this procedure was retained for the following multimodal functional parcellation.

3.3 Robust levels of subdivisions across CBP modalities

After defining the optimal denoising strategy (FIX+WM/CSF) from the voxels' properties, as well as from the parcellation's stability perspective, we examined which level of partition, in other words, granularity, promotes consistency across CBP modalities. We focused on the consistency measure instead of stability since we aimed to promote biological validity estimated through comparisons across modalities. To examine consistency across partition's levels, we computed one-way ANOVAs with number of clusters (k = 2-7) as factor and ARI index measuring similarity as the dependent variable, separately for each pair of modality (RSFC vs MACM, RSFC vs SC and MACM vs SC).

Cross-modal comparisons between SC and functional modalities (RSFC, MACM) resulted in less consistency than between the two functional CBP modalities (RSFC vs MACM). The highest similarity between RSFC and SC was achieved for a partition of 2 (M = .58, SE = .03) and 6 clusters (M = .41, SE = .05) [F (5, 119999) = 167974.16, $p < .0001$] (see **Figure 3**). The comparison between MACM and SC revealed that the highest consistency occurred at a 2- (M = .54, SE = .15), 3- (M = .47, SE = .04) and 5-cluster partition (M = .43, SE = .06), [F (5, 119999) = 17685.1, $p < .0001$]. All *post-hoc* Bonferroni-corrected comparisons were significant ($p < .0001$).

Visual examination suggested that the highest convergence between SC and functional modalities could be observed at low granularity, that is, for 2-cluster partition in which all modalities subdivided the hippocampus into an anterior and a posterior cluster. At the next subdivision level, partitions already differed markedly between modalities. Namely, the pattern of subdivisions based on SC is dominated by a medial-lateral organization that strikingly mimics cytoarchitecture differentiation between subiculum and CA subfields. Such a medial-lateral subdivision first concerns the posterior portion of the hippocampus (at 3-cluster partition) but extends into the hippocampus head at 4-cluster partition (see **Figure 3**).

In turn, functional convergence between RSFC and MACM showed a significant effect on the ARI [F (5, 719999) = 12506.39, $p < .0001$], with the highest convergence being observed for partitions of 5 (M = .55, SE = .10), 3 (M = .49, SE = .03), and 7 clusters (M = .48, SE = .02)(see Supplementary results II.2, Table 2). Consequently, partitions into 3, 5 and 7 subregions were considered as optimal level of partitions for defining robust functional maps of the hippocampus.

In addition to the quantitative analysis, the visual examination of the partition schemes also proposed high convergence for 3, 5 and 7 clusters, revealing that the 3-cluster partition divided the hippocampus into anterior, intermediate and posterior subregions in both modalities (**Figure 3**). In turn, the 5-cluster partition divided the hippocampus into one

anterior cluster (head), three intermediate clusters (intermediate caudal, intermediate lateral and medial, for the body) and lastly, a posterior cluster (tail). Finally, the 7-cluster partition included three anterior, three intermediate clusters and one posterior subregion (see **Figure 3**).

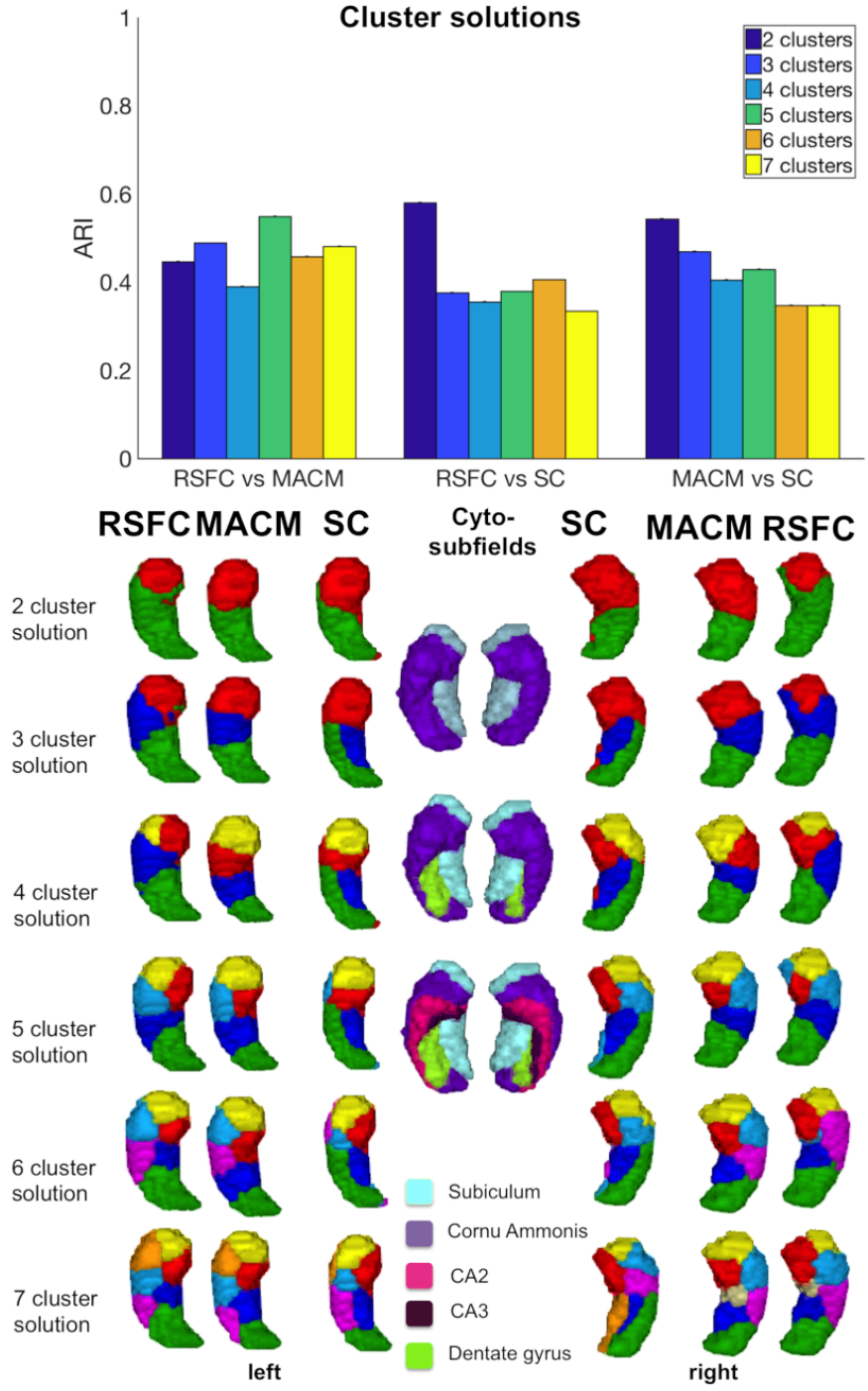

Figure 3. Hippocampus partitions based on SC, MACM, RSFC and cytoarchitecture mapping. Mean ARI (±standard error). All comparisons between cluster solutions showed significant differences.

3.5 Cross-modal functional consensus map

Cross-modal comparisons of CBP modalities revealed high convergence between RSFC and MACM, especially at higher granularities, whereas SC showed an idiosyncratic subdivision that deviated from pure functional modalities. For this reason we established a pure functional cross-modal map of the hippocampus using bootstrap resampling as described in section 2.9 and based on RSFC and MACM parcellations while excluding SC. Importantly, we created functional maps at different granularity levels (3,5 and 7 clusters) reflecting convergence between modalities as an approximation of biological validity. These functional maps at different partition levels should allow the community to investigate hippocampus' function and dysfunction at various levels of organization. In the present study, we focused on the 7 cluster partition to study hippocampus function as this high level of partition offers a detailed architecture along the anterior-posterior axis with small functional units.

As illustrated in **Figure 4**, each and every retained level of granularity revealed a specific aspect of hippocampal functional organization. The cross-modal 3-cluster partition subdivided the left and right hippocampi into an anterior (head), intermediate (body) and a posterior (tail) subregion. At the next subdivision (5-cluster granularity), bilateral hippocampi were partitioned into a posterior, intermediate part including 3 subregions - intermediate caudal, intermediate lateral rostral and intermediate medial rostral -, and finally an anterior subregion. The 7-cluster cross-modal partition showed hemispheric asymmetry. The body of the right hippocampus was subdivided into one intermediate lateral and two intermediate medial clusters. In contrast, the left hippocampus was partitioned into two intermediate lateral clusters and one intermediate medial cluster (see **Figure 4**). However, the posterior tail-cluster as well as the head, which was subdivided into three clusters (anterior rostral, anterior lateral and anterior medial), were found in both hemispheres.

We hypothesized that the subdivision into medial vs lateral subregions could partially reflect the already known cytoarchitectonic subdivision. The lateral segments in the body of the hippocampus corresponded mainly to the CA1-3 subfields and the medial clusters mainly to the subiculum. This hypothesis was supported by a quantitative comparison of our clusters with cytoarchitecture from the Anatomy Toolbox (see **Table 1**).

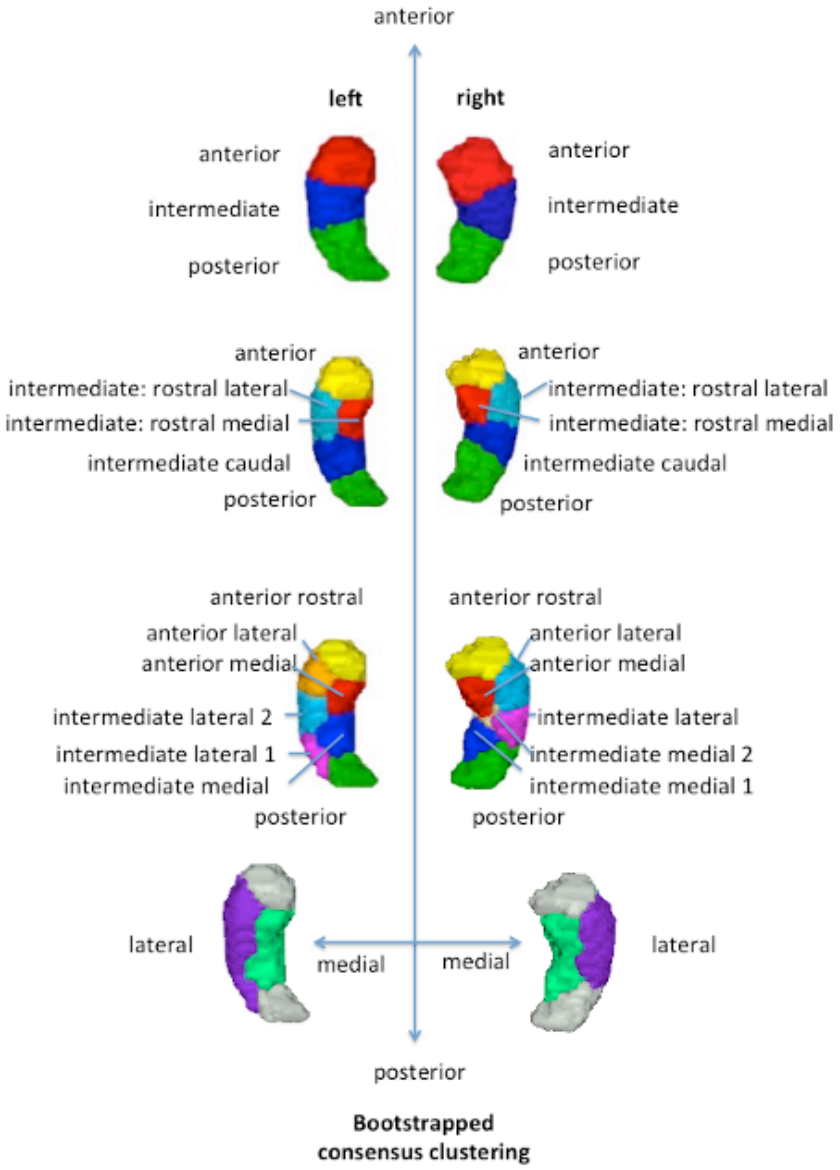

Figure 4. Functional multimodal maps across different granularities showing differentiation along the anterior-posterior and the medial-lateral dimension.

Table 1 Consensus hippocampus in comparison to cytoarchitecture

Consensus cluster	Cluster size	x	y	z	Overlap with cytoarchitectonic subfields
Right hippocampus					
Anterior rostral cluster (yellow)	161	22	-10	-24	CA1, Subiculum

Anterior lateral cluster (light blue)	181	31	-16	-20	CA1, DG, Subiculum, CA2
Anterior medial cluster (red)	139	21	-17	-17	Subiculum, CA3
Intermediate lateral cluster (purple)	128	33	-26	-12	DG, CA1, CA2
Intermediate medial 2 cluster (ocher)	34	26	-22	-16	Subiculum
Intermediate medial 1 cluster (dark blue)	86	24	-31	-9	Subiculum, DG
Posterior cluster (green)	129	26	-37	-2	DG, CA1
Left hippocampus cluster					
Anterior rostral cluster (yellow)	166	-23	-11	-24	CA1, Subiculum
Anterior lateral cluster (orange)	122	-31	-15	-21	CA1, DG, CA2
Anterior medial cluster (red)	149	-24	-20	-18	Subiculum, CA3
Intermediate lateral 2 cluster (light blue)	133	-33	-24	-14	DG, CA1, CA2
Intermediate lateral 1 cluster (purple)	76	-31	-35	-7	DG, CA1
Intermediate medial cluster (dark blue)	112	-26	-30	-9	Subiculum, DG
Posterior cluster (green)	73	-20	-35	1	DG, CA1

3.6 Cluster characterization

After having defined a functional parcellation map of the hippocampus we characterized the subregions with regard to behavioral functions using BrainMap and NeuroSynth activation databases. We focused on the finer partitions (7 subregions) since an examination of changes in behavioral associations across subregions at this high partition level could provide novel

insights into the functional dimensions, which has not been investigated previously. More concretely, at this high level of partitions, we could both track behavioral associations across the anterior-posterior gradient and explore medial-lateral differentiation.

3.6.1 Anterior vs. posterior functional differentiation

The characterization with BrainMap and NeuroSynth revealed a functional gradient along the anterior-posterior axis of the hippocampus that, on the one hand, supported the hypothesis of an emotion-cognition gradient, and on the other hand, suggested a self-world centric processing gradient.

In BrainMap anterior clusters were more likely engaged in emotion processing whereas posterior subregions displayed a sparse functionality emphasizing higher cognition functions requiring abstract representations (e.g. Cognition.memory, Cognition.memory.explicit, Cognition.memory.language.semantics). (see **Figure 5**). In addition, the anterior clusters were associated with various behavioral domains such as perception, interoception and cognition, demonstrating a diverse behavioral spectrum.

NeuroSynth provided a more detailed functional distinction along the anterior-posterior axis suggesting a gradient from self-centric (anterior parts) to more world-centric processing (posterior parts) as represented in **Figure 6**. The more anterior head clusters were engaged in cognitive and emotional processes related to personal experiences (e.g. episodic memory, experiences, autobiographical memory), whereas the more posterior clusters were associated with behavior like navigation (which requires the use of an abstract representation) and the processing of information in its environmental context. All the other intermediate-body and head subregions showed a graduated profile within this qualitative behavioral gradient (see **Figure 6**) and all clusters, independent of their position along the anterior-posterior axis, were associated with encoding, memory and retrieval processes. Interestingly, the gradients were especially evident in the lateral clusters (green, purple, light blue (orange) and yellow) of the hippocampus that were associated with CA subfields along the anterior-posterior axis as illustrated in **Figure 5 and 6**.

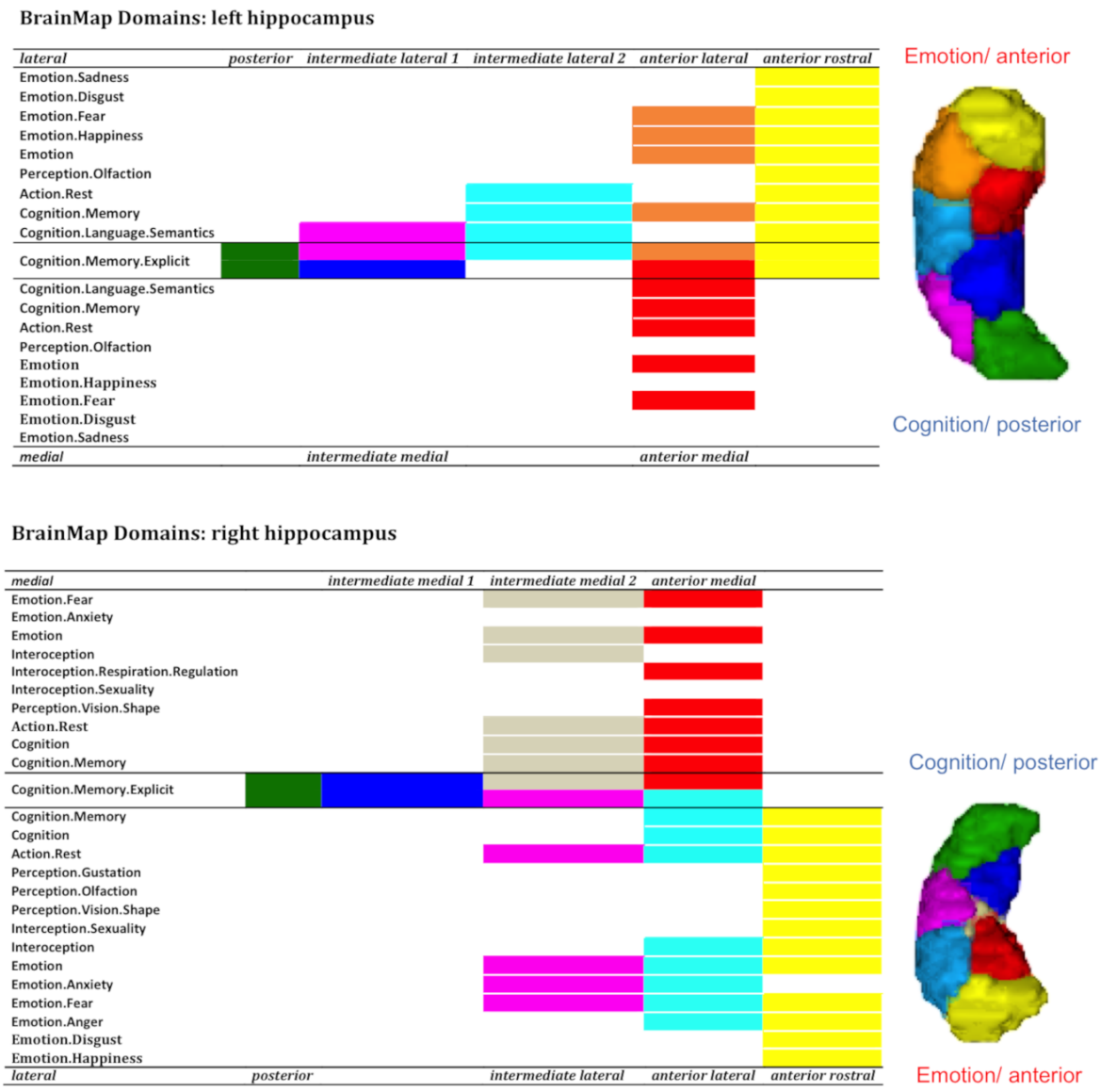

Figure 5. **Anterior to posterior characterization with BrainMap**.

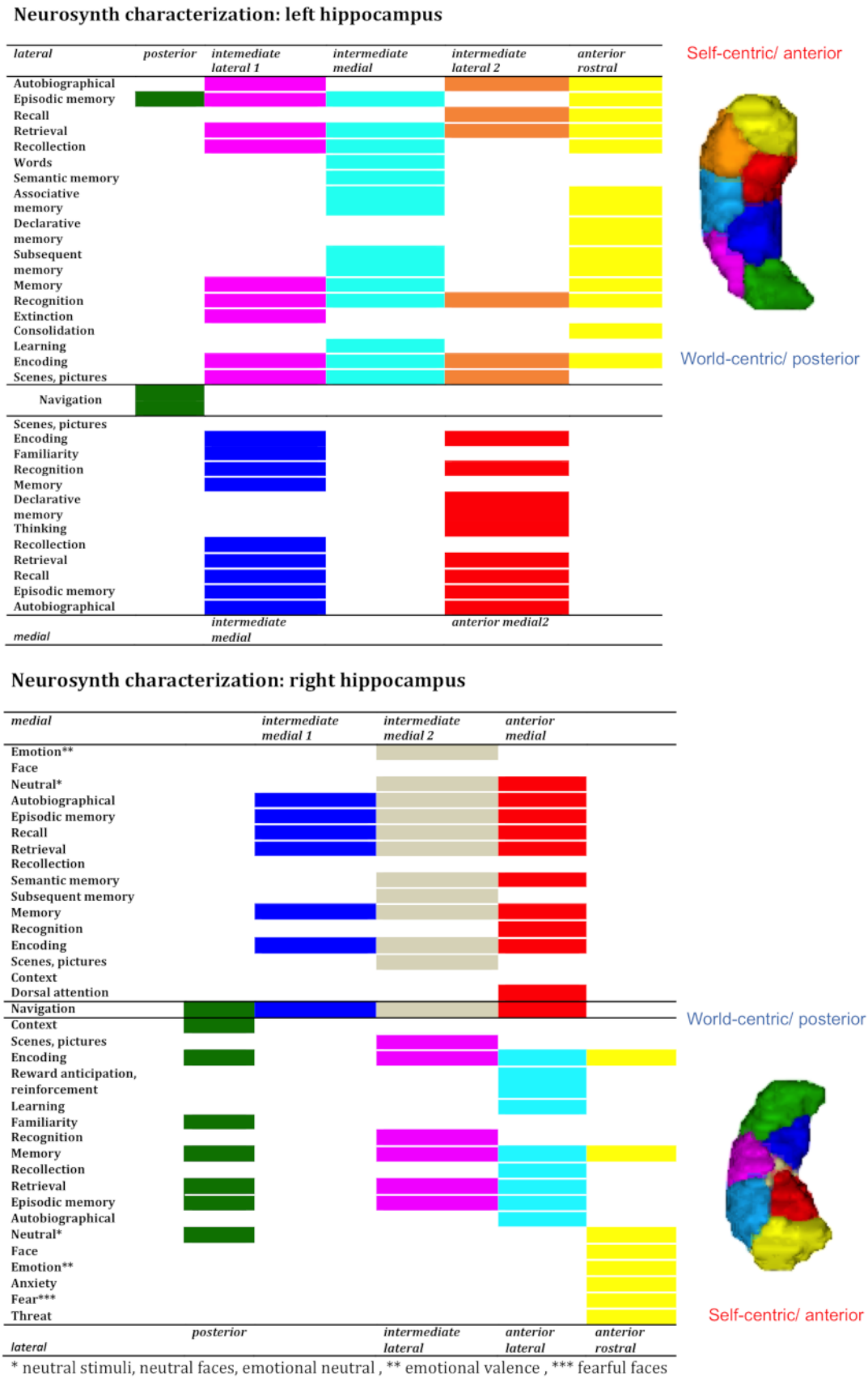

Figure 6. **Anterior to posterior characterization with NeuroSynth**.

3.6.2 Medial vs. lateral functional differentiation

In addition to an anterior-posterior organization the parcellation yielded a medial vs lateral differentiation predominantly in the body and partly in the head. In order to explore the functional relevance of the medial-lateral axis, we merged the intermediate clusters into one medial VOI segment and one lateral VOI segment, while anterior rostral and posterior subregions were not integrated (see **Figure 4**). Along the medial-lateral dimension the functional differentiation was less obvious with only slight differences between the two segments (see **Figure 5 and 6**). The medial segments were engaged in perception (visual shape discrimination), interoception (respiration regulation), dorsal attention and familiarity. Navigation, declarative memory and thinking were also associated with medial parts. In contrast, the lateral segments seemed to assimilate information into the hippocampal memory-system hence being engaged in associative memory, learning, reinforcement and extinction. Finally, we observed a lateralization effect in the sense that left lateral parts were involved in words and language processing and the right lateral subregions in emotion processing of happiness, anger and anxiety.

4 Discussion

In this study, we investigated the hippocampal organization in humans bridging the gap between hippocampal architecture and function using multi-modal CBP and two complementary databases for functional characterization. In contrast to other CBP modalities, RSFC, which is especially sensitive to noise, required a preliminary optimal denoising, which we evaluated in this study in regard to clustering stability and voxels' properties. Our results showed that the combination of a model-based (FIX) and a model-free (WM/CSF regression) denoising technique resulted in stable and biological plausible parcellations estimated through convergence across modalities. Especially, both pure functional modalities, MACM and RSFC, displayed high convergence at lower and higher parcellation granularities and could therefore be combined to derive a cross-modal functional map. We excluded SC from the cross-modal map as this modality demonstrated a relatively specific organization partly reflecting functional, as well as micro-architectonic characteristics. We emphasized and characterized the cross-modal seven-cluster-hippocampus yielding a subdivision into one posterior cluster, three head clusters and depending on lateralization two or three intermediate

clusters along the anterior-posterior and medial-lateral dimension. Following this, our behavioral profiling of the clusters revealed a functional emotion-cognition and a self-world centric gradient along the anterior-posterior dimension, which seemed to be particularly evident along the lateral subregion and more pronounced in the right hemisphere. In the following sections, after briefly discussing our new methodological findings regarding denoising for RSFC-CBP, we discuss the new insight into hippocampus organization and function brought by the current study with regard to previous literature.

4.1 Optimal denoising for RSFC-CBP

Our preliminary goal was to find a stable and consistent RSFC parcellation. But in the absence of unanimous guidelines of denoising approaches for RSFC-CBP in the scientific literature, we investigated various strategies with regard to stability, and voxels' properties such as time-course similarity and connectivity profile dissimilarity.

FIX+WM/CSF was found to contribute to highly stable partitions of RSFC-CBP, although other denoising techniques showed likewise high stability of parcellations. The subsequent examination of voxels' properties on which the clustering builds suggested two potential mechanisms underlying higher stability of FIX+WM/CSF. First, the part of variance neutralized by FIX+WM/CSF seemed to contain structured noise, as seed voxels' time-course similarity highly decreased when this strategy was applied (when compared to not denoised data and other denoising strategies, except for FIX+GSR). Secondly, and more importantly in the application-driven perspective, FIX+WM/CSF increased the discrimination between voxels as reflected by the significant improvement of seed voxels' connectivity profile dissimilarity. These influences eventually resulted in a better assignment of voxels to clusters. Overall our investigation promoted the combination of a model-based (FIX) and a model-free (WM/CSF regression) technique as an optimal denoising method, both from voxel-wise properties and partition-wise clustering. Burgess et al. (2016) already proposed to use FIX and GSR simultaneously in order to eliminate both local spatial artifacts and global drifts in fMRI data. Our results also suggested that the combination of FIX and GSR successfully removed structured noise outperforming FIX or GSR applied separately. FIX+GSR also led to stable parcellations in a similar extent than FIX+WM/CSF, but the use of FIX+WM/CSF was further supported by its improvement of voxels connectivity fingerprint discriminability, which is especially important in the clustering context. The reason why FIX+GSR performed less efficiently might be that GSR on one hand effectively neutralized motion artifacts, but on

other hand, distorted distance relationships (Murphy, Birn, Handwerker, Jones, & Bandettini, 2009; Power et al., 2014; Satterthwaite et al., 2017; Satterthwaite et al., 2013; Yan et al., 2013) that influenced connectivity measures. Based on these considerations, we can assume that GSR can have detrimental effects for parcellation and that WM/CSF represents a better alternative for combination with FIX. It has been suggested that WM/CSF regression eliminates more effectively respiration and cardiac effects (Anderson et al., 2011; Jo et al., 2010; Liu, 2016) and more generally, any slow undulations compared to GSR or FIX. FIX, in turn, could catch local or spatial related artifacts, which cannot be captured by WM/CSF in the same way. For these reasons, we here suggest that the combination of FIX with WM/CSF represents the most sophisticated double-approach for denoising, in particular in the context of CBP.

4.2 A convergent functional topography of the hippocampus across different measures of functional connectivity

In our study, two functional CBP modalities, task-independent (RSFC) and task-dependent (MACM), yielded CBP results with high convergence at the granularity of 3-, 5- and 7-cluster partitions, despite divergent methodological procedures. This high similarity between conceptually related methods, but based on completely different procedures and independent objects of investigation (i.e. co-activations across paradigms vs participants' RS-fMRI) argued for biological relevance of the revealed topographical pattern. Importantly, the convergence in partition scheme between the two modalities can not be attributed to an artifact intrinsic to the k-means clustering as a similar clustering procedure applied to structural covariance data revealed a different partition scheme. Indeed, SC-CBP parcellations deviated substantially from functional organizations already at low granularity even though at high granularity this modality also contained a functional head separation, the medial-lateral differentiation within body and tail seemed to mirror cytoarchitectonic differentiation between cornu ammonis and subiculum. Although our goal was not to elucidate the relationship between functional aspects, microstructure and SC, our parcellation work suggested that SC pattern could to a greater extent than functional connectivity be influenced by microstructural aspects. Future studies should further investigate the relationships between SC, microstructure and functional connectivity across the human brain.

Overall, our findings converged with previous literature reporting studies in different methods and species, which further supported the biological validity of the obtained parcellations. In

this context, one of the most prominent subdivisions for the hippocampus along the anterior-posterior axis is the tripartite model found in human and non-human segmentations. According to that model, the hippocampus is subdivided in an anterior (ventral, head), intermediate (body) and posterior (dorsal, tail) subregion, shown by anatomical (Swanson & Cowan, 1977) and gene expression data in rodents (Dong, Swanson, Chen, Fanselow, & Toga, 2009), and CBP research in humans (Robinson et al., 2015; Robinson et al., 2016).

Furthermore, Robinson et al. (2015) and Chase et al. (2015) extended the subdivision of the hippocampus and revealed an organization into five subregions for the entire hippocampus as well as for subiculum subfield using CBP. Robinson's (2015) MACM parcellation yielded four serial clusters along the anterior-posterior axis and a fifth anterior head-cluster tilted medially (see **Figure 1**). Of note, this pattern was replicated in the current study by RSFC parcellation but does not appear as a prominent pattern retained in the cross-modal map. Beyond these minor differences between studies, non-species studies divided the CA1 subfield in rodents in five serial segments along the dorsoventral axis (Petrovich, Canteras, & Swanson, 2001; Risold & Swanson, 1996), supporting the observation and potential biological meaningfulness of serially aligned clusters in our and Robinson's work.

To investigate hippocampus' function, we capitalized on the consensual 7-cluster partition scheme as it provides a very detailed functional architecture representing anterior-posterior gradient into small units, which was never achieved before. Our cross-modal map of the hippocampus at this level exhibited three head clusters, three or two intermediate clusters dependent on lateralization and one tail cluster. Interestingly, the posterior cluster in the tail remained as a relatively homogeneous functional region across functional modalities and granularities. This level of fine parcellation also contains a medial-lateral differentiation, which seemed to reflect differences between cornu ammonis and subiculum, respectively. According to the current parcellation, these two regions could be partitioned into serially positioned clusters along the anterior-posterior axis, which is in line with other studies (Dong et al., 2009; Fanselow & Dong, 2010). In other words, our clustering of seven subregions seemed to reflect on one hand the differentiation between cornu ammonis and subiculum and on the other hand further subdivisions along the anterior-posterior axis.

4.3 Functional organization of the hippocampus and human behavior

Based on the high convergence between RSFC and MACM we computed a fine consensual parcellation combining both modalities. We then drew up the behavioral profile of each

subregion using BrainMap and NeuroSynth as two complementary databases. We hence behaviorally characterized the anterior-posterior gradient and the medial-lateral differentiation taking an overarching view with activation databases.

4.3.1 Medial-lateral differentiation

We hypothesized that our organization along the medial-lateral axis reflected the differentiation between the subiculum (medial) and the CA subfields (lateral) evidenced by cytoarchitecture. Our behavioral profiling suggested that the medial segments participated in navigation, declarative memory and familiarity, whereas the lateral segments were associated with reinforcement, learning and extinction. Overall functional differences along the medial-lateral axis were sparse. Based on these behavioral descriptions we can only speculate that the lateral clusters were functionally involved in storing potentially integrating information into other systems and networks, whereas the functional specificity of the medial subregion was less evident. The conceptual inferences of the present study are limited on one hand by the spatial precision of standard MRI measurements and on the other hand, by current cognitive ontologies which have been derived by the study of human behavior and mind. By making all our partitions openly available to the scientific community, we invite future studies to further complement these first integrative findings on hippocampus organization and function. Nevertheless and importantly, the medial-lateral differentiation in the current fine parcellation has revealed that the functional gradient proposed in previous studies is mainly evident along the lateral segment. This aspect of functional organization of the hippocampus has presumably complicated or obscured the characterization and understanding of the gradient. In the current study, extensive behavioral profiling of fine subdivisions has allowed us to discuss new hypothesis beyond common psychology distinctions of behavioral functions.

4.3.2 Anterior-posterior organization

Evidence for an emotion-cognition and self-world centric gradient

The present study brought new integrative insights across research fields on the longitudinal functional differentiation of the hippocampus previously demonstrated in rats (de Hoz, Knox, & Morris, 2003; Jung, Wiener, & McNaughton, 1994; E. Moser, Moser, & Andersen, 1993;

M. B. Moser & Moser, 1998; Vann, Brown, Erichsen, & Aggleton, 2000), monkeys (Colombo, Fernandez, Nakamura, & Gross, 1998) and humans (Poppenk et al., 2013; Robinson et al., 2015; Robinson et al., 2016; Small et al., 2001) by revealing an emotion-cognition gradient within the broad behavioral domains of BrainMap and a self-world centric gradient based on more specific behavioral concepts in NeuroSynth. For reader's convenience the main pattern is illustrated in **Figure 7** in which we focused on lateral clusters. Below we discuss these patterns with regard to previous hypotheses proposed in the literature.

Besides the already often discussed differentiation of emotion-cognition along the anterior-posterior dimension, that we replicated with both databases integrating the scientific knowledge of thousand of studies, we also speculated that hippocampal organization along the anterior-posterior axis could be better explained with a self-world centric gradient. As actually almost all subregions are associated with memory processes, we speculate a self-centric information processing mode in the most anterior cluster with psychological functions such as autobiographical memory and emotion (see **Figure 7**) contrasting with a world-centric processing of information calling concepts such as navigation, scene and context processing associated with the most posterior hippocampal subregions. In other words, the overall pattern of behavioral concepts along the anterior-posterior axis suggest, in our view, a latent or underlying functional change from one pole of self-related processing to another pole of world-related processing. Importantly, general processes like encoding, and retrieval appeared equally distributed along the longitudinal axis. Thus, altogether our findings are more in favor of a self-world centric information processing gradient rather than a behavioral domain-wise (imagination-perception (Zeidman & Maguire, 2016) or encoding-retrieval organization (H. Kim, 2015; Lepage et al., 1998; Prince et al., 2005)) along the anterior-posterior axis of the hippocampus. Importantly, this self- and world-centric distinction may be reminiscent of egocentric vs allocentric distinction suggested by studies of spatial processing in rodents (R. G. Morris, Hagan, & Rawlins, 1986) and is particularly evident in the right hemisphere, but their meaning in the human cognitive system should nevertheless be considered beyond spatial representation, that is, also in relation to memory and decision making domains. If this hypothesis holds true, it has important implications for our understanding of psychiatric and neurological disease but its validity remains to be further evaluated in future studies using hypothesis-based experiments.

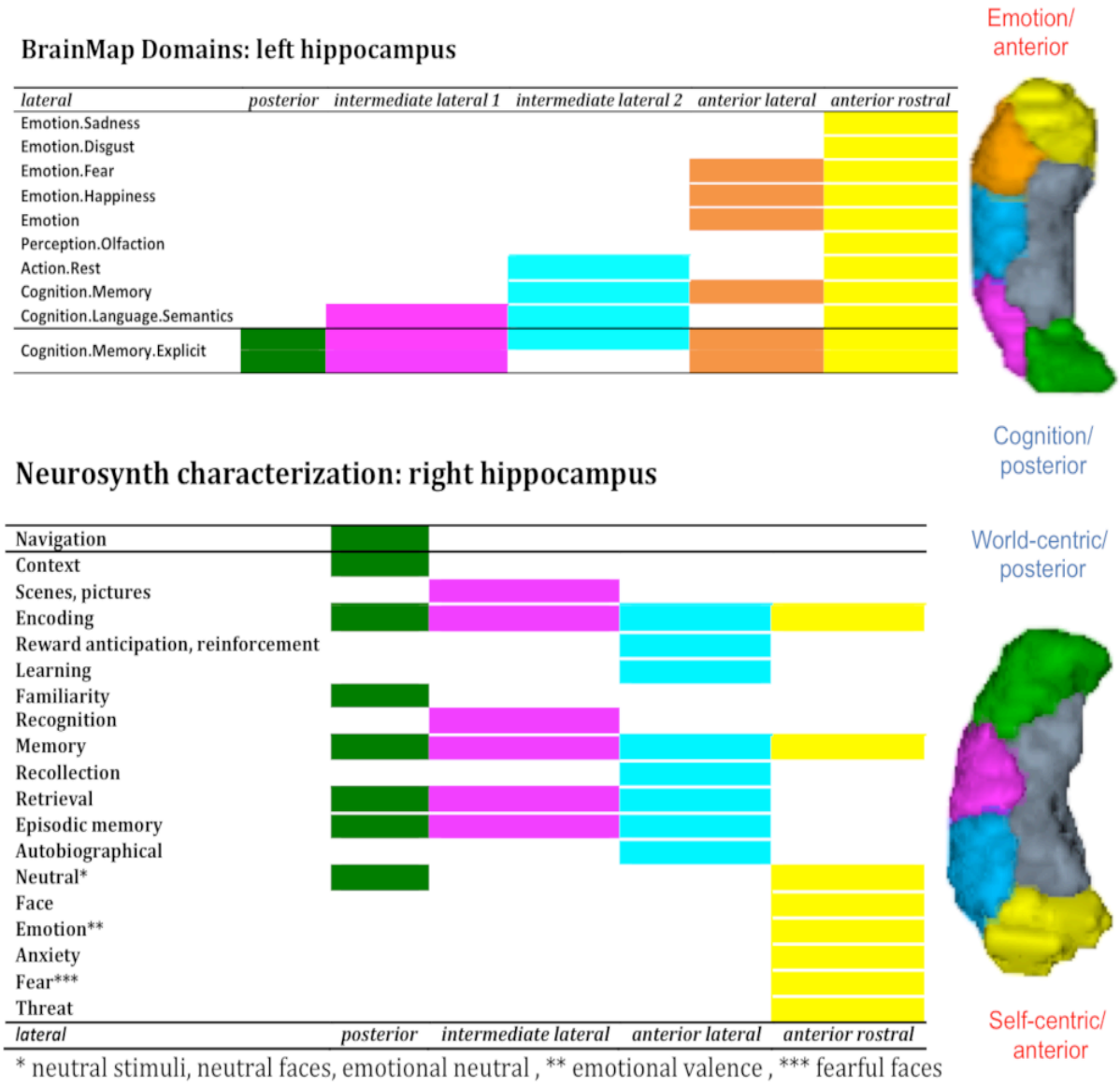

Figure 7. **Emotion-cognition and self-world centric functional gradient along the anterior-posterior axis.** Lateral clusters display an emotion-cognition gradient yielded with BrainMap and a self-world centric gradient found with NeuroSynth.

Limitations

The large-scale data aggregation on which the current study capitalized also comes with specific limitations. First, we focused on MRI, a method, which has a relatively limited spatial resolution and a relatively limited signal-to-noise ratio in the subcortical structures. Therefore, the clusters we have obtained can only be considered as homogeneous regions with respect to the usual MRI signal. Accordingly, we assume that our lateral segment actually represents an aggregation of the known different CA subfields showing different cytoarchitecture and

function. In particular, rodent studies suggested that CA1 and CA3 differ in their involvement in processes such as pattern separation and pattern completion (Guzowski, Knierim, & Moser, 2004). While these differentiations remain debated in humans (Deuker, Doeller, Fell, & Axmacher, 2014; Koster et al., 2018) in whom processes such as encoding, retrieval and association between unrelated items have been additionally proposed to differentiate distinct subfields (Bakker, Kirwan, Miller, & Stark, 2008; Deuker et al., 2014; Dimsdale-Zucker, Ritchey, Ekstrom, Yonelinas, & Ranganath, 2018). These differentiations could not be investigated in the present study due to a lack of behavioral precision in the representative concepts of both activation databases, in addition to the aforementioned limited spatial resolution. Future studies should therefore investigate how the anterior-posterior functional differentiation could be integrated with the subfields functional specialization in the hippocampus.

Another relevant limiting point refers to the complex structure of the hippocampus itself and its consequences for the optimal number of clusters. The human hippocampus is characterized by angulation and a variable number of digitations (Ding & Van Hoesen, 2015; Treit, Steve, Gross, & Beaulieu, 2018; Wisse et al., 2012). Both features could have influenced our results in terms of the optimal number of clusters. Due to the limited spatial resolution of MRI data, we may have missed differences in connectivity profiles of conflated subfields in the posterior hippocampus hence leading to a single tail cluster in the present study. Additionally, hippocampal gyrification, known as digitations, vary between individuals and have been previously discussed as a possible factor for inter-individual variability in the hippocampus (C. Chang et al., 2018; DeKraker et al., 2018; Ding & Van Hoesen, 2015; Treit et al., 2018). How this affects cognition and psychopathology (Oppenheim et al., 1998) and whether different digitations have different connectivity profiles and hence could influence clustering pattern is still unclear. This question should be addressed in future studies with high spatial precision techniques. Overall, the maps and conceptual findings reported in the present study are useful for the specific mapping modality they have been derived from, that is, conventional field MRI in humans.

Conclusions

In the present study we established for the first time a robust and stable RSFC hippocampal parcellation by applying a combination of a model-free and a model-based denoising framework. By combining partitions based on spontaneous connectivity with partitions based

on task-based connectivity, we built the first cross-modal generic hippocampal map at different levels of partition. Extensive behavioral profiling of the finest partition allowed inferences regarding the nature of information processing principles along the anterior-posterior axis in the hippocampus, beyond the concepts derived from psychological studies in specific fields. Importantly, while previous characterization of the anterior-posterior differentiation based on these concepts cannot be refuted and were partially supported, they could not account for the range of associations observed by our quantitative approaches. In turn, we proposed a self-world centric processing mode gradient along the anterior-posterior axis in humans, a data-based hypothesis that should be further investigated with specific model-based approaches. Further functional decoding allowed us to speculate that the medial-lateral distinction represented an assimilating process for the lateral part integrating information across different systems. Importantly, our medial-lateral distinction for the first time evidenced that the anterior-posterior gradient is predominantly observed in the lateral part of the hippocampus and an independent mapping approach based on structural data (structural covariance) further evidenced a medial-lateral distinction. Finally, the pattern of separation revealed by structural covariance appeared as a hybridization of functional connectivity and microstructure hence bringing new light into this relatively understudied mapping modality and offering an alternative and potentially better partition for compression of structural data (cfr. (Varikuti et al., 2018)). All our uni-modal and cross-modal maps are available in the ANIMA database (http://anima.fz-juelich.de/) to support future hippocampal investigations of hippocampal function in healthy or pathological populations.

Acknowledgments

Our research was supported by the Deutsche Forschungsgemeinschaft (DFG, GE 2835/1-1, EI 816/4-1), the National Institute of Mental Health (R01-MH074457), the Helmholtz Portfolio Theme 'Supercomputing and Modelling for the Human Brain', and the European Union's Horizon 2020 Research and Innovation Programme under Grant Agreement No. 720270 (HBP SGA1) and No. 785907 (HBP SGA2). The authors also thank Dr. Nicola Palomero-Gallagher and Shahrzad Kharabian for fruitful discussions.

I. Supplemental methods

I.1 HCP functional data

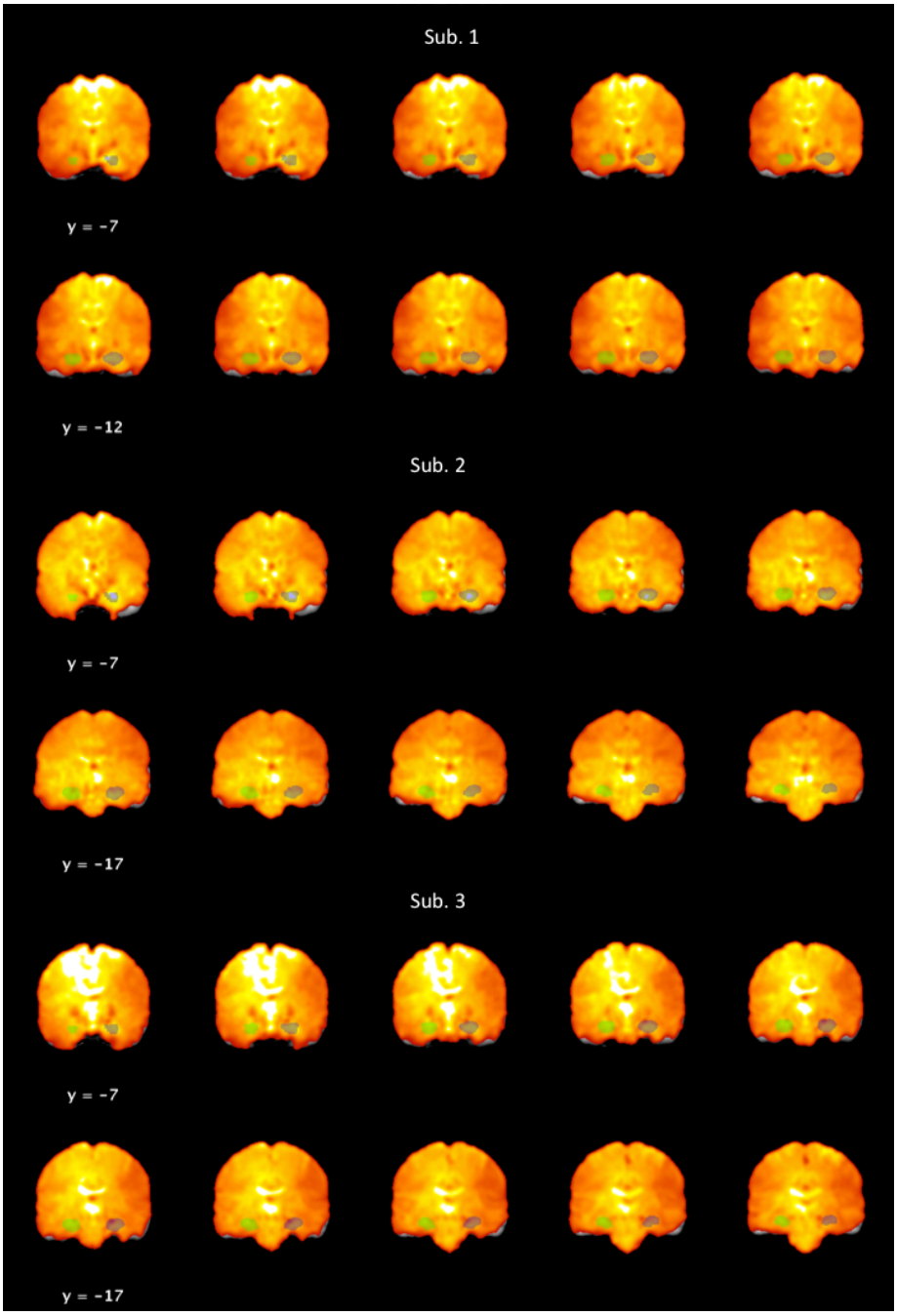

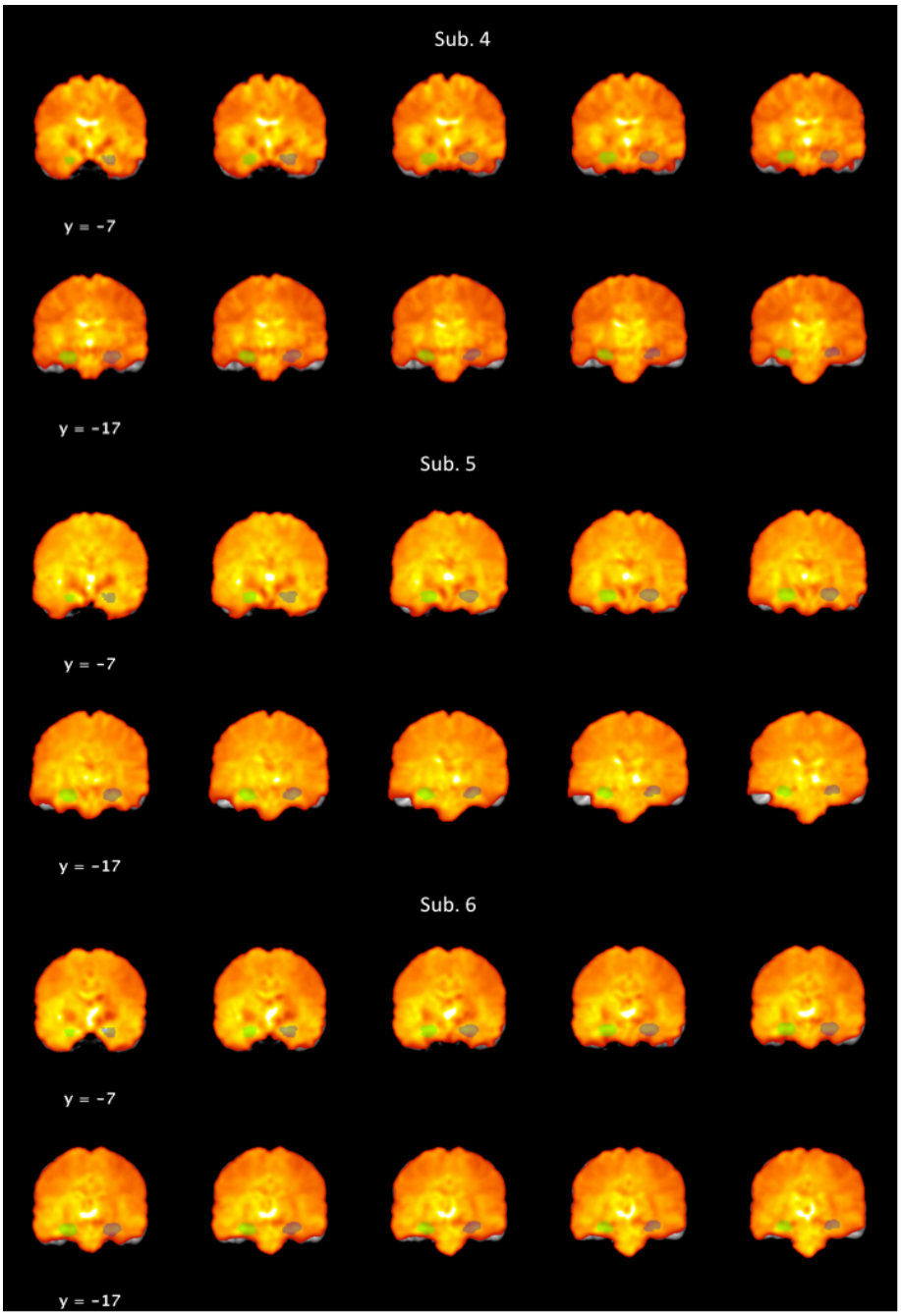
Sub. 4
y = -7
y = -17
Sub. 5
y = -7
y = -17
Sub. 6
y = -7
y = -17

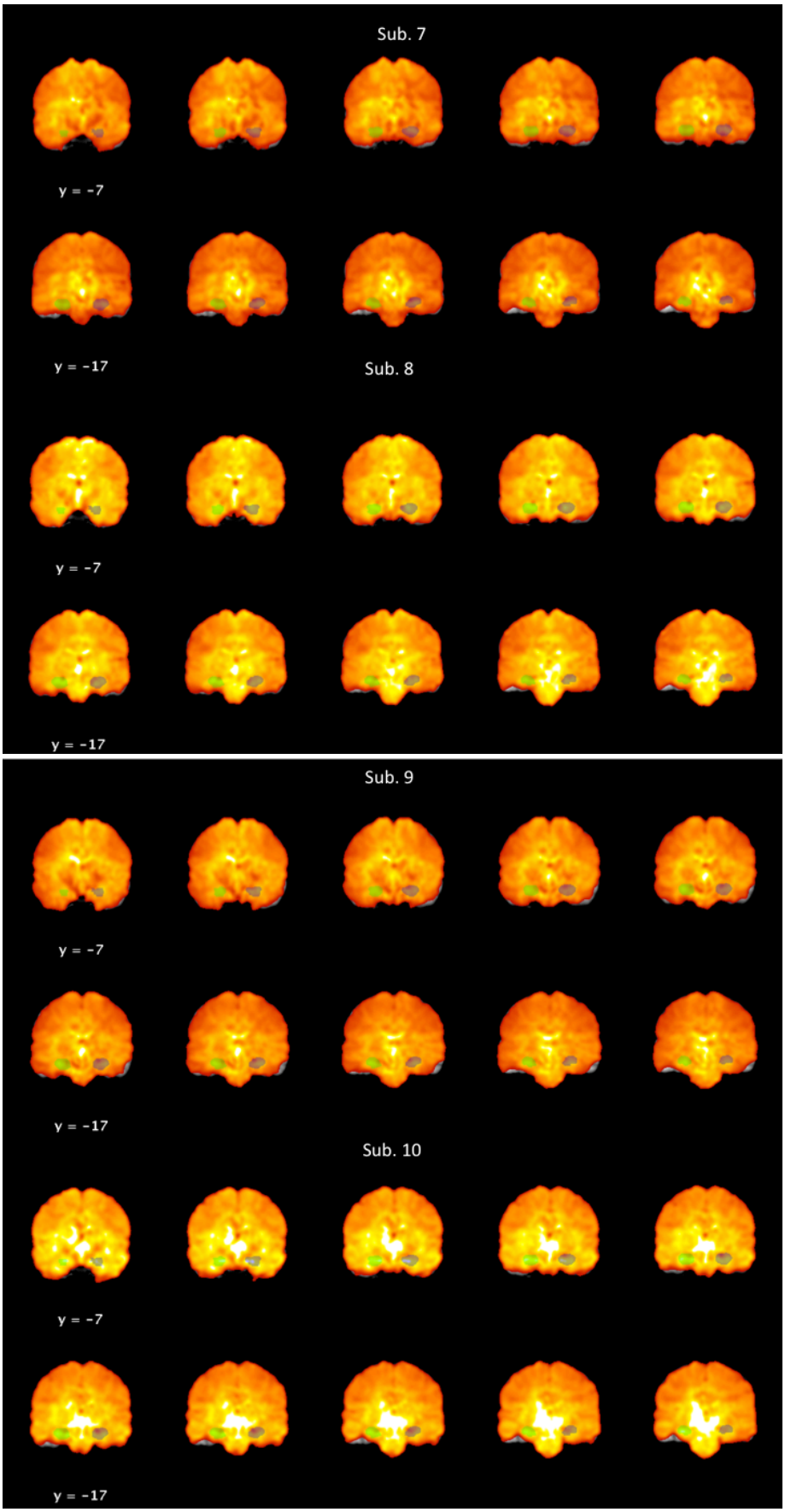

Figure 1. Resting-state functional signal in the hippocampus (green and blue ROI) of the HCP dataset on coronal slices.

I.2 Circularity assumption

A circularity limitation has been raised several times in previous studies parcellating brain regions based on MACM-CBP and characterizing these regions using the BrainMap database again. In those studies (Clos et al., 2013), MACM-CBP was performed in terms of whole-brain co-activation profiles of BrainMap to delineate subregions, and in the second step, the defined subregions were characterized in regard to associated behavioral concepts in this same database. Importantly, although both methods require BrainMap data, the underlying statistical computations and the type of data differ considerably.

The initial analysis of identifying clusters for CBP is of exploratory nature and is based on an exploratory statistical framework (S. B. Eickhoff et al., 2015) using co-activations across studies and paradigms that were published. The next step of behavioral characterization is based on *post-hoc* inferential statistics (i.e. reverse inference P(Activation|Task) on associations between peaks and behavioral labels of the BrainMap database. Therefore we would like to emphasize that even though BrainMap data is used for both steps, MACM-CBP and behavioral profiling, the underlying statistical frameworks were different and were also applied on different types of data (whole brain co-activation maps vs behavioral domains) hence were less circular then assumed. Nevertheless, in the present study, we further addressed this potential circularity by first externally validate the pattern of MACM-CBP with RSFC-CBP and hence building a robust subdivision scheme. Furthermore, we validated externally the behavioral profiling of our clusters revealed by the analyses of the BrainMap database with an additional, independent database i.e. NeuroSynth. This procedure should have avoided circularity at any steps, parcellation and behavioral profiling.

I.3. Parcellation based on meta-analytic connectivity modeling (MACM-CBP)

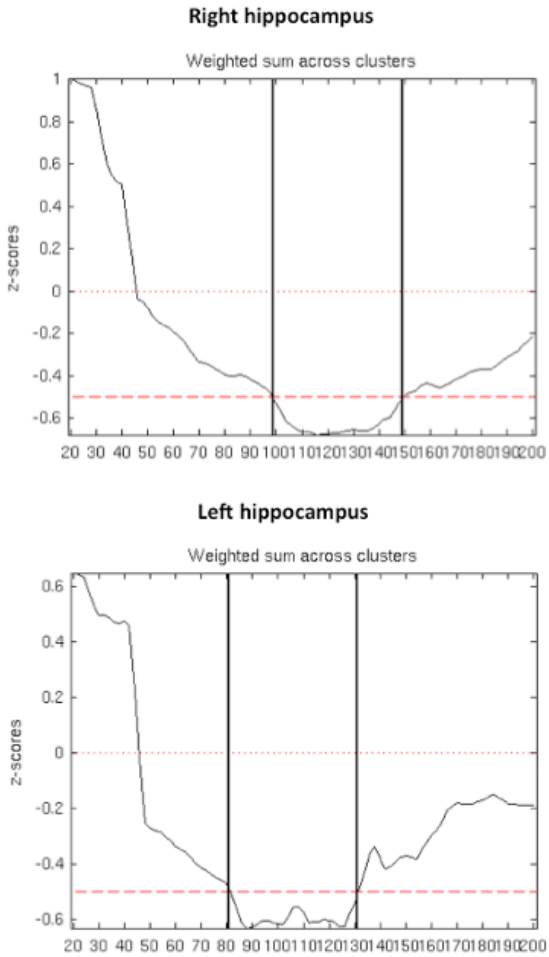

Figure 2. Filter range for MACM-CBP. Deviants and stability z-scores on median- filtered deviants. The vertical lines indicate the selected, most stable range of filter sizes (i.e., range with least deviants across k). Maximum z- score of median-filtered deviants.

I.4 Combination of denoising strategies

In the history of fMRI and denoising the application of several subsequent cleanup strategies is not unusual. Different approaches were introduced in the past to remove different types of artifacts. The most common approach is to regress out confounders such as realignment parameters, tissue-specific signals (WM and/or CSF), global signals, and signals either from principal component or independent component analyses as stated in a recent report by (Satterthwaite et al., 2017).

Another recent work examined systematically what are the most common denoising approaches in use and how do they influence the resting state test-retest reliability (Varikuti et al., 2017). The literature survey of the authors revealed that combinations of different confounders are often performed. In particular, the most common strategies were global and tissue-class specific mean signal regression (either only WM/CSF or in combination with GSR) followed by principal component analysis in addition to GSR or with tissue specific confounders (Varikuti et al., 2017). ICA-based models like those underlying FIX, which is based on a machine learning approach, were less likely to be applied possibly because of its training requirements of the classifiers. Nevertheless, Griffanti et al. (2014) demonstrated the high accuracy performance (99%) of these classifiers on HCP data to detect spatial artifacts, hence making FIX the first choice for such dataset. From a purely mathematical point of view, however, FIX was not designed to capture global or slow waves in the data, since it aims for an independent component separation (Griffanti et al., 2014) that does not apply to the interlocking global noise. In other words, it is highly sensitive for spatial artifacts in particular, but cannot capture global drifts. On the other hand, GSR is not selective at all but removes global waves with the negative effect of spatial distortions in functional connectivity, which can represent a major problem for parcellation work.

In line with this argument, Burgess et al. (2016), pointed out the limitation of using only FIX or GSR separately and combined both methods investigating its influence on motion-artifacts. These were significantly reduced after both approaches were applied together and not separately (Burgess et al., 2016). In addition, Satterthwaite et al. (2017) pursued the same goal and confirmed that adding GSR to ICA-AROMA reduced motion artifacts significantly and provided the same performance as the classical denoising strategy with six realignment parameters, WM, CSF regression, and GSR applied jointly to the data. All their high performance models contained GSR. However, the use of GSR remains controversial because long-distance connections benefit from this approach, while short-distance connections do not as regionally specific artifacts cannot be captured by GSR (Satterthwaite et al., 2017). ICA-based denoising, on the other hand, did not show distance dependency, but left spurious stripes of motion artifacts unless GSR was added (Satterthwaite et al., 2017). In order to avoid distance dependency effects in our study (which could flawed the clustering), we included and tested another approach combining FIX with WM/CSF regression. We assumed that FIX would identify spatial artifacts and WM/CSF regression would compensate for physiological noise and, like GSR, all undulation influences of movement in the data.

To demonstrate the effects of denoising we prepared some examples of grey ordinate plots for three subjects (**Fig**. 3) showing that the combination of model-based and model-free techniques do not distort the data. As expected, the plots show that the model-free strategies indeed additionally removed stripes present in the data that were not identified by FIX. Thus, in addition to the previous assumptions about the usefulness of a combined approach, our results also suggested that such a combination did not incorrectly distort the data.

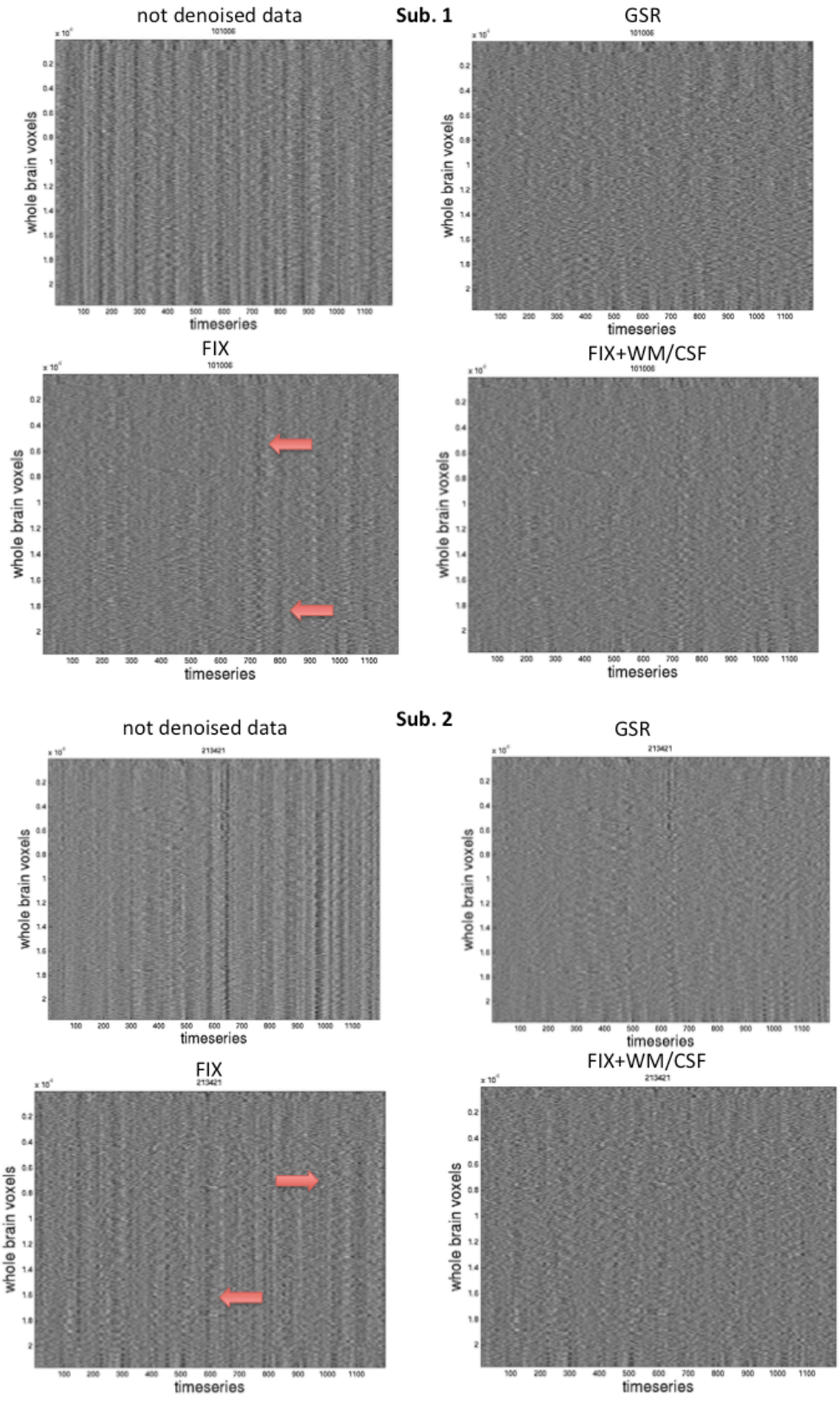
not denoised data
Sub. 1
GSR
FIX
FIX+WM/CSF
Sub. 2
not denoised data
GSR
FIX
FIX+WM/CSF
whole brain voxels
timeseries

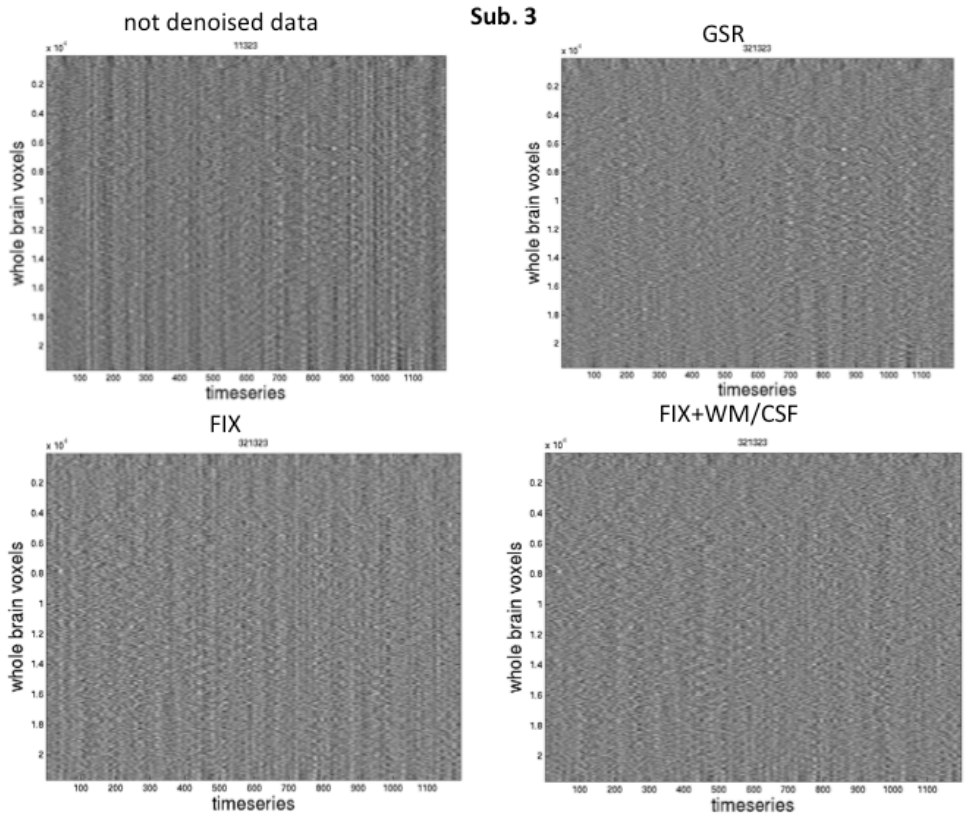

Figure 3. Influence of denoising on RS-fMRI signal. Grey ordinate plots for subject 1-3 for resting-state fMRI data either not denoised or denoised with different techniques demonstrating the removal of artifacts especially with FIX+WM/CSF achieving best results through removing stripes in the data as indicated with arrows.

I.5 Measure of RSFC-CBP and SC-CBP

For SC-CBP we had a matrix with 'participants x hippocampal grey matter values', which we correlated with another group-level matrix containing 'participants x whole brain grey matter values' resulting in a group-level 'seed x whole brain voxels' matrix. In contrast, for RSFC we correlated the seed voxels matrix across the time-series with whole brain voxels across time-series for every single subject (see **Fig.** 4).

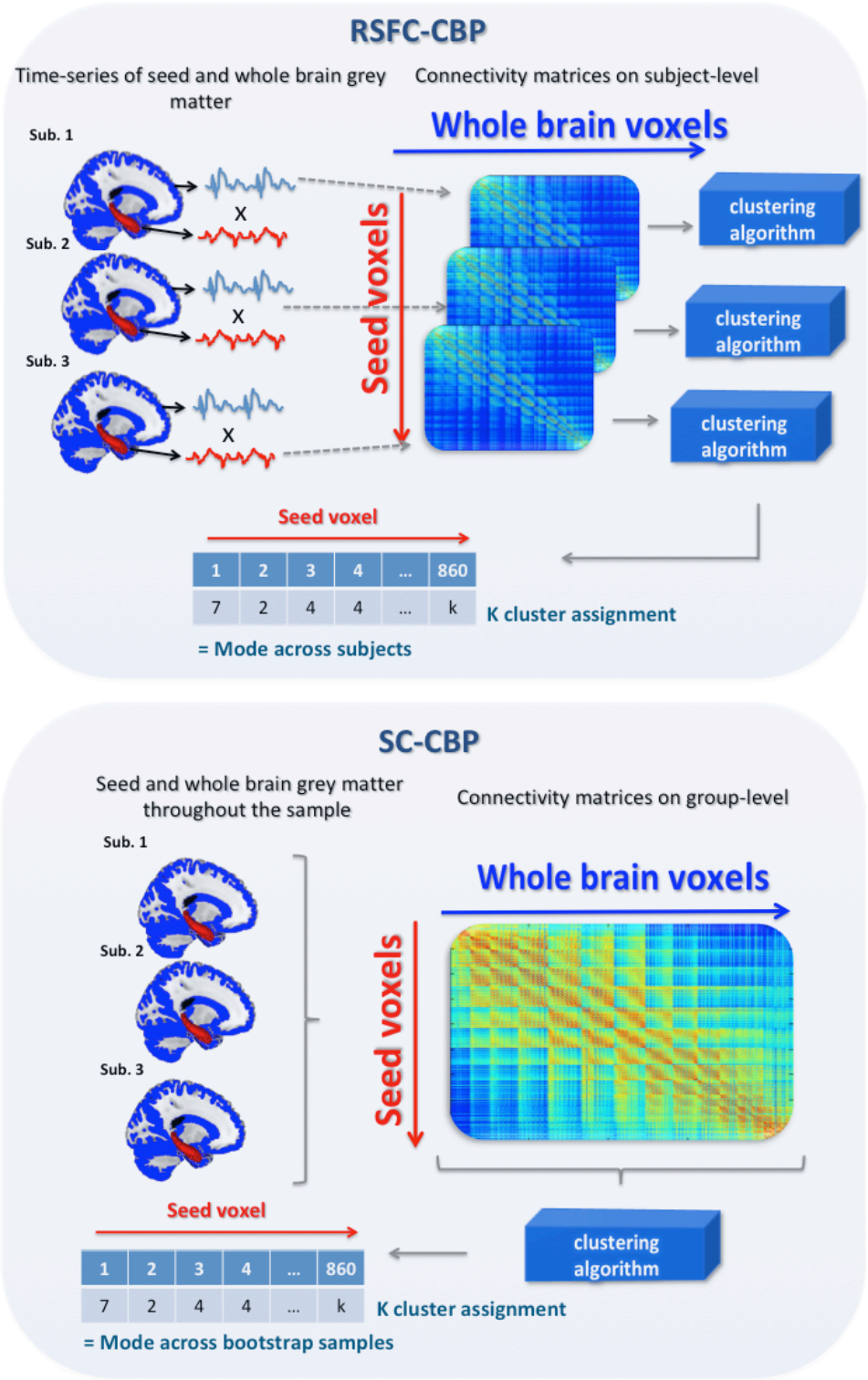

Figure 4. Connectivity input of RSFC-CBP and SC-CBP for the clustering algorithm and its output vector of seed voxels assigned to clusters.

I.6 Adjusted Rand Index

The adjusted rand index reflects the dissimilarity between partitions based on the number of pairs of elements (here voxels) that are either clustered together or separately in partitions. For example, if two given, voxel A and voxel B, are clustered together in partition X and also in partition Y, these two partitions agrees for this pair of voxels A-B. In contrast, if voxel A and voxel B are clustered together in partition X, while voxel A and voxel B are assigned to different clusters in partition Y, the two partitions, X and Y disagree for this pair of voxels A-B. Taking into account the total number of pairs, we can make a statement about how many pairs of voxels in both parts agree, and how many do not. Therefore in the numerator the agreement between clusterings is expressed (pairs of voxels that are found in both clusterings) whereas in the dominator the total number of pairs is specified.

In order to compare two partitions/clusterings we used a matrix containing for each hippocampal voxel the cluster number to which it was assigned across participants (RSFC, SC) or filter sizes (MACM). For stability measures in RSFC, we divided the matrix randomly into two halves based on the number of participants. Each half contained all hippocampal voxels assigned to clusters within one half of the participants. We computed the mode of cluster assignment across this half, resulting in a vector containing only the hippocampal voxels and their most frequent cluster labels for the specific half. We compared the two vectors resulting from the two halves with each other using the ARI as shown in **Fig**. 5. For validity measurements, we used the same procedure except that the entire matrix with all bootstrapped participants (or filter sizes) was used to generate the hippocampal vectors (see **Fig**. 5).

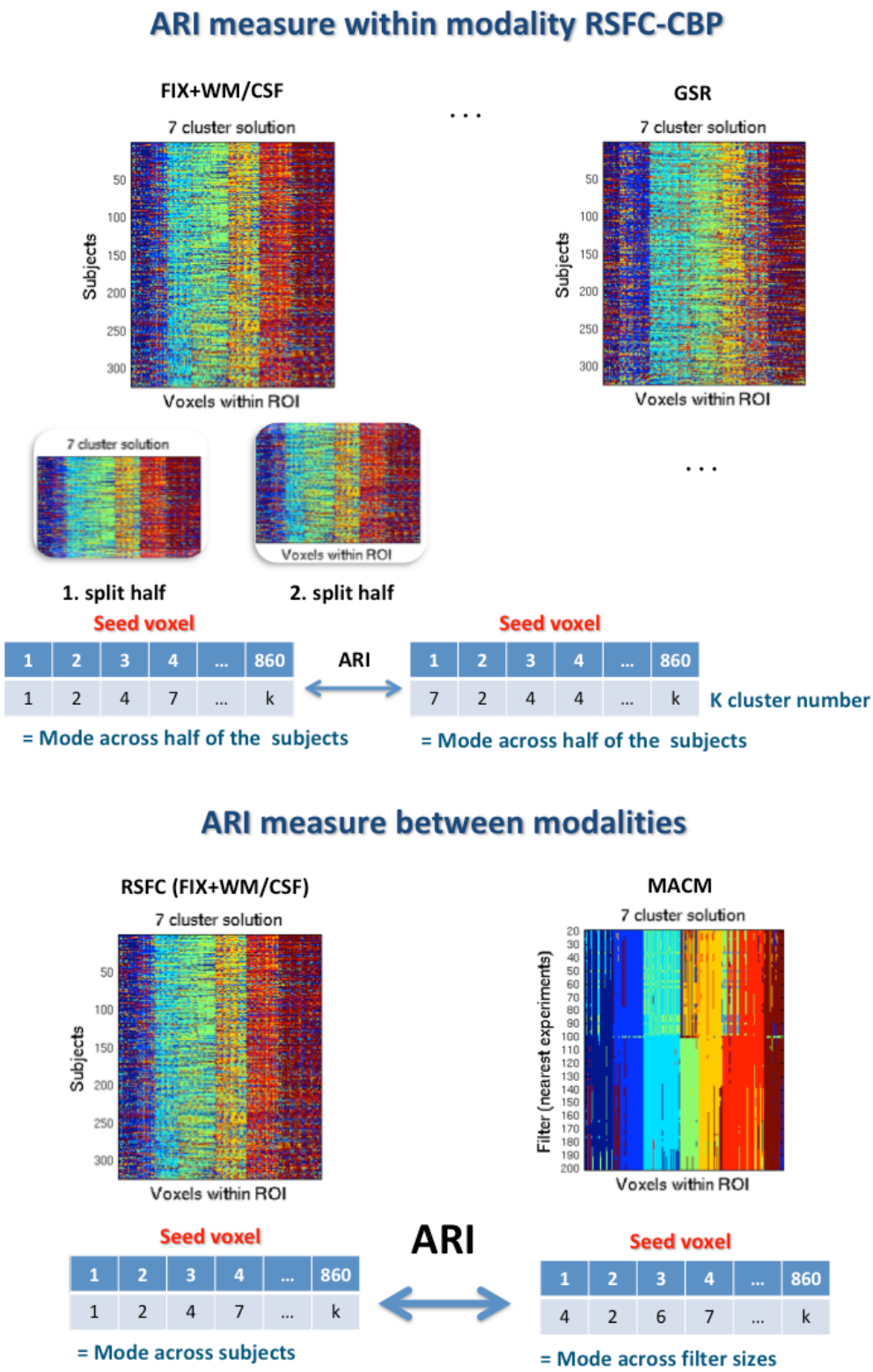

Figure 5. ARI measure within and between modalities.

I.7 Cluster characterization with BrainMap and NeuroSynth databases

For NeuroSynth we used the following centroid coordinates of each cluster in MNI152 space in order to associate specific behavioral profiles to the partitions.

Consensus cluster	**x**	**y**	**z**
Right hippocampus			
Anterior rostral cluster	22	-10	-24
Anterior lateral cluster	31	-16	-20
Anterior medial cluster	21	-17	-17
Intermediate lateral cluster	33	-26	-12
Intermediate medial 2 cluster	26	-22	-16
Intermediate medial 1 cluster	24	-31	-9
Posterior cluster	26	-37	-2
Left hippocampus			
Anterior rostral cluster	-23	-11	-24
Anterior lateral cluster	-31	-15	-21
Anterior medial cluster	-24	-20	-18
Intermediate lateral 2 cluster	-33	-24	-14
Intermediate lateral 1 cluster	-31	-35	-7
Intermediate medial cluster	-26	-30	-9
Posterior cluster	-20	-35	1

Table 1. Coordinates of the generic hippocampal map for NeuroSynth characterization

II. Supplemental results

II.1 Extending decision criteria for optimal cluster number

Throughout our work two major criteria were responsible for our decision for the optimal number of partitions: stability measured with split-half cross-validation and biological

meaningfulness estimated by bootstrap resampling across MRI modalities and compared with the ARI. For the sake of completeness we also examined an index of data representation within each connectivity modality. We here used Variation of Information (VI) as suggested by Kelly et al. (2012). This metric measures the distance between two clusterings and indicates how much information is lost or captured when switching from one cluster solution to another clustering (Meilă, 2007). Accordingly, a cluster solution is considered as optimal when it does not show an increase of VI compared to other cluster solutions so that low values show optimal solutions in relation to previous or subsequent cluster solutions. We here examined this metric for cluster solutions ranging from two to ten cluster solutions. Overall, VI further supported the 7 cluster solution as an optimal level of compression for both functional connectivity measures as summarized in **Fig**. **6**.

In particular, for RSFC, VI tends to decrease from the 6-cluster to the 7-cluster solution, but either to remain stable (right hippocampus) or to increase (left hippocampus) from the 7-cluster solution to the 8-cluster solution. For MACM, VI showed a clear decrease from the 6-cluster solution to the 7-cluster solution, but an increase from the latter to the next solution in the left hippocampus. Somewhat surprisingly, the pattern was different in the right hippocampus with VI showing a progressive increase from the 5-cluster solution up to the 9 cluster solution, thus a pattern that differs with what is observed with RSFC. We could therefore assume that this difference is related to technical factors (such as overall more variance in activation peaks reported in the left hippocampus), despite the influence of a biological factor for this observation cannot be ruled out. Although SC parcellation was not incorporated in our consensus functional parcellation (based on RSFC and MACM), for the sake of completeness, we also examined VI in clustering based on SC. This reveals that VI decreases from a 5-cluster solution to a 6-cluster solution, but then shows a "plateau" until the 10 cluster solution for which it increases when compared to the 9 cluster-solution in the right hemisphere. In contrast, on the left hippocampus, VI clearly reaches an optimum at a 7-cluster level.

Thus, in sum, the VI criterion supported the 7 cluster solution as an optimal representation of connectivity variance as estimated by different features (MACM, RSFC, SC) in particular in the left hippocampus. We noted that the right hippocampus showed a slightly more complex pattern with differences across features; nevertheless, hemispheric differences are beyond the scope of the current study. Overall, both the investigation of VI across cluster solution and our previous investigation of stability support a 7-cluster subdivision as an optimal compression of MRI functional connectivity features in the hippocampus.

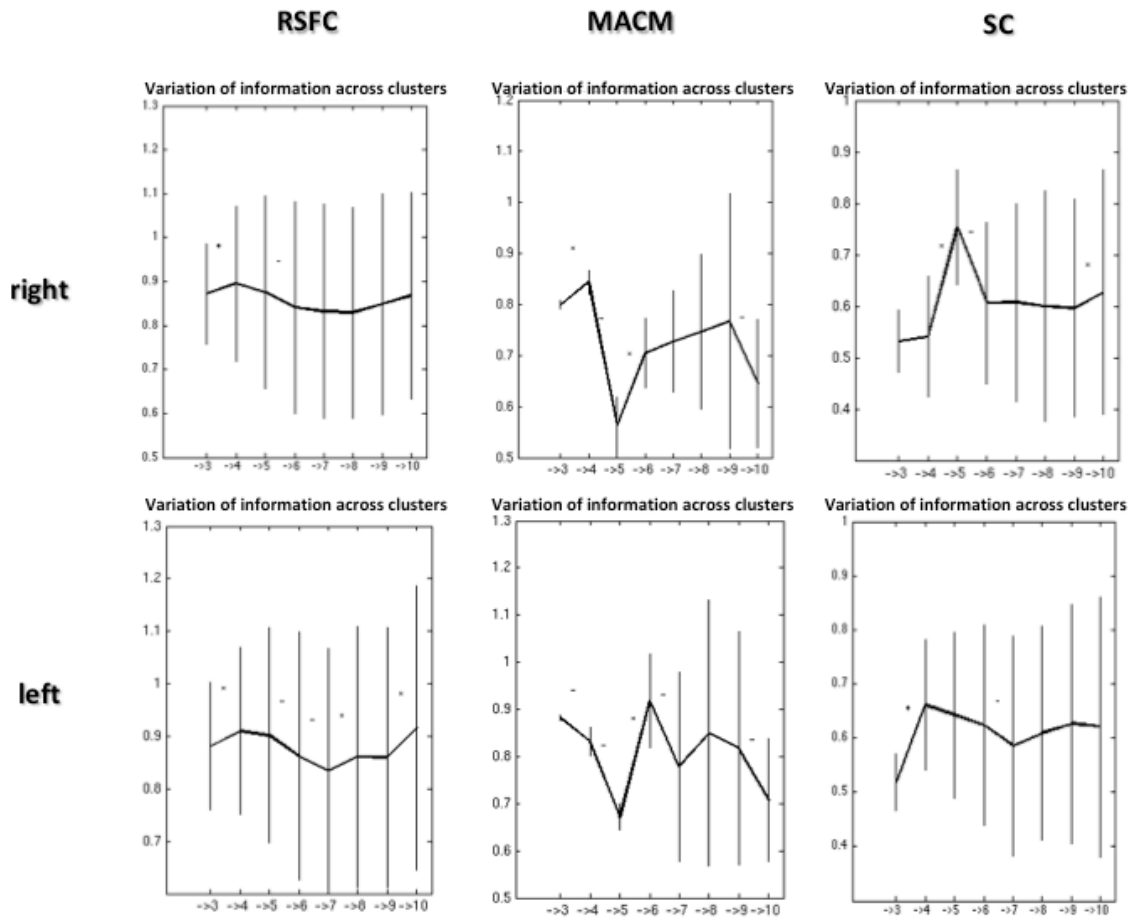

Figure 6. **Variation of information across modalities and hemispheres supported cluster solution 7 for RSFC and SC-CBP, and 5 for MACM-CBP.**

II.2 Functional consensus map

In order to be able to establish a consensus map that was generally representing functional architecture of the hippocampus we decided to merge the 10 000 generated bootstrap samples of MACM and RSFC as these two modalities exposed the highest convergence across modalities visually and in regard to the ARI index as represented in the following table 2. SC, on the other hand, had a hybrid-like nature with a functional head division that was similar to MACM and RSFC and a body and tail partitioning reminding of the cytoarchitectonic subfields for which it was excluded from the cross-modal map.

right	**cluster solution 3**	
	MACM-CBP	SC-CBP
RSFC-CBP	0.4645	0.3891
MACM-CBP	1	0.5260
	cluster solution 5	
RSFC-CBP	0.6514	0.3984
MACM-CBP	1	0.3686
	cluster solution 7	
RSFC-CBP	0.4641	0.2937
MACM-CBP	1	0.3361
left	**cluster solution 3**	
RSFC-CBP	0.4963	0.3751
MACM-CBP	1	0.4667
	cluster solution 5	
RSFC-CBP	0.4642	0.3759
MACM-CBP	1	0.4838
	cluster solution 7	
RSFC-CBP	0.5116	0.3715
MACM-CBP	1	0.3592

Table 2. Clustering similarity (measured with ARI index) across CBP modalities.

II.3 Clustering based on unsmoothed data

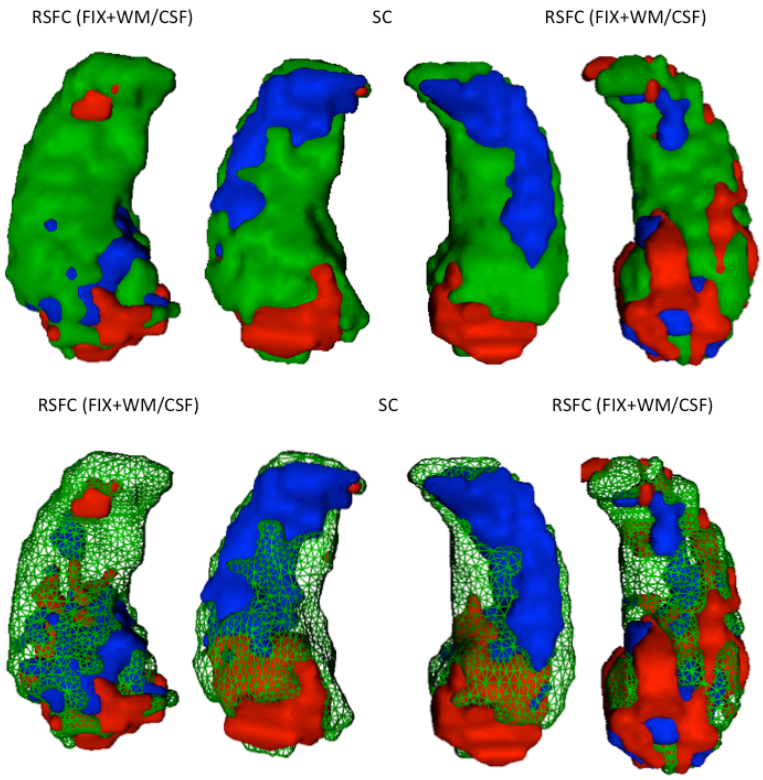

Figure 7. Unsmoothed hippocampi for RSFC and SC modality. Fragmented clustering still indicates the already known pattern from smoothed data, with RSFC showing an anterior-posterior differentiation and SC a cytoarchitectonic-like pattern. Lower row shows green transparent clusters in order to illustrate the underlying organization.

References

Adler DH, Pluta J, Kadivar S, Craige C, Gee JC, Avants BB, Yushkevich PA. 2014. Histology-derived volumetric annotation of the human hippocampal subfields in postmortem mri. NeuroImage. 84:505-523.

Adler DH, Wisse LEM, Ittyerah R, Pluta JB, Ding SL, Xie L, Wang J, Kadivar S, Robinson JL, Schuck T et al. 2018. Characterizing the human hippocampus in aging and alzheimer's disease using a computational atlas derived from ex vivo mri and histology. Proceedings of the National Academy of Sciences of the United States of America. 115(16):4252-4257.

Adnan A, Barnett A, Moayedi M, McCormick C, Cohn M, McAndrews MP. 2016. Distinct hippocampal functional networks revealed by tractography-based parcellation. Brain structure & function. 221(6):2999-3012.

Alexander-Bloch A, Raznahan A, Bullmore E, Giedd J. 2013. The convergence of maturational change and structural covariance in human cortical networks. The Journal of neuroscience : the official journal of the Society for Neuroscience. 33(7):2889-2899.

Amunts K, Kedo O, Kindler M, Pieperhoff P, Mohlberg H, Shah NJ, Habel U, Schneider F, Zilles K. 2005. Cytoarchitectonic mapping of the human amygdala, hippocampal region and entorhinal cortex: Intersubject variability and probability maps. Anatomy and embryology. 210(5-6):343-352.

Anderson JS, Druzgal TJ, Lopez-Larson M, Jeong EK, Desai K, Yurgelun-Todd D. 2011. Network anticorrelations, global regression, and phase-shifted soft tissue correction. Human brain mapping. 32(6):919-934.

Arslan S, Ktena SI, Makropoulos A, Robinson EC, Rueckert D, Parisot S. 2018. Human brain mapping: A systematic comparison of parcellation methods for the human cerebral cortex. NeuroImage. 170:5-30.

Ashburner J, Friston KJ. 2005. Unified segmentation. NeuroImage. 26(3):839-851.

Bakker A, Kirwan CB, Miller M, Stark CE. 2008. Pattern separation in the human hippocampal ca3 and dentate gyrus. Science (New York, NY). 319(5870):1640-1642.

Beckmann CF, Smith SM. 2004. Probabilistic independent component analysis for functional magnetic resonance imaging. IEEE transactions on medical imaging. 23(2):137-152.

Behrens TE, Johansen-Berg H, Woolrich MW, Smith SM, Wheeler-Kingshott CA, Boulby PA, Barker GJ, Sillery EL, Sheehan K, Ciccarelli O et al. 2003. Non-invasive mapping of connections between human thalamus and cortex using diffusion imaging. Nature neuroscience. 6(7):750-757.

Bellec P, Rosa-Neto P, Lyttelton OC, Benali H, Evans AC. 2010. Multi-level bootstrap analysis of stable clusters in resting-state fmri. NeuroImage. 51(3):1126-1139.

Bianciardi M, Fukunaga M, van Gelderen P, Horovitz SG, de Zwart JA, Shmueli K, Duyn JH. 2009. Sources of functional magnetic resonance imaging signal fluctuations in the human brain at rest: A 7 t study. Magnetic resonance imaging. 27(8):1019-1029.

Birn RM, Diamond JB, Smith MA, Bandettini PA. 2006. Separating respiratory-variation-related fluctuations from neuronal-activity-related fluctuations in fmri. NeuroImage. 31(4):1536-1548.

Biswal B, Yetkin FZ, Haughton VM, Hyde JS. 1995. Functional connectivity in the motor cortex of resting human brain using echo-planar mri. Magnetic resonance in medicine. 34(4):537-541.

Buckner RL, Krienen FM, Yeo BT. 2013. Opportunities and limitations of intrinsic functional connectivity mri. Nature neuroscience. 16(7):832-837.

Burgess GC, Kandala S, Nolan D, Laumann TO, Power JD, Adeyemo B, Harms MP, Petersen SE, Barch DM. 2016. Evaluation of denoising strategies to address motion-correlated artifacts in resting-state functional magnetic resonance imaging data from the human connectome project. Brain connectivity. 6(9):669-680.

Caballero-Gaudes C, Reynolds RC. 2017. Methods for cleaning the bold fmri signal. NeuroImage. 154:128-149.

Chang C, Huang C, Zhou N, Li SX, Ver Hoef L, Gao Y. 2018. The bumps under the hippocampus. Human brain mapping. 39(1):472-490.

Chase HW, Clos M, Dibble S, Fox P, Grace AA, Phillips ML, Eickhoff SB. 2015. Evidence for an anterior-posterior differentiation in the human hippocampal formation revealed by meta-analytic parcellation of fmri coordinate maps: Focus on the subiculum. NeuroImage. 113:44-60.

Clos M, Amunts K, Laird AR, Fox PT, Eickhoff SB. 2013. Tackling the multifunctional nature of broca's region meta-analytically: Co-activation-based parcellation of area 44. NeuroImage. 83:174-188.

Clos M, Rottschy C, Laird AR, Fox PT, Eickhoff SB. 2014. Comparison of structural covariance with functional connectivity approaches exemplified by an investigation of the left anterior insula. NeuroImage. 99:269-280.

Cole DM, Smith SM, Beckmann CF. 2010. Advances and pitfalls in the analysis and interpretation of resting-state fmri data. Frontiers in systems neuroscience. 4:8.

Colombo M, Fernandez T, Nakamura K, Gross CG. 1998. Functional differentiation along the anterior-posterior axis of the hippocampus in monkeys. J Neurophysiol. 80(2):1002-1005.

Dagli MS, Ingeholm JE, Haxby JV. 1999. Localization of cardiac-induced signal change in fmri. NeuroImage. 9(4):407-415.
de Flores R, La Joie R, Chetelat G. 2015. Structural imaging of hippocampal subfields in healthy aging and alzheimer's disease. Neuroscience. 309:29-50.
de Hoz L, Knox J, Morris RG. 2003. Longitudinal axis of the hippocampus: Both septal and temporal poles of the hippocampus support water maze spatial learning depending on the training protocol. Hippocampus. 13(5):587-603.
de Munck JC, Goncalves SI, Faes TJ, Kuijer JP, Pouwels PJ, Heethaar RM, Lopes da Silva FH. 2008. A study of the brain's resting state based on alpha band power, heart rate and fmri. NeuroImage. 42(1):112-121.
DeKraker J, Ferko KM, Lau JC, Kohler S, Khan AR. 2018. Unfolding the hippocampus: An intrinsic coordinate system for subfield segmentations and quantitative mapping. NeuroImage. 167:408-418.
Desikan RS, Segonne F, Fischl B, Quinn BT, Dickerson BC, Blacker D, Buckner RL, Dale AM, Maguire RP, Hyman BT et al. 2006. An automated labeling system for subdividing the human cerebral cortex on mri scans into gyral based regions of interest. NeuroImage. 31(3):968-980.
Desjardins AE, Kiehl KA, Liddle PF. 2001. Removal of confounding effects of global signal in functional mri analyses. NeuroImage. 13(4):751-758.
Deuker L, Doeller CF, Fell J, Axmacher N. 2014. Human neuroimaging studies on the hippocampal ca3 region - integrating evidence for pattern separation and completion. Frontiers in cellular neuroscience. 8:64.
Dimsdale-Zucker HR, Ritchey M, Ekstrom AD, Yonelinas AP, Ranganath C. 2018. Ca1 and ca3 differentially support spontaneous retrieval of episodic contexts within human hippocampal subfields. Nature communications. 9(1):294.
Ding SL, Van Hoesen GW. 2015. Organization and detailed parcellation of human hippocampal head and body regions based on a combined analysis of cyto- and chemoarchitecture. The Journal of comparative neurology. 523(15):2233-2253.
Dong HW, Swanson LW, Chen L, Fanselow MS, Toga AW. 2009. Genomic-anatomic evidence for distinct functional domains in hippocampal field ca1. Proceedings of the National Academy of Sciences of the United States of America. 106(28):11794-11799.
Efron B. 1979. Bootstrap methods: Another look at the jackknife. Ann Statist. 7(1):1-26.
Eickhoff SB, Bzdok D, Laird AR, Kurth F, Fox PT. 2012. Activation likelihood estimation meta-analysis revisited. NeuroImage. 59(3):2349-2361.
Eickhoff SB, Stephan KE, Mohlberg H, Grefkes C, Fink GR, Amunts K, Zilles K. 2005. A new spm toolbox for combining probabilistic cytoarchitectonic maps and functional imaging data. NeuroImage. 25(4):1325-1335.
Eickhoff SB, Thirion B, Varoquaux G, Bzdok D. 2015. Connectivity-based parcellation: Critique and implications. Human brain mapping. 36(12):4771-4792.
Eickhoff SB, Yeo, T., Genon, S. in press. Imaging-based parcellations of the human brain. Nature Review Neuroscience.
Evans AC. 2013. Networks of anatomical covariance. NeuroImage. 80:489-504.
Fanselow MS, Dong HW. 2010. Are the dorsal and ventral hippocampus functionally distinct structures? Neuron. 65(1):7-19.
Genon S, Li H, Fan L, Muller VI, Cieslik EC, Hoffstaedter F, Reid AT, Langner R, Grefkes C, Fox PT et al. 2017. The right dorsal premotor mosaic: Organization, functions, and connectivity. Cerebral cortex (New York, NY : 1991). 27(3):2095-2110.
Genon S, Reid A, Langner R, Amunts K, Eickhoff SB. 2018a. How to characterize the function of a brain region. Trends in cognitive sciences.

Genon S, Reid A, Langner R, Amunts K, Eickhoff SB. 2018b. How to characterize the function of a brain region. Trends in cognitive sciences. 22(4):350-364.
Genon S, Reid A, Li H, Fan L, Muller VI, Cieslik EC, Hoffstaedter F, Langner R, Grefkes C, Laird AR et al. 2018c. The heterogeneity of the left dorsal premotor cortex evidenced by multimodal connectivity-based parcellation and functional characterization. NeuroImage. 170:400-411.
Glasser MF, Coalson TS, Robinson EC, Hacker CD, Harwell J, Yacoub E, Ugurbil K, Andersson J, Beckmann CF, Jenkinson M et al. 2016. A multi-modal parcellation of human cerebral cortex. Nature. 536(7615):171-178.
Griffanti L, Salimi-Khorshidi G, Beckmann CF, Auerbach EJ, Douaud G, Sexton CE, Zsoldos E, Ebmeier KP, Filippini N, Mackay CE et al. 2014. Ica-based artefact removal and accelerated fmri acquisition for improved resting state network imaging. NeuroImage. 95:232-247.
Guzowski JF, Knierim JJ, Moser EI. 2004. Ensemble dynamics of hippocampal regions ca3 and ca1. Neuron. 44(4):581-584.
Hallquist MN, Hwang K, Luna B. 2013. The nuisance of nuisance regression: Spectral misspecification in a common approach to resting-state fmri preprocessing reintroduces noise and obscures functional connectivity. NeuroImage. 82:208-225.
Hutchison RM, Womelsdorf T, Gati JS, Everling S, Menon RS. 2013. Resting-state networks show dynamic functional connectivity in awake humans and anesthetized macaques. Human brain mapping. 34(9):2154-2177.
Jo HJ, Gotts SJ, Reynolds RC, Bandettini PA, Martin A, Cox RW, Saad ZS. 2013. Effective preprocessing procedures virtually eliminate distance-dependent motion artifacts in resting state fmri. Journal of applied mathematics. 2013.
Jo HJ, Saad ZS, Simmons WK, Milbury LA, Cox RW. 2010. Mapping sources of correlation in resting state fmri, with artifact detection and removal. NeuroImage. 52(2):571-582.
Johansen-Berg H, Behrens TE, Robson MD, Drobnjak I, Rushworth MF, Brady JM, Smith SM, Higham DJ, Matthews PM. 2004. Changes in connectivity profiles define functionally distinct regions in human medial frontal cortex. Proceedings of the National Academy of Sciences of the United States of America. 101(36):13335-13340.
Jung M, Wiener S, McNaughton B. 1994. Comparison of spatial firing characteristics of units in dorsal and ventral hippocampus of the rat. The Journal of Neuroscience. 14(12):7347-7356.
Kelly C, Toro R, Di Martino A, Cox CL, Bellec P, Castellanos FX, Milham MP. 2012. A convergent functional architecture of the insula emerges across imaging modalities. NeuroImage. 61(4):1129-1142.
Kim H. 2015. Encoding and retrieval along the long axis of the hippocampus and their relationships with dorsal attention and default mode networks: The hernet model. Hippocampus. 25(4):500-510.
Koster R, Chadwick MJ, Chen Y, Berron D, Banino A, Duzel E, Hassabis D, Kumaran D. 2018. Big-loop recurrence within the hippocampal system supports integration of information across episodes. Neuron. 99(6):1342-1354.e1346.
Kotkowski E, Price LR, Mickle Fox P, Vanasse TJ, Fox PT. 2018. The hippocampal network model: A transdiagnostic metaconnectomic approach. NeuroImage Clinical. 18:115-129.
LaConte S, Anderson J, Muley S, Ashe J, Frutiger S, Rehm K, Hansen LK, Yacoub E, Hu X, Rottenberg D et al. 2003. The evaluation of preprocessing choices in single-subject bold fmri using npairs performance metrics. NeuroImage. 18(1):10-27.

Laird AR, Eickhoff SB, Fox PM, Uecker AM, Ray KL, Saenz JJ, Jr., McKay DR, Bzdok D, Laird RW, Robinson JL et al. 2011. The brainmap strategy for standardization, sharing, and meta-analysis of neuroimaging data. BMC research notes. 4:349.

Lambert C, Simon H, Colman J, Barrick TR. 2017. Defining thalamic nuclei and topographic connectivity gradients in vivo. NeuroImage. 158:466-479.

Lepage M, Habib R, Tulving E. 1998. Hippocampal pet activations of memory encoding and retrieval: The hiper model. Hippocampus. 8(4):313-322.

Liu TT. 2016. Noise contributions to the fmri signal: An overview. NeuroImage. 143:141-151.

Macey PM, Macey KE, Kumar R, Harper RM. 2004. A method for removal of global effects from fmri time series. NeuroImage. 22(1):360-366.

Mechelli A, Friston KJ, Frackowiak RS, Price CJ. 2005. Structural covariance in the human cortex. The Journal of neuroscience : the official journal of the Society for Neuroscience. 25(36):8303-8310.

Meilă M. 2007. Comparing clusterings—an information based distance. Journal of Multivariate Analysis. 98(5):873-895.

Morris RG, Hagan JJ, Rawlins JN. 1986. Allocentric spatial learning by hippocampectomised rats: A further test of the "spatial mapping" and "working memory" theories of hippocampal function. The Quarterly journal of experimental psychology B, Comparative and physiological psychology. 38(4):365-395.

Moser E, Moser MB, Andersen P. 1993. Spatial learning impairment parallels the magnitude of dorsal hippocampal lesions, but is hardly present following ventral lesions. The Journal of neuroscience : the official journal of the Society for Neuroscience. 13(9):3916-3925.

Moser MB, Moser EI. 1998. Functional differentiation in the hippocampus. Hippocampus. 8(6):608-619.

Mueller S, Wang D, Fox MD, Yeo BT, Sepulcre J, Sabuncu MR, Shafee R, Lu J, Liu H. 2013. Individual variability in functional connectivity architecture of the human brain. Neuron. 77(3):586-595.

Murphy K, Birn RM, Handwerker DA, Jones TB, Bandettini PA. 2009. The impact of global signal regression on resting state correlations: Are anti-correlated networks introduced? NeuroImage. 44(3):893-905.

Nanetti L, Cerliani L, Gazzola V, Renken R, Keysers C. 2009. Group analyses of connectivity-based cortical parcellation using repeated k-means clustering. NeuroImage. 47(4):1666-1677.

Ojemann JG, Akbudak E, Snyder AZ, McKinstry RC, Raichle ME, Conturo TE. 1997. Anatomic localization and quantitative analysis of gradient refocused echo-planar fmri susceptibility artifacts. NeuroImage. 6(3):156-167.

Oppenheim C, Dormont D, Biondi A, Lehericy S, Hasboun D, Clemenceau S, Baulac M, Marsault C. 1998. Loss of digitations of the hippocampal head on high-resolution fast spin-echo mr: A sign of mesial temporal sclerosis. AJNR American journal of neuroradiology. 19(3):457-463.

Petrovich GD, Canteras NS, Swanson LW. 2001. Combinatorial amygdalar inputs to hippocampal domains and hypothalamic behavior systems. Brain research Brain research reviews. 38(1-2):247-289.

Poppenk J, Evensmoen HR, Moscovitch M, Nadel L. 2013. Long-axis specialization of the human hippocampus. Trends in cognitive sciences. 17(5):230-240.

Power JD, Barnes KA, Snyder AZ, Schlaggar BL, Petersen SE. 2012. Spurious but systematic correlations in functional connectivity mri networks arise from subject motion. NeuroImage. 59(3):2142-2154.

Power JD, Mitra A, Laumann TO, Snyder AZ, Schlaggar BL, Petersen SE. 2014. Methods to detect, characterize, and remove motion artifact in resting state fmri. NeuroImage. 84:320-341.
Power JD, Schlaggar BL, Petersen SE. 2015. Recent progress and outstanding issues in motion correction in resting state fmri. NeuroImage. 105:536-551.
Prince SE, Daselaar SM, Cabeza R. 2005. Neural correlates of relational memory: Successful encoding and retrieval of semantic and perceptual associations. The Journal of neuroscience : the official journal of the Society for Neuroscience. 25(5):1203-1210.
Reid AT, Bzdok D, Langner R, Fox PT, Laird AR, Amunts K, Eickhoff SB, Eickhoff CR. 2016. Multimodal connectivity mapping of the human left anterior and posterior lateral prefrontal cortex. Brain structure & function. 221(5):2589-2605.
Risold PY, Swanson LW. 1996. Structural evidence for functional domains in the rat hippocampus. Science (New York, NY). 272(5267):1484-1486.
Robinson JL, Barron DS, Kirby LA, Bottenhorn KL, Hill AC, Murphy JE, Katz JS, Salibi N, Eickhoff SB, Fox PT. 2015. Neurofunctional topography of the human hippocampus. Human brain mapping. 36(12):5018-5037.
Robinson JL, Salibi N, Deshpande G. 2016. Functional connectivity of the left and right hippocampi: Evidence for functional lateralization along the long-axis using meta-analytic approaches and ultra-high field functional neuroimaging. NeuroImage. 135:64-78.
Salimi-Khorshidi G, Douaud G, Beckmann CF, Glasser MF, Griffanti L, Smith SM. 2014. Automatic denoising of functional mri data: Combining independent component analysis and hierarchical fusion of classifiers. NeuroImage. 90:449-468.
Satterthwaite TD, Ciric R, Roalf DR, Davatzikos C, Bassett DS, Wolf DH. 2017. Motion artifact in studies of functional connectivity: Characteristics and mitigation strategies. Human brain mapping.
Satterthwaite TD, Elliott MA, Gerraty RT, Ruparel K, Loughead J, Calkins ME, Eickhoff SB, Hakonarson H, Gur RC, Gur RE et al. 2013. An improved framework for confound regression and filtering for control of motion artifact in the preprocessing of resting-state functional connectivity data. NeuroImage. 64:240-256.
Schaefer A, Kong R, Gordon EM, Laumann TO, Zuo XN, Holmes AJ, Eickhoff SB, Yeo BTT. 2017. Local-global parcellation of the human cerebral cortex from intrinsic functional connectivity mri. Cerebral cortex (New York, NY : 1991).1-20.
Seeley WW, Crawford RK, Zhou J, Miller BL, Greicius MD. 2009. Neurodegenerative diseases target large-scale human brain networks. Neuron. 62(1):42-52.
Small SA, Nava AS, Perera GM, DeLaPaz R, Mayeux R, Stern Y. 2001. Circuit mechanisms underlying memory encoding and retrieval in the long axis of the hippocampal formation. Nature neuroscience. 4(4):442-449.
Smith SM, Beckmann CF, Andersson J, Auerbach EJ, Bijsterbosch J, Douaud G, Duff E, Feinberg DA, Griffanti L, Harms MP et al. 2013. Resting-state fmri in the human connectome project. NeuroImage. 80:144-168.
Strange BA, Fletcher PC, Henson RN, Friston KJ, Dolan RJ. 1999. Segregating the functions of human hippocampus. Proceedings of the National Academy of Sciences of the United States of America. 96(7):4034-4039.
Strange BA, Witter MP, Lein ES, Moser EI. 2014. Functional organization of the hippocampal longitudinal axis. Nature reviews Neuroscience. 15(10):655-669.
Strother SC, Anderson J, Hansen LK, Kjems U, Kustra R, Sidtis J, Frutiger S, Muley S, LaConte S, Rottenberg D. 2002. The quantitative evaluation of functional neuroimaging experiments: The npairs data analysis framework. NeuroImage. 15(4):747-771.

Swanson LW, Cowan WM. 1977. An autoradiographic study of the organization of the efferent connections of the hippocampal formation in the rat. The Journal of comparative neurology. 172(1):49-84.
Treit S, Steve T, Gross DW, Beaulieu C. 2018. High resolution in-vivo diffusion imaging of the human hippocampus. NeuroImage. 182:479-487.
Ugurbil K, Xu J, Auerbach EJ, Moeller S, Vu AT, Duarte-Carvajalino JM, Lenglet C, Wu X, Schmitter S, Van de Moortele PF et al. 2013. Pushing spatial and temporal resolution for functional and diffusion mri in the human connectome project. NeuroImage. 80:80-104.
Van Dijk KR, Hedden T, Venkataraman A, Evans KC, Lazar SW, Buckner RL. 2010. Intrinsic functional connectivity as a tool for human connectomics: Theory, properties, and optimization. J Neurophysiol. 103(1):297-321.
Van Dijk KR, Sabuncu MR, Buckner RL. 2012. The influence of head motion on intrinsic functional connectivity mri. NeuroImage. 59(1):431-438.
Van Essen DC, Ugurbil K. 2012. The future of the human connectome. NeuroImage. 62(2):1299-1310.
Vann SD, Brown MW, Erichsen JT, Aggleton JP. 2000. Fos imaging reveals differential patterns of hippocampal and parahippocampal subfield activation in rats in response to different spatial memory tests. The Journal of neuroscience : the official journal of the Society for Neuroscience. 20(7):2711-2718.
Varikuti DP, Genon S, Sotiras A, Schwender H, Hoffstaedter F, Patil KR, Jockwitz C, Caspers S, Moebus S, Amunts K et al. 2018. Evaluation of non-negative matrix factorization of grey matter in age prediction. NeuroImage. 173:394-410.
Varikuti DP, Hoffstaedter F, Genon S, Schwender H, Reid AT, Eickhoff SB. 2017. Resting-state test-retest reliability of a priori defined canonical networks over different preprocessing steps. Brain structure & function. 222(3):1447-1468.
Weissenbacher A, Kasess C, Gerstl F, Lanzenberger R, Moser E, Windischberger C. 2009. Correlations and anticorrelations in resting-state functional connectivity mri: A quantitative comparison of preprocessing strategies. NeuroImage. 47(4):1408-1416.
Windischberger C, Langenberger H, Sycha T, Tschernko EM, Fuchsjager-Mayerl G, Schmetterer L, Moser E. 2002. On the origin of respiratory artifacts in bold-epi of the human brain. Magnetic resonance imaging. 20(8):575-582.
Wise RG, Ide K, Poulin MJ, Tracey I. 2004. Resting fluctuations in arterial carbon dioxide induce significant low frequency variations in bold signal. NeuroImage. 21(4):1652-1664.
Wisse LE, Gerritsen L, Zwanenburg JJ, Kuijf HJ, Luijten PR, Biessels GJ, Geerlings MI. 2012. Subfields of the hippocampal formation at 7 t mri: In vivo volumetric assessment. NeuroImage. 61(4):1043-1049.
Yan CG, Cheung B, Kelly C, Colcombe S, Craddock RC, Di Martino A, Li Q, Zuo XN, Castellanos FX, Milham MP. 2013. A comprehensive assessment of regional variation in the impact of head micromovements on functional connectomics. NeuroImage. 76:183-201.
Yarkoni T, Poldrack RA, Nichols TE, Van Essen DC, Wager TD. 2011. Large-scale automated synthesis of human functional neuroimaging data. Nature methods. 8(8):665-670.
Yee Y, Fernandes DJ, French L, Ellegood J, Cahill LS, Vousden DA, Spencer Noakes L, Scholz J, van Eede MC, Nieman BJ et al. 2017. Structural covariance of brain region volumes is associated with both structural connectivity and transcriptomic similarity. bioRxiv.
Zeidman P, Maguire EA. 2016. Anterior hippocampus: The anatomy of perception, imagination and episodic memory. Nature reviews Neuroscience. 17(3):173-182.

Zhang X, Mormino EC, Sun N, Sperling RA, Sabuncu MR, Yeo BT. 2016. Bayesian model reveals latent atrophy factors with dissociable cognitive trajectories in alzheimer's disease. Proceedings of the National Academy of Sciences of the United States of America. 113(42):E6535-e6544.

3 Study 2: Hippocampus' co-atrophy pattern in dementia deviates from covariance patterns across the lifespan

Running title: **Hippocampus' co-plasticity and co-atrophy**

Anna Plachti[1,2], Shahrzad Kharabian[1,2], Simon B. Eickhoff[1,2], Somayeh Maleki Balajoo[2], Felix Hoffstaedter[2], Deepthi P. Varikuti[2], Christiane Jockwitz[2,4], Svenja Caspers[2,5,6], Katrin Amunts[2,3,5] and Sarah Genon[2,7].

[1]Institute of Systems Neuroscience, Heinrich Heine University Düsseldorf, Düsseldorf 40225, Germany,
[2]Institute of Neuroscience and Medicine (INM-1, INM-7), Research Centre Jülich, Jülich, Germany,
[3]C. & O. Vogt Institute for Brain Research, Heinrich Heine University, Düsseldorf. Germany,
[4]Department of Psychiatry, Psychotherapy and Psychosomatics, Medical Faculty, RWTH Aachen University, Aachen, Germany,
[5]JARA-BRAIN, Jülich-Aachen Research Alliance, Jülich, Germany,
[6]Institute for Anatomy I, Medical Faculty, Heinrich Heine University, Düsseldorf, Germany,
[7]GIGA-CRC In vivo Imaging, University of Liege, Liege, Belgium

Correspondence to: Anna Plachti

Institute of Neuroscience and Medicine (INM-7, Brain & Behavior), Research Centre Jülich,

Wilhelm-Johnen-Straße, 52425 Jülich, Germany

Email: a.plachti@fz-juelich.de

Brain (2020)
Doi: 10.1093/brain/awaa222
Impact Factor (2019): 11.3

Own contributions	Conception and design of study
	Reviewing and adapting analysis code
	Statistical data analysis
	Interpretation of results
	Preparing figures
	Writing paper
	Total contribution 80

Abstract

The hippocampus is a plastic region and highly susceptible to aging and dementia. Previous studies explicitly imposed *apriori* models of hippocampus when investigating aging and dementia specific atrophy but led to inconsistent results. Consequently, the basic question of whether macro-structural changes follow a cytoarchitectonic or functional organization across the adult lifespan and in age-related neurodegenerative disease remained open. The aim of this cross-sectional study was to identify the spatial pattern of hippocampus differentiation based on structural covariance with a data-driven approach across structural magnetic resonance imaging data of large cohorts (n=2594). We examined the pattern of structural covariance of hippocampus' voxels in young, middle-aged, elderly, mild cognitive impairment and dementia disease samples by applying a clustering algorithm revealing differentiation in SC within the hippocampus. In all the healthy and in the mild cognitive impaired participants, the hippocampus was robustly divided into anterior, lateral and medial subregions reminiscent of cytoarchitectonic division. In contrast, in dementia patients, the pattern of subdivision was closer to known functional differentiation into an anterior, body and tail subregions. These results not only contribute to a better understanding of co-plasticity and co-atrophy in the hippocampus across the lifespan and in dementia, but also provide robust data-driven spatial representations (i.e. maps) for structural studies.

Keywords: dementia, temporal lobe, structural covariance, parcellation, elderly

Abbreviations: 1000BRAINS = MRI dataset from Forschungszentrum Juelich, AD = Alzheimer's disease, ADNI= Alzheimer's Disease Neuroimaging Initiative dataset, aRI = adjusted Rand Index, CA1= Cornu Ammonis subfield 1, CA2= Cornu Ammonis subfield 2, CA3= Cornu Ammonis subfield 3, CA4= Cornu Ammonis subfield 4, CamCAN = Cambridge Centre for Ageing and Neuroscience dataset, CAT12= Computational anatomy toolbox, CDR= Clinical dementia rating, eNKI= Enhanced Nathan Kline Institute-Rockland Sample, FWE = family wise error, HCP= Human Connectome Project dataset, IQR=interquartile range, MCI= mild cognitive impairment, OASIS3= Open Access Series of Imaging Studies dataset, SC = structural covariance, SPM= statistical parametric mapping

Introduction

The hippocampus is a notable brain region from its lifelong plasticity potential (Moreno-Jiménez et al., 2019), which can be observed with microstructural and molecular investigations but also at the macro-structural level using morphologic measurements of structural MRI. From macro-structural studies, the plasticity of the hippocampus seems to relate to experience and more particularly to cognitive training (Boyke, Driemeyer, Gaser, Buchel, & May, 2008; Maguire et al., 2006). Relatedly morphological measurements of the hippocampus across individuals suggest an important inter-individual variability (Fleming Beattie et al., 2017; Llera, Wolfers, Mulders, & Beckmann, 2019; Van Petten, 2004).

Since aging and Alzheimer's disease atrophy patterns resemble each other, in particular, showing important atrophy in temporal lobes, several authors suggested that dementia simply represents a more severe or accelerated aging process (Fjell et al., 2014). It has been frequently pointed out that clinically normal individuals demonstrate an accumulation of amyloid-beta and tau pathologies in the hippocampus and entorhinal cortex suggesting that neurobiological features associated with Alzheimer's disease can also be found in apparently healthy elderly populations (Sperling et al., 2019; Ziontz et al., 2019). Thus the neurobiological relationship between healthy aging and dementia and in particular the hypothesis of dementia as a form of increased aging process remains controversial and poorly understood.

Most researches have focused on hippocampal atrophy assessed at the macro-structural level and as representing the most straightforward non-invasive estimates of age-related structural changes. In other words, a large amount of investigations have aimed to identify specific pattern of atrophy across hippocampus' organization. Two different models of hippocampus' organization were referred to: the subfield model (based on cytoarchitecture features) and the tripartite model differentiating regions along the longitudinal axis such as the head-body and tail (based on functional and large-scale connectivity features). Since subfields and subregions are suggested to be characterized by different neurobiological features, they are likely to be differently affected by ageing and pathological processes. Despite several studies have investigated this question, no convergence towards individual subfields and subregions as being specifically affected by atrophy has emerged from these studies hindering our understanding of the underlying mechanisms.

In sum, our fundamental understanding of structural changes in the human hippocampus across the adult lifespan and in dementia remain fairly limited, but several issues should be pointed out to account for the current state of art. First, as described above, most studies were based on an a-priori model of hippocampus organization while it is unclear which model is the most appropriate. On the one hand, one could expect macro-structural changes to be constrained by the topology defined by cytoarchitecture, but on the other hand, as plasticity has been related to behavioral function, one could expect macro-structural changes to follow the functional organization of the human hippocampus along the longitudinal axis. Second, partly related to the first conundrum, the question of whether the pattern of structural changes in aging and dementia follow a similar topological pattern remains as a completely open question.

In this study, we have probed morphological changes across large datasets of structural MRI in healthy subjects and dementia patients applying a data-driven approach to reveal latent patterns of differentiation in the hippocampus. Using the pattern of covariance with other brain regions across individuals to guide the clustering, importantly, allows the integration of interrelationships between the hippocampus and the whole brain hence revealing a more systemic pattern of change.

To implement the aforementioned objectives practically, we used a parcellation approach applied on hippocampus' structural co-variance in five different age and disease groups: young, middle-aged, elderly adults, mild cognitive impairment patients (MCI) and patients with dementia coming from independent datasets. We use the term "co-variance" to refer to healthy life-span changes in structural co-variation, which are assumed to be driven mainly by co-plasticity (e.g. regions developing together) and partly by co-atrophy, especially in older adults (e.g. regions degenerating together). In contrast, in dementia, we expect co-variation to be primarily driven by co-degeneration of brain regions. Accordingly, we use the term "co-atrophy" in the context of dementia patients (even though technically, the same "structural covariance" measure was applied across age and disease groups.

In this framework, a data-driven approach of structural covariance offers a bottom-up examination of the topological patterns of co-plasticity/co-variation in the first adult life periods and co-atrophy in elderly and dementia. Importantly, we examined the stability of the pattern across datasets by using split-half cross validation and robustness across groups with bootstrapping approaches. We explored the possible mechanisms explaining these patterns by examining the similarity of these topological patterns with the pattern of functional organization of the hippocampus, and investigated the structural networks that underlie the

different hippocampus subregions. Finally, we characterized these structural networks with regards to behavioral functions and compared these structural networks with functional networks.

Materials and methods

Datasets, cohort samples and age-phenotypical groups

We included six different datasets: Human Connectome Project (HCP) (http://www.humanconnectome.org), Enhanced Nathan Kline Institute-Rockland Sample (eNKI) (http://fcon_1000.projects.nitrc.org/indi/enhanced/), Cambridge Centre for Ageing and Neuroscience (CamCAN) (https://www.cam-can.org/) (Shafto et al., 2014; Taylor et al., 2017), 1000BRAINS from Forschungszentrum Juelich (https://www.frontiersin.org/articles/10.3389/fnagi.2014.00149/full), Alzheimer's Disease Neuroimaging Initiative (ADNI) (http://adni.loni.usc.edu/) and Open Access Series of Imaging Studies (OASIS3) (https://www.oasis-brains.org/). From these datasets, we formed five cohort samples: young, middle-aged, elderly, MCI and dementia participants. The age range of the group of young adults was set to 20-35 years. In turn, the age range of the middle-aged group was 35-55 years and for the elderly, we set a conservative age range of 60-80 years. MCI and AD patients were selected within the same age range as the elderly group. For the dementia group we included patients with probable Alzheimer's type pathology by selecting Alzheimer's disease patients from the OASIS3 dataset and ADNI dataset, as well as the late cognitive impaired individuals from the ADNI dataset who are considered as patients at the early stage of Alzheimer's disease (Qiu, Li, Zhou, & Lu, 2014). The MCI group was formed by the participants with the diagnosis 'early MCI' (ADNI dataset) and by participants with a CDR score of 0.5 from the OASIS3 dataset. The demographic data of each study samples and groups are reported in Table 1 and Tab 2 below. The analyses of these data were approved by the ethical committee of the Heinrich Heine University Düsseldorf.

Table 1. Demographic data of all collected samples

Samples	Sample size (n)	Mean age (SD; age range)	% females	Education	CDR	MMSE
Young_HCP	n= 304	27.8 (SD=3.55;	50.6%	SSAGA_Educ: 14.8 (SD= 1.75;	/	29.0 (SD =1.07; 23-

		22-34)		11-17); NAs: 0		30); NAs: 0
Young_eNKI	n= 140	24.8 (SD=3.85; 20-34)	50%	SES-Adult Education code, 5.4 SD=0.8; 4-7; 14.8 (SD = 1.6; 11-18); NAs: 0	/	/
MiddleAged_eNKI	n= 72	43.6 (SD=5.7; 35-54)	52.7%	SES-Adult Education code, 5.5 (SD=1; 3-7); 15.1 (SD=2.3; 10-21); missing n=2	/	/
Old_eNKI	n= 76	68.3 (SD=5.5; 60-79)	51.3%	SES-Adult Education code, 6.0 (SD=1.0 4-7); 16.1 (SD=2.4; 12-24); NAs: 0	/	/
Young_ CamCAN	n= 94	28.4 (SD=3.97; 20-34)	50%	Education scoring: 6.2 (SD=1.7; 2-8); missing n=21	/	29.4 (SD=1.17, 25-30); NAs: 0
MiddleAged_CamCAN	n =207	44.3 (SD=5.78; 35-54)	50.7%	5.7 (SD=1.8, 1-8); missing n=35	/	29.1 (SD=1.17, 26-30); NAs: 0
Old_CamCAN	n = 213	69.8 (SD=5.96; 60-79)	50.2%	5.0 (SD=2.2, 1-8); missing n=65	/	28.4 (SD=1.47, 25-30); missing n=1
Old_1000BRAINS	n = 492	66.9 (SD=4.24; 60-75)	50%	Education years: 13.7 (SD= 3.7, 3-27); missing n=1	/	/ Demtec: 15.2 (SD=2.3, 8-18); missing n=9
Old_ADNI	n = 139	71.6 (SD=4.65; 61-79)	51.7%	Education years: 16.6 (SD=2.6, 12-20); NAs: 0	CDR sum of boxes: 0.02, SD= 0.11, 0-0.5; NAs: 0	28.9 (SD=1.24, 24-30); NAs: 0
MCI_ADNI	n = 213	69.2 (SD=5.05;	50.2%	Education years: 15.9 (SD=2.6, 10-	CDR sum of boxes:	28.4 (SD=1.5,

		60-79)		20); NAs: 0	1.22, SD=0.76, 0.5-4; NAs: 0	23-30); NAs: 0
AD_ADNI	n = 219	71.0 (SD=5.42; 60-79)	51.1%	Education years: 16.1 (SD= 2.6, 11-20); NAs: 0	CDR sum of boxes: 2.9, SD= 1.8, 0.5-10; NAs: 0	25.8 (SD= 3.0, 19-30); NAs: 0
Old_OASIS3	n = 298	70.3 (SD=4.42; 60-79)	50%	Education years: 16.0 (SD=2.7, 8-24); NAs: 0	0, SD = 0, 0-0; NAs: 0	28.8 (SD=1.8, 9-30); missing n =2
MCI_OASIS3	n = 74	70.9 (SD=4.58; 61-79)	50%	Education years: 15.3 (SD=2.7, 8-20); NAs: 0	0.5, SD=0, 0.5-0.5; NAs: 0	26.7 (SD=3.4, 13-30); missing n=2
AD_OASIS3	n = 53	69.9 (SD=5.58; 60-79)	47.2%	Education years: 15.1 (SD=2.8, 11-20); NAs: 0	0.92, SD=0.57, 0-2; NAs: 0	23.5 (SD=4.8, 10-30); missing n=1

Table 2. Demographic data of the age and disease groups created from independent samples

Phenotypical group	Size (n)	Mean age (SD; age range)	% females
Young	n = 538	27.1 (SD = 3.95; 20-34)	50.5
Middle age	n= 279	44.0 (SD=5.77; 35-54)	51.0%
Elderly	n= 1218	68.9 (SD=5.07; 60-79)	50.2%
MCI	n= 287	69.7 (SD=4.98; 60-79)	50.2%
AD	n= 272	70.7 (SD = 5.46; 60-79)	50.4%

Structural MRI acquisition, preprocessing and structural covariance computation

Only 3T MRI anatomical scans were included in this study acquired with different scanning parameters (Tab. 3). All images were preprocessed with SPM12 and the CAT12 toolbox, running on Matlab R2016a. The normalization was performed with the DARTEL algorithm to the ICBM-152 template using both affine and non-linear spatial normalization. The MRI images were bias-field corrected and segmented into gray, white matter, and cerebrospinal fluid tissues. The gray matter segments were then modulated for non-linear transformations only and subsequently smoothed with an isotropic Gaussian kernel (full-width-half-maximum = 8).

We used a mask of the human hippocampus created in a previous study (Plachti et al., 2019) from macro-anatomical atlas and cytoarchitecture maps. Structural covariance was computed by correlating hippocampal voxels with all other grey matter voxels using Pearson correlation, which were z-transformed. For each dataset, hundreds of bootstrap samples (corresponding to the size of the dataset) were created and a respective structural covariance matrix was computed for each bootstrap sample (see Supplemental material Methods).

Table 3. Sequence parameters of the different datasets

Datasets	Sequence parameters
HCP	T1 (3D-MPRAGE), Siemens Skyra, 256 slices, TR=2400 ms, TE=2.14 ms, TI =1000ms, FoV=224x224mm^2, flip angle = 8◦, voxel size = 0.7 x 0.7 x 0.7 mm^3
eNKI	Cross Sectional Lifespan Connectomics and Longitudinal Developmental Connectomics study: T1 (3D-MPRAGE), Tim Trio, 176, TR= 1900 ms, TE = 2.52 ms, TI= 900 ms, FoV = 250 x 250 mm^2, flip angle = 9◦, voxel size = 1 x 1 x 1 mm^3; Neurofeedback study: T1 (3D-MPRAGE), Tim Trio, 192 slices, TR = 2600 ms, TE = 3.02 ms, TI = 900 ms, flip angle = 8◦, voxel size = 1 x 1 x 1 mm^3
CamCAN	T1 (3D-MPRAGE), Tim Trio, 192, TR=2250 ms TE= 2.98 ms, TI= 900 ms, FoV = 256 x 256 mm^2, flip angle = 9◦, voxel size = 1 x 1 x 1 mm^3
1000BRAINS	T1 (3D-MPRAGE), Tim-TRIO, 176 slices, TR = 2.25 s, TE = 3.03 ms, TI = 900ms, FoV = 256 x 256mm^2, flip angle = 9◦, voxel resolution = 1 x 1 x 1mm^3

ADNI	ADNI1: T1 (3D-MPRAGE), TR = 0.65 s, TE = min full, FoV = 256 x 256 mm^2, flip angle = 8◦, voxel resolution = 1.2 mm^3; ADNIGO/2: T1 (3D-MPRAGE), TR = 0.4 s, TE = min full, FoV = 256 x 256 mm^2, flip angle = 11◦, voxel size = 1.2 mm^3; ADNI3: T1 (3D-MPRAGE), TR = 2300 ms, TE = min full echo, TI = 900 ms, FoV = 256 mm, resolution = 1 x 1 x 1mm^3;
OASIS3	T1 (3D-MPRAGE), Tim Trio, TR = 2400 ms, TE = 3.08 ms, TI = 1, FoV = 256 x 256 mm^2, flip angle = 8 ◦, voxel size = 1 x 1 x 1 mm^3

Parcellation – clustering of hippocampus' voxels— based on structural covariance

Clustering

To identify patterns of similar and different structural covariance among hippocampus voxels, we used an unsupervised clustering approach extensively applied in the field of brain parcellation. More precisely, for each voxel within the hippocampus, an individual structural covariance profile to all other brain voxels across subjects was computed. In the next step, hippocampus' voxels were clustered based on the similarity/dissimilarity of their profiles. As a clustering algorithm we applied the k-means ++ algorithm in Matlab identifying two to seven parcels. We used 255 iteration and 500 repetition parameters in line with Plachti et al. (2019) to allow comparison with previous parcellations.

Split-half cross validation as stability measure

In order to identify which cluster solution best summarized similarity and dissimilarity in the pattern of structural covariance of hippocampus' voxels, we used split-half cross validation to estimate the stability of differentiations. We divided each sample into halves 10 000 times (splits) and compared with the adjusted Rand Index (aRI) the convergence between the two halves. The aRI estimates the consistency of two clusterings and is adjusted for chance. It can have values between 0 (not similar at all) and 1 (identical). A higher convergence reflects a higher consistency of the clusterings indicating high stability. In order to quantify statistically the stability of the different cluster solutions, we performed an ANOVA.

Cross-dataset group parcellation

To obtain robust patterns of structural covariance parcellation in each age/disease group, we merged after the clustering the parcellation results from different datasets corresponding to the same age and disease group. This procedure aimed to extract patterns that captured the relevant features under investigation (e.g. aging or dementia effects) rather than dataset specific effects (Jockwitz et al., 2019). First, the clustering approach was applied on hippocampus' voxels structural covariance profiles within each sample and age group resulting in sample-group-specific matrices. We then concatenated the solution matrix of one sample (e.g. Young_HCP) with all the other samples (e.g. Young_eNKI, Young_CamCAN) belonging to the same age or disease group (e.g. Young) and applied bootstrapping (10 000 resampling) on the 'merged' solution matrix across bootstrap samples (see Supplemental material Methods and Fig. 1).

Clusters' covariance network and their relationship to functional large-scale networks

In order to identify the pattern of structural covariance underlying the clustering in each age/disease group (n=2584), we examined the network of structural covariance more specifically associated to each cluster. To do so, we used the general linear model as implemented in SPM, hence at the voxel level. Accordingly, at each voxel, the linear relationship with the average grey matter value of the cluster of interest is tested. This procedure provided some insight into the individual pattern of structural covariance of the different subregions of the hippocampus that have driven the clustering. As the clustering is not performed on any thresholded values but based on the full pattern of structural covariance, we here examined the map of structural covariance of each cluster across the whole brain at an uncorrected level of $P < 0.001$ with a threshold of T=1. Nevertheless, we additionally corrected for multiple comparisons using family wise error (FWE) rate at the significance level of $P < 0.05$ to examine the brain patterns that survived at a strict statistical threshold (Supplementary Fig. 7).

To test whether structural covariance networks in dementia follow functional co-activation networks, we examined the functional connectivity of the subregions derived in dementia but in a sample of healthy participants. Our underlying hypothesis was that the pattern of co-

atrophy in dementia could mirror functional connectivity patterns observed in late life (but before dementia). To explore this question, we performed a similar general linear model analysis using resting-state fMRI time-series in the group of healthy elderly (n=428 in 1000BRAINS; EPI, 36 slices, TR=2.2 s, TE=30 ms, FOV = 200 x 200 mm^2, flip angel = 90 °, voxel resolution =3.1 x 3.1 x 3.1 mm^3) for the hippocampus' subregions derived from the dementia group. Preprocessing included movement correction by affine 2-pass registration and alignment of the images to the first volume and to the mean of the volumes. The six motion parameters and their first derivatives from the realignment step were regressed out. Spatial normalization was performed to the MNI-152 Template for the average EPI scans for each subject using the unified segmentation approach. Images were band-pass filtered with cut-off values of 0.01-0.08 Hz and smoothed with the isotropic Gaussian kernel (full-width-half-maximum = 5 mm). Denoising was performed using white-matter and CSF signal regression.

For each grey matter voxel, a linear relationship with the average BOLD-response of the cluster of interest was computed. In this way, we obtained the functional connectivity network of each individual cluster and contrasted it against the whole brain pattern of association of other clusters.

Clusters' covariance network and their behavioral associations

After having identified the structural covariance network for each cluster, we characterized those networks in terms of associated behavioral functions using NeuroSynth database (https://neurosynth.org/) and its cognitive decoding tool with above 1 300 terms included. For the most frequent terms reported in the literature (such as "episodic memory"), NeuroSynth provides meta-analytic maps of the most frequently associated voxels in activation studies. It therefore offers the possibility to compare any given brain pattern, such as the whole brain structural co-variation patterns in the present study, to the collection of maps related to each term using the cognitive decoding tool. Accordingly, we used the uncorrected whole-brain maps of each cluster and ran Pearson correlations between our structural covariance maps and the meta-analytic maps of NeuroSynth. As our objective here was not to identify specific behavioral functions associated to a specific network but rather to identify the broad pattern of behavioral associations of cluster's network, we included all correlations for associated terms above 0.1, we excluded non-behavioral terms (e.g. hippocampus, dementia) and summarized

similar lexical terms into a summary label (e.i. 'emotions', 'affect', 'happy', 'fear' -> emotion). The pattern of associated behavioral terms, which could differ in number depending on the spatial extent the of clusters' covariance pattern, was then interpreted qualitatively rather than with regards to magnitude of association.

Data availability statement

The data that support the findings of this study are available from open science initiatives reported and cited above. Code can be shared upon reasonable request from the corresponding author. The derived clusters are available at (http://anima.fz-juelich.de/) as ROI in .nii format.

Results

Stable clustering level

We used split-half cross-validation (10 000 splits) to identify the most stable cluster solution based on similarity across splits as measured by the aRI index. We performed a 6 (datasets: HCP, eNKI, CamCAN, 1000BRAINS, ADNI, OASIS3) x 6 (cluster solution: 2-7) ANOVA with the aRI as dependent variable. The ANOVAs were performed separately for each hemisphere.

Overall, examining cluster solutions' main effect $F(5,839964) = 32365.18$, $P < 0.001$), in the right hippocampus, parcellations into 2 and 3 clusters were the most stable solutions even though the differences between all cluster solutions were marginal: 2 (M=0.97,), 3 (M=0.96), 4 (M=0.95) (Fig. 1A). For the left hippocampus, cluster solution two and three were also the most stable: 2 (M= 0.97), 3 (M= 0.96), 4 (M= 0.94), $F(5,839964) = 25194.75$, $P < 0.001$(Fig. 1A). The significant interaction effects in right and left hippocampi indicated that the stability of parcellations was dependent on dataset, $F(25, 839964) = 2006.7$, $P < 0.001$, $F(25,839964) = 4884.36$, $P < 0.001$ (Supplementary Fig. 2).

In line with previous clustering studies, our first exploration showed a relatively linear decrease in the stability as the number of cluster increases, suggesting that the simpler, more parsimonious models are the most robust ones (additionally supported by silhouette plots in Supplemental material 2.2). In particular here, the 2- and 3- cluster solutions are the most stable levels of differentiation.

Similarity/consistency of the hippocampal differentiation

To further ensure that the stability of cluster solutions 2-4 was driven by intrinsic properties of the structural covariance pattern rather than by intrinsic properties of the dataset, we examined the pattern of similarity (measured by the aRI) between the different cohort samples (Fig. 1B).

The inspection of the similarity matrices revealed that, cluster solution 2 showed a general pattern of high similarity, whatever the dataset or age group. This suggested a global differentiation being robust across data and age/disease group (Fig. 1B). The 3-cluster solution mainly and remarkably showed a high within group (age and disease) and between group consistency suggesting a differentiation pattern driven by intrinsic features of the age/disease groups rather than by the intrinsic features of the dataset. This suggests that neurobiological rather than technical factors specific to the dataset guided the parcellation.

In contrast, the 4-cluster solution showed high within age group consistency only for the healthy elderly group in the right hippocampus, questioning its usability to study lifespan and disease related changes. Finally, the higher clustering levels (5, 6 and 7-cluster solution) showed overall relatively low similarity between samples (Supplementary Fig 2). Thus, the investigations of consistency/similarity between samples supported the focus on the 3-cluster solution as the most stable and most likely biological relevant pattern of differentiation of hippocampus' voxels.

In sum, our first 'bottom-up' examination of the differentiation of the hippocampus based on structural covariance across different datasets suggested that a 3-cluster solution could represent the data in a stable manner. Furthermore, our examination of consistency within age and disease group suggested that this high stability is not primarily driven by characteristics that were intrinsic to the dataset but rather by characteristics that were intrinsic to the population group and hence driven by neurobiological factors. Thus, altogether, hippocampus voxels within different age/disease groups could be optimally summarized with a 3-cluster solution ideally applicable to study lifespan and disease alterations. Importantly, such parsimonious 3-partition model also meets previous theories on hippocampus' organization.

Even though cluster solution 2 and 4 displayed high stability and consistency compared to higher differentiations, they were either less informative as in the case of cluster solution two (Supplementary Fig. 5) or demonstrated qualitatively divergent parcellations less comparable across age/disease group as in the case of cluster solution four (Supplementary Fig. 5).

Building on these explorations of the data and previous knowledge, we then focused on the 3-cluster solution pattern.

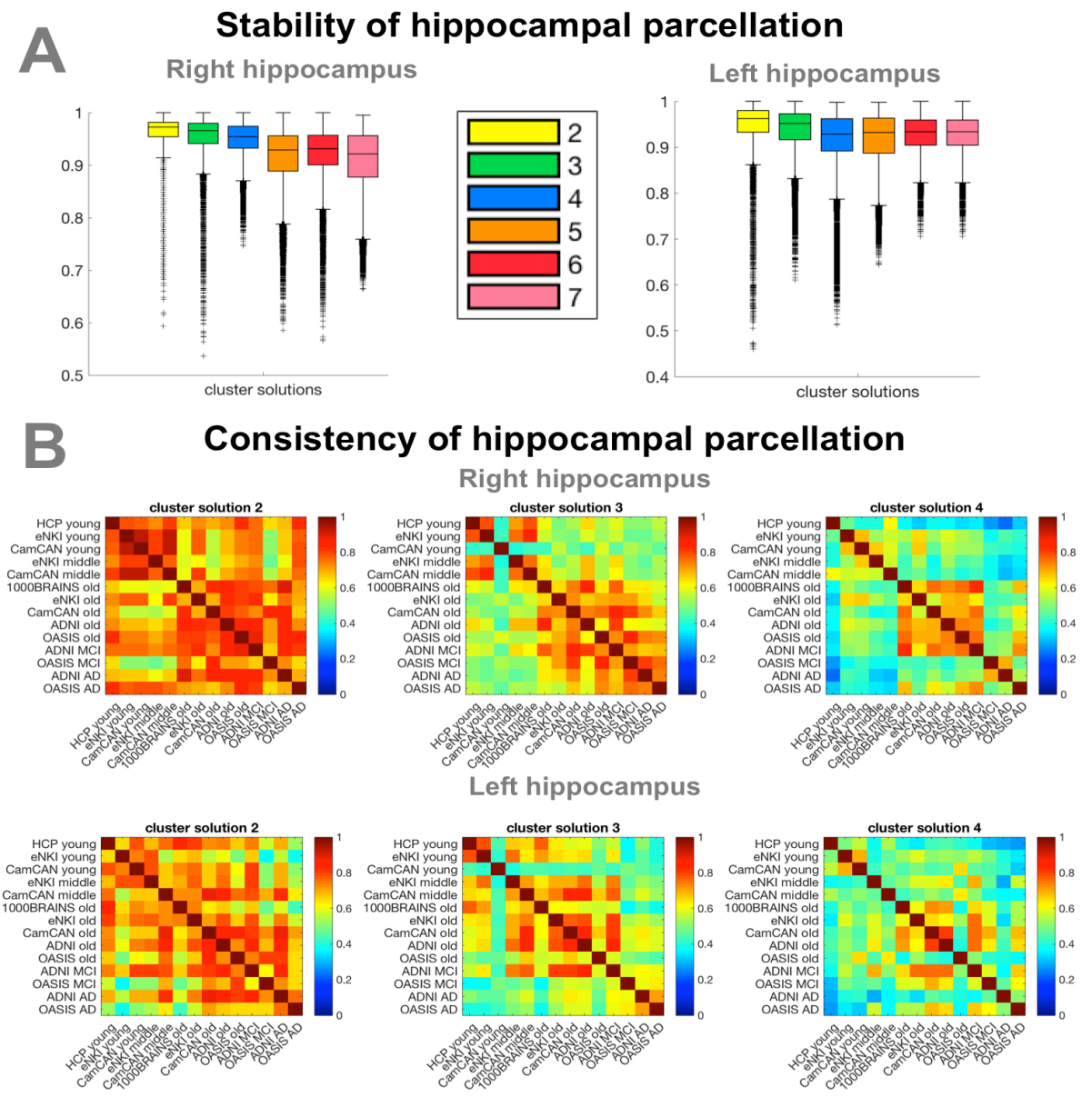

Figure 1. A) Stable organizational patterns were found for right and left hippocampus for cluster solution 2-4 estimated with split-half cross-validation. All clusterings reached very high stability > 0.9 aRI. B) Cross-sample consistency of lower cluster solutions measured with the aRI. Despite overall high stability, the simple parcellation schemes 2-4 were also very consistent > 0.6 across datasets and within age/disease specific groups (e.g. young, elderly) suggesting biological relevance in those differentiations. Cluster solution 3 was exceptionally useful to study age and disease related patterns, because this scheme demonstrated not only high within age/disease similarity but to some extent also across age/diesease groups indicating relatedness, which did not apply for cluster solution 4. In

contrast cluster solution 2 showed very high similarity independent of age/disease and dataset suggesting on the one hand a robust biological differentiation, but on the other hand a less flexible scheme to represent lifespan and pathological alterations. Boxplots with median, 1.5 interquartile range, min. Q1-1.5*IQR, max. Q3+1.5*IQR.

Cross-dataset age and disease group parcellation

After deriving parcellations in each cohort sample, we merged them to obtain a robust pattern of differentiation of hippocampus voxels for five different age and disease groups: young, middle-aged, elderly, MCI and dementia patients using a bootstrapping approach to further promote stability. This aggregation was done separately for the left and right hippocampi. Nevertheless, a very symmetrical pattern of differentiation could be observed across hemispheres. For both hippocampi, our maps (Fig. 2) showed a very similar pattern for the young, middle-aged, elderly and the MCI group. This pattern highlighted a division in the medial-lateral dimension of the hippocampus' body and to some extent, of the tail while the head appeared as a relatively homogeneous region. This pattern replicated the findings from our previous parcellation work in the hippocampus performed in a sample of young participants from the HCP dataset (Plachti et al., 2019), and as already highlighted in our previous study, is reminiscent of the medial-lateral differentiation between CA and subiculum subfields known from cytoarchitecture. Of note, it seemed that with increasing age the head cluster decreased slightly in size, while the medial (blue) cluster expanded into the tail area and the lateral (green) cluster expanded into the anterior direction (Fig. 2).

Remarkably, the differentiation of the hippocampus in the dementia group deviated from the pattern that was observed in healthy population across adult age. Despite the anterior subregion also appeared as a relatively homogeneous region, the lateral (green) cluster was focused on the hippocampus body while the medial (blue) cluster appeared more prominent in the tail. As illustrated in Figure 2, this pattern was reminiscent of the functional differentiation along the anterior-posterior dimension (and hence "head-body-tail" tripartite model) observed in parcellations using large-scale functional connectivity. In order to further quantitatively evaluate these apparent divergences and resemblances, we compared the similarity of the age and disease groups among each other and with the functional map of the hippocampus derived in healthy adult fMRI data (Plachti et al., 2019) using the aRI.

Strikingly, the highest similarity with the hippocampus' functional map was found for the parcellation pattern obtained in dementia. This finding suggested that over time, the structural changes in the hippocampus in the pathological condition of dementia followed the large-scale functional organization of the hippocampus. Interestingly, this tendency was higher for the right than for the left hippocampus. Finally, it is worth noting that the pattern in participants with MCI was more similar to the healthy middle-aged and elderly participants than to the pattern observed in dementia.

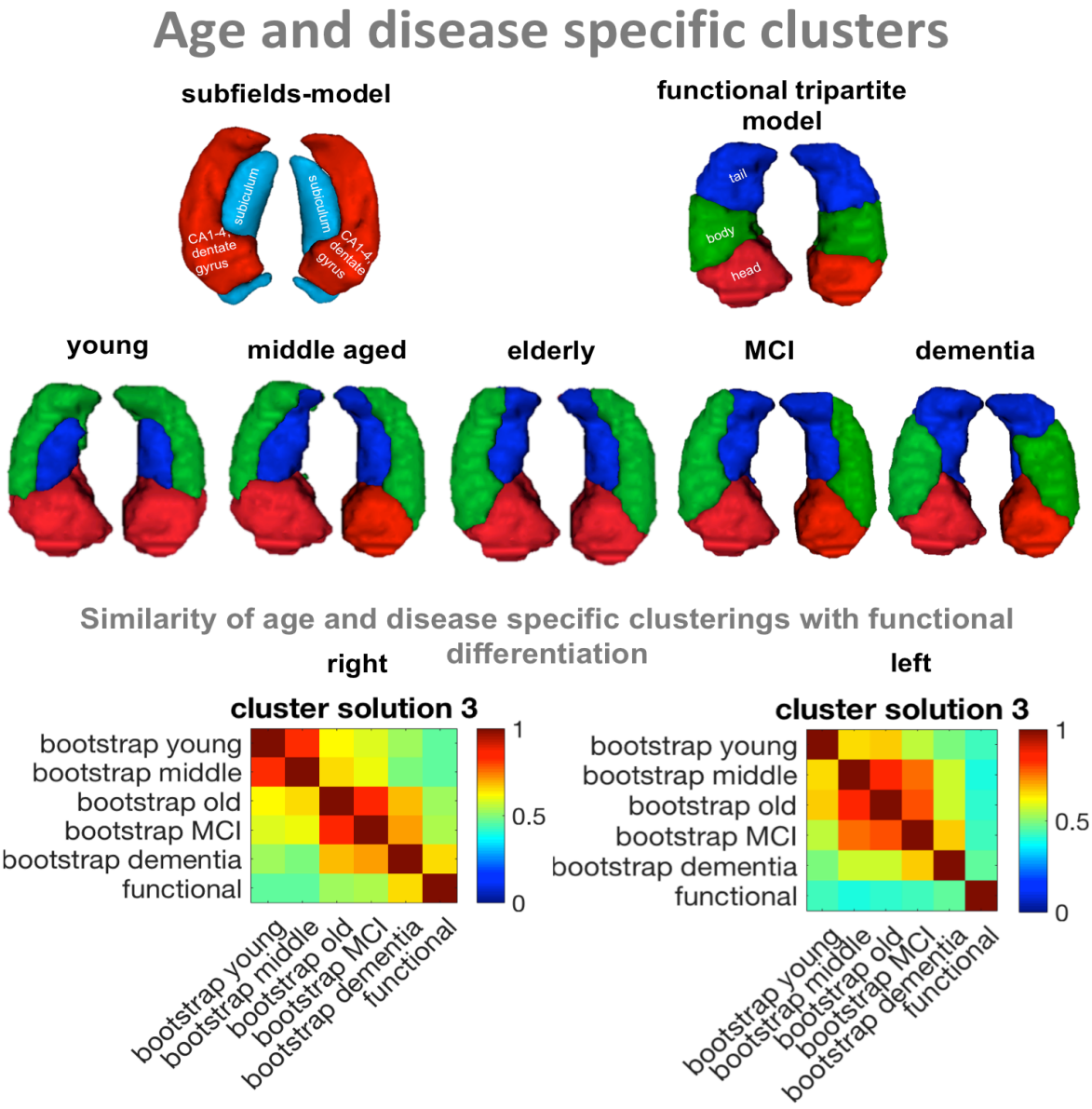

Figure 2. Age and disease specific clusterings of the hippocampus and its similarity to functional differentiation into head, body and tail parcellation. In younger age the hippocampal differentiation was reminiscent of the differentiation between subiculum vs. CA1-4 and dentate gyrus subfields. With increasing age the lateral subregion decreased from

the tail, whereas the differentiation in dementia was reminiscent of the functional differentiation into head, body and tail also suggested by the similarity estimation.

Whole brain structural covariance patterns of each cluster

In order to better understand the structural covariance patterns that drove the differentiation among hippocampus' voxels in each age/disease group, we examined the specific structural covariance pattern of each cluster and this, separately in each age/disease group. The structural covariance networks for young, elderly adults and dementia patients are presented below while the results obtained in middle aged and MCI participants (that were in line with other non-demented groups) are presented in Supplementary Fig. 6.

In young participants the (red) anterior cluster was associated with wide fronto-temporal and parietal networks including frontal medial cortex, superior frontal gyrus, orbitofrontal cortex, cingulate cortex, temporal lobe, parahippocampal gyrus, (pre-)cuneal cortex, calcarine cortex, lingual gyrus and occipital pole. In addition, the putamen, pallidum, amygdala, insular cortex belonged to this network. A similar pattern was found in healthy elderly participants despite a slight expansion, additionally covering the inferior frontal gyrus, the whole cerebellum, pre- and postcentral gyri (Fig. 3).

The lateral (green) cluster in the young group was mainly associated with subcortical structures such as putamen, pallidum, nucleus caudatus, thalamus but also with the cingulate gyrus, lingual gyrus, precuneous cortex and intracalcarine/supracalcarine cortex. Additionally, frontal and temporal brain regions were included such as frontal orbital cortex, frontal operculum cortex, inferior frontal gyrus, pars opercularis and superior temporal gyrus. In the older group, this network mainly reduced to the parieto-occipital (posterior cingulate cortex, precuneous, lingual and intracalcarine gyrus) and frontal medial (frontal medial cortex, subcallocal cortex, frontal pole) brain regions reminiscent of the Default mode network.

The blue medial cluster in the group of young adults was mostly related to middle frontal, middle temporal gyri, cerebellum and lateral occipital cortex. Subcortical regions such as the caudate and thalamus, but also the insula were included. Interestingly, the (blue) medial cluster showed in the group of healthy elderly a very broad pattern of structural covariation (Fig 3), especially in the posterior brain regions (e.g. parietal, occipital lobes and motor related regions: cerebellum, pre-postcentral gyrus, thalamus, putamen, but also occipital gyrus, superior parietal lobule, and temporal gyri). Some smaller associated regions were also found in the inferior frontal and middle frontal cortex.

In contrast, in the group of patients with dementia, the pattern of structural covariance of each cluster was less spatially extended compared to all the other groups (Fig 3). Furthermore, the pattern was also qualitatively different when compared to the patterns of the three clusters in the other age/disease groups confirming that the differentiation into subregions within the hippocampus itself is qualitatively different and did not follow the known pattern of healthy aging. Hence, the (green) lateral-body cluster was not associated with posterior subcortical structures as the lateral (green) cluster in other groups but rather was more specifically associated with structures in the frontal (inferior frontal gyrus pars opercularis, frontal pole, opercular gyrus), temporal (middle temporal gyrus, Heschl's gyrus) and occipital brain regions (Fig. 3). In contrast, the (blue) tail cluster was more associated with posterior brain regions (posterior parts of the temporal lobe, postcentral gyrus and (pre)cuneous, angular gyrus) while the anterior cluster was more associated with temporal, temporo-occipital fusiform cortex, and parietal regions loosing mainly its co-variation with frontal regions compared to younger healthy adults.

Because of apparent similarity between structural differentiation of the hippocampus in the dementia group with the functional organization model of the hippocampus known from previous studies in the healthy population, we further explored the relationship between functional and structural networks. More concretely, we investigated the pattern of resting-state functional connectivity in the later life period of healthy participants (i.e. in healthy older adults) of the hippocampus' cluster derived in dementia patients. This exploratory analysis suggested that the functional networks of the anterior and the lateral clusters that can be observed in an aging population are very similar to their structural networks observed in patients with dementia hence further supporting the hypothesis of a an influence of large-scale functional interaction in the co-atrophy pattern in dementia.

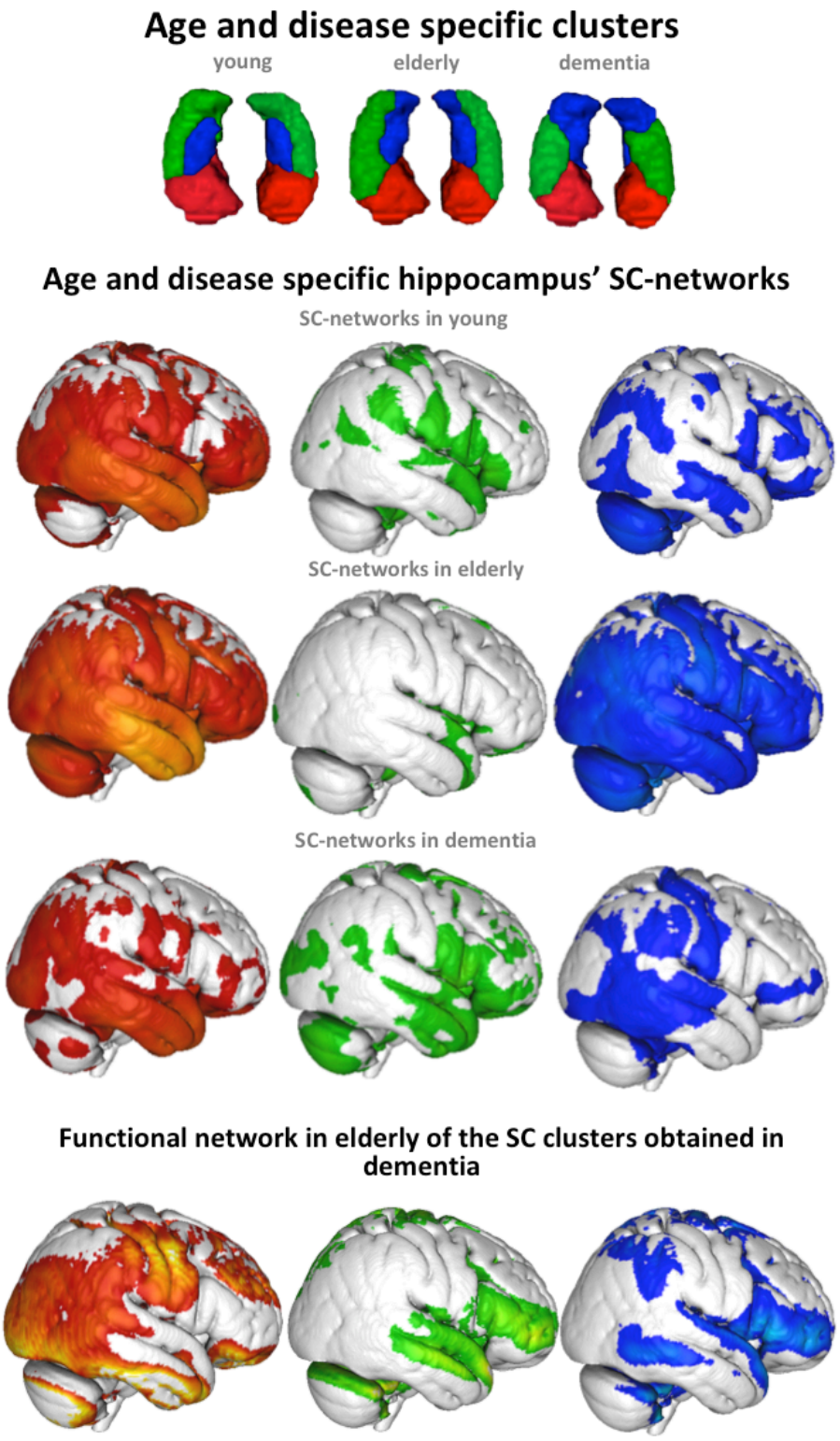

Figure 3. Patterns of structural covariance of each hippocampus' subregions in young, elderly and dementia groups. Relative resting state-functional connectivity networks of dementia-hippocampus in healthy elderly resembled structural co-variation networks of dementia hippocampus in dementia group. Uncorrected ($P < 0.001$), thresholded T=1.

Behavioral characterization of clusters' structural covariance networks

In order to explore whether the structural covariance patterns of each cluster could reflect functional networks subserving specific behavioral functions, we characterized the spatial pattern of each cluster's covariance network with regards to behavioral terms with NeuroSynth. Results of middle aged and MCI patients are presented in Supplementary (Fig. 10) while we here focused on the associations in the young, elderly and the dementia group, as showing a slightly different pattern.

Overall, the spatial pattern of the anterior (red) cluster was primarily associated with emotional, perceptual (olfactory, viewing) and self-related (autobiographical) terms, but also with other less ontologically defined terms such as faces, ratings and reactivity (Fig. 4). Overall, this behavioral pattern pointed to an automatic and more perceptual-emotional processing and integration of information into self-related internal states. This behavioral profile of the anterior subregion was even preserved in dementia pathology. In contrast, the pattern of the lateral (green) and the medial (blue) clusters' diverged depending on the age and disease group. Whereas the medial blue clusters' networks in the group of healthy young adults was associated with visual processing of objects and places, in the group of elderly and dementia patients, however, it was behaviorally additionally associated with motor/movement and orientation (Fig.4).

Most changes in structural co-variation and behavior were observed for the lateral (green) cluster. In the group of young healthy adults the network was associated with motor-related behavior (e.g. motor, navigation), whereas in the elderly the behavioral association suggested an involvement of storing self-related information (e.g. autobiographic memory, episodic memory). In the group of dementia patients, on the other hand, the network was primarily associated with communication and social cognition, both of its own internal states (e.g. pain) as well as external information (e.g. comprehension, theory of mind). Overall, these results suggested that, the changes in the patterns of structural co-variation of the medial and lateral clusters over the lifespan and in pathology could be related to associations with different behavioral functions.

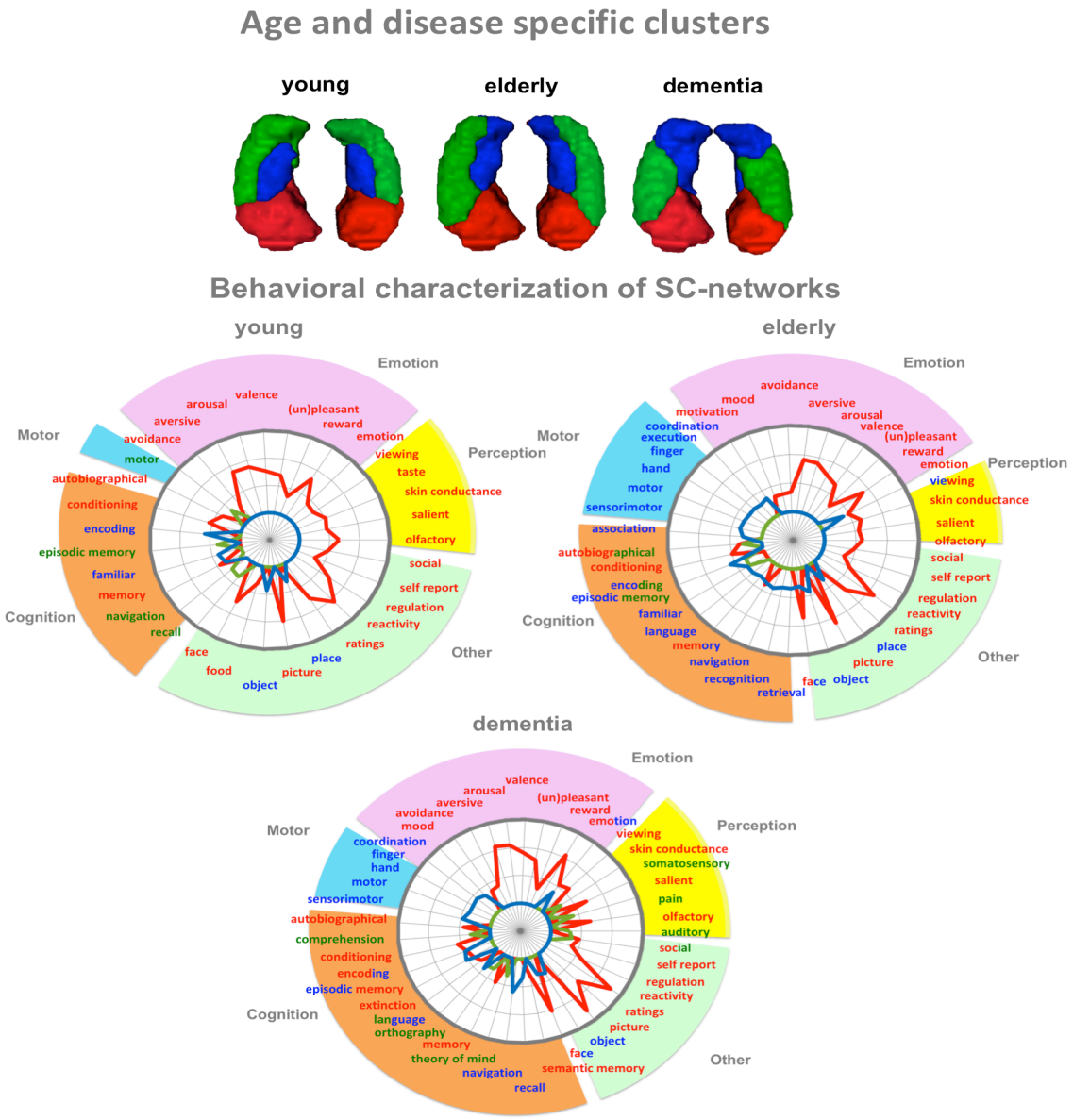

Figure 4. Behavioral characterization of clusters' co-variance network in age and disease groups using NeuroSynth. Behavioral profiles of anterior cluster's co-variance network remained relatively stable across the lifespan and in disease playing a major role in automatic perceptual-emotional approach-behavior in learning, establishing self-related memories. Across the lifespan the medial (blue) subregion's network changed from being associated with visual processing in younger years to being also motor-related in older age. The lateral-body (green) subregion in the group of dementia was behaviorally associated with language and theory of mind processing while the lateral subregion did not show a clear behavioral specificity in the second half of lifespan compared to the anterior subregion.

Discussion

The hippocampus is susceptible to senescence and neurodegenerative processes but the patterns of structural changes at the macro-scale revealed inconsistencies across studies. Observed changes in grey matter volume could be either constrained by micro-anatomical organization of the cytoarchitecture or follow an organization determined by lifelong functional large-scale networks.

In a previous recent study, we used a parcellation approach to study human hippocampus organization with a multimodal parcellation approach. We hence examined the pattern of structural covariance in the human hippocampus in healthy young adults and found a topology that mimics both medial-lateral differentiation from cytoarchitecture and anterior-posterior differentiation shown by functional connectivity profiles (Plachti et al., 2019). A similar pattern was found in a very recent study using a similar population but different parcellation approaches (Ge et al., 2019), and was reproduced again in this study, hence suggesting that this pattern reflects a robust pattern of co-plasticity in young adults.

We here investigated if structural changes represented in co-variations in older age and dementia follow or deviate from the patterns of co-plasticity observed in young adults. Our results indicated that during aging the overall pattern of structural covariance follows the pattern of structural covariance observed in young adult age with some small differences discussed below. However, in participants with probable dementia disease, the pattern of co-atrophy in the hippocampus deviates from what was observed in these healthy populations. In patients with dementia, the co-atrophy seems to follow the functional large-scale networks with a pattern that resembles more than the functional model of hippocampus' organization than what was observed in other groups. Overall, the most prominent differences between groups in the differentiation patterns of the hippocampus were found in the body and tail whereas the head always appears as a uniform region. Group differences were shown not only in the topological pattern within the hippocampus, but also in the whole brain structural covariance pattern that drove the clustering and their associated behavioral associations.

Consistent pattern of head differentiation in hippocampus' structural covariance across the lifespan

Independent of age and disease, the head of the hippocampus, emerged consistently as one homogeneous subregion, except for some minor reductions with higher age and ongoing

pathology. But the actual underlying covariance pattern of the anterior hippocampal subregion changed across age/disease groups. In young adulthood the anterior hippocampal co-variation pattern was characterized by a broad network extending across frontal, temporal and occipital lobes as well as (inferior) parietal regions. In accordance with the large spatial distribution of this network, behavioral associations showed a relatively broader spectrum including emotional, cognitive and perceptual processes. These results could suggest that the hippocampus head is a plastic region (based for example on cell proliferation in the dentate gyrus, (van Praag, Shubert, Zhao, & Gage, 2005) during the lifespan), which structure is modulated by rich functional interaction with large-scale brain networks subserving various behavioral functions. The structural covariance networks of the hippocampus head in early and late adulthood demonstrated that the anterior hippocampus co-varied with the same brain regions in both halves of healthy lifespan suggesting a perseverance of co-plasticity and resilience. However, in dementia the structural covariance network of the anterior subregion decreased mainly to the temporal lobe suggesting a loss of network.

Consistent pattern of medial-lateral differentiation in hippocampus' structural covariance

Across different age groups of the healthy population, we found a consistent differentiation pattern along the medial-lateral dimension of the hippocampus dividing it into a lateral and a medial subregion. This pattern replicated previous findings and seemed to follow the cytoarchitectonic differentiation between the CA and subiculum subfields (Plachti et al., 2019). Importantly, this pattern, like the head subregion, appeared to remain stable across the whole adult lifespan suggesting a very strong and robust scheme of structural covariance that should be referred to when studying structural changes with MRI in adults. This scheme was even further retained when subdividing the hippocampus into 4 subregions in healthy adults and MCI patients (Supplementary Fig. 5), even if, one additional cluster appeared either in the anterior or posterior-lateral region depending on the age/disease group. Even though the differentiation into a lateral and medial parcel was preserved over the lifespan, the lateral cluster decreased posteriorly with age and the medial cluster expanded into the tail. This change in the cluster pattern was reflected both in the associated structural pattern and the related behavioral associations.

The medial hippocampal subdivision showed a co-variation pattern with occipito-parietal, temporal (middle temporal gyrus), and frontal (inferior and middle frontal gyri) brain regions. Furthermore, the network included subcortical brain regions such as thalamus, caudate, and insula. With increasing age, the covariance network expanded highly in size, especially covering posterior brain regions. The shift from mostly anteriorly associated brain regions in younger years to posteriorly associated regions in elderly is not unusual for the hippocampus. It has already been reported in functional connectivity (Blum, Habeck, Steffener, Razlighi, & Stern, 2014; Stark, Frithsen, & Stark, 2019), in structural covariance studies (X. Li, Li, Wang, Li, & Li, 2018), and for anatomical connectivity with strengthened connections to medial occipital regions (Maller et al., 2019), which was in line with our results, even though the responsible mechanisms remain to be elucidated.

These alterations were also mirrored in the behavioral association patterns. While in younger adults visual cognition (e.g. object, place, encoding, familiarity) was prominent, in elderly, however, the behavioral spectrum expanded to language processing as well as to motor related (learning) behavior. Both, structural co-variation networks and behavioral profiling, suggest that brain regions connected by the inferior longitudinal fasciculus (ILF) co-vary more likely with the medial subregion of the hippocampus. The ILF is an occipito-temporal association tract with close relationships to the occipital radiations and hippocampus through the tapetum (Herbet, Zemmoura, & Duffau, 2018). The ILF is behaviorally associated with visual object and face recognition, reading as well as lexical and semantic processing (Herbet et al., 2018), which is in accordance with our behavioral profiling of the medial subregion across the lifespan.

While the medial cluster expanded into the tail during healthy aging, the lateral cluster decreased from the tail. The lateral subregion's co-variance network in young adulthood yielded primarily associations with subcortical regions (e.g. thalamus, caudate nuclei) and additionally with the parieto-occipital fissure. Anatomically those associated brain regions were reminiscent to some extent to the grey matter regions around the dorsal hippocampal commissure, being connected with posterior cingulum, tapetum, and fornix (Postans et al., 2019). The dorsal hippocampal commissure is associated with learning, memory and recently also with recognition (Postans et al., 2019). The fornix is the white matter output of the hippocampus through the tail (R. S. C. Amaral et al., 2018) whereas the tapetum transfers information between hemispheres. The hippocampus is connected via the fornix with limbic structures (e.i. hypothalamus, thalamus, nucleus accumbens) (Douet & Chang, 2015), and has

been suggested to play a major role in transferring information from short-term to long-term memory via the Papez circuit and is accordingly, involved in long-term memory encoding and retrieval (Douet & Chang, 2015; Eichenbaum, Yonelinas, & Ranganath, 2007; Foster, Kennedy, Hoagey, & Rodrigue, 2019).

Structural covariance pattern in the hippocampus in dementia resemble functional organization

In healthy population, structural covariance across the brain is assumed to reflect maturational, developmental and experience-based co-plasticity (Alexander-Bloch et al., 2013; Geng et al., 2017). In patients with neurodegenerative disorders, structural covariance across the brain could be expected to mainly reflect brain structure co-atrophy. The moderate to high convergence between structural covariance and task-(un)related functional connectivity (Kotkowski et al., 2018; Paquola, Bennett, & Lagopoulos, 2018; Reid et al., 2016; Shah et al., 2018) suggests that abnormalities in structural and functional network topology is predictive of brain disorders (Goodkind et al., 2015; Seeley et al., 2009) and weaker cognitive performance (McTeague, Goodkind, & Etkin, 2016; Montembeault et al., 2016; Spreng & Turner, 2013). However, the question remains fully open whether structural atrophy changes functional BOLD response (He et al., 2007) or the other way around (Chang, Huang, Chang, Lee, & Chang, 2018). From a neuropathological standpoint, Alzheimer's pathology is assumed to follow a specific topological pattern distributed along large-scale networks (Braak & Braak, 1991; Corder et al., 2000; Montembeault et al., 2016). For example, amyloid-plaque distribution in the brain seems to follow functional organization mirrored in the Default mode network (DMN) (Buckner et al., 2005; Klunk et al., 2004; Montembeault et al., 2016). Similarly, the spreading of tau neurofibrillary tangles seems to follow a functional pattern, which is not explained by spatial proximity (Franzmeier et al., 2019). In other words, brain regions that are more likely to be functionally coupled together share a stronger tau covariance, which is not explained by pure spatial neighborhood. This apparent convergence between spatial distribution of pathology markers and the spatial organization of functional networks may be explained by the fact that synchronous neuronal firing establishes a network-based synaptogenesis (Bi & Poo, 1999; Katz & Shatz, 1996), which can then be assumed to be vulnerable to pathological processes.

Linking these neuropathological considerations to the pattern of differentiation based on structural covariance found in the hippocampus of patients with probable AD in this study, we can hypothesize that the pattern of co-atrophy in these patients followed the pattern of functional organization subserving broad behavioral functions. In this regard, we can note that the pattern of structural covariance networks of the hippocampal body in dementia patients in this study was associated with temporal and frontal regions in turn associated with comprehension, language, orthography and theory of mind. We hypothesize that the structural covariance network of the hippocampus' body reflects a functional network of higher cognitive functions of social cognition additionally supported by the functional co-activation pattern of the lateral-body subregion when applied to healthy elderly. It therefore emphasizes, that the hippocampal differentiation based on structural covariance in dementia follows functional differentiation. Overall our findings point to the necessity of accounting for hippocampus' functional organization related to large-scale networks subserving broad behavioral functions when studying hippocampus' structural changes at the macro-scale in dementia.

Acknowledgments

Some of the data used in preparation of this article were obtained from the Alzheimer's Disease Neuroimaging Initiative (ADNI) database (adni.loni.usc.edu). As such, the investigators within the ADNI contributed to the design and implementation of ADNI and/or provided data but did not participate in analysis or writing of this report. A complete listing of ADNI investigators can be found at: http://adni.loni.usc.edu/wp-content/uploads/how_to_apply/ADNI_Acknowledgement_List.pdf.

Clinical data collection and sharing for this project was funded by the Alzheimer's Disease Neuroimaging Initiative (ADNI) (National Institutes of Health Grant U01 AG024904) and DOD ADNI (Department of Defense award number W81XWH-12-2-0012). ADNI is funded by the National Institute on Aging, the National Institute of Biomedical Imaging and Bioengineering, and through generous contributions from the following: AbbVie, Alzheimer's Association; Alzheimer's Drug Discovery Foundation; Araclon Biotech; BioClinica, Inc; Biogen; Bristol-Myers Squibb Company; CereSpir, Inc; Cogstate; Eisai Inc; Elan Pharmaceuticals, Inc; Eli Lilly and Company; EuroImmun; F Hoffmann-La Roche Ltd and its affiliated company Genentech, Inc; Fujirebio; GE Healthcare; IXICO Ltd.; Janssen Alzheimer Immunotherapy Research and Development, LLC; Johnson and Johnson

Pharmaceutical Research and Development LLC; Lumosity; Lundbeck; Merck and Co, Inc; Meso Scale Diagnostics, LLC; NeuroRx Research; Neurotrack Technologies; Novartis Pharmaceuticals Corporation; Pfizer Inc; Piramal Imaging; Servier; Takeda Pharmaceutical Company; and Transition Therapeutics. The Canadian Institutes of Health Research is providing funds to support ADNI clinical sites in Canada. Private sector contributions are facilitated by the Foundation for the National Institutes of Health (www.fnih.org). The grantee organization is the Northern California Institute for Research and Education, and the study is coordinated by the Alzheimer's Therapeutic Research Institute at the University of Southern California. ADNI data are disseminated by the Laboratory for Neuro Imaging at the University of Southern California.

Data collection and sharing for this project was provided by the Cambridge Centre for Ageing and Neuroscience (CamCAN). CamCAN funding was provided by the UK Biotechnology and Biological Sciences Research Council (grant number BB/H008217/1), together with support from the UK Medical Research Council and University of Cambridge, UK.

Funding

This study was supported by Deutsche Forschungsgemeinschaft (GE 2835/1–1), Helmholtz-Gemeinschaft (Helmholtz Portfolio Theme 'Supercomputing and Modelling for the Human Brain'), Horizon 2020 Framework Programme (720270 (HBP SGA1)), Horizon 2020 Framework Programme (785907 (HBP SGA2)), and Deutsche Forschungsgemeinschaft (EI 816/4–1).

Competing interests

The authors report no competing interests.

Supplemental Material

References

Alexander-Bloch A, Raznahan A, Bullmore E, Giedd J. The convergence of maturational change and structural covariance in human cortical networks. The Journal of neuroscience : the official journal of the Society for Neuroscience 2013; 33(7): 2889-99.

Amaral RSC, Park MTM, Devenyi GA, Lynn V, Pipitone J, Winterburn J*, et al.* Manual segmentation of the fornix, fimbria, and alveus on high-resolution 3T MRI: Application via fully-automated mapping of the human memory circuit white and grey matter in healthy and pathological aging. NeuroImage 2018; 170: 132-50.

Bi G, Poo M. Distributed synaptic modification in neural networks induced by patterned stimulation. Nature 1999; 401(6755): 792-6.

Blum S, Habeck C, Steffener J, Razlighi Q, Stern Y. Functional connectivity of the posterior hippocampus is more dominant as we age. Cognitive neuroscience 2014; 5(3-4): 150-9.
Boyke J, Driemeyer J, Gaser C, Buchel C, May A. Training-induced brain structure changes in the elderly. The Journal of neuroscience : the official journal of the Society for Neuroscience 2008; 28(28): 7031-5.

Braak H, Braak E. Neuropathological stageing of Alzheimer-related changes. Acta neuropathologica 1991; 82(4): 239-59.

Buckner RL, Snyder AZ, Shannon BJ, LaRossa G, Sachs R, Fotenos AF*, et al.* Molecular, structural, and functional characterization of Alzheimer's disease: evidence for a relationship between default activity, amyloid, and memory. The Journal of neuroscience : the official journal of the Society for Neuroscience 2005; 25(34): 7709-17.

Chang Y-T, Huang C-W, Chang W-N, Lee J-J, Chang C-C. Altered Functional Network Affects Amyloid and Structural Covariance in Alzheimer's Disease. Biomed Res Int 2018; 2018: 8565620-.

Corder EH, Woodbury MA, Volkmann I, Madsen DK, Bogdanovic N, Winblad B. Density profiles of Alzheimer disease regional brain pathology for the huddinge brain bank: pattern recognition emulates and expands upon Braak staging. Experimental gerontology 2000; 35(6-7): 851-64.

Douet V, Chang L. Fornix as an imaging marker for episodic memory deficits in healthy aging and in various neurological disorders. Frontiers in aging neuroscience 2015; 6: 343-.

Eichenbaum H, Yonelinas AP, Ranganath C. The medial temporal lobe and recognition memory. Annual review of neuroscience 2007; 30: 123-52.

Fjell AM, McEvoy L, Holland D, Dale AM, Walhovd KB. What is normal in normal aging? Effects of aging, amyloid and Alzheimer's disease on the cerebral cortex and the hippocampus. Progress in neurobiology 2014; 117: 20-40.

Fleming Beattie J, Martin RC, Kana RK, Deshpande H, Lee S, Cure J*, et al.* Hippocampal dentation: Structural variation and its association with episodic memory in healthy adults. Neuropsychologia 2017; 101: 65-75.

Foster CM, Kennedy KM, Hoagey DA, Rodrigue KM. The role of hippocampal subfield volume and fornix microstructure in episodic memory across the lifespan. Hippocampus 2019.

Franzmeier N, Rubinski A, Neitzel J, Kim Y, Damm A, Na DL*, et al.* Functional connectivity associated with tau levels in ageing, Alzheimer's, and small vessel disease. Brain : a journal of neurology 2019; 142(4): 1093-107.

Ge R, Kot P, Liu X, Lang DJ, Wang JZ, Honer WG*, et al.* Parcellation of the human hippocampus based on gray matter volume covariance: Replicable results on healthy young adults. Human brain mapping 2019; 40(13): 3738-52.

Geng X, Li G, Lu Z, Gao W, Wang L, Shen D*, et al.* Structural and Maturational Covariance in Early Childhood Brain Development. Cerebral cortex (New York, NY : 1991) 2017; 27(3): 1795-807.

Goodkind M, Eickhoff SB, Oathes DJ, Jiang Y, Chang A, Jones-Hagata LB*, et al.* Identification of a common neurobiological substrate for mental illness. JAMA psychiatry 2015; 72(4): 305-15.

He Y, Wang L, Zang Y, Tian L, Zhang X, Li K*, et al.* Regional coherence changes in the early stages of Alzheimer's disease: a combined structural and resting-state functional MRI study. NeuroImage 2007; 35(2): 488-500.

Herbet G, Zemmoura I, Duffau H. Functional Anatomy of the Inferior Longitudinal Fasciculus: From Historical Reports to Current Hypotheses. Frontiers in neuroanatomy 2018; 12: 77-.

Jockwitz C, Mérillat S, Liem F, Oschwald J, Amunts K, Caspers S*, et al.* Generalizing age effects on brain structure and cognition: A two-study comparison approach. Human brain mapping 2019; 40(8): 2305-19.

Katz LC, Shatz CJ. Synaptic activity and the construction of cortical circuits. Science (New York, NY) 1996; 274(5290): 1133-8.

Klunk WE, Engler H, Nordberg A, Wang Y, Blomqvist G, Holt DP*, et al.* Imaging brain amyloid in Alzheimer's disease with Pittsburgh Compound-B. Annals of neurology 2004; 55(3): 306-19.

Kotkowski E, Price LR, Mickle Fox P, Vanasse TJ, Fox PT. The hippocampal network model: A transdiagnostic metaconnectomic approach. NeuroImage Clinical 2018; 18: 115-29.

Li X, Li Q, Wang X, Li D, Li S. Differential Age-Related Changes in Structural Covariance Networks of Human Anterior and Posterior Hippocampus. Frontiers in physiology 2018; 9: 518.

Llera A, Wolfers T, Mulders P, Beckmann CF. Inter-individual differences in human brain structure and morphology link to variation in demographics and behavior. eLife 2019; 8: e44443.

Maguire EA, Woollett K, Spiers HJ. London taxi drivers and bus drivers: a structural MRI and neuropsychological analysis. Hippocampus 2006; 16(12): 1091-101.

Maller JJ, Welton T, Middione M, Callaghan FM, Rosenfeld JV, Grieve SM. Revealing the Hippocampal Connectome through Super-Resolution 1150-Direction Diffusion MRI. Scientific Reports 2019; 9(1): 2418.

McTeague LM, Goodkind MS, Etkin A. Transdiagnostic impairment of cognitive control in mental illness. J Psychiatr Res 2016; 83: 37-46.

Montembeault M, Rouleau I, Provost JS, Brambati SM. Altered Gray Matter Structural Covariance Networks in Early Stages of Alzheimer's Disease. Cerebral cortex (New York, NY : 1991) 2016; 26(6): 2650-62.

Moreno-Jiménez EP, Flor-García M, Terreros-Roncal J, Rábano A, Cafini F, Pallas-Bazarra N*, et al.* Adult hippocampal neurogenesis is abundant in neurologically healthy subjects and drops sharply in patients with Alzheimer's disease. Nature Medicine 2019; 25(4): 554-60.

Paquola C, Bennett MR, Lagopoulos J. Structural and Functional Connectivity Underlying Gray Matter Covariance: Impact of Developmental Insult. Brain connectivity 2018; 8(5): 299-310.

Plachti A, Eickhoff SB, Hoffstaedter F, Patil KR, Laird AR, Fox PT*, et al.* Multimodal Parcellations and Extensive Behavioral Profiling Tackling the Hippocampus Gradient. Cerebral cortex (New York, NY : 1991) 2019.

Postans M, Parker GD, Lundell H, Ptito M, Hamandi K, Gray WP*, et al.* Uncovering a Role for the Dorsal Hippocampal Commissure in Recognition Memory. Cerebral Cortex 2019.

Qiu Y, Li L, Zhou TY, Lu W. Alzheimer's disease progression model based on integrated biomarkers and clinical measures. Acta pharmacologica Sinica 2014; 35(9): 1111-20.

Reid AT, Bzdok D, Langner R, Fox PT, Laird AR, Amunts K*, et al.* Multimodal connectivity mapping of the human left anterior and posterior lateral prefrontal cortex. Brain structure & function 2016; 221(5): 2589-605.

Seeley WW, Crawford RK, Zhou J, Miller BL, Greicius MD. Neurodegenerative diseases target large-scale human brain networks. Neuron 2009; 62(1): 42-52.

Shafto MA, Tyler LK, Dixon M, Taylor JR, Rowe JB, Cusack R*, et al.* The Cambridge Centre for Ageing and Neuroscience (Cam-CAN) study protocol: a cross-sectional, lifespan, multidisciplinary examination of healthy cognitive ageing. BMC neurology 2014; 14: 204.

Shah P, Bassett DS, Wisse LEM, Detre JA, Stein JM, Yushkevich PA*, et al.* Mapping the structural and functional network architecture of the medial temporal lobe using 7T MRI. Human brain mapping 2018; 39(2): 851-65.

Sperling RA, Mormino EC, Schultz AP, Betensky RA, Papp KV, Amariglio RE*, et al.* The impact of amyloid-beta and tau on prospective cognitive decline in older individuals. Annals of neurology 2019; 85(2): 181-93.

Spreng RN, Turner GR. Structural covariance of the default network in healthy and pathological aging. The Journal of neuroscience : the official journal of the Society for Neuroscience 2013; 33(38): 15226-34.

Stark SM, Frithsen A, Stark CEL. Age-related alterations in functional connectivity along the longitudinal axis of the hippocampus and its subfields. bioRxiv 2019: 577361.

Taylor JR, Williams N, Cusack R, Auer T, Shafto MA, Dixon M*, et al.* The Cambridge Centre for Ageing and Neuroscience (Cam-CAN) data repository: Structural and functional MRI, MEG, and cognitive data from a cross-sectional adult lifespan sample. NeuroImage 2017; 144(Pt B): 262-9.
Van Petten C. Relationship between hippocampal volume and memory ability in healthy individuals across the lifespan: review and meta-analysis. Neuropsychologia 2004; 42(10): 1394-413.

van Praag H, Shubert T, Zhao C, Gage FH. Exercise enhances learning and hippocampal neurogenesis in aged mice. The Journal of neuroscience : the official journal of the Society for Neuroscience 2005; 25(38): 8680-5.

Ziontz J, Bilgel M, Shafer AT, Moghekar A, Elkins W, Helphey J*, et al.* Tau pathology in cognitively normal older adults: Associations with brain atrophy and cognitive decline. bioRxiv 2019: 611186.

Supplemental material

Supplementary material is available at Brain online.

1 Methods

Age and disease specific cluster solutions based on bootstrapping

In this study, a bootstrapping approach was applied following a two steps procedure. First, we created bootstrap samples at the step of computation of the covariance matrices (correlating seed and target grey matter values) (Fig. 1). In a second step, bootstrapping was applied after having generated the clustering of each bootstrap samples.

In the first case, the bootstrap number was identical to the sample size generating as many bootstrap samples as participants in the sample. As bootstrapping is resampling with replacement, different versions of the original sample were generated. The covariance matrices for each bootstrap sample were computed by correlating the seed and target matrices within each generated bootstrap sample. Afterwards, we applied the clustering algorithm on these covariance matrices resulting in a solution matrix for each dataset-group (e.g. HCP_young, eNKI_old etc). This solution matrix contained, for each bootstrap sample (i.e. for each different version of the original sample), the assignment of each seed voxel to a cluster (i.e. the clustering). We merged the dataset and group specific matrices into one group-specific matrix (e.g. HCP_Young, eNKI_Young and CamCAN_Young => Young) containing for each bootstrap sample, the cluster assignment of each voxel. We again applied bootstrapping (10 000 iterations) on the group specific merged (across datasets) solution matrix to ensure further stability and to eliminate further noise. In other words, we bootstrapped the bootstrap samples containing the clustering (assignment of voxels to clusters). After this step the final matrix contained the final ("stable") cluster assignment of each seed-voxel by taking the mode for each seed-voxel across 10 000 bootstrap samples (Fig. 1).

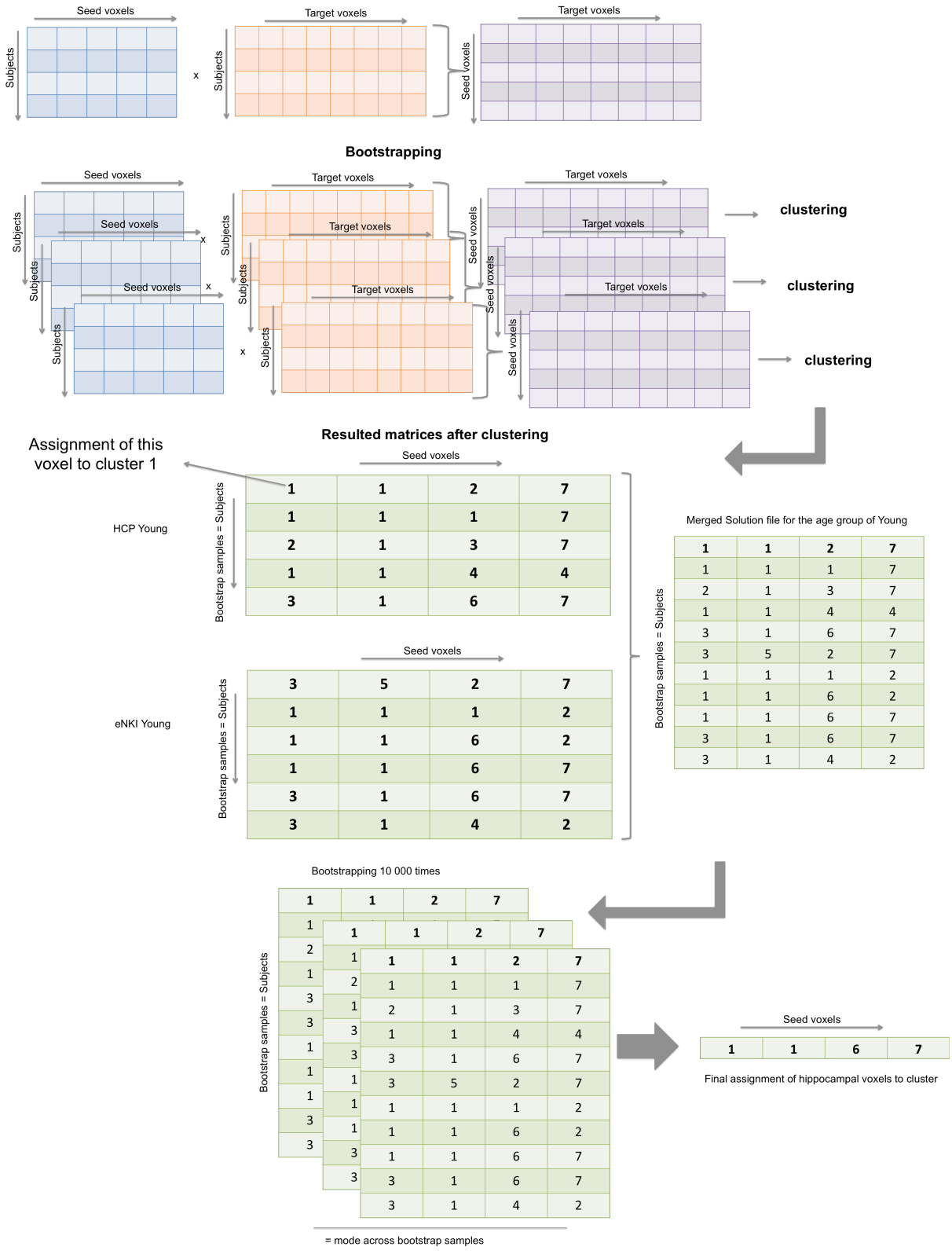

Figure 1. Illustration for the computation of a stable clustering with a bootstrapping approach.

2 Results

2.1 Clusters' stability and consistency

Simple cluster solutions (2 and 3) were more stable than partitions of higher granularity and were dependent on dataset and age/disease group. In several datasets, stability seemed to increase (or to remain stable) from 2 to 3 cluster solutions in both the right (in HCP, 1000BRAINS and eNKI) and left (in eNKI, 1000BRAINS and OASIS3) hippocampi (Fig.1). In contrast, a clear increase in stability from 3 to 4 clusters solution was only observed in the CamCAN dataset (n=94) suggesting that this pattern could be dataset specific.

We additionally examined whether stability of clusters was also dependent on age and disease group and performed a 5 (age/disease group: young, middle age, elderly, MCI, dementia) x 6 (cluster solution: 2-7) ANOVA with the aRI as dependent variable. The ANOVAs were performed separately for each hemisphere.

For the right hippocampus all main and the interaction effects were significant: cluster solution, $F(5,839970)=45388.74$, $P < 0.001$, age/disease group, $F(4,839970) = 24244.72$, $P < 0.001$, cluster solution x age/disease group, $F(20,839970) = 5406.63$, $P < 0.001$. Post-hoc Bonferroni corrected multiple comparison computations revealed that MCI was the age/disease group with the most stable cluster solutions (aRI=0.95), followed by young (aRI=0.94) and elderly (aRI = 0.94), middle aged (aRI=93), and dementia (aRI= 0.90).

For the left hippocampus all main and the interaction effects were also significant: cluster solution, $F(5,839970) = 20243.24$, $P < 0.001$, age/disease group, $F(4,839970) = 8929.86$, $P < 0.001$, cluster solution x age/disease group, $F(20,839970) = 259.13$, $P < 0.001$. Post-hoc Bonferroni corrected multiple comparison computations revealed that elderly had the most stable partitions (aRI=0.94), followed by MCI (aRI=0.94), young (aRI = 0.93), middle aged (aRI = 0.92) and dementia (aRI = 0.93).

The most stable cluster solutions were 2 (right aRI=0.96, left aRI =0.96), 3 (right aRI=0.95, left aRI=0.95), and 4 (right aRI=0.94, left aRI =0.94) followed by 5 (right aRI=0.91, left aRI =0.92) and 6 (right aRI=0.91, left aRI = 0.92), and 7 (right aRI=0.90, left aRI = 0.93).

Overall, more basic cluster solutions such as 2, 3 and 4 were preferred compared to higher granularities in different age/disease groups (Fig. 2). Except for the MCI group the stability for all the other groups dropped after cluster solution 4 indicating less consistency in the differentiations.

Cluster stability dependent on dataset

Right hippocampus

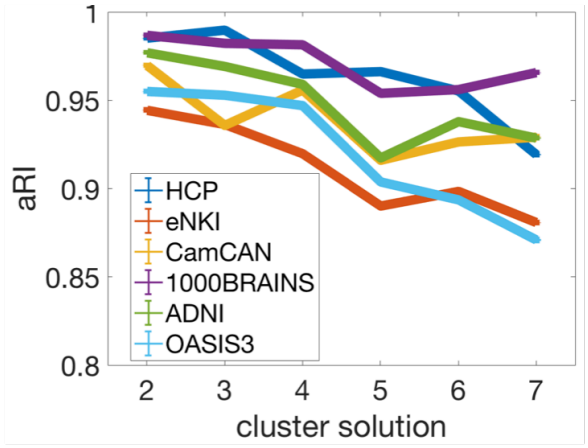

Left hippocampus

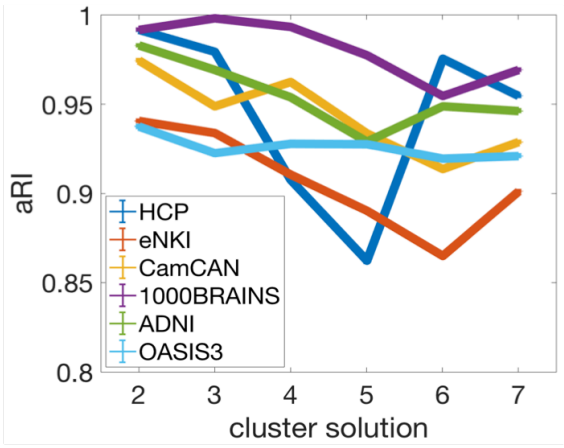

Cluster stability of age and disease groups

Right hippocampus

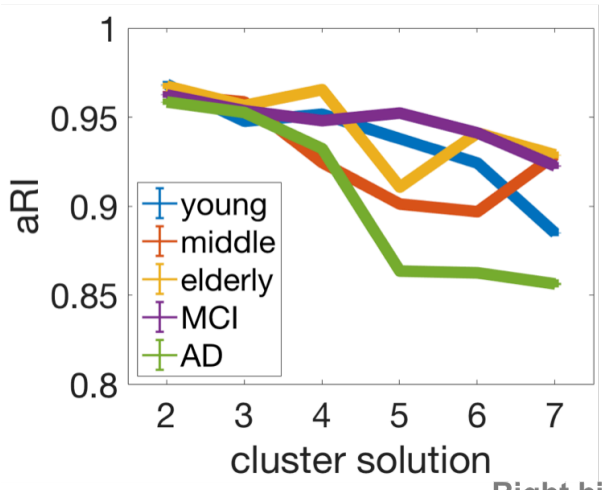

Left hippocampus

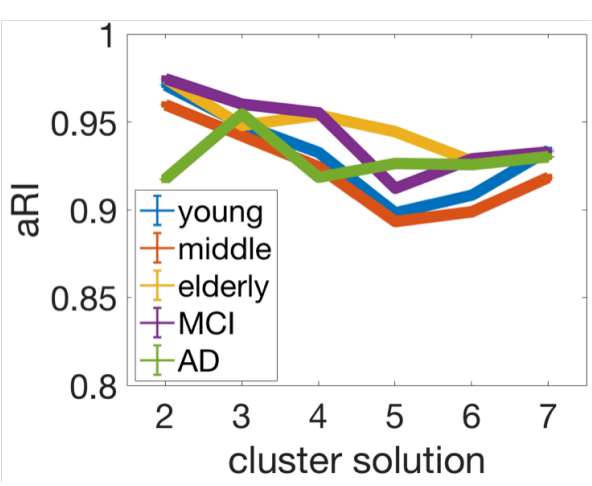

Right hippocampus

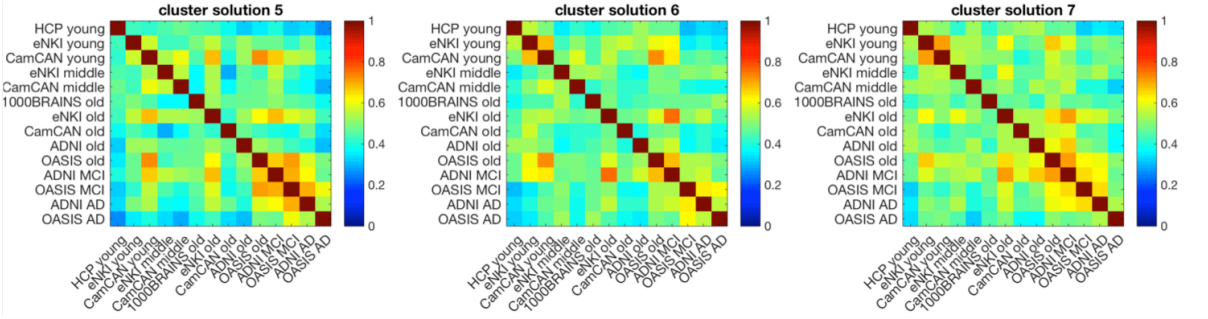

Left hippocampus

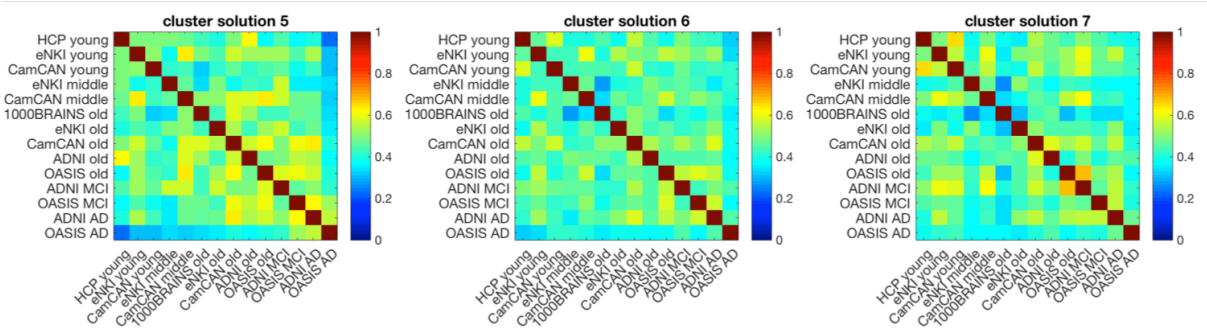

Figure 2. A) Clusters' stability dependent on dataset and age/disease groups. Lower cluster solutions (2-4) demonstrated a higher stability compared to higher cluster solutions, even though the stability was overall high > .85. B) Clusters' consistency across dataset and age/disease was low for higher cluster solutions (5-7) indicating higher heterogeneity in higher granularities possibly due to dataset intrinsic features.

2.2 Silhouette estimation of clusterings

The choice of the optimal cluster solution was guided by three criteria. To estimate the internal validity, we used stability measures estimated with split-half cross-validation and consistency measure using the mean silhouette values. As an approximation of external validity, we assessed the consistency of parcellations across datasets and age/disease specific groups.

Based on the silhouette value, our results indicated that cluster solution 2 and 3 (across all age and disease groups) provide the best data representation of voxels' differentiation in the hippocampus (Fig. 3). This result was in accordance with our previous results based on split-half cross validation and based on consistency across groups and datasets.

The silhouette value was defined in terms of both similarity and distance metric comparing cluster compactness to cluster separation. Silhouette values can range between -1 and +1. Higher positive values indicate a better fit of each individual voxel to the cluster it was assigned to. Negative values indicate a poor fit in the assignment.

We tested with an ANOVA whether silhouette values were significantly different between groups (young, middle-aged, elderly, MCI and dementia) and cluster solutions (k=2:7), revealing significant main effects of group, [$F(4,25920) = 30.26$, $P < 0.0001$ for right hippocampus; $F(4,24900)=25.73$, $P < 0.001$ for the left hippocampus], cluster solutions, [$F(5,25920)=693.6$, $P < 0.0001$ for right hippocampus; $F(5,24900)=586.27$, $P < 0.001$ for left hippocampus] and the interaction effect, [$F(20,25920) = 17.48$, $P < 0.0001$ for right hippocampus; $F(20,24900)=8.09$, $P < 0.001$ for left hippocampus].

More simplistic differentiations into 2, 3 and 4 clusters had significantly higher silhouette values compared to subdivision patterns of higher granularity for both, right and left hippocampus ($P < 0.001$, Bonferroni corrected comparisons revealed ($P < 0.001$). But there was no significant difference between cluster solution 5 and 6 ($P =0.32$ for right hippocampus and $P = 0.62$ for left hippocampus).

Post-hoc Bonferroni corrected multiple comparisons showed that parcellations in young and middle-aged participants had lower silhouette values compared to all the other groups (young vs all the other groups $P < 0.001$ for right hippocampus; young and middle aged ($P = 0.77$) compared to all the other groups $P < 0.001$ for the left hippocampus). There was no significant difference in silhouette values between the group of elderly and dementia patients ($P = 0.39$ for left hippocampus).

In sum, the silhouette metric supported cluster solution 2 and 3 as optimal subdivisions for the hippocampus across age and disease groups.

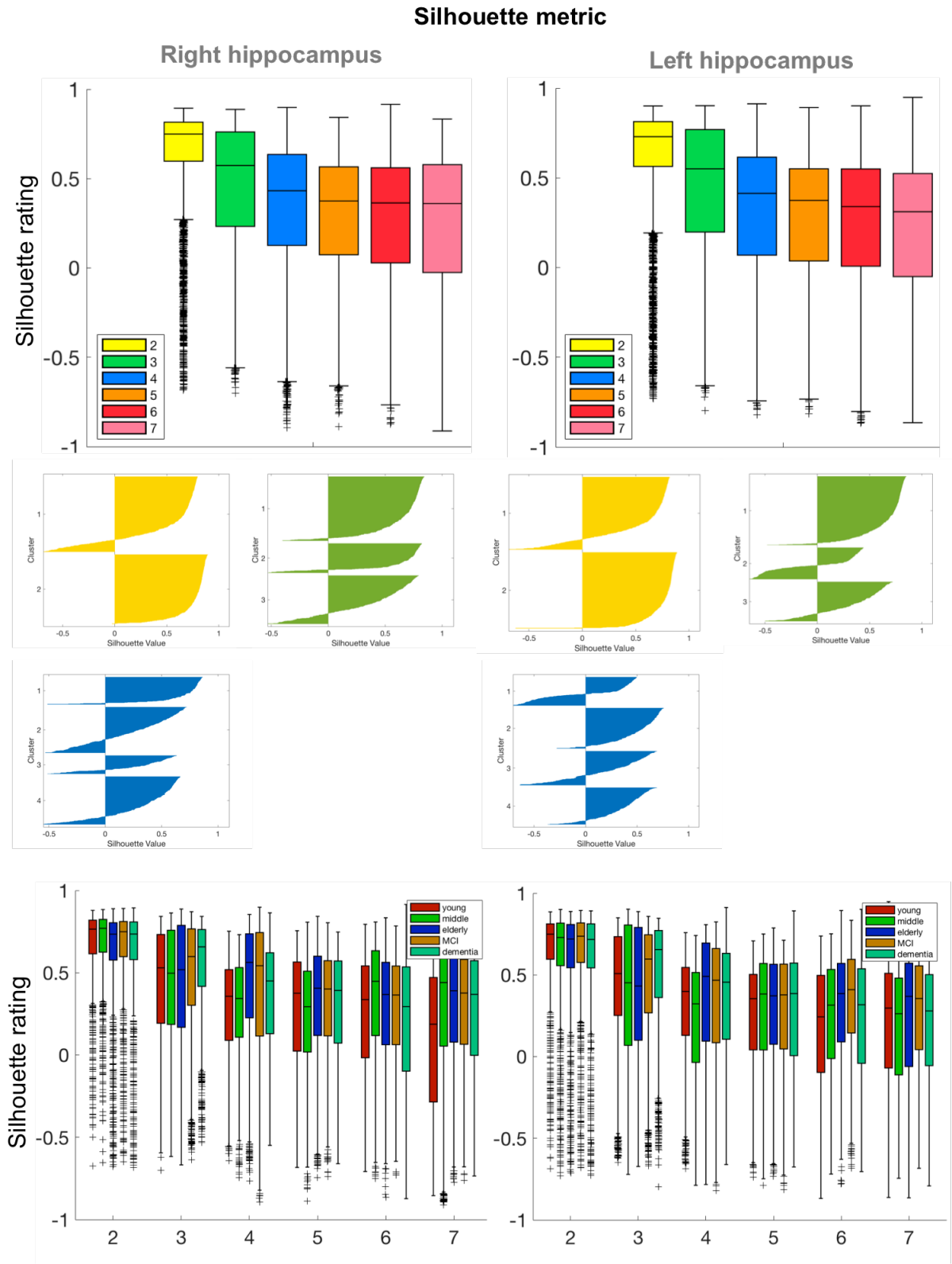

Figure 3. Silhouette measure for right and left hippocampus across age and disease groups and cluster solutions. Boxplots show the median, 1.5 interquartile range, min. Q1-1.5*IQR, max. Q3+1.5*IQR.

2.3 Dataset specific similarity of cluster solution three

Cluster solution 3 showed very high similarity across datasets and age/disease groups dividing the hippocampus in an anterior head region, lateral and medial subregions. Independent of dataset, in the group of young adulthood the tail was covered by the lateral (green) parcel, whereas with increasing age the lateral subregion decreased gradually from the tail. The parcellation in the CamCAN young sample did not follow this differentiation probably due to either a high variability within a small sample size (n=94) or dataset specific intrinsic features.

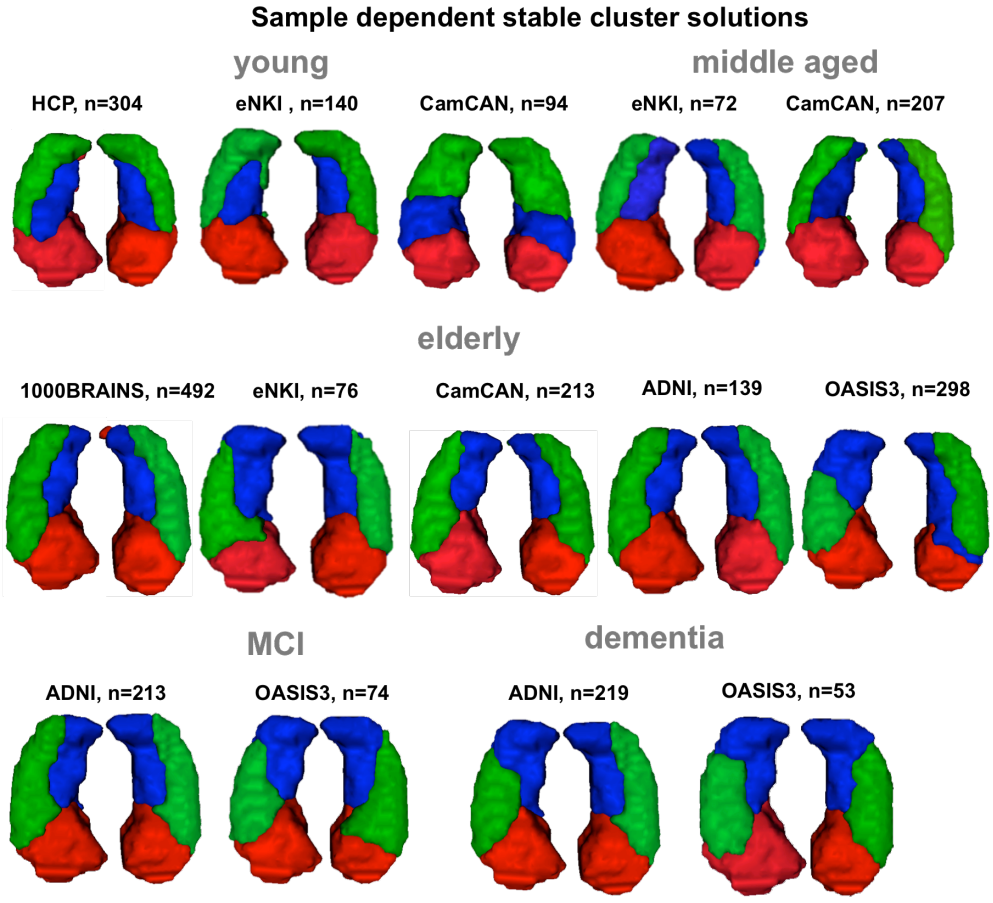

Figure 4. Sample and age/disease specific 3-cluster solution differentiation. Overall hippocampal parcellation showed a high similarity for each age/disease group even though derived from different datasets. In cases where high variability is to expect (young, middle aged and MCI patients) clusterings diverged slightly coming from different datasets. CamCAN_young and OASIS_old slightly dropped out from the overall phenotype parcellation pattern.

2.4 Age and disease specific differentiation of cluster solution two and three

Based on stability and consistency measures we chose cluster solution 3 to study lifespan and disease related alterations, as this differentiation seemed to be more neurobiologically informative than others. First, the differentiation into 3 clusters was stable enough to ensure that we measured the same biological feature. Secondly, despite stability, it also captured age and disease dependent divergences that better reflected co-plasticity and co-atrophy than cluster solution 2. Indeed the differentiation into 2 clusters was more stable than cluster solution 3 but it was less suitable to study alterations, as this differentiation mirrored a very stable simple partition into one anterior and one posterior subregion independent of age and disease condition (Fig. 5). On the other hand, cluster solution 4 was less stable and more diverse in its qualitatively unique differentiation pattern across age/disease groups, which showed less convergence between groups (Fig. 5), and therefore challenging to study related features of aging and dementia. In the group of young and middle aged healthy adults, the subdivision into 4 parcels resulted in an additional cluster in the head hippocampus, whereas in healthy elderly and in MCI patients the posterior lateral subregion was subdivided additionally in the tail. In dementia, however, the fourth subregion emerged in the medial head-body region, illustrating high divergence between age/disease groups.

Overall, as already summarized in our analysis the composition of stability and consistency of differentiations driven by age/disease specific intrinsic characteristics are better represented in cluster solution 3 compared to 2 and 4.

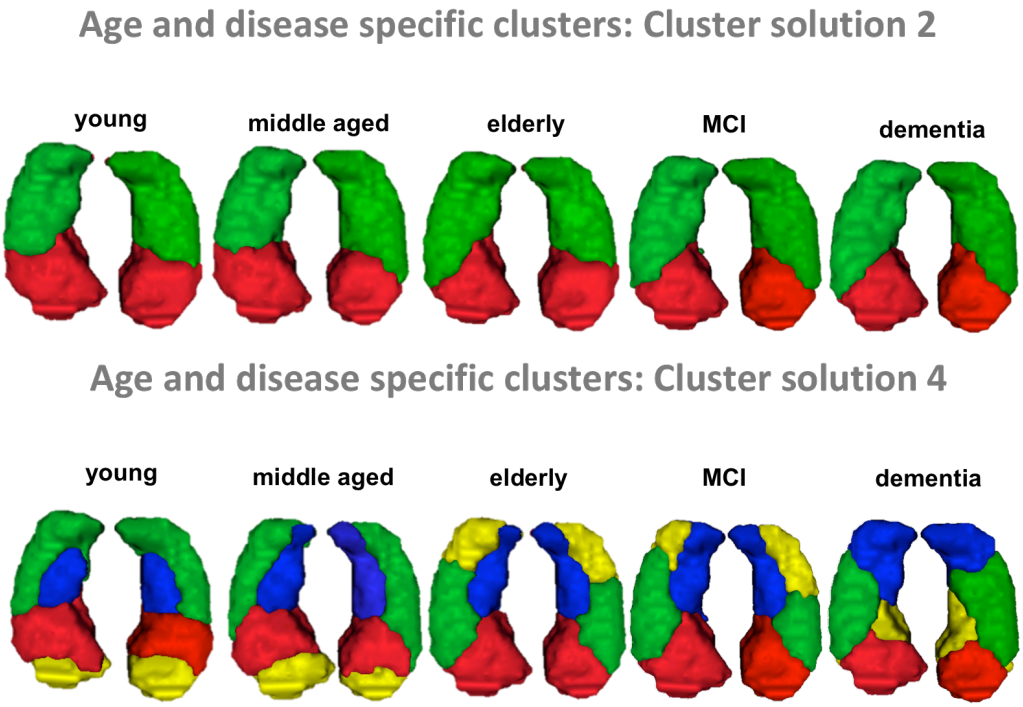

Figure 5. Age/disease specific and stable differentiations of the hippocampus into 2 and 4 parcels.

2.5 Hippocampal structural covariance networks

Uncorrected and corrected structural co-variance networks across age/disease groups.

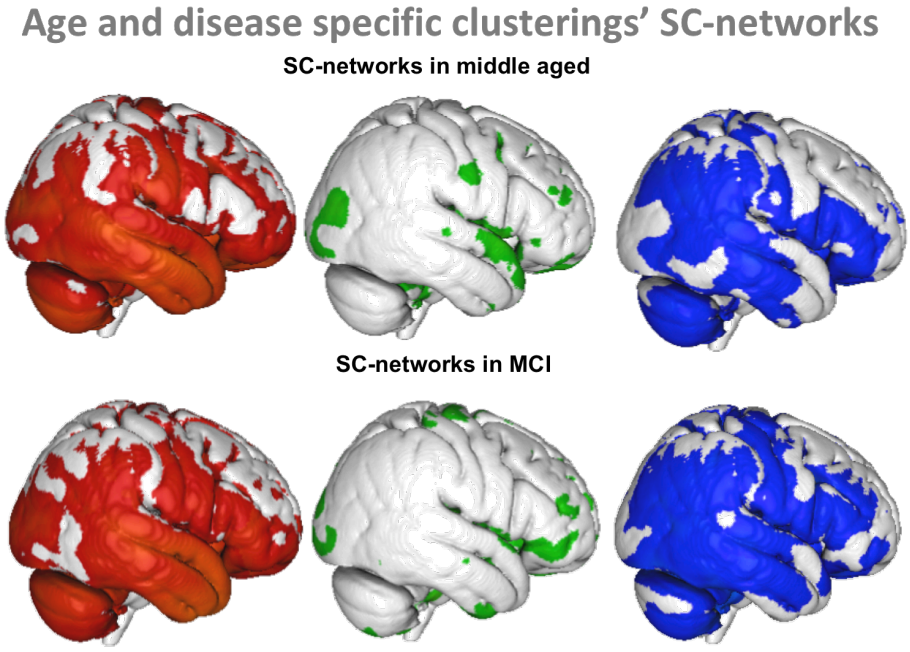

Figure 6. Uncorrected ($P < 0.001$, T=1) structural covariance networks of hippocampal clusters in middle age and MCI age/disease group.

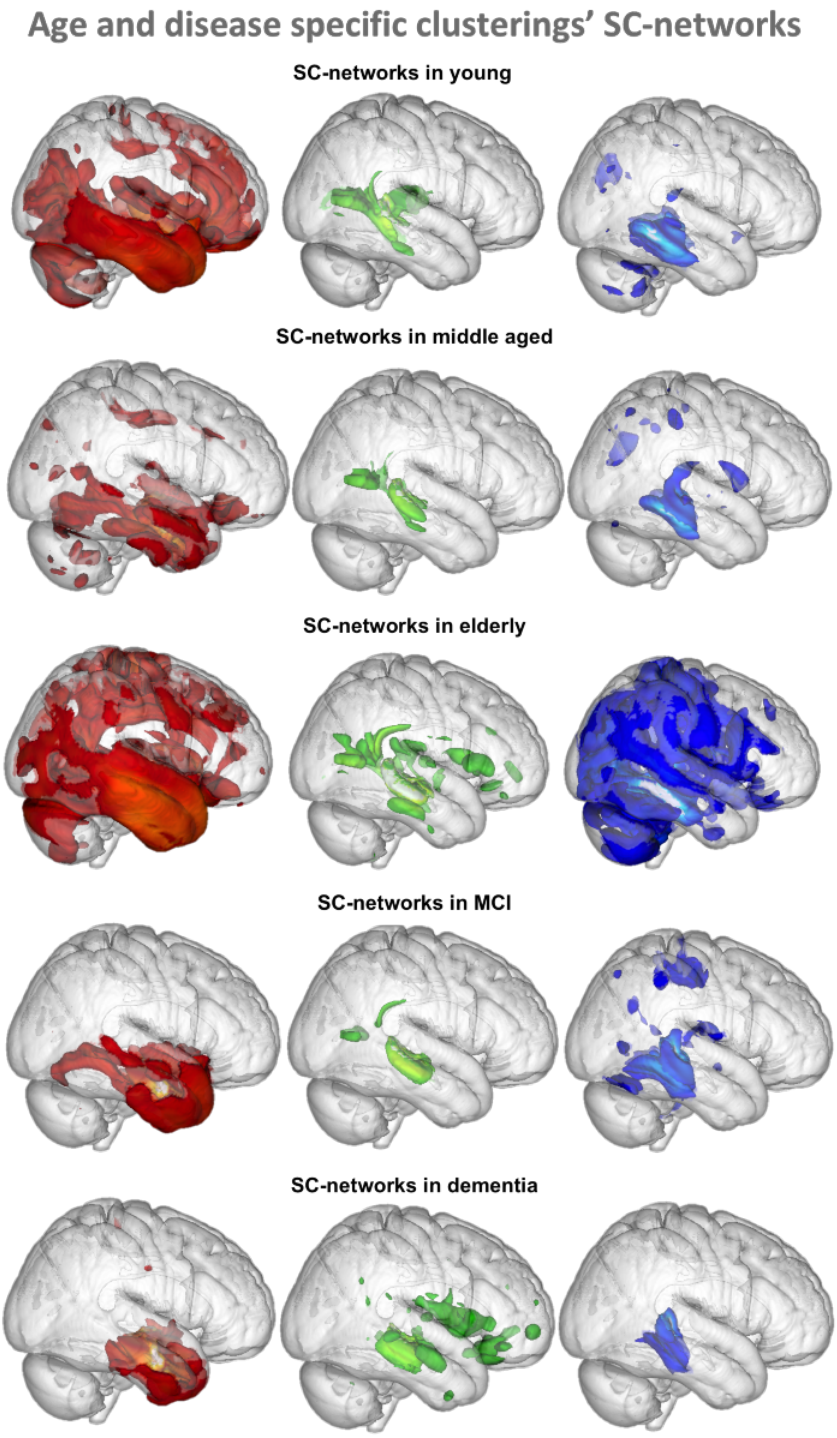

Figure 7. Corrected (FWE, $P < 0.05$, T=4.46) structural covariance networks of hippocampal clusters dependent on age/disease groups.

2.6 Harmonized hippocampal structural covariance networks

In order to account for data coming from different sites the grey matter values that were used for the general linear model in SPM to obtain underlying structural covariance networks of hippocampal subregions, were harmonized. To reduce site related noise, we harmonized the

grey matter values (https://github.com/Jfortin1/ComBatHarmonization) (Fortin et al., 2018) across sites n=71, before performing general linear model computations. The primary function of harmonization is to reduce unwanted, non-biological sources of variance related to MRI scanners and sites such as field strength, manufacturer and divergent scanning protocols (Fortin et al., 2018). Harmonized hippocampal structural covariance networks are represented in Fig. 8 and Fig. 9 showing similar patterns compared to non-harmonized data.

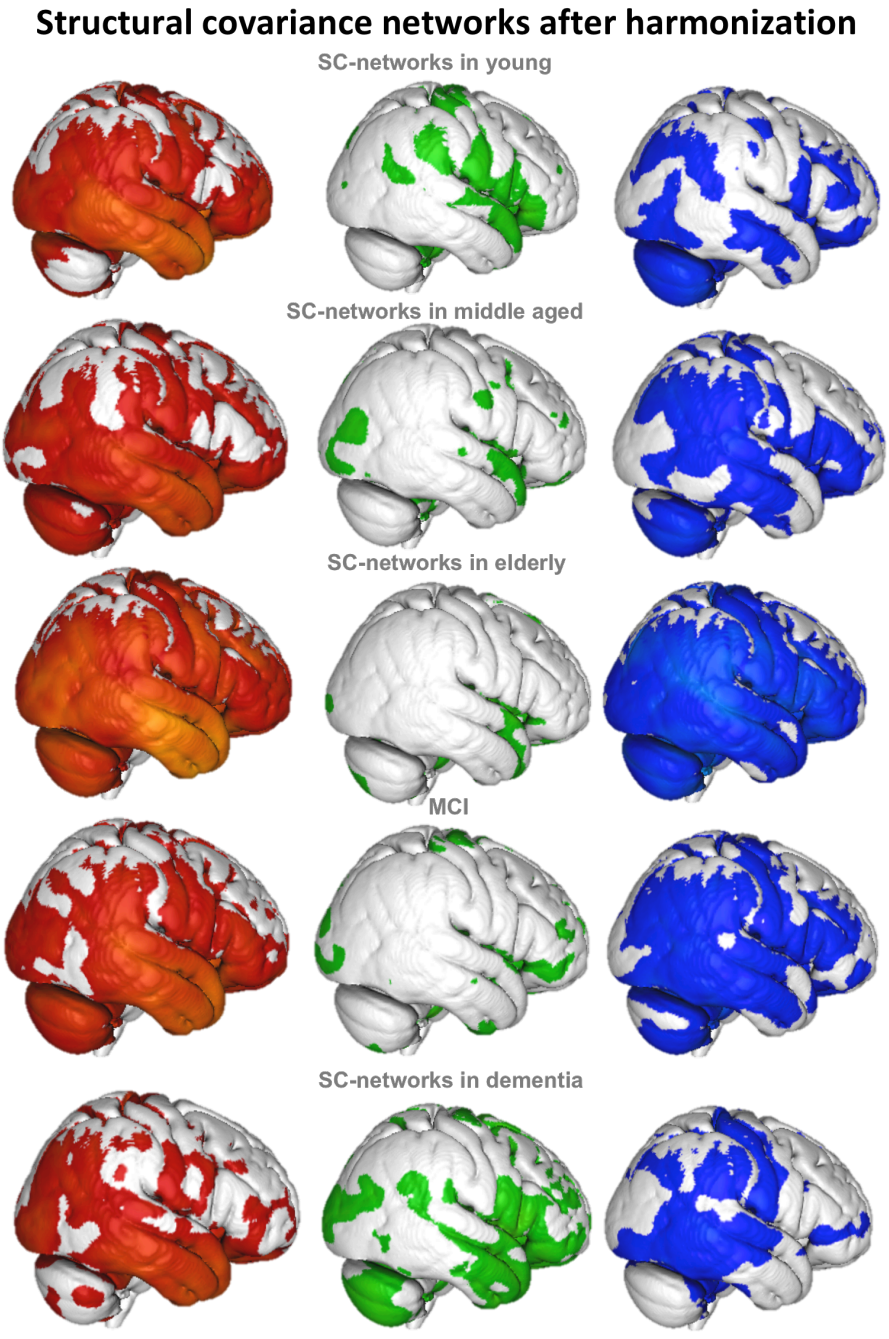

Figure 8. Uncorrected ($P < 0.001$, T=1) hippocampus associated structural covariance networks derived after harmonization of grey matter values.

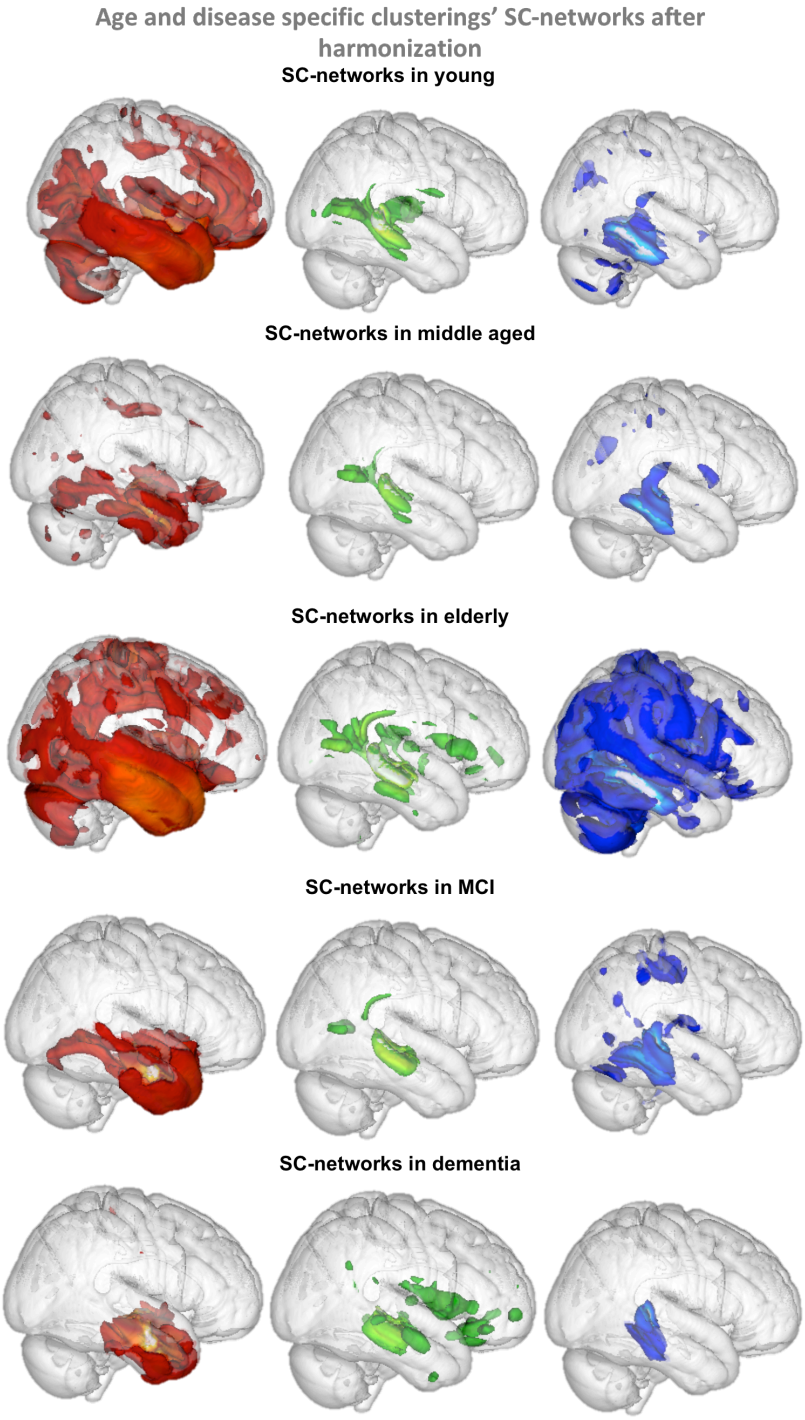

Figure 9. Corrected (FWE, $P < 0.05$, T=4.46) structural covariance networks of hippocampal clusters derived after harmonization of grey matter values.

2.7 Behavioral profiling of clusters' structural covariance networks

In the group of middle-aged participants and MCI patients the behavioral profile of the anterior and medial cluster did not change compared to other healthy age groups. The anterior cluster was involved in the perceptual-emotional-regulatory processing of information into self-relevant internal memories. The medial (blue) cluster was associated with motor exploration and orientation behavior (Fig. 10), but in MCI patients the medial (blue) cluster was additionally related to behavioral terms such as recognition, recollection and retrieval.

In both groups of middle-aged and MCI patients, the behavioral association of the lateral (green) cluster was less distinctive compared to the anterior and medial clusters. In MCI patients it was related to autobiographical memory, episodic memory and retrieval, all terms also related to either the medial or anterior parcel.

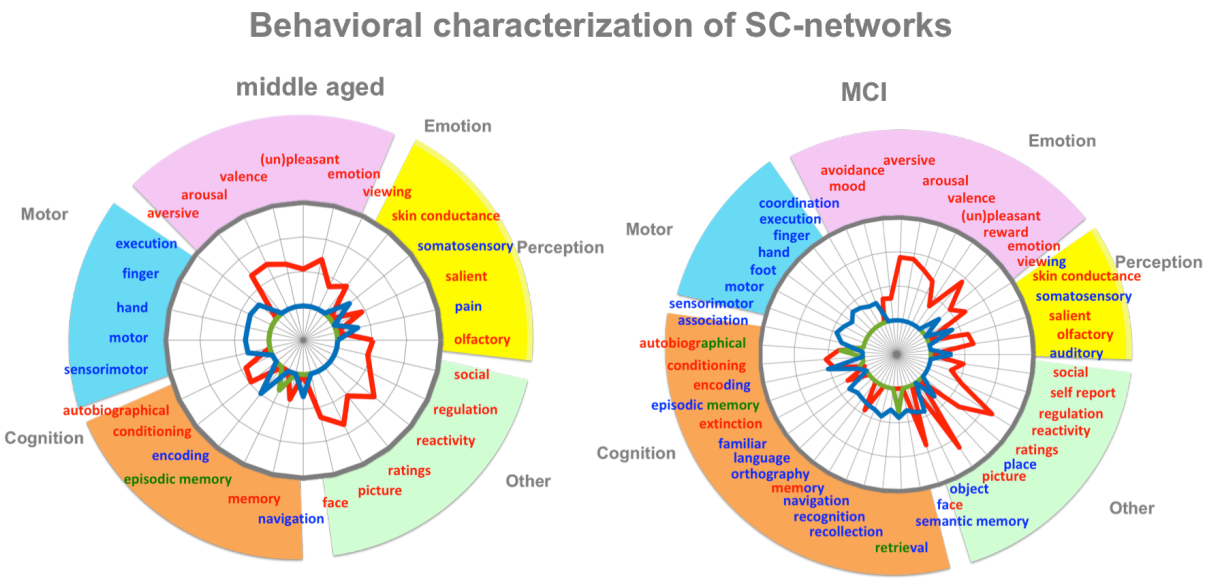

Figure 10. Behavioral characterization of structural covariance networks in the group of middle aged healthy adults and MCI patients.

3 Discussion

Structural covariance pattern in the hippocampus in MCI resemble healthy adults' pattern

In addition to our observations that the pattern of hippocampus differentiation based on structural covariance remained similar across age groups, we also found that this pattern was replicated in patients with mild cognitive impairment, despite an ongoing decrease in the tail of the lateral (green) subregion. Accordingly, the hippocampus' differentiation pattern in MCI represents a transition model between normal covariance in healthy aging and co-atrophy caused by pathology of dementia. One reason for a higher similarity with healthy elderly in this study might be the criteria of selection of the MCI patients. We here selected only patients with a strict *very mild* cognitive impairment (e.g. ADNI sample) by excluding patients with more pronounced memory deficits associated with Alzheimer's disease. In other words, we have excluded patients who were likely to be patients with Alzheimer-type pathology at the early stage of the disease (*late MCI*). We therefore hypothesize that some participants were patients at a so early stage of Alzheimer's disease that pathology hasn't affected brain structure in a way that would result in qualitatively different disease-related structural covariance patterns.

Asymmetrical differentiation pattern of the hippocampus in dementia

We found asymmetric differentiation patterns in our study for the right and left hippocampus, which were especially evident in the MCI and dementia group with the left hippocampus seemingly being more affected by disease. In MCI, this could be inferred by a higher decrease of the lateral-green cluster from the tail and, in dementia, by a higher extension of the lateral-body cluster into the medial direction. Higher left hippocampal susceptibility was already reported several times in the context of volume reductions in dementia and MCI (Lindberg et al., 2012; Müller et al., 2005; Shi et al., 2009). It has been hypothesized that aging and disease affect more likely the left hemisphere than the right hemisphere. Nevertheless, a meta-analysis by Minkova et al. (2017) suggested a lack of support for this hypothesis, despite a tendency for the right hippocampus to be more atrophied in MCI and the left hippocampus being more affected in AD. Global lateralized atrophy as assessed by Minkova et al. (2017) might appear late in pathology or with increase in disease severity. In contrast, lateralized

differentiation patterns as investigated in the present study, seem to be more evident in the hippocampus in dementia. Future studies could reveal under which circumstances lateralized differentiation patterns and lateralized atrophy arise.

References

Fortin J-P, Cullen N, Sheline YI, Taylor WD, Aselcioglu I, Cook PA*, et al.* Harmonization of cortical thickness measurements across scanners and sites. NeuroImage 2018; 167: 104-20.

Lindberg O, Walterfang M, Looi JC, Malykhin N, Ostberg P, Zandbelt B*, et al.* Hippocampal shape analysis in Alzheimer's disease and frontotemporal lobar degeneration subtypes. Journal of Alzheimer's disease : JAD 2012; 30(2): 355-65.

Minkova L, Habich A, Peter J, Kaller CP, Eickhoff SB, Kloppel S. Gray matter asymmetries in aging and neurodegeneration: A review and meta-analysis. Human brain mapping 2017; 38(12): 5890-904.

Müller MJ, Greverus D, Dellani PR, Weibrich C, Wille PR, Scheurich A*, et al.* Functional implications of hippocampal volume and diffusivity in mild cognitive impairment. NeuroImage 2005; 28(4): 1033-42.

Shi F, Liu B, Zhou Y, Yu C, Jiang T. Hippocampal volume and asymmetry in mild cognitive impairment and Alzheimer's disease: Meta-analyses of MRI studies. Hippocampus 2009; 19(11): 1055-64.

4 General Discussion

Hippocampal organization was primary known based on micro-anatomical features of cytoarchitecture revealing a differentiation pattern along the medial-lateral and dorsal-ventral dimensions, whereas functional studies suggested a differentiation along the longitudinal axis. Since hippocampal maps based on large-scale networks at the macro-level were missing, the overarching aim of this thesis was to explore hippocampal organization based on large-scale networks. Therefore different MRI modalities such as task-(un)related functional connectivity and structural covariance were used in order to investigate the hippocampus from different perspectives.

As hypothesized hippocampal maps of both functional MRI modalities, MACM and RSFC, were more similar to each other than to structural covariance. Moreover, as already indicated by animal studies and suggested by some researchers in humans, we found that the hippocampus was primarily organized along the longitudinal axis based on functional connectivity, especially for simpler patterns of 3 and 5 clusters. More complex differentiation patterns of 7 subregions, however, indicated a differentiation along the medial-lateral dimension in addition to the anterior-posterior dimension. Hippocampal maps based on structural covariance revealed an extraordinary differentiation pattern. With a head subregion the maps mirrored an anterior-posterior subdivision but with the posterior hippocampus being divided into a medial and a lateral subregion, they represented mainly a pattern along the medial-lateral dimension.

One of the challenges of the first study was to ensure stable differentiation patterns while using RSFC, which is especially prone to noise, be it motion or respiration artifacts. To test for the best denoising strategy, two criteria were applied: a) how well were artifacts removed and b) how well was it possible to discriminate between voxels within the hippocampus, which was relevant for stable clustering patterns. Optimal results were achieved with the combination of a model-based and a model-free denoising strategy, FIX+WM/CSF regression. It reduced structured noise and enhanced the dissimilarity of connectivity profiles of hippocampal voxels, facilitating to differentiate between voxels' profiles and hence clustering.

Another aim of the study was to test whether hippocampal organization is related to a specific behavioral profile as indicated in rodent studies. Our behavioral characterization of hippocampal subregions along the longitudinal axis, on the one hand, reproduced the emotion-cognition gradient suggested in rodents (M. B. Moser & Moser, 1998), but also

indicated an additional behavioral gradient, of self-centric vs. world-centric information processing summarizing previous proposed behavioral theories of the hippocampus.

After having extracted our hippocampal maps based on different MRI measures, I was interested in investigating whether they remain stable across the lifespan and in disease. Given the lack of consistency and specificity in atrophy patterns across studies and given the lack of age and disease dependent hippocampal maps, the second study aimed extract age and disease-specific maps. Using structural covariance the hippocampus was separately parcellated in the group of young, middle-aged, and elderly healthy participants, as well as in MCI and dementia patients. Overall, stable and consistent differentiation patterns were found for basic parcellation schemes of 3 clusters dividing the hippocampus into head, lateral and medial subregions reminding of the cytoarchitectonic differentiation between CA and subiculum.

The differentiation into 3 subregions optimally captured age and disease dependent changes. In study 2, we reproduced the map of the hippocampus of young participants based on structural covariance as reported in study 1, pointing to a robust differentiation pattern based on macro-structural measures. Moreover, high similarity of differentiation patterns across dataset samples (e.g. young, elderly, dementia) was found, supporting the assumption that alterations in hippocampal organization were driven by aging and disease and not due to dataset specific measurement noise.

Prominent age-related changes were detected in the posterior hippocampus, as the lateral subregion decreased with higher age from the tail. In dementia, however, the lateral subregion expanded into the medial direction covering the body of the hippocampus, resembling the tripartite organization (i.e. head-body-tail) found with functional connectivity measures in the first study.

Behavioral characterization of underlying subregions' structural covariance networks revealed that the head subregion was consistently associated with self-related automatic processing of information (e.g. autobiographical memory, emotions, reactivity) independent of age or disease. This was however not the case for the behavioral associations of the lateral and medial subregions, which underwent alterations across the lifespan due to co-plasticity and co-atrophy in aging and dementia. In the first period of life, the medial subregion (Study 2, Fig. 4) was primarily associated with the processing of visual information (e.g. place, objects, encoding), while in the second half of life, the medial subregion was additionally associated with motoric coordination and navigation. Substantial behavioral alterations were found for the lateral subregion in dementia (Study 2, Fig. 4). While being less defined in healthy

populations, it was behaviorally associated in dementia with theory of mind, comprehension, orthography and language, indicating its involvement in a functional network probably related to communication.

Both studies demonstrate that the organization of the hippocampus can be studied from different perspectives such as functional connectivity and structural covariance. Hippocampal organization based on functional connectivity suggests mainly a differentiation along the anterior-posterior dimension whereas organization based on structural covariance mainly suggests a differentiation along the medial-lateral dimension resembling micro-anatomical differentiation. Finally, it should be emphasized that hippocampal differentiation is dependent on changes of large-scale networks over the course of lifetime and in pathology influencing behavior.

4.1 Hippocampal organization along the medial-lateral vs. anterior-posterior dimension

Despite a rough resemblance, hippocampal organizations derived from functional connectivity and structural covariance contrasted with the organization pattern known from histology along the medial-lateral and ventral-dorsal dimension. Parcellations based on functional connectivity were mainly organized along the anterior-posterior dimension whereas parcellations based on structural covariance mainly displayed an organization along the medial-lateral dimension.

This raises the question, which organization pattern represents better the underlying biological composition of the hippocampus? And, could different organization patterns co-exist along both dimensions?

In line with our results, previous studies indicated that the preliminary organizational dimension of the hippocampus primarily depends on the feature by which the hippocampus is differentiated. A differentiation along the anterior-posterior dimension was proposed by studies investigating theta propagation in electrophysiological recordings in rodents (Lubenov & Siapas, 2009), intra-hippocampal functional (Dalton et al., 2019) and anatomical connectivity (Beaujoin et al., 2018), size of place fields (Jung et al., 1994; Kjelstrup et al., 2008; Maurer, VanRhoads, Sutherland, Lipa, & McNaughton, 2005), and gene expressions (Fanselow & Dong, 2010; Vogel et al., 2020). Within the subfields anatomical (in monkeys) (R. Insausti & Munoz, 2001) and functional connectivity in humans is also organized along the longitudinal axis (Dalton et al., 2019; Libby et al., 2012; Maass, Berron, Libby, Ranganath, & Düzel, 2015; Vos de Wael et al., 2018). Recent work focusing on gradients in

contrast to parcellations, also proposed a functional gradient (Przeździk, Faber, Fernández, Beckmann, & Haak, 2019) and a gradient of gene expression along the longitudinal axis (Vogel et al., 2020). Vos de Wael et al. (2018) identified two organizational gradients, one along the anterior-posterior dimension based on functional connectivity and a second one along the medial-lateral dimension based on microstructure supporting our own findings.

Studies that primarily found an organization along the medial-lateral dimension often investigated microstructural features within the hippocampus not taking extra-hippocampal connectivity into account. DeKraker, Lau, Ferko, Khan, and Köhler (2020), for example, chose morphological and laminar features for hippocampal mapping and demonstrated that thickness, gyrification, and mean neural density (previously the main feature in classical histological mapping) reveal a differentiation pattern along the medial-lateral dimension dividing the hippocampus into the known subfields. Gyrification, however, indicated a differentiation pattern along the anterior-posterior dimension, when studying it within subfields.

Thus, these studies and findings highly emphasize that there are at least two main organizational dimensions in the hippocampus. Moreover, our parcellation work did not suggest exclusively either a differentiation schema along the one or exclusively along the other dimension, but rather a combination of both supporting the assumption that differentiation patterns along both dimensions are valid and complement each other.

Very recent work by Kharabian Masouleh, Plachti, Hoffstaedter, Eickhoff, and Genon (2020) identified even a third potential organizational dimension along the ventral-dorsal axis based on structural covariance, which was in line with Bajada et al. (2017), who reported patterns of connectivity along the medial-lateral and anteroventral-posterodorsal dimension in the temporal lobe.

4.2 Behavioral characterization of hippocampus' subregions and associated structural covariance networks

While there is general agreement that the anterior hippocampus is related to episodic memory, and spatial navigation is associated with posterior hippocampus (Persson, Stening, Nordin, & Söderlund, 2018), there is so far no systematic and broad behavioral characterization bridging the gap between hippocampus organization and behavior. However, such a systematic overview would help to understand hippocampus' involvement in human's behavior and to detect early deviations in pathological conditions. Therefore, we established a behavioral

profiling of hippocampus' subregions (study 1) and the underlying structural covariance networks associated with the subregions (study 2). Both characterizations yielded similar pattern of associated behavior despite using different inputs (e.g. subregions and networks). Based on the findings of the first study, we suggest that a behavioral gradient along the anterior-posterior axis is present. Anterior subregions were more likely involved in self-centric (e.g. autobiographical memory, emotions) and posterior subregions more likely involved in world-centric information processing (e.g. navigation, objects, scenes).

In contrast to other studies (H. Kim, 2015), we did not find a clear differentiation for general psychological processes such as encoding, memory and recollection along the anterior-posterior axis. Our self-vs. world-centric processing hypothesis rather suggests that not the psychological process matters, but the quality of the information to be processed (e.g. anterior: anger, happy; posterior: visual information, navigation). I speculate that this is related to extra-hippocampal connectivity since posterior hippocampus is more likely connected to occipital and parietal cortices, while the anterior hippocampus being more connected to amygdala, anterior cingulum and orbitofrontal cortex.

In line with other studies, our behavioral profiling indicated that spatial behavior, navigation, and retrieval were more likely associated with posterior hippocampus whereas episodic memory and emotion were more likely associated with anterior hippocampus (H. Kim, 2015; Kühn & Gallinat, 2014; M. B. Moser & Moser, 1998; Nadel et al., 2013). Behavioral terms such as vestibular, imagination, recent memories and abstraction are very specific and were not found in our behavioral profiling, as suggested by previous literature (Bowman & Zeithamova, 2018; Hufner et al., 2011; Zeidman & Maguire, 2016).

The most related theory to ours is probably pattern integration vs. pattern separation (Morton et al., 2017; Zeidman & Maguire, 2016). Being able to discriminate between stimuli while exploring environments requires the ability to separate patterns or stimuli from each other, being able to differentiate between similar but not identical items. This is in line with our suggested world-centric information processing idea, namely the ability to process and to differentiate between stimuli coming from outside, which also requires to encode and to store the information. On the other hand, establishing coherent memories requires the integration of different patterns in one memory trace, which is described by our self-centric information processing or by the term pattern completion or integration. However, the theory of pattern integration vs. pattern separation was also suggested in the context of subfield organization of the hippocampus. CA3 and dentate gyrus were associated with pattern separation whereas CA1 was associated with pattern integration (Bakker et al., 2008; Dimsdale-Zucker et al.,

2018; Leutgeb, Leutgeb, Moser, & Moser, 2007). Therefore, it is unclear whether pattern integration and separation are organized along the medial-lateral or anterior-posterior axis.

In contrast to study 1, in study 2 we characterized structural covariance networks associated with hippocampal subregions instead of characterizing subregions themselves. Our results of study 1 and 2 were convergent for the anterior hippocampus showing that it is associated with self-related information processing including autobiographical memory, emotions, but also reactivity and regulation. In addition, study 2 revealed that the medial hippocampal subregion is probably involved in visual-motoric coordination and language production or processing. While visual processing was more dominant in younger years, motoric coordination and execution became more evident in the second period of life. This finding suggested that the structural covariance network of the medial subregion might co-vary with the inferior longitudinal fasciculus (ILF) associated with motoric learning, visual recognition and lexical language processing (Herbet et al., 2018). The ILF was recently identified as one of the six long-range pathways of the hippocampus (Maller et al., 2019) (Fig. 5) supporting our assumptions.

In sum, we suggest a behavioral gradient along the anterior-posterior axis of self-centric vs. world-centric information processing established on functional connectivity. The medial hippocampal subregion is more likely involved in visual and motoric behavior whereas the behavioral meaning of the network associated with the lateral subregion has to be further determined in future studies.

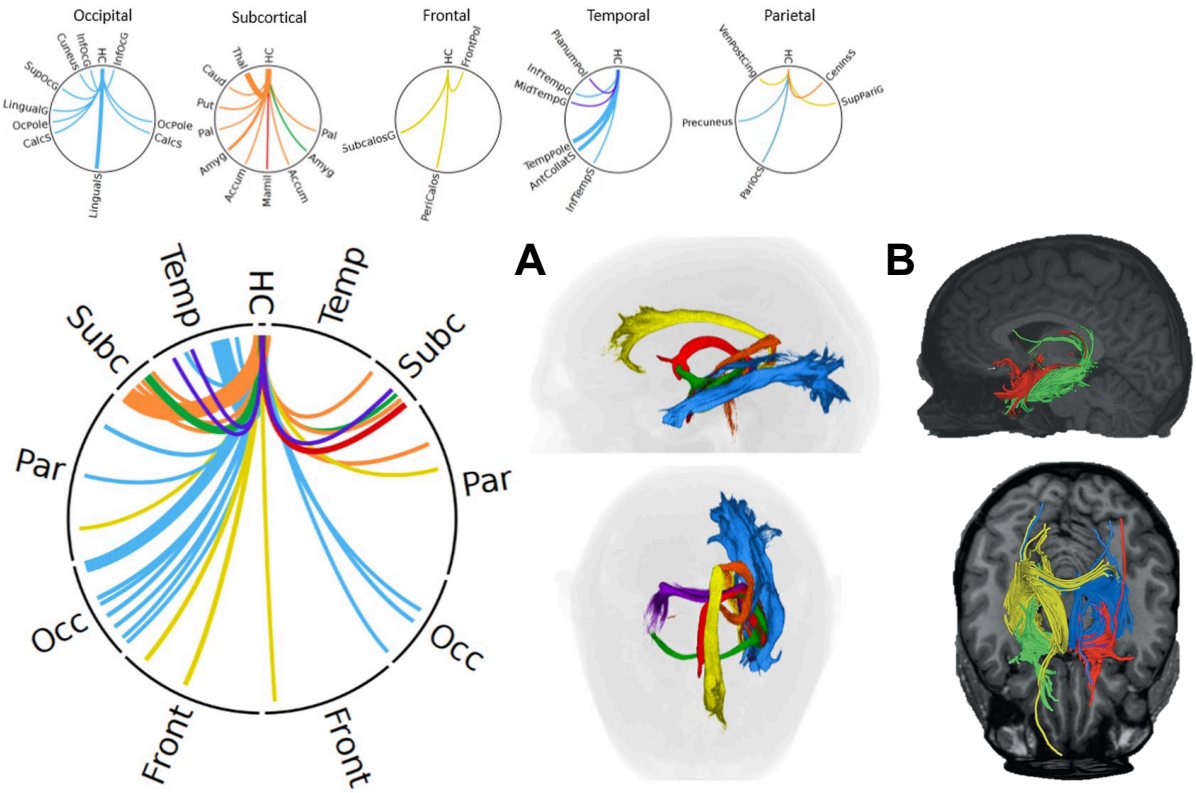

Figure 5. Hippocampal associated pathways and tracts. A) blue: inferior longitudinal fasciculus, orange: spinal-limbic pathway, yellow: cingulate bundle, green: anterior commissure, purple: tapetum, red: fornix; Adapted from Maller et al. (2019) under the Creative Commons Attribution 4.0 International License http://creativecommons.org/licenses/by/4.0/. B) Red and green fibers cross the amygdala and hippocampus. Those fibers that cross the amygdala join the orbitofrontal area and the temporal area through the uncinate fasciculus. The blue and yellow fibers follow the shape of the fornix. Some fibers join the splenium of the corpus callosum and some fibers extend to the occipital area (Colnat-Coulbois et al., 2010). Adapted with the permissions of AANS Publication.

4.3 Aging and dementia disrupt large-scale networks beyond hippocampal atrophy

Previous studies primarily examined volume reductions in the hippocampus during aging and dementia, but network reorganizations in the context of hippocampus were less intensively explored. Therefore study 2, examined changes in differentiation patterns within the hippocampus influenced by alterations of large-scale networks due to either co-plasticity or co-atrophy during aging and dementia.

If certain voxels in the hippocampus do not co-vary with certain brain regions but with other regions instead (if any), this would reflect changes in their connectivity profiles and would be

reflected in differentiation patterns within the hippocampus. Therefore, alterations in hippocampus' map would suggest that either 'connections' (meant in a statistical manner) would be lost or 'new connections' would be established, representing some kind of reorganization.

Reorganization processes were already reported in healthy aging focusing on resting-state functional connectivity (Koch et al., 2010; Zonneveld et al., 2019) and task-related co-activation networks (Stern et al., 2005), which was attributed to either functional disconnections[6] (Koch et al., 2010) or white matter tract disruptions (O'Sullivan et al., 2001).

Networks related to higher order cognition such as language-related semantic network, executive control network but also the default mode network revealed reduced structural associations in higher age compared to younger adults (Montembeault et al., 2012). In younger age structural covariance networks seem to be more distributed but get more localized with advanced age (Montembeault et al., 2012; Montembeault et al., 2016). This process speeds up in pathology, as graph theoretical analysis showed that long-range connections decrease but local connectivity increases in MCI and dementia. The consequence is a loss of network integrity and an acceleration of fragmentation of networks (He, Chen, & Evans, 2008; H.-J. Kim et al., 2016; Pereira et al., 2016).

But aging is not simply accompanied by a decrease or decline of networks, as shown in the context of medial temporal lobe and functional connectivity. A. Salami, Wahlin, Kaboodvand, Lundquist, and Nyberg (2016) reported in a cross-sectional (Alireza Salami, Pudas, & Nyberg, 2014) and in a longitudinal study a decrease in functional connectivity for anterior medial temporal lobe (including the hippocampus) during aging on the one hand. But they also reported an increase of functional connectivity for the posterior temporal lobe on the other hand (Alireza Salami et al., 2014; A. Salami et al., 2016). We also found a decrease and increase of structural covariance networks for different subregions of the hippocampus. While the lateral-green cluster decreased from the tail with higher age[7], the medial-blue cluster

---

[6] Higher task-related activity in older participants seems to contradict the disruption hypothesis. Andrews-Hanna et al. (2007) argued that disrupted and therefore segregated large-scale networks are difficult to coordinate, which results in an inefficient processing of information. In order to compensate this inefficiency, increased functional activity is recruited to get more resources in order to solve the task (Sala-Llonch, Bartres-Faz, & Junque, 2015). Morcom and Henson (2018), however, suggested that the higher frontal activity is unspecific and mirrors inefficiency and not compensation.

[7] The low behavioral specificity of structural covariance network of the lateral-green subregion and its almost linear decrease from the tail with age might be related to anatomical changes rather than behavioral changes. In younger age, the network yielded primarily associations with subcortical regions (e.g. thalamus, caudate nuclei) and decreased with higher age to parieto-occipital regions. Anatomically it was reminiscent to some extent to the grey matter regions around the dorsal hippocampal commissure, posterior cingulum, tapetum, and fornix (Postans et al., 2019), those white matter fibers/tracts connect the posterior hippocampus with contralateral hippocampus, subcortical, and posterior brain regions.
The fornix is the white matter output of the hippocampus through the tail (R. S. C. Amaral et al., 2018) and connects the hippocampus with limbic structures (i.e. hypothalamus, thalamus, nucleus accumbens) (Douet & Chang, 2015), similar to our network of the lateral subregion. The fornix has been suggested to transfer information from short-term to long-term memory

expanded more into the tail demonstrating an almost proportional relationship between age and the amount of decrease/increase. The same mechanism also applied to the underlying structural covariance networks. The associated network of the lateral-green cluster decreased with higher age to subcortical regions but the network of the medial-blue cluster expanded covering a major posterior part of the brain. In dementia, however, we found especially a decrease of the structural covariance network for the anterior subregion, being more restricted to the temporal and parietal lobes.

Nordin et al. (2018), however, yielded stable structural covariance networks for the anterior and posterior hippocampus across age groups and found no changes for anterior and posterior hippocampus except for an overall decrease in network integrity. To add to the inconsistencies, other studies reported decreased functional connectivity of the posterior hippocampus in groups of higher age (Andrews-Hanna et al., 2007; Damoiseaux, Viviano, Yuan, & Raz, 2016).

The divergences in findings are probably related to previous studies' selection criteria of the regions of interest (i.e. anterior and posterior hippocampus), differences in sample sizes and age groups. It is therefore noteworthy that we did not impose prior selection criteria on the region of interest for anterior and posterior hippocampus (in study 1 and 2) but used a purely data driven approach. Taken together, our results and some of the other studies indicate that aging is a process accompanied by co-plasticity at the functional and structural level.

In contrast to aging, Alzheimer dementia is additionally characterized by a high burden and distribution of pathogens such as amyloid plaques and tau neurofibrillary tangles (Braak & Braak, 1991; Corder et al., 2000). Amyloid plaque distributes along the default mode network (Buckner et al., 2005; Klunk et al., 2004; Montembeault et al., 2016) and tau neurofibrillary tangles co-vary strongly with functional networks (Franzmeier et al., 2019) probably resulting in a functional disconnection of the hippocampus from parietal brain regions (Pasquini et al., 2015). Previous results strongly suggest that amyloid beta and tau pathology afflict functional network integrity and contribute independently to the disruption of functional connectivity of

via the Papez circuit and is accordingly, involved in long-term memory, encoding and retrieval (Douet & Chang, 2015; Eichenbaum et al., 2007; Foster et al., 2019). The tapetum and the posterior hippocampal commissure, which are associated with learning, memory and recognition (Postans et al., 2019), transfer information between hemispheres (Maller et al., 2019). Several studies suggested that posterior hippocampal connectivity is more likely influenced by white matter disruption either of the fornix (Metzler-Baddeley et al., 2019) or of the cingulum (Catheline et al., 2010), which might explain the decrease of the lateral subregion from the tail found in study 2. The fornix starts to atrophy early after its peak in adolescence (Douet & Chang, 2015), which might explain why we see a decrease of the lateral subregion already in the group of middle aged participants. Damage of white matter glia of the fornix seems to cause grey matter damage such as neuronal loss in the hippocampus with higher age (Metzler-Baddeley et al., 2019). Grey matter alterations in the hippocampus are probably determined by these white matter changes (Spreng & Turner, 2013). In sum this raises the question whether the observed shift in hippocampal organization of the posterior part (lateral and medial subregions) reflect white matter thinning affecting grey matter co-variation of the hippocampus in healthy aging.

the medial temporal lobe (including the hippocampus) (L. Wang et al., 2013). But dementia similar to aging does not exclusively demonstrate disconnection but also increased functional connectivity as was shown between prefrontal, parietal and occipital lobes (K. Wang et al., 2007). If this also applies to structural covariance of the hippocampus, has to be shown in future studies. Our own results showed that the structural covariance network of the lateral-body subregion follows functional networks associated with theory of mind, comprehension and language suggesting a qualitative change in network co-variations.

Together this represents strong implications that dementia is not a simple accelerated aging process but functionally afflicted by pathogens, which again reshape functional and structural covariance networks influencing hippocampal differentiation patterns. These results highly suggest that the hippocampus reorganizes its structural covariance networks beyond hippocampal atrophy in healthy aging and disease. While underlying networks associated with hippocampal subregions primarily decrease in dementia, increased covariance for the posterior hippocampus in addition to decreases was observed in healthy aging.

4.4 Mild cognitive impairment - a state in between

Mild cognitive impairment is considered to be a pre-clinical stage of Alzheimer's disease especially the amnestic type of MCI seems to develop more likely Alzheimer's symptoms later on (Dubois et al., 2016). As MCI represents the silent preclinical stage, it is more related to dementia, so that we would expect differentiation patterns of the hippocampus to be more similar to dementia patients rather than to healthy elderly. In this thesis, however, late MCI patients, who are expected to be more prone to dementia than early MCI patients, were included in the dementia group and not in the MCI group. Therefore our group of MCI patients was probably healthier than a typical MCI group. Accordingly, it was not surprising that hippocampal maps of MCI patients were more similar to healthy elderly than dementia patients.

The apolipoprotein E (APOE) genotype is a risk factor for developing Alzheimer's disease and influences large-scale structural covariance networks by enhancing atrophy between thalamus, hippocampus and caudate nucleus in MCI participants (Novellino et al., 2019). As we did not differentiate between genotypes of MCI participants future studies might investigate whether genotype expressions have an influence on hippocampal differentiation patterns.

Overall MCI seems to be very similar to dementia in terms of identified atrophy in subfields (Liana G. Apostolova et al., 2006; Susanne G. Mueller et al., 2010), and disruptions in networks even though MCI also displayed an individual pattern of decreased activation in fronto-parietal network and default mode network, which differed from Alzheimer's patients (Chand, Hajjar, & Qiu, 2018; H. J. Li et al., 2015). Our group of MCI patients was probably more preserved challenging the scientific field to account for both, health and risk factors in future studies.

4.5 Cytoarchitectonic hippocampus model less supported by behavior and extra-hippocampal connectivity

Many scientists focus on the cytoarchitectonic subdivision of the hippocampus even in the context of behavior and connectivity, although D. G. Amaral and Witter (1989) already suggested to consider, not only the cytoarchitectonic-lamina subdivision, but also the anterior-posterior organization of the hippocampus in rodents. Besides histological differences, the cytoarchitectonic model was further justified by assuming that a) subfields are supported by specific behavior and b) are characterized by specific connectivity profiles, which will be discussed briefly.

It was suggested that the dentate gyrus and CA3 are involved in pattern separation and completion (Bakker et al., 2008; Leutgeb et al., 2007). CA2 was associated with social memory in rats (Alexander et al., 2016; Hitti & Siegelbaum, 2014). CA1, on the other hand, was associated with novelty detection (Barbeau, Chauvel, Moulin, Regis, & Liégeois-Chauvel, 2017), and autobiographical memory (Bartsch, Döhring, Rohr, Jansen, & Deuschl, 2011), but also CA3 was associated with novelty detection in rodents (Kesner, Lee, & Gilbert, 2004). The subiculum was related to emotion, reward, motivation and navigation (S. O'Mara, 2005; S. M. O'Mara, Sanchez-Vives, Brotons-Mas, & O'Hare, 2009). Even if subfields were associated with certain behavior, there are no consistent results on the meta-analytical level to support this assumption. The association between subfields and behavior was assessed in individual experiments mostly in rodents but the transfer to humans is difficult. Furthermore, fMRI studies often have not the spatial resolution to reliably distinguish between some subfields such as CA3 and the dentate gyrus (Yassa & Stark, 2011) hampering to investigate the relationship between subfields and human behavior. In sum, much more investigations are needed to clarify the specific link. It is furthermore essential to determine, whether the activity or lesion of the whole subfield was assessed or the subfield at a specific location along the longitudinal axis (for instance in the anterior head). There are neither consistent nor

sufficient studies available to draw a clear conclusion on how subfields are associated with human behavior, which has to be resolved in future.

In terms of connectivity and subfields, previous work primarily focused on intra-hippocampal connectivity of the hippocampus. Doing so, the trisynaptic[8] and the polysynaptic pathways[9] were identified to be essential to transfer signals within the hippocampus across lamina and subfields. On the other hand, extra-hippocampal connectivity was poorly described so far, with connections to the anterior nuclei of the thalamus, mammillary bodies, posterior cingulate cortex, retrosplenial cortex and anterior cingulate (Duvernoy, 2013)(p. 27ff) (Colon-Perez et al., 2015; Ly et al.; Zeineh, Holdsworth, Skare, Atlas, & Bammer, 2012; Zeineh et al., 2017). However, it is still rather vague how the subfields are specifically connected to the rest of the brain, as subfield's specific characterizations are lacking. Dalton et al. (2019) attempted to do so, and replicated the trisynaptic pathway using functional connectivity. But besides this, we do not know much about subfields' whole brain connectivity profiles.

In contrast, in both studies of this work I focused on large-scale networks of the hippocampus, which are considered to represent extra-hippocampal co-variation with the rest of the brain. It is unclear, whether those covariance networks represent direct connections between the hippocampus and the revealed networks, or if its relationship is mediated by functional connectivity. Independent of the underlying mechanism, our structural covariance networks of the subregions mirrored the revealed connectome of the hippocampus reported by Maller et al. (2019) and by Colnat-Coulbois et al. (2010) (Fig. 5). Their work showed that the ILF, the fornix, cingulum, tapetum, anterior commissure, spinal limbic pathway, fibers to the occipital areas and the uncinate fasciculus (which is still debatable whether it is connecting the hippocampus with frontal regions) are connections associated with the hippocampus to the rest of the brain. Overall, future studies should clarify, which brain regions are specifically connected with the subfields and lamina of the hippocampus and which connections are related to subregions as they were revealed in this work.

So far, relatively poor support is available for the assumption that the laminar and cytoarchitectonic organization is supported by specific behavior and is on top characterized by specific extra-hippocampal connectivity profiles, which has to be examined in detail in

---

[8] The trisynaptic pathway starts with the entorhinal cortex, which provides the primary input to the hippocampus. The entorhinal cortex projects to the dentate gyrus, which projects via mossy fibers to CA3, which neurons project to CA1 via Schaffer collaterals. CA1 projects back to the enthorinal cortex (Duvernoy, 2013) (p. 28f) (Knierim, 2015).

[9] The trisynaptic pathway is part of the polysynaptic pathway, which starts with the entorhinal cortex, projects to the dentate gyrus, and transverses to CA4 and CA3 via mossy fibers. From the entorhinal cortex the perforant pathway perforates the subiculum projecting to the dentate gyrus. Some axons of CA3 and CA4 emit Schaffer collaterals, which in turn communicate with the apical dendrites of CA1. Other axons access the alveus and then the fimbria, which represents the major hippocampal output pathway through the fornix. Axons of CA1 produce collaterals reaching the subiculum. Other axons of CA1 and subiculum also project back to the entorhinal cortex (Duvernoy, 2013)(p. 27ff).

future studies. In sum, I suggest to establish a three-dimensional perspective of the hippocampus with both differentiation patterns along the medial-lateral and anterior-posterior dimension, which is more supported by extra-hippocampal connectivity and heterogeneity of behavior as revealed by both studies in this work. The two organizational patterns are not contradictory to each other but complementary.

4.6 Parcellation: Science or art?

The title is inspired by the paper 'Clustering: Science or art?' by Luxburg, Williamson, and Guyon (2012) and is intended to remind of the challenges of the method of clustering and especially referring to the quote that ‘clustering is in the eye of the beholder’ (Jain, 2010). Therefore, some of the caveats will be briefly discussed in this section.

Both studies of this thesis were established using the method of CBP, which relies on an unsupervised clustering algorithm to divide the hippocampus into subregions/clusters to reveal its underlying organization. So far, a considerable number of regions have been parcellated providing a broad range of comparisons between different topographical schemas assessed with divergent approaches. These comparisons can be used to evaluate whether the method is reliable and valid. I define validity here in terms of biological meaningfulness, which is not directly measurable. In both studies we assessed validity indirectly by investigating whether parcellations show a re-occurring pattern either across modalities (study 1) or across dataset samples (study 2). Previous studies referred to validity in the context of how well parcellations match histological mapping, which does not fit to the goals of our investigation since different measures were used (micro-anatomical tissue composition vs. macro-anatomical large-scale networks).

However, parcellations based on diffusion MRI on the thalamus and medial frontal cortex reveal high correspondence with nuclei and subregions known from histology (Behrens et al., 2003; Johansen-Berg et al., 2004) suggesting high correspondence between diffusion MRI and histology (Simon B. Eickhoff, Yeo, & Genon, 2018). But parcellations based on MACM, resting-state functional connectivity and structural covariance, performed on the insula, (pre)-supplementary motor area, striatum, orbitofrontal cortex and amygdala yielded either convergent or divergent topographical patterns challenging the interpretation of results (Balsters, Mantini, & Wenderoth, 2018; Cauda et al., 2012; Clos et al., 2014; Cohen, Lombardo, & Blumenfeld, 2008; S. B. Eickhoff et al., 2011; Genon et al., 2017; Genon, Reid, Li, et al., 2018; Kahnt, Chang, Park, Heinzle, & Haynes, 2012; Kelly et al., 2012; Mishra,

Rogers, Chen, & Gore, 2014). This can have different reasons besides from the fact that different measures and techniques were used. The next section will address the main caveats associated with clustering.

Clustering algorithm

Clustering is an unsupervised machine learning approach with the purpose to assign objects to classes or clusters that are not predefined so that the whole approach is exploratory in nature (Jain, 2010; Luxburg et al., 2012).

CBP does not provide a ground truth solution of differentiation patterns but rather what is the optimal partition best mining and describing the data (S. B. Eickhoff et al., 2015). This provoked the statement that 'clustering is in the eye of the beholder' (Jain, 2010) and therefore highly subjective, raising the question, how to ensure scientific validity of clusterings (e.i. biological meaningful parcellations).

The user should be aware that dependent on the algorithm, be it k-means, spectral clustering or hierarchical clustering different assumptions about the data and the expected outcome are made implicitly (S. B. Eickhoff et al., 2015). To be more precisely, k-means performs best on data, which clusters are expected to be small in size and its features are spherical to the cluster center (S. B. Eickhoff et al., 2015). Spectral clustering is capable to find more complicated shapes in the data, which are discontinuous but at the same time it forces the clusters to be equal in size (S. B. Eickhoff et al., 2015). Hierarchical clustering is applied on data, which is nested, so that no specification of cluster number is required. However, hierarchical clustering is sensitive to effects of close spatial relationships of neighboring objects (S. B. Eickhoff et al., 2015).

Therefore, one major limitation of this work is that we did not test replicability of partitions across clustering algorithms, which should be kept in mind for future work. In this context, Thirion, Varoquaux, Dohmatob, and Poline (2014) suggested to prefer Ward's algorithm to cluster functional MRI data based on reproducibility and accuracy that was achieved. While Arslan et al. (2018) did not prefer any algorithm, k-means performed better on functional MRI data due to validity (e.g. measured with Silhouette values and parcel homogeneity) even though with poor reproducibility.

It is however worth mentioning, that no algorithm was developed so far to satisfy all criteria that are posed on a clustering algorithm such as scale invariance, richness and consistency (Jain, 2010; Kleinberg, 2002). Scale invariance means, that a rescaling of the similarity metric

would not change the clustering solution. In other words, to prefer the Mahalabonis to Euclidean distance, should lead to the same cluster solution. Richness refers to the ability of the algorithm to find any possible partition of the data in regard of size and shape of the clusters. Consistency means that a spatial change of distances due to stretching or shrinking would not change the clustering solution (Jain, 2010; Kleinberg, 2002).
Overall, while it is highly recommended to apply different clustering algorithms on the data, there is likely no one clustering algorithm that will always provide a perfect solution.

Predefining k-clusters using k-means

Using k-means requires the predefinition of the number of clusters in which the data must be parcellated but it does not guarantee to find the true biological topography. Therefore, the decision of the right number of partitions was guided by previous work already identified 3 and 5 parcels as optimal (Robinson et al., 2015; Robinson et al., 2016). By increasing the cluster number up to 7, we ensured to capture higher differentiation patterns as well. In the first study, we also tested for k: 2-10 achieving similar performances compared to k: 2-7.
Future studies should however evaluate the possibility of a higher k for parcellations of the hippocampus, especially using structural covariance as modality.

Connectivity and distance metric

Our definition of connectivity was based on Pearson's correlation but other measures such as Spearman rank correlation are potentially less prone to outliers and should be tested more systematically in future work. Geerligs, Cam, and Henson (2016) showed that multivariate distance correlations are more reliable than Pearson's correlation but Carmon et al. (2019) found no major differences using Spearman's compared to Pearson's correlation.
In addition, we here used the Euclidean distance as a distance metric but we did not test for other distance metrics such as cosine, Mahalanobis or Manhattan distance (Ronan, Qi, & Naegle, 2016), which might better account for outliers or noisy data.

Validity criteria

In the absence of a ground truth, the evaluation of clustering results poses another challenge. In the current work we emphasized to replicate our parcellation results either in a different

dataset sample like in study 2, or in a different related modality like in study 1 (functional modalities: MACM and RSFC). If parcellation schemas were highly similar to each other, we assumed biological meaningful clusterings since reoccurring patterns share a common basis, which is less likely structured noise, as different samples and modalities have different sources of noise.

In addition, in both studies we focused on robustness and consistency of parcellations estimating the internal validity of clusterings using measures such as stability, silhouette values (study 1 and 2), variation of information, inter/intra cluster distance, percentage of voxels misclassified (study 1).

Overall, parcellation schemas that fulfilled our criteria of reproducibility, stability and consistency were chosen to optimally describe hippocampal organization.

Features of the data

Another challenge for clustering algorithms is the high-dimensional nature of biological data (Ronan et al., 2016). K-means works best in low dimensional data as it has been defined to find the nearest neighbor (Ronan et al., 2016), which is difficult in high dimensional data (more features than participants). When the number of potential neighbors increases, the probability of misclassification is also increased. In the current work, we did not apply principal component analysis in order to reduce dimensionality and to capture only those voxels in the hippocampus with the most meaningful amount of variance that probably drives the clustering (Ronan et al., 2016). Future studies should evaluate whether dimensionality reduction before applying the clustering algorithm would have a benefit on parcellation schemas of the hippocampus.

In addition to the restrictions that are imposed by the clustering algorithm itself, neuroimaging data is noisy due to technical limitations on top of inter-individual variability challenging to extract signal from noise (S. B. Eickhoff et al., 2015; Ronan et al., 2016). To overcome the problem of inter-individual variability and to be able to extract a general differentiation pattern of the hippocampus, we tried to use datasets of large numbers of participants. In addition, we applied bootstrapping on structural covariance measures in order to resample within the seed and the target masks to reduce the risk to obtain deviant or very unlikely parcellations. We also applied the mode-function (to find most frequent values in array) across participants in each MRI modality accounting for the most likely clustering solution and reducing the probability of unusual parcellation schemes at the same time.

To reduce noise in resting-state functional connectivity data, we tested several denoising strategies, model-based and model-free, and applied them on the data to identify the best way of reducing structured noise (e.g. motion, physiological artifacts). At the time I started the study, model-based strategies such as FIX were only available for the spatial dimension but were developed further for the temporal dimension (Matthew F. Glasser et al., 2018), which we did not test in this work. Future studies have therefore to evaluate whether model-based strategies applied on spatial and temporal dimensions outperform our combination of model-based spatial FIX and model-free denoising using white matter/CSF regression.

All in all, despite some shortcomings such as not having tested another clustering algorithm, a different connectivity measure and a different distance metric or not having used dimensionality reduction, our validation criteria still suggested convergent and consistent parcellation schemas in study 1 across modalities and in study 2 across dataset samples supporting reliable and valid differentiation patterns. Moreover, we did not define initialization centers of the clusters and therefore did not constrain our parcellation results, being completely data driven. Instead we used a high number of repetitions ensuring to find the optimal convergence of data points (voxels) to clusters' centers.

To answer the question raised at the beginning, whether clustering represents art rather than science, my answer is a clear no. Clustering and therefore parcellation is a challenging scientific tool with a lot of constraints, which other scientific tools also have. But with clustering it is possible to unravel underlying schemas and relationships that might have been overlooked otherwise. The interpretation of results, however, is challenging and depends highly on the subjective knowledge that a scientist has about the object of investigation. Therefore, the interpretation of cluster solutions rather than clustering itself might be in the eye of the beholder as scientists have to separate unlikely differentiation patterns from more meaningful ones.

Conclusions

In contrast to known histological differentiation patterns based on micro-anatomical tissue composition, hippocampal organization based on functional large-scale networks, be it task-related (MACM) or task-unrelated connectivity (RSFC), revealed a differentiation pattern mainly along the longitudinal axis. Hippocampal organization based on structural covariance networks, however, revealed a differentiation pattern mainly along the medial-lateral dimension resembling partly cytoarchitectonic differentiation. These findings emphasize that

at least two different dimensions (e.g. anterior-posterior vs. medial-lateral) govern the differentiation pattern of the hippocampus at different spatial-scales depending on the feature of interest (cytoarchitecture vs. large-scale networks). Both dimensions are related to each other, since functional patterns showed at higher differentiation levels also a medial-lateral schema and macro-structural patterns showed an anterior head in addition to the medial-lateral subregions. Therefore a three-dimensional integrative view on the hippocampus should be taken.

In addition, we also observed that hippocampal organization based on structural covariance is under constant change across healthy lifespan, in MCI and in dementia pathology. This has to be further examined in a longitudinal research design to identify the driving mechanism. While the highest age-related change was found in the posterior hippocampus, the highest change in dementia was found for the lateral subregion expanding into the medial direction. Thus, hippocampal organization in dementia follows more likely functional organization. Divergences in hippocampal organization between healthy aging and dementia highly suggest that different mechanisms are driving these alterations. For example, white matter thinning could drive changes in aging, while pathogen distribution along functional networks might be the reason for changes in dementia. Investigating large-scale networks in the context of lifespan and pathology represents a more sensitive measure than purely atrophy, which is probably only detectable in severe cases as inconsistencies in the literature suggest.

The behavioral profiling of the hippocampus confirmed its involvement in a broad range of behavior including perception, emotion, motor and cognition stressing its high importance for human life. Moreover, our studies exemplify a strong relationship between hippocampal organization, its associated networks and behavior suggesting a self-centric vs. world-centric information processing along the anterior-posterior dimension, and with the medial subregion involved in vision-motor behavior.

Investigations of hippocampal organization should be further expanded on modalities such as positron emission tomography, diffusion weighted MRI, and magnet encephalography recordings. The combination of these modalities will help us to have an overarching perspective on hippocampal organization, functioning and behavior. Data driven approaches, even though challenging, could reveal additional organizational dimensions, which might help to establish a detailed coordinate system for the hippocampus being able to detect and track deviations in organization, connectivity and hence behavior.

Acknowledgements

Ich möchte mich vor allem bei den Menschen ganz herzlich bedanken, die mich in all dieser Zeit unterstützt und mitgetragen haben. Im privaten Bereich gehören dazu meine Familie, meine Eltern Wladimir und Olga, meine Brüder, Vitali und Alexander und meine Oma, Lydia. Ein großes Dankeschön geht auch an Marina, Swetlana, Juri, Hakim, Oleg, Anton, Viktoria, Yunis und Susann. Geduldig habt ihr meine Probleme angehört und mir Mut zugesprochen. Ohne eure Zuversicht und Optimismus wäre es einsamer Weg gewesen. Vielen herzlichen Dank, dass ihr da gewesen seid!

Ein unglaublich großes Dankeschön geht an meinen Partner Simon Steinkamp, der viele meiner Tränen getrocknet hat, und mit mir durch Täler gegangen ist und (Fast)-Gipfel erklommen hat. Ohne dich, Simon, wäre alles fahl und langweilig gewesen, mit dir dagegen war Wissenschaft eine nie enden wollende Diskussionsreise.

In the scientific field my deepest thanks go to Sarah Genon und Simon B. Eickhoff. Thank you so much for giving me the freedom to do the research that I was interested in, being open to ideas, even those, which were less promising, being supportive in any situation and having given the feedback to improve my work. Those early years as a scientist were highly influenced by you, and I am thankful for having the chance to have them with you.

I would also like to thank all the colleagues who made the working environment more attractive, spicy and exciting, who listened to all my complaints and who shared the lunchtime with me discussing all the irrelevant things not related to science.

References

Adachi, M., Kawakatsu, S., Hosoya, T., Otani, K., Honma, T., Shibata, A., & Sugai, Y. (2003). Morphology of the Inner Structure of the Hippocampal Formation in Alzheimer Disease. *American Journal of Neuroradiology, 24*(8), 1575-1581.

Adams, M. M., Shi, L., Linville, M. C., Forbes, M. E., Long, A. B., Bennett, C., . . . Brunso-Bechtold, J. K. (2008). Caloric restriction and age affect synaptic proteins in hippocampal CA3 and spatial learning ability. *Exp Neurol, 211*(1), 141-149. doi:10.1016/j.expneurol.2008.01.016

Adler, D. H., Pluta, J., Kadivar, S., Craige, C., Gee, J. C., Avants, B. B., & Yushkevich, P. A. (2014). Histology-derived volumetric annotation of the human hippocampal subfields in postmortem MRI. *Neuroimage, 84*, 505-523. doi:10.1016/j.neuroimage.2013.08.067

Adler, D. H., Wisse, L. E. M., Ittyerah, R., Pluta, J. B., Ding, S. L., Xie, L., . . . Yushkevich, P. A. (2018). Characterizing the human hippocampus in aging and Alzheimer's disease using a computational atlas derived from ex vivo MRI and histology. *Proc Natl Acad Sci U S A, 115*(16), 4252-4257. doi:10.1073/pnas.1801093115

Adnan, A., Barnett, A., Moayedi, M., McCormick, C., Cohn, M., & McAndrews, M. P. (2016). Distinct hippocampal functional networks revealed by tractography-based parcellation. *Brain Struct Funct, 221*(6), 2999-3012. doi:10.1007/s00429-015-1084-x

Alexander, G. M., Farris, S., Pirone, J. R., Zheng, C., Colgin, L. L., & Dudek, S. M. (2016). Social and novel contexts modify hippocampal CA2 representations of space. *Nat Commun, 7*(1), 10300. doi:10.1038/ncomms10300

Alexander-Bloch, A., Raznahan, A., Bullmore, E., & Giedd, J. (2013). The convergence of maturational change and structural covariance in human cortical networks. *J Neurosci, 33*(7), 2889-2899. doi:10.1523/jneurosci.3554-12.2013

Amaral, D. G., & Witter, M. P. (1989). The three-dimensional organization of the hippocampal formation: A review of anatomical data. *Neuroscience, 31*(3), 571-591. doi:https://doi.org/10.1016/0306-4522(89)90424-7

Amaral, R. S. C., Park, M. T. M., Devenyi, G. A., Lynn, V., Pipitone, J., Winterburn, J., . . . Chakravarty, M. M. (2018). Manual segmentation of the fornix, fimbria, and alveus on high-resolution 3T MRI: Application via fully-automated mapping of the human memory circuit white and grey matter in healthy and pathological aging. *Neuroimage, 170*, 132-150. doi:10.1016/j.neuroimage.2016.10.027

Amunts, K., Kedo, O., Kindler, M., Pieperhoff, P., Mohlberg, H., Shah, N. J., . . . Zilles, K. (2005). Cytoarchitectonic mapping of the human amygdala, hippocampal region and entorhinal cortex: intersubject variability and probability maps. *Anat Embryol (Berl), 210*(5-6), 343-352. doi:10.1007/s00429-005-0025-5

Amunts, K., & Zilles, K. (2015). Architectonic Mapping of the Human Brain beyond Brodmann. *Neuron, 88*(6), 1086-1107. doi:https://doi.org/10.1016/j.neuron.2015.12.001

Andersen, P., David Amaral, P. A. J. O. K. R. M., Collection, E. B., Morris, R., Amaral, D., O'Keefe, J., . . . Bliss, T. (2007). *The Hippocampus Book*: Oxford University Press, USA.

Anderson, J. S., Druzgal, T. J., Lopez-Larson, M., Jeong, E. K., Desai, K., & Yurgelun-Todd, D. (2011). Network anticorrelations, global regression, and phase-shifted soft tissue correction. *Hum Brain Mapp, 32*(6), 919-934. doi:10.1002/hbm.21079

Andrews-Hanna, J. R., Snyder, A. Z., Vincent, J. L., Lustig, C., Head, D., Raichle, M. E., & Buckner, R. L. (2007). Disruption of large-scale brain systems in advanced aging. *Neuron, 56*(5), 924-935. doi:10.1016/j.neuron.2007.10.038

Apostolova, L. G., Dinov, I. D., Dutton, R. A., Hayashi, K. M., Toga, A. W., Cummings, J. L., & Thompson, P. M. (2006). 3D comparison of hippocampal atrophy in amnestic mild cognitive impairment and Alzheimer's disease. *Brain, 129*(Pt 11), 2867-2873. doi:10.1093/brain/awl274

Apostolova, L. G., Dutton, R. A., Dinov, I. D., Hayashi, K. M., Toga, A. W., Cummings, J. L., & Thompson, P. M. (2006). Conversion of Mild Cognitive Impairment to Alzheimer Disease Predicted by Hippocampal Atrophy Maps. *Arch Neurol, 63*(5), 693-699. doi:10.1001/archneur.63.5.693

Apostolova, L. G., Mosconi, L., Thompson, P. M., Green, A. E., Hwang, K. S., Ramirez, A., . . . de Leon, M. J. (2010). Subregional hippocampal atrophy predicts Alzheimer's dementia in the cognitively normal. *Neurobiol Aging, 31*(7), 1077-1088. doi:10.1016/j.neurobiolaging.2008.08.008

Arslan, S., Ktena, S. I., Makropoulos, A., Robinson, E. C., Rueckert, D., & Parisot, S. (2018). Human brain mapping: A systematic comparison of parcellation methods for the human cerebral cortex. *Neuroimage, 170*, 5-30. doi:10.1016/j.neuroimage.2017.04.014

Ashburner, J., & Friston, K. J. (2005). Unified segmentation. *Neuroimage, 26*(3), 839-851. doi:10.1016/j.neuroimage.2005.02.018

Atienza, M., Atalaia-Silva, K. C., Gonzalez-Escamilla, G., Gil-Neciga, E., Suarez-Gonzalez, A., & Cantero, J. L. (2011). Associative memory deficits in mild cognitive impairment: the role of hippocampal formation. *Neuroimage, 57*(4), 1331-1342. doi:10.1016/j.neuroimage.2011.05.047

Bajada, C. J., Jackson, R. L., Haroon, H. A., Azadbakht, H., Parker, G. J. M., Lambon Ralph, M. A., & Cloutman, L. L. (2017). A graded tractographic parcellation of the temporal lobe. *Neuroimage, 155*, 503-512. doi:10.1016/j.neuroimage.2017.04.016

Bakker, A., Kirwan, C. B., Miller, M., & Stark, C. E. (2008). Pattern separation in the human hippocampal CA3 and dentate gyrus. *Science, 319*(5870), 1640-1642. doi:10.1126/science.1152882

Balsters, J. H., Mantini, D., & Wenderoth, N. (2018). Connectivity-based parcellation reveals distinct cortico-striatal connectivity fingerprints in Autism Spectrum Disorder. *Neuroimage, 170*, 412-423. doi:https://doi.org/10.1016/j.neuroimage.2017.02.019

Barbeau, E. J., Chauvel, P., Moulin, C. J. A., Regis, J., & Liégeois-Chauvel, C. (2017). Hippocampus duality: Memory and novelty detection are subserved by distinct mechanisms. *Hippocampus, 27*(4), 405-416. doi:10.1002/hipo.22699

Bartsch, T., Döhring, J., Rohr, A., Jansen, O., & Deuschl, G. (2011). CA1 neurons in the human hippocampus are critical for autobiographical memory, mental time travel, and autonoetic consciousness. *Proceedings of the National Academy of Sciences, 108*(42), 17562-17567. doi:10.1073/pnas.1110266108

Beaujoin, J., Palomero-Gallagher, N., Boumezbeur, F., Axer, M., Bernard, J., Poupon, F., . . . Poupon, C. (2018). Post-mortem inference of the human hippocampal connectivity and microstructure using ultra-high field diffusion MRI at 11.7 T. *Brain Struct Funct*. doi:10.1007/s00429-018-1617-1

Beckmann, C. F., & Smith, S. M. (2004). Probabilistic independent component analysis for functional magnetic resonance imaging. *IEEE Trans Med Imaging, 23*(2), 137-152. doi:10.1109/tmi.2003.822821

Behrens, T. E., Johansen-Berg, H., Woolrich, M. W., Smith, S. M., Wheeler-Kingshott, C. A., Boulby, P. A., . . . Matthews, P. M. (2003). Non-invasive mapping of connections between human thalamus and cortex using diffusion imaging. *Nat Neurosci, 6*(7), 750-757. doi:10.1038/nn1075

Bellec, P., Rosa-Neto, P., Lyttelton, O. C., Benali, H., & Evans, A. C. (2010). Multi-level bootstrap analysis of stable clusters in resting-state fMRI. *Neuroimage, 51*(3), 1126-1139. doi:10.1016/j.neuroimage.2010.02.082

Bettio, L. E. B., Rajendran, L., & Gil-Mohapel, J. (2017). The effects of aging in the hippocampus and cognitive decline. *Neurosci Biobehav Rev, 79*, 66-86. doi:10.1016/j.neubiorev.2017.04.030

Bi, G., & Poo, M. (1999). Distributed synaptic modification in neural networks induced by patterned stimulation. *Nature, 401*(6755), 792-796. doi:10.1038/44573

Bianciardi, M., Fukunaga, M., van Gelderen, P., Horovitz, S. G., de Zwart, J. A., Shmueli, K., & Duyn, J. H. (2009). Sources of functional magnetic resonance imaging signal fluctuations in the human brain at rest: a 7 T study. *Magn Reson Imaging, 27*(8), 1019-1029. doi:10.1016/j.mri.2009.02.004

Birn, R. M., Diamond, J. B., Smith, M. A., & Bandettini, P. A. (2006). Separating respiratory-variation-related fluctuations from neuronal-activity-related fluctuations in fMRI. *Neuroimage, 31*(4), 1536-1548. doi:10.1016/j.neuroimage.2006.02.048

Biswal, B., Yetkin, F. Z., Haughton, V. M., & Hyde, J. S. (1995). Functional connectivity in the motor cortex of resting human brain using echo-planar MRI. *Magn Reson Med, 34*(4), 537-541.

Blum, S., Habeck, C., Steffener, J., Razlighi, Q., & Stern, Y. (2014). Functional connectivity of the posterior hippocampus is more dominant as we age. *Cogn Neurosci, 5*(3-4), 150-159. doi:10.1080/17588928.2014.975680

Bobinski, M., Wegiel, J., Tarnawski, M., Bobinski, M., Reisberg, B., de Leon, M. J., . . . Wisniewski, H. M. (1997). Relationships between regional neuronal loss and neurofibrillary changes in the hippocampal formation and duration and severity of Alzheimer disease. *J Neuropathol Exp Neurol, 56*(4), 414-420. doi:10.1097/00005072-199704000-00010

Bobinski, M., Wegiel, J., Wisniewski, H. M., Tarnawski, M., Reisberg, B., Mlodzik, B., . . . Miller, D. C. (1995). Atrophy of hippocampal formation subdivisions correlates with stage and duration of Alzheimer disease. *Dementia, 6*(4), 205-210.

Boedhoe, P. S., Schmaal, L., Abe, Y., Ameis, S. H., Arnold, P. D., Batistuzzo, M. C., . . . van den Heuvel, O. A. (2017). Distinct Subcortical Volume Alterations in Pediatric and Adult OCD: A Worldwide Meta- and Mega-Analysis. *Am J Psychiatry, 174*(1), 60-69. doi:10.1176/appi.ajp.2016.16020201

Bowman, C. R., & Zeithamova, D. (2018). Abstract Memory Representations in the Ventromedial Prefrontal Cortex and Hippocampus Support Concept Generalization. *The Journal of Neuroscience, 38*(10), 2605-2614. doi:10.1523/jneurosci.2811-17.2018

Boyke, J., Driemeyer, J., Gaser, C., Buchel, C., & May, A. (2008). Training-induced brain structure changes in the elderly. *J Neurosci, 28*(28), 7031-7035. doi:10.1523/jneurosci.0742-08.2008

Braak, H., & Braak, E. (1991). Neuropathological stageing of Alzheimer-related changes. *Acta Neuropathol, 82*(4), 239-259. doi:10.1007/bf00308809

Buckner, R. L., Krienen, F. M., & Yeo, B. T. (2013). Opportunities and limitations of intrinsic functional connectivity MRI. *Nat Neurosci, 16*(7), 832-837. doi:10.1038/nn.3423

Buckner, R. L., Snyder, A. Z., Shannon, B. J., LaRossa, G., Sachs, R., Fotenos, A. F., . . . Mintun, M. A. (2005). Molecular, structural, and functional characterization of Alzheimer's disease: evidence for a relationship between default activity, amyloid, and memory. *J Neurosci, 25*(34), 7709-7717. doi:10.1523/jneurosci.2177-05.2005

Burgess, G. C., Kandala, S., Nolan, D., Laumann, T. O., Power, J. D., Adeyemo, B., . . . Barch, D. M. (2016). Evaluation of Denoising Strategies to Address Motion-Correlated Artifacts in Resting-State Functional Magnetic Resonance Imaging Data from the Human Connectome Project. *Brain Connect, 6*(9), 669-680. doi:10.1089/brain.2016.0435

Caballero-Gaudes, C., & Reynolds, R. C. (2017). Methods for cleaning the BOLD fMRI signal. *Neuroimage, 154*, 128-149. doi:10.1016/j.neuroimage.2016.12.018

Carmon, J., Heege, J., Necus, J., Owen, T., Pipa, G., Kaiser, M., . . . Wang, Y. (2019). *Reliability and comparability of human brain structural covariance networks*.

Catani, M., Dell'acqua, F., & Thiebaut de Schotten, M. (2013). A revised limbic system model for memory, emotion and behaviour. *Neurosci Biobehav Rev, 37*(8), 1724-1737. doi:10.1016/j.neubiorev.2013.07.001

Catani, M., & Thiebaut de Schotten, M. (2008). A diffusion tensor imaging tractography atlas for virtual in vivo dissections. *Cortex, 44*(8), 1105-1132. doi:10.1016/j.cortex.2008.05.004

Catheline, G., Periot, O., Amirault, M., Braun, M., Dartigues, J. F., Auriacombe, S., & Allard, M. (2010). Distinctive alterations of the cingulum bundle during aging and Alzheimer's disease. *Neurobiol Aging, 31*(9), 1582-1592. doi:10.1016/j.neurobiolaging.2008.08.012

Cauda, F., Costa, T., Torta, D. M., Sacco, K., D'Agata, F., Duca, S., . . . Vercelli, A. (2012). Meta-analytic clustering of the insular cortex: characterizing the meta-analytic connectivity of the insula when involved in active tasks. *Neuroimage, 62*(1), 343-355. doi:10.1016/j.neuroimage.2012.04.012

Chand, G. B., Hajjar, I., & Qiu, D. (2018). Disrupted interactions among the hippocampal, dorsal attention, and central-executive networks in amnestic mild cognitive impairment. *Hum Brain Mapp, 39*(12), 4987-4997. doi:10.1002/hbm.24339

Chang, C., Huang, C., Zhou, N., Li, S. X., Ver Hoef, L., & Gao, Y. (2018). The bumps under the hippocampus. *Hum Brain Mapp, 39*(1), 472-490. doi:10.1002/hbm.23856

Chang, Y.-T., Huang, C.-W., Chang, W.-N., Lee, J.-J., & Chang, C.-C. (2018). Altered Functional Network Affects Amyloid and Structural Covariance in Alzheimer's Disease. *BioMed research international, 2018*, 8565620-8565620. doi:10.1155/2018/8565620

Chase, H. W., Clos, M., Dibble, S., Fox, P., Grace, A. A., Phillips, M. L., & Eickhoff, S. B. (2015). Evidence for an anterior-posterior differentiation in the human hippocampal formation revealed by meta-analytic parcellation of fMRI coordinate maps: focus on the subiculum. *Neuroimage, 113*, 44-60. doi:10.1016/j.neuroimage.2015.02.069

Chen, K. H. M., Chuah, L. Y. M., Sim, S. K. Y., & Chee, M. W. L. (2010). Hippocampal region-specific contributions to memory performance in normal elderly. *Brain and Cognition, 72*(3), 400-407. doi:https://doi.org/10.1016/j.bandc.2009.11.007

Chetelat, G., Desgranges, B., Landeau, B., Mezenge, F., Poline, J. B., de la Sayette, V., . . . Baron, J. C. (2008). Direct voxel-based comparison between grey matter hypometabolism and atrophy in Alzheimer's disease. *Brain, 131*(Pt 1), 60-71. doi:10.1093/brain/awm288

Clos, M., Amunts, K., Laird, A. R., Fox, P. T., & Eickhoff, S. B. (2013). Tackling the multifunctional nature of Broca's region meta-analytically: co-activation-based parcellation of area 44. *Neuroimage, 83*, 174-188. doi:10.1016/j.neuroimage.2013.06.041

Clos, M., Rottschy, C., Laird, A. R., Fox, P. T., & Eickhoff, S. B. (2014). Comparison of structural covariance with functional connectivity approaches exemplified by an investigation of the left anterior insula. *Neuroimage, 99*, 269-280. doi:10.1016/j.neuroimage.2014.05.030

Cohen, M. X., Lombardo, M. V., & Blumenfeld, R. S. (2008). Covariance-based subdivision of the human striatum using T1-weighted MRI. *Eur J Neurosci, 27*(6), 1534-1546. doi:10.1111/j.1460-9568.2008.06117.x

Cole, D. M., Smith, S. M., & Beckmann, C. F. (2010). Advances and pitfalls in the analysis and interpretation of resting-state FMRI data. *Front Syst Neurosci, 4*, 8. doi:10.3389/fnsys.2010.00008

Collin, S. H., Milivojevic, B., & Doeller, C. F. (2015). Memory hierarchies map onto the hippocampal long axis in humans. *Nat Neurosci, 18*(11), 1562-1564. doi:10.1038/nn.4138

Colnat-Coulbois, S., Mok, K., Klein, D., Pénicaud, S., Tanriverdi, T., & Olivier, A. (2010). Tractography of the amygdala and hippocampus: anatomical study and application to selective amygdalohippocampectomy. *J Neurosurg, 113*(6), 1135-1143. doi:10.3171/2010.3.jns091832

Colombo, M., Fernandez, T., Nakamura, K., & Gross, C. G. (1998). Functional differentiation along the anterior-posterior axis of the hippocampus in monkeys. *J Neurophysiol, 80*(2), 1002-1005. doi:10.1152/jn.1998.80.2.1002

Colon-Perez, L. M., King, M., Parekh, M., Boutzoukas, A., Carmona, E., Couret, M., . . . Carney, P. R. (2015). High-field magnetic resonance imaging of the human temporal lobe. *NeuroImage: Clinical, 9*, 58-68. doi:https://doi.org/10.1016/j.nicl.2015.07.005

Corder, E. H., Woodbury, M. A., Volkmann, I., Madsen, D. K., Bogdanovic, N., & Winblad, B. (2000). Density profiles of Alzheimer disease regional brain pathology for the huddinge brain bank: pattern recognition emulates and expands upon Braak staging. *Exp Gerontol, 35*(6-7), 851-864.

Csernansky, J. G., Wang, L., Joshi, S., Miller, J. P., Gado, M., Kido, D., . . . Miller, M. I. (2000). Early DAT is distinguished from aging by high-dimensional mapping of the hippocampus. Dementia of the Alzheimer type. *Neurology, 55*(11), 1636-1643. doi:10.1212/wnl.55.11.1636

Csernansky, J. G., Wang, L., Swank, J., Miller, J. P., Gado, M., McKeel, D., . . . Morris, J. C. (2005). Preclinical detection of Alzheimer's disease: hippocampal shape and volume predict dementia onset in the elderly. *Neuroimage, 25*(3), 783-792. doi:10.1016/j.neuroimage.2004.12.036

Dagli, M. S., Ingeholm, J. E., & Haxby, J. V. (1999). Localization of cardiac-induced signal change in fMRI. *Neuroimage, 9*(4), 407-415. doi:10.1006/nimg.1998.0424

Dalton, M. A., McCormick, C., & Maguire, E. A. (2019). Differences in functional connectivity along the anterior-posterior axis of human hippocampal subfields. *Neuroimage, 192*, 38-51. doi:https://doi.org/10.1016/j.neuroimage.2019.02.066

Damoiseaux, J. S., Viviano, R. P., Yuan, P., & Raz, N. (2016). Differential effect of age on posterior and anterior hippocampal functional connectivity. *Neuroimage, 133*, 468-476. doi:10.1016/j.neuroimage.2016.03.047

Daugherty, A. M., Bender, A. R., Raz, N., & Ofen, N. (2016). Age differences in hippocampal subfield volumes from childhood to late adulthood. *Hippocampus, 26*(2), 220-228. doi:10.1002/hipo.22517

de Flores, R., La Joie, R., & Chetelat, G. (2015). Structural imaging of hippocampal subfields in healthy aging and Alzheimer's disease. *Neuroscience, 309*, 29-50. doi:10.1016/j.neuroscience.2015.08.033

de Hoz, L., Knox, J., & Morris, R. G. (2003). Longitudinal axis of the hippocampus: both septal and temporal poles of the hippocampus support water maze spatial learning depending on the training protocol. *Hippocampus, 13*(5), 587-603. doi:10.1002/hipo.10079

de Munck, J. C., Goncalves, S. I., Faes, T. J., Kuijer, J. P., Pouwels, P. J., Heethaar, R. M., & Lopes da Silva, F. H. (2008). A study of the brain's resting state based on alpha band power, heart rate and fMRI. *Neuroimage, 42*(1), 112-121. doi:10.1016/j.neuroimage.2008.04.244

DeKraker, J., Ferko, K. M., Lau, J. C., Kohler, S., & Khan, A. R. (2018). Unfolding the hippocampus: An intrinsic coordinate system for subfield segmentations and quantitative mapping. *Neuroimage, 167*, 408-418. doi:10.1016/j.neuroimage.2017.11.054

DeKraker, J., Lau, J. C., Ferko, K. M., Khan, A. R., & Köhler, S. (2020). Hippocampal subfields revealed through unfolding and unsupervised clustering of laminar and morphological features in 3D BigBrain. *Neuroimage, 206*, 116328. doi:https://doi.org/10.1016/j.neuroimage.2019.116328

Desikan, R. S., Segonne, F., Fischl, B., Quinn, B. T., Dickerson, B. C., Blacker, D., . . . Killiany, R. J. (2006). An automated labeling system for subdividing the human cerebral cortex on MRI scans into gyral based regions of interest. *Neuroimage, 31*(3), 968-980. doi:10.1016/j.neuroimage.2006.01.021

Desjardins, A. E., Kiehl, K. A., & Liddle, P. F. (2001). Removal of confounding effects of global signal in functional MRI analyses. *Neuroimage, 13*(4), 751-758. doi:10.1006/nimg.2000.0719

Deuker, L., Doeller, C. F., Fell, J., & Axmacher, N. (2014). Human neuroimaging studies on the hippocampal CA3 region - integrating evidence for pattern separation and completion. *Front Cell Neurosci, 8*, 64. doi:10.3389/fncel.2014.00064

Dimsdale-Zucker, H. R., Ritchey, M., Ekstrom, A. D., Yonelinas, A. P., & Ranganath, C. (2018). CA1 and CA3 differentially support spontaneous retrieval of episodic contexts within human hippocampal subfields. *Nat Commun, 9*(1), 294. doi:10.1038/s41467-017-02752-1

Ding, S. L., & Van Hoesen, G. W. (2015). Organization and Detailed Parcellation of Human Hippocampal Head and Body Regions Based on a Combined Analysis of Cyto- and Chemoarchitecture. *J Comp Neurol, 523*(15), 2233-2253. doi:10.1002/cne.23786

Dong, H. W., Swanson, L. W., Chen, L., Fanselow, M. S., & Toga, A. W. (2009). Genomic-anatomic evidence for distinct functional domains in hippocampal field CA1. *Proc Natl Acad Sci U S A, 106*(28), 11794-11799. doi:10.1073/pnas.0812608106

Douet, V., & Chang, L. (2015). Fornix as an imaging marker for episodic memory deficits in healthy aging and in various neurological disorders. *Frontiers in Aging Neuroscience, 6*, 343-343. doi:10.3389/fnagi.2014.00343

Driscoll, I., Hamilton, D. A., Petropoulos, H., Yeo, R. A., Brooks, W. M., Baumgartner, R. N., & Sutherland, R. J. (2003). The aging hippocampus: cognitive, biochemical and structural findings. *Cereb Cortex, 13*(12), 1344-1351. doi:10.1093/cercor/bhg081

Dubois, B., Hampel, H., Feldman, H. H., Scheltens, P., Aisen, P., Andrieu, S., . . . Washington Dc, U. S. A. (2016). Preclinical Alzheimer's disease: Definition, natural history, and

diagnostic criteria. *Alzheimers Dement, 12*(3), 292-323. doi:10.1016/j.jalz.2016.02.002
Duvernoy, H. C., Francoise; Risold Pierre-Yves. (2013). *The Human Hippocampus*.
Efron, B. (1979). Bootstrap Methods: Another Look at the Jackknife. *Ann. Statist., 7*(1), 1-26. doi:10.1214/aos/1176344552
Eichenbaum, H., Yonelinas, A. P., & Ranganath, C. (2007). The medial temporal lobe and recognition memory. *Annu Rev Neurosci, 30*, 123-152. doi:10.1146/annurev.neuro.30.051606.094328
Eickhoff, S. B., Bzdok, D., Laird, A. R., Kurth, F., & Fox, P. T. (2012). Activation likelihood estimation meta-analysis revisited. *Neuroimage, 59*(3), 2349-2361. doi:10.1016/j.neuroimage.2011.09.017
Eickhoff, S. B., Bzdok, D., Laird, A. R., Roski, C., Caspers, S., Zilles, K., & Fox, P. T. (2011). Co-activation patterns distinguish cortical modules, their connectivity and functional differentiation. *Neuroimage, 57*(3), 938-949. doi:10.1016/j.neuroimage.2011.05.021
Eickhoff, S. B., Stephan, K. E., Mohlberg, H., Grefkes, C., Fink, G. R., Amunts, K., & Zilles, K. (2005). A new SPM toolbox for combining probabilistic cytoarchitectonic maps and functional imaging data. *Neuroimage, 25*(4), 1325-1335. doi:10.1016/j.neuroimage.2004.12.034
Eickhoff, S. B., Thirion, B., Varoquaux, G., & Bzdok, D. (2015). Connectivity-based parcellation: Critique and implications. *Hum Brain Mapp, 36*(12), 4771-4792. doi:10.1002/hbm.22933
Eickhoff, S. B., Yeo, B. T. T., & Genon, S. (2018). Imaging-based parcellations of the human brain. *Nature Reviews Neuroscience, 19*(11), 672-686. doi:10.1038/s41583-018-0071-7
Eickhoff, S. B., Yeo, T., Genon, S. (in press). Imaging-based parcellations of the human brain. *Nature Review Neuroscience*.
Evans, A. C. (2013). Networks of anatomical covariance. *Neuroimage, 80*, 489-504. doi:10.1016/j.neuroimage.2013.05.054
Fan, L., Li, H., Zhuo, J., Zhang, Y., Wang, J., Chen, L., . . . Jiang, T. (2016). The Human Brainnetome Atlas: A New Brain Atlas Based on Connectional Architecture. *Cerebral Cortex, 26*(8), 3508-3526. doi:10.1093/cercor/bhw157
Fanselow, M. S., & Dong, H. W. (2010). Are the dorsal and ventral hippocampus functionally distinct structures? *Neuron, 65*(1), 7-19. doi:10.1016/j.neuron.2009.11.031
Fjell, A. M., McEvoy, L., Holland, D., Dale, A. M., & Walhovd, K. B. (2014). What is normal in normal aging? Effects of aging, amyloid and Alzheimer's disease on the cerebral cortex and the hippocampus. *Prog Neurobiol, 117*, 20-40. doi:10.1016/j.pneurobio.2014.02.004
Fleming Beattie, J., Martin, R. C., Kana, R. K., Deshpande, H., Lee, S., Cure, J., & Ver Hoef, L. (2017). Hippocampal dentation: Structural variation and its association with episodic memory in healthy adults. *Neuropsychologia, 101*, 65-75. doi:10.1016/j.neuropsychologia.2017.04.036
Fortin, J.-P., Cullen, N., Sheline, Y. I., Taylor, W. D., Aselcioglu, I., Cook, P. A., . . . Shinohara, R. T. (2018). Harmonization of cortical thickness measurements across scanners and sites. *Neuroimage, 167*, 104-120. doi:10.1016/j.neuroimage.2017.11.024
Foster, C. M., Kennedy, K. M., Hoagey, D. A., & Rodrigue, K. M. (2019). The role of hippocampal subfield volume and fornix microstructure in episodic memory across the lifespan. *Hippocampus*. doi:10.1002/hipo.23133

Fouquet, M., Desgranges, B., La Joie, R., Riviere, D., Mangin, J. F., Landeau, B., . . . Chetelat, G. (2012). Role of hippocampal CA1 atrophy in memory encoding deficits in amnestic Mild Cognitive Impairment. *Neuroimage, 59*(4), 3309-3315. doi:10.1016/j.neuroimage.2011.11.036

Franko, E., & Joly, O. (2013). Evaluating Alzheimer's disease progression using rate of regional hippocampal atrophy. *PLoS One, 8*(8), e71354. doi:10.1371/journal.pone.0071354

Franzmeier, N., Rubinski, A., Neitzel, J., Kim, Y., Damm, A., Na, D. L., . . . Ewers, M. (2019). Functional connectivity associated with tau levels in ageing, Alzheimer's, and small vessel disease. *Brain, 142*(4), 1093-1107. doi:10.1093/brain/awz026

Fraser, M. A., Shaw, M. E., & Cherbuin, N. (2015). A systematic review and meta-analysis of longitudinal hippocampal atrophy in healthy human ageing. *Neuroimage, 112*, 364-374. doi:10.1016/j.neuroimage.2015.03.035

Frisoni, G. B., Ganzola, R., Canu, E., Rub, U., Pizzini, F. B., Alessandrini, F., . . . Thompson, P. M. (2008). Mapping local hippocampal changes in Alzheimer's disease and normal ageing with MRI at 3 Tesla. *Brain, 131*(Pt 12), 3266-3276. doi:10.1093/brain/awn280

Frisoni, G. B., Sabattoli, F., Lee, A. D., Dutton, R. A., Toga, A. W., & Thompson, P. M. (2006). In vivo neuropathology of the hippocampal formation in AD: a radial mapping MR-based study. *Neuroimage, 32*(1), 104-110. doi:10.1016/j.neuroimage.2006.03.015

Gao, A. F., Keith, J. L., Gao, F. Q., Black, S. E., Moscovitch, M., & Rosenbaum, R. S. (2020). Neuropathology of a remarkable case of memory impairment informs human memory. *Neuropsychologia, 140*, 107342. doi:10.1016/j.neuropsychologia.2020.107342

Ge, R., Kot, P., Liu, X., Lang, D. J., Wang, J. Z., Honer, W. G., & Vila-Rodriguez, F. (2019). Parcellation of the human hippocampus based on gray matter volume covariance: Replicable results on healthy young adults. *Hum Brain Mapp, 40*(13), 3738-3752. doi:10.1002/hbm.24628

Geerligs, L., Cam, C., & Henson, R. N. (2016). Functional connectivity and structural covariance between regions of interest can be measured more accurately using multivariate distance correlation. *Neuroimage, 135*, 16-31. doi:10.1016/j.neuroimage.2016.04.047

Gemmell, E., Bosomworth, H., Allan, L., Hall, R., Khundakar, A., Oakley, A. E., . . . Kalaria, R. N. (2012). Hippocampal neuronal atrophy and cognitive function in delayed poststroke and aging-related dementias. *Stroke, 43*(3), 808-814. doi:10.1161/strokeaha.111.636498

Geng, X., Li, G., Lu, Z., Gao, W., Wang, L., Shen, D., . . . Gilmore, J. H. (2017). Structural and Maturational Covariance in Early Childhood Brain Development. *Cereb Cortex, 27*(3), 1795-1807. doi:10.1093/cercor/bhw022

Genon, S., Li, H., Fan, L., Muller, V. I., Cieslik, E. C., Hoffstaedter, F., . . . Eickhoff, S. B. (2017). The Right Dorsal Premotor Mosaic: Organization, Functions, and Connectivity. *Cereb Cortex, 27*(3), 2095-2110. doi:10.1093/cercor/bhw065

Genon, S., Reid, A., Langner, R., Amunts, K., & Eickhoff, S. B. (2018a). How to Characterize the Function of a Brain Region. *Trends Cogn Sci*. doi:10.1016/j.tics.2018.01.010

Genon, S., Reid, A., Langner, R., Amunts, K., & Eickhoff, S. B. (2018b). How to Characterize the Function of a Brain Region. *Trends Cogn Sci, 22*(4), 350-364. doi:10.1016/j.tics.2018.01.010

Genon, S., Reid, A., Li, H., Fan, L., Muller, V. I., Cieslik, E. C., . . . Eickhoff, S. B. (2018). The heterogeneity of the left dorsal premotor cortex evidenced by multimodal

connectivity-based parcellation and functional characterization. *Neuroimage, 170*, 400-411. doi:10.1016/j.neuroimage.2017.02.034

Gilboa, A., Winocur, G., Grady, C. L., Hevenor, S. J., & Moscovitch, M. (2004). Remembering our past: functional neuroanatomy of recollection of recent and very remote personal events. *Cereb Cortex, 14*(11), 1214-1225. doi:10.1093/cercor/bhh082

Glasser, M. F., Coalson, T. S., Bijsterbosch, J. D., Harrison, S. J., Harms, M. P., Anticevic, A., . . . Smith, S. M. (2018). Using temporal ICA to selectively remove global noise while preserving global signal in functional MRI data. *Neuroimage, 181*, 692-717. doi:10.1016/j.neuroimage.2018.04.076

Glasser, M. F., Coalson, T. S., Robinson, E. C., Hacker, C. D., Harwell, J., Yacoub, E., . . . Van Essen, D. C. (2016). A multi-modal parcellation of human cerebral cortex. *Nature, 536*(7615), 171-178. doi:10.1038/nature18933

Goodkind, M., Eickhoff, S. B., Oathes, D. J., Jiang, Y., Chang, A., Jones-Hagata, L. B., . . . Etkin, A. (2015). Identification of a common neurobiological substrate for mental illness. *JAMA Psychiatry, 72*(4), 305-315. doi:10.1001/jamapsychiatry.2014.2206

Gordon, B. A., Blazey, T., Benzinger, T. L., & Head, D. (2013). Effects of aging and Alzheimer's disease along the longitudinal axis of the hippocampus. *J Alzheimers Dis, 37*(1), 41-50. doi:10.3233/jad-130011

Gordon, E. M., Laumann, T. O., Adeyemo, B., Huckins, J. F., Kelley, W. M., & Petersen, S. E. (2014). Generation and Evaluation of a Cortical Area Parcellation from Resting-State Correlations. *Cerebral Cortex, 26*(1), 288-303. doi:10.1093/cercor/bhu239

Griffanti, L., Salimi-Khorshidi, G., Beckmann, C. F., Auerbach, E. J., Douaud, G., Sexton, C. E., . . . Smith, S. M. (2014). ICA-based artefact removal and accelerated fMRI acquisition for improved resting state network imaging. *Neuroimage, 95*, 232-247. doi:10.1016/j.neuroimage.2014.03.034

Guzowski, J. F., Knierim, J. J., & Moser, E. I. (2004). Ensemble dynamics of hippocampal regions CA3 and CA1. *Neuron, 44*(4), 581-584. doi:10.1016/j.neuron.2004.11.003

Hallquist, M. N., Hwang, K., & Luna, B. (2013). The nuisance of nuisance regression: spectral misspecification in a common approach to resting-state fMRI preprocessing reintroduces noise and obscures functional connectivity. *Neuroimage, 82*, 208-225. doi:10.1016/j.neuroimage.2013.05.116

Hanseeuw, B. J., Van Leemput, K., Kavec, M., Grandin, C., Seron, X., & Ivanoiu, A. (2011). Mild cognitive impairment: differential atrophy in the hippocampal subfields. *AJNR Am J Neuroradiol, 32*(9), 1658-1661. doi:10.3174/ajnr.A2589

He, Y., Chen, Z., & Evans, A. (2008). Structural insights into aberrant topological patterns of large-scale cortical networks in Alzheimer's disease. *J Neurosci, 28*(18), 4756-4766. doi:10.1523/jneurosci.0141-08.2008

He, Y., Wang, L., Zang, Y., Tian, L., Zhang, X., Li, K., & Jiang, T. (2007). Regional coherence changes in the early stages of Alzheimer's disease: a combined structural and resting-state functional MRI study. *Neuroimage, 35*(2), 488-500. doi:10.1016/j.neuroimage.2006.11.042

Herbet, G., Zemmoura, I., & Duffau, H. (2018). Functional Anatomy of the Inferior Longitudinal Fasciculus: From Historical Reports to Current Hypotheses. *Front Neuroanat, 12*, 77-77. doi:10.3389/fnana.2018.00077

Hitti, F. L., & Siegelbaum, S. A. (2014). The hippocampal CA2 region is essential for social memory. *Nature, 508*(7494), 88-92. doi:10.1038/nature13028

Hufner, K., Binetti, C., Hamilton, D. A., Stephan, T., Flanagin, V. L., Linn, J., . . . Brandt, T. (2011). Structural and functional plasticity of the hippocampal formation in professional dancers and slackliners. *Hippocampus, 21*(8), 855-865. doi:10.1002/hipo.20801

Hutchison, R. M., Womelsdorf, T., Gati, J. S., Everling, S., & Menon, R. S. (2013). Resting-state networks show dynamic functional connectivity in awake humans and anesthetized macaques. *Hum Brain Mapp, 34*(9), 2154-2177. doi:10.1002/hbm.22058

Hyman, B. T., Van Hoesen, G. W., Damasio, A. R., & Barnes, C. L. (1984). Alzheimer's disease: cell-specific pathology isolates the hippocampal formation. *Science, 225*(4667), 1168-1170. doi:10.1126/science.6474172

Insausti, R., & Munoz, M. (2001). Cortical projections of the non-entorhinal hippocampal formation in the cynomolgus monkey (Macaca fascicularis). *Eur J Neurosci, 14*(3), 435-451. doi:10.1046/j.0953-816x.2001.01662.x

Insausti, R., Muñoz-López, M., Insausti, A. M., & Artacho-Pérula, E. (2017). The Human Periallocortex: Layer Pattern in Presubiculum, Parasubiculum and Entorhinal Cortex. A Review. *Front Neuroanat, 11*, 84-84. doi:10.3389/fnana.2017.00084

Jack, C. R., Jr., Lowe, V. J., Senjem, M. L., Weigand, S. D., Kemp, B. J., Shiung, M. M., . . . Petersen, R. C. (2008). 11C PiB and structural MRI provide complementary information in imaging of Alzheimer's disease and amnestic mild cognitive impairment. *Brain, 131*(Pt 3), 665-680. doi:10.1093/brain/awm336

Jack, C. R., Jr., Petersen, R. C., Xu, Y. C., Waring, S. C., O'Brien, P. C., Tangalos, E. G., . . . Kokmen, E. (1997). Medial temporal atrophy on MRI in normal aging and very mild Alzheimer's disease. *Neurology, 49*(3), 786-794. doi:10.1212/wnl.49.3.786

Jain, A. K. (2010). Data clustering: 50 years beyond K-means. *Pattern Recognition Letters, 31*(8), 651-666. doi:https://doi.org/10.1016/j.patrec.2009.09.011

Jo, H. J., Gotts, S. J., Reynolds, R. C., Bandettini, P. A., Martin, A., Cox, R. W., & Saad, Z. S. (2013). Effective Preprocessing Procedures Virtually Eliminate Distance-Dependent Motion Artifacts in Resting State FMRI. *J Appl Math, 2013*. doi:10.1155/2013/935154

Jo, H. J., Saad, Z. S., Simmons, W. K., Milbury, L. A., & Cox, R. W. (2010). Mapping sources of correlation in resting state FMRI, with artifact detection and removal. *Neuroimage, 52*(2), 571-582. doi:10.1016/j.neuroimage.2010.04.246

Jockwitz, C., Mérillat, S., Liem, F., Oschwald, J., Amunts, K., Caspers, S., & Jäncke, L. (2019). Generalizing age effects on brain structure and cognition: A two-study comparison approach. *Hum Brain Mapp, 40*(8), 2305-2319. doi:10.1002/hbm.24524

Johansen-Berg, H., Behrens, T. E., Robson, M. D., Drobnjak, I., Rushworth, M. F., Brady, J. M., . . . Matthews, P. M. (2004). Changes in connectivity profiles define functionally distinct regions in human medial frontal cortex. *Proc Natl Acad Sci U S A, 101*(36), 13335-13340. doi:10.1073/pnas.0403743101

Jung, M., Wiener, S., & McNaughton, B. (1994). Comparison of spatial firing characteristics of units in dorsal and ventral hippocampus of the rat. *The Journal of Neuroscience, 14*(12), 7347-7356. doi:10.1523/jneurosci.14-12-07347.1994

Kahn, I., Andrews-Hanna, J. R., Vincent, J. L., Snyder, A. Z., & Buckner, R. L. (2008). Distinct cortical anatomy linked to subregions of the medial temporal lobe revealed by intrinsic functional connectivity. *J Neurophysiol, 100*(1), 129-139. doi:10.1152/jn.00077.2008

Kahnt, T., Chang, L. J., Park, S. Q., Heinzle, J., & Haynes, J. D. (2012). Connectivity-based parcellation of the human orbitofrontal cortex. *J Neurosci, 32*(18), 6240-6250. doi:10.1523/jneurosci.0257-12.2012

Kalpouzos, G., Chetelat, G., Baron, J. C., Landeau, B., Mevel, K., Godeau, C., . . . Desgranges, B. (2009). Voxel-based mapping of brain gray matter volume and glucose

metabolism profiles in normal aging. *Neurobiol Aging, 30*(1), 112-124. doi:10.1016/j.neurobiolaging.2007.05.019
Katz, L. C., & Shatz, C. J. (1996). Synaptic activity and the construction of cortical circuits. *Science, 274*(5290), 1133-1138. doi:10.1126/science.274.5290.1133
Kelly, C., Toro, R., Di Martino, A., Cox, C. L., Bellec, P., Castellanos, F. X., & Milham, M. P. (2012). A convergent functional architecture of the insula emerges across imaging modalities. *Neuroimage, 61*(4), 1129-1142. doi:10.1016/j.neuroimage.2012.03.021
Kesner, R. P., Lee, I., & Gilbert, P. (2004). A behavioral assessment of hippocampal function based on a subregional analysis. *Rev Neurosci, 15*(5), 333-351. doi:10.1515/revneuro.2004.15.5.333
Kesslak, J. P., Nalcioglu, O., & Cotman, C. W. (1991). Quantification of magnetic resonance scans for hippocampal and parahippocampal atrophy in Alzheimer's disease. *Neurology, 41*(1), 51-54. doi:10.1212/wnl.41.1.51
Kharabian Masouleh, S., Plachti, A., Hoffstaedter, F., Eickhoff, S., & Genon, S. (2020). Characterizing the gradients of structural covariance in the human hippocampus. *Neuroimage, 218*, 116972. doi:https://doi.org/10.1016/j.neuroimage.2020.116972
Kim, H. (2015). Encoding and retrieval along the long axis of the hippocampus and their relationships with dorsal attention and default mode networks: The HERNET model. *Hippocampus, 25*(4), 500-510. doi:10.1002/hipo.22387
Kim, H.-J., Shin, J.-H., Han, C. E., Kim, H. J., Na, D. L., Seo, S. W., . . . Alzheimer's Disease Neuroimaging, I. (2016). Using Individualized Brain Network for Analyzing Structural Covariance of the Cerebral Cortex in Alzheimer's Patients. *Front Neurosci, 10*, 394-394. doi:10.3389/fnins.2016.00394
Kjelstrup, K. B., Solstad, T., Brun, V. H., Hafting, T., Leutgeb, S., Witter, M. P., . . . Moser, M. B. (2008). Finite scale of spatial representation in the hippocampus. *Science, 321*(5885), 140-143. doi:10.1126/science.1157086
Kleinberg, J. (2002). *An impossibility theorem for clustering*. Paper presented at the Proceedings of the 15th International Conference on Neural Information Processing Systems.
Klunk, W. E., Engler, H., Nordberg, A., Wang, Y., Blomqvist, G., Holt, D. P., . . . Langstrom, B. (2004). Imaging brain amyloid in Alzheimer's disease with Pittsburgh Compound-B. *Ann Neurol, 55*(3), 306-319. doi:10.1002/ana.20009
Knierim, J. J. (2015). The hippocampus. *Current Biology, 25*(23), R1116-R1121. doi:https://doi.org/10.1016/j.cub.2015.10.049
Koch, W., Teipel, S., Mueller, S., Buerger, K., Bokde, A. L., Hampel, H., . . . Meindl, T. (2010). Effects of aging on default mode network activity in resting state fMRI: does the method of analysis matter? *Neuroimage, 51*(1), 280-287. doi:10.1016/j.neuroimage.2009.12.008
Koster, R., Chadwick, M. J., Chen, Y., Berron, D., Banino, A., Duzel, E., . . . Kumaran, D. (2018). Big-Loop Recurrence within the Hippocampal System Supports Integration of Information across Episodes. *Neuron, 99*(6), 1342-1354.e1346. doi:10.1016/j.neuron.2018.08.009
Kotkowski, E., Price, L. R., Mickle Fox, P., Vanasse, T. J., & Fox, P. T. (2018). The hippocampal network model: A transdiagnostic metaconnectomic approach. *Neuroimage Clin, 18*, 115-129. doi:10.1016/j.nicl.2018.01.002
Kühn, S., & Gallinat, J. (2014). Segregating cognitive functions within hippocampal formation: A quantitative meta-analysis on spatial navigation and episodic memory. *Hum Brain Mapp, 35*(4), 1129-1142. doi:10.1002/hbm.22239

La Joie, R., Fouquet, M., Mezenge, F., Landeau, B., Villain, N., Mevel, K., . . . Chetelat, G. (2010). Differential effect of age on hippocampal subfields assessed using a new high-resolution 3T MR sequence. *Neuroimage, 53*(2), 506-514. doi:10.1016/j.neuroimage.2010.06.024

La Joie, R., Perrotin, A., de La Sayette, V., Egret, S., Doeuvre, L., Belliard, S., . . . Chetelat, G. (2013). Hippocampal subfield volumetry in mild cognitive impairment, Alzheimer's disease and semantic dementia. *Neuroimage Clin, 3*, 155-162. doi:10.1016/j.nicl.2013.08.007

Laakso, M. P., Lehtovirta, M., Partanen, K., Riekkinen, P. J., & Soininen, H. (2000). Hippocampus in Alzheimer's disease: a 3-year follow-up MRI study. *Biol Psychiatry, 47*(6), 557-561. doi:10.1016/s0006-3223(99)00167-5

LaConte, S., Anderson, J., Muley, S., Ashe, J., Frutiger, S., Rehm, K., . . . Strother, S. (2003). The evaluation of preprocessing choices in single-subject BOLD fMRI using NPAIRS performance metrics. *Neuroimage, 18*(1), 10-27.

Laird, A. R., Eickhoff, S. B., Fox, P. M., Uecker, A. M., Ray, K. L., Saenz, J. J., Jr., . . . Fox, P. T. (2011). The BrainMap strategy for standardization, sharing, and meta-analysis of neuroimaging data. *BMC Res Notes, 4*, 349. doi:10.1186/1756-0500-4-349

Lambert, C., Simon, H., Colman, J., & Barrick, T. R. (2017). Defining thalamic nuclei and topographic connectivity gradients in vivo. *Neuroimage, 158*, 466-479. doi:10.1016/j.neuroimage.2016.08.028

Lazic, S. E. (2012). Modeling hippocampal neurogenesis across the lifespan in seven species. *Neurobiol Aging, 33*(8), 1664-1671. doi:10.1016/j.neurobiolaging.2011.03.008

Lepage, M., Habib, R., & Tulving, E. (1998). Hippocampal PET activations of memory encoding and retrieval: the HIPER model. *Hippocampus, 8*(4), 313-322. doi:10.1002/(SICI)1098-1063(1998)8:4<313::AID-HIPO1>3.0.CO;2-I

Leutgeb, J. K., Leutgeb, S., Moser, M. B., & Moser, E. I. (2007). Pattern separation in the dentate gyrus and CA3 of the hippocampus. *Science, 315*(5814), 961-966. doi:10.1126/science.1135801

Li, H. J., Hou, X. H., Liu, H. H., Yue, C. L., He, Y., & Zuo, X. N. (2015). Toward systems neuroscience in mild cognitive impairment and Alzheimer's disease: a meta-analysis of 75 fMRI studies. *Hum Brain Mapp, 36*(3), 1217-1232. doi:10.1002/hbm.22689

Li, X., Li, Q., Wang, X., Li, D., & Li, S. (2018). Differential Age-Related Changes in Structural Covariance Networks of Human Anterior and Posterior Hippocampus. *Front Physiol, 9*, 518. doi:10.3389/fphys.2018.00518

Libby, L. A., Ekstrom, A. D., Ragland, J. D., & Ranganath, C. (2012). Differential connectivity of perirhinal and parahippocampal cortices within human hippocampal subregions revealed by high-resolution functional imaging. *J Neurosci, 32*(19), 6550-6560. doi:10.1523/jneurosci.3711-11.2012

Lindberg, O., Walterfang, M., Looi, J. C., Malykhin, N., Ostberg, P., Zandbelt, B., . . . Wahlund, L. O. (2012). Hippocampal shape analysis in Alzheimer's disease and frontotemporal lobar degeneration subtypes. *J Alzheimers Dis, 30*(2), 355-365. doi:10.3233/jad-2012-112210

Liu, T. T. (2016). Noise contributions to the fMRI signal: An overview. *Neuroimage, 143*, 141-151. doi:10.1016/j.neuroimage.2016.09.008

Llera, A., Wolfers, T., Mulders, P., & Beckmann, C. F. (2019). Inter-individual differences in human brain structure and morphology link to variation in demographics and behavior. *eLife, 8*, e44443. doi:10.7554/eLife.44443

Lowe, A. J., Paquola, C., Vos de Wael, R., Girn, M., Lariviere, S., Tavakol, S., . . . Bernhardt, B. C. (2019). Targeting Age-Related Differences in Brain and Cognition with Multimodal Imaging and Connectome Topography Profiling. *bioRxiv*, 601146. doi:10.1101/601146

Lubenov, E. V., & Siapas, A. G. (2009). Hippocampal theta oscillations are travelling waves. *Nature, 459*(7246), 534-539. doi:10.1038/nature08010

Lupien, S. J., Evans, A., Lord, C., Miles, J., Pruessner, M., Pike, B., & Pruessner, J. C. (2007). Hippocampal volume is as variable in young as in older adults: implications for the notion of hippocampal atrophy in humans. *Neuroimage, 34*(2), 479-485. doi:10.1016/j.neuroimage.2006.09.041

Luxburg, U. v., Williamson, R. C., & Guyon, I. (2012). *Clustering: Science or Art?* Paper presented at the Proceedings of ICML Workshop on Unsupervised and Transfer Learning, Proceedings of Machine Learning Research. http://proceedings.mlr.press

Ly, M., Foley, L., Manivannan, A., Hitchens, T. K., Richardson, R. M., & Modo, M. Mesoscale diffusion magnetic resonance imaging of the ex vivo human hippocampus. *Hum Brain Mapp, n/a*(n/a). doi:10.1002/hbm.25119

Maass, A., Berron, D., Libby, L. A., Ranganath, C., & Düzel, E. (2015). Functional subregions of the human entorhinal cortex. *eLife, 4*, e06426. doi:10.7554/eLife.06426

Macey, P. M., Macey, K. E., Kumar, R., & Harper, R. M. (2004). A method for removal of global effects from fMRI time series. *Neuroimage, 22*(1), 360-366. doi:10.1016/j.neuroimage.2003.12.042

Maguire, E. A., Woollett, K., & Spiers, H. J. (2006). London taxi drivers and bus drivers: a structural MRI and neuropsychological analysis. *Hippocampus, 16*(12), 1091-1101. doi:10.1002/hipo.20233

Maller, J. J., Welton, T., Middione, M., Callaghan, F. M., Rosenfeld, J. V., & Grieve, S. M. (2019). Revealing the Hippocampal Connectome through Super-Resolution 1150-Direction Diffusion MRI. *Scientific Reports, 9*(1), 2418. doi:10.1038/s41598-018-37905-9

Malykhin, N. V., Bouchard, T. P., Camicioli, R., & Coupland, N. J. (2008). Aging hippocampus and amygdala. *Neuroreport, 19*(5), 543-547. doi:10.1097/WNR.0b013e3282f8b18c

Malykhin, N. V., Huang, Y., Hrybouski, S., & Olsen, F. (2017). Differential vulnerability of hippocampal subfields and anteroposterior hippocampal subregions in healthy cognitive aging. *Neurobiol Aging, 59*, 121-134. doi:10.1016/j.neurobiolaging.2017.08.001

Maurer, A. P., VanRhoads, S. R., Sutherland, G. R., Lipa, P., & McNaughton, B. L. (2005). Self-motion and the origin of differential spatial scaling along the septo-temporal axis of the hippocampus. *Hippocampus, 15*(7), 841-852. doi:10.1002/hipo.20114

McTeague, L. M., Goodkind, M. S., & Etkin, A. (2016). Transdiagnostic impairment of cognitive control in mental illness. *J Psychiatr Res, 83*, 37-46. doi:10.1016/j.jpsychires.2016.08.001

Mechelli, A., Friston, K. J., Frackowiak, R. S., & Price, C. J. (2005). Structural covariance in the human cortex. *J Neurosci, 25*(36), 8303-8310. doi:10.1523/jneurosci.0357-05.2005

Meilă, M. (2007). Comparing clusterings—an information based distance. *Journal of Multivariate Analysis, 98*(5), 873-895. doi:https://doi.org/10.1016/j.jmva.2006.11.013

Metzler-Baddeley, C., Mole, J. P., Sims, R., Fasano, F., Evans, J., Jones, D. K., . . . Baddeley, R. J. (2019). Fornix white matter glia damage causes hippocampal gray matter damage during age-dependent limbic decline. *Scientific Reports, 9*(1), 1060. doi:10.1038/s41598-018-37658-5

Minkova, L., Habich, A., Peter, J., Kaller, C. P., Eickhoff, S. B., & Kloppel, S. (2017). Gray matter asymmetries in aging and neurodegeneration: A review and meta-analysis. *Hum Brain Mapp, 38*(12), 5890-5904. doi:10.1002/hbm.23772

Mishra, A., Rogers, B. P., Chen, L. M., & Gore, J. C. (2014). Functional connectivity-based parcellation of amygdala using self-organized mapping: a data driven approach. *Hum Brain Mapp, 35*(4), 1247-1260. doi:10.1002/hbm.22249

Montembeault, M., Joubert, S., Doyon, J., Carrier, J., Gagnon, J. F., Monchi, O., . . . Brambati, S. M. (2012). The impact of aging on gray matter structural covariance networks. *Neuroimage, 63*(2), 754-759. doi:10.1016/j.neuroimage.2012.06.052

Montembeault, M., Rouleau, I., Provost, J. S., & Brambati, S. M. (2016). Altered Gray Matter Structural Covariance Networks in Early Stages of Alzheimer's Disease. *Cereb Cortex, 26*(6), 2650-2662. doi:10.1093/cercor/bhv105

Morcom, A. M., & Henson, R. N. A. (2018). Increased Prefrontal Activity with Aging Reflects Nonspecific Neural Responses Rather than Compensation. *The Journal of Neuroscience, 38*(33), 7303-7313. doi:10.1523/jneurosci.1701-17.2018

Moreno-Jiménez, E. P., Flor-García, M., Terreros-Roncal, J., Rábano, A., Cafini, F., Pallas-Bazarra, N., . . . Llorens-Martín, M. (2019). Adult hippocampal neurogenesis is abundant in neurologically healthy subjects and drops sharply in patients with Alzheimer's disease. *Nature Medicine, 25*(4), 554-560. doi:10.1038/s41591-019-0375-9

Morris, J. C., Roe, C. M., Grant, E. A., Head, D., Storandt, M., Goate, A. M., . . . Mintun, M. A. (2009). Pittsburgh compound B imaging and prediction of progression from cognitive normality to symptomatic Alzheimer disease. *Arch Neurol, 66*(12), 1469-1475. doi:10.1001/archneurol.2009.269

Morris, R. G., Hagan, J. J., & Rawlins, J. N. (1986). Allocentric spatial learning by hippocampectomised rats: a further test of the "spatial mapping" and "working memory" theories of hippocampal function. *Q J Exp Psychol B, 38*(4), 365-395.

Morton, N. W., Sherrill, K. R., & Preston, A. R. (2017). Memory integration constructs maps of space, time, and concepts. *Current opinion in behavioral sciences, 17*, 161-168. doi:10.1016/j.cobeha.2017.08.007

Moser, E., Moser, M. B., & Andersen, P. (1993). Spatial learning impairment parallels the magnitude of dorsal hippocampal lesions, but is hardly present following ventral lesions. *J Neurosci, 13*(9), 3916-3925.

Moser, M. B., & Moser, E. I. (1998). Functional differentiation in the hippocampus. *Hippocampus, 8*(6), 608-619. doi:10.1002/(SICI)1098-1063(1998)8:6<608::AID-HIPO3>3.0.CO;2-7

Mueller, S., Wang, D., Fox, M. D., Yeo, B. T., Sepulcre, J., Sabuncu, M. R., . . . Liu, H. (2013). Individual variability in functional connectivity architecture of the human brain. *Neuron, 77*(3), 586-595. doi:10.1016/j.neuron.2012.12.028

Mueller, S. G., Schuff, N., Yaffe, K., Madison, C., Miller, B., & Weiner, M. W. (2010). Hippocampal atrophy patterns in mild cognitive impairment and Alzheimer's disease. *Hum Brain Mapp, 31*(9), 1339-1347. doi:10.1002/hbm.20934

Mueller, S. G., Stables, L., Du, A. T., Schuff, N., Truran, D., Cashdollar, N., & Weiner, M. W. (2007). Measurement of hippocampal subfields and age-related changes with high resolution MRI at 4T. *Neurobiol Aging, 28*(5), 719-726. doi:10.1016/j.neurobiolaging.2006.03.007

Mueller, S. G., & Weiner, M. W. (2009). Selective effect of age, Apo e4, and Alzheimer's disease on hippocampal subfields. *Hippocampus, 19*(6), 558-564. doi:10.1002/hipo.20614

Müller, M. J., Greverus, D., Dellani, P. R., Weibrich, C., Wille, P. R., Scheurich, A., . . . Fellgiebel, A. (2005). Functional implications of hippocampal volume and diffusivity in mild cognitive impairment. *Neuroimage, 28*(4), 1033-1042. doi:https://doi.org/10.1016/j.neuroimage.2005.06.029

Murphy, K., Birn, R. M., Handwerker, D. A., Jones, T. B., & Bandettini, P. A. (2009). The impact of global signal regression on resting state correlations: are anti-correlated networks introduced? *Neuroimage, 44*(3), 893-905. doi:10.1016/j.neuroimage.2008.09.036

Naber, P. A., & Witter, M. P. (1998). Subicular efferents are organized mostly as parallel projections: A double-labeling, retrograde-tracing study in the rat. *Journal of Comparative Neurology, 393*(3), 284-297. doi:10.1002/(sici)1096-9861(19980413)393:3<284::aid-cne2>3.0.co;2-y

Nadel, L., Hoscheidt, S., & Ryan, L. R. (2013). Spatial cognition and the hippocampus: the anterior-posterior axis. *J Cogn Neurosci, 25*(1), 22-28. doi:10.1162/jocn_a_00313

Nanetti, L., Cerliani, L., Gazzola, V., Renken, R., & Keysers, C. (2009). Group analyses of connectivity-based cortical parcellation using repeated k-means clustering. *Neuroimage, 47*(4), 1666-1677. doi:10.1016/j.neuroimage.2009.06.014

Nordin, K., Persson, J., Stening, E., Herlitz, A., Larsson, E.-M., & Söderlund, H. (2018). Structural whole-brain covariance of the anterior and posterior hippocampus: Associations with age and memory. *Hippocampus, 28*(2), 151-163. doi:10.1002/hipo.22817

Novellino, F., López, M. E., Vaccaro, M. G., Miguel, Y., Delgado, M. L., & Maestu, F. (2019). Association Between Hippocampus, Thalamus, and Caudate in Mild Cognitive Impairment APOEε4 Carriers: A Structural Covariance MRI Study. *Front Neurol, 10*, 1303. doi:10.3389/fneur.2019.01303

O'Mara, S. (2005). The subiculum: what it does, what it might do, and what neuroanatomy has yet to tell us. *J Anat, 207*(3), 271-282. doi:10.1111/j.1469-7580.2005.00446.x

O'Mara, S. M., Sanchez-Vives, M. V., Brotons-Mas, J. R., & O'Hare, E. (2009). Roles for the subiculum in spatial information processing, memory, motivation and the temporal control of behaviour. *Prog Neuropsychopharmacol Biol Psychiatry, 33*(5), 782-790. doi:10.1016/j.pnpbp.2009.03.040

O'Sullivan, M., Jones, D. K., Summers, P. E., Morris, R. G., Williams, S. C., & Markus, H. S. (2001). Evidence for cortical "disconnection" as a mechanism of age-related cognitive decline. *Neurology, 57*(4), 632-638. doi:10.1212/wnl.57.4.632

Ojemann, J. G., Akbudak, E., Snyder, A. Z., McKinstry, R. C., Raichle, M. E., & Conturo, T. E. (1997). Anatomic localization and quantitative analysis of gradient refocused echo-planar fMRI susceptibility artifacts. *Neuroimage, 6*(3), 156-167. doi:10.1006/nimg.1997.0289

Oppenheim, C., Dormont, D., Biondi, A., Lehericy, S., Hasboun, D., Clemenceau, S., . . . Marsault, C. (1998). Loss of digitations of the hippocampal head on high-resolution fast spin-echo MR: a sign of mesial temporal sclerosis. *AJNR Am J Neuroradiol, 19*(3), 457-463.

Palomero-Gallagher, N., Kedo, O., Mohlberg, H., Zilles, K., & Amunts, K. (2020). Multimodal mapping and analysis of the cyto- and receptorarchitecture of the human hippocampus. *Brain Structure and Function*. doi:10.1007/s00429-019-02022-4

Paquola, C., Bennett, M. R., & Lagopoulos, J. (2018). Structural and Functional Connectivity Underlying Gray Matter Covariance: Impact of Developmental Insult. *Brain Connect, 8*(5), 299-310. doi:10.1089/brain.2018.0584

Pasquini, L., Scherr, M., Tahmasian, M., Meng, C., Myers, N. E., Ortner, M., . . . Sorg, C. (2015). Link between hippocampus' raised local and eased global intrinsic connectivity in AD. *Alzheimers Dement, 11*(5), 475-484. doi:10.1016/j.jalz.2014.02.007

Pereira, J. B., Mijalkov, M., Kakaei, E., Mecocci, P., Vellas, B., Tsolaki, M., . . . Westman, E. (2016). Disrupted Network Topology in Patients with Stable and Progressive Mild Cognitive Impairment and Alzheimer's Disease. *Cereb Cortex, 26*(8), 3476-3493. doi:10.1093/cercor/bhw128

Pereira, J. B., Valls-Pedret, C., Ros, E., Palacios, E., Falcon, C., Bargallo, N., . . . Junque, C. (2014). Regional vulnerability of hippocampal subfields to aging measured by structural and diffusion MRI. *Hippocampus, 24*(4), 403-414. doi:10.1002/hipo.22234

Persson, J., Stening, E., Nordin, K., & Söderlund, H. (2018). Predicting episodic and spatial memory performance from hippocampal resting-state functional connectivity: Evidence for an anterior–posterior division of function. *Hippocampus, 28*(1), 53-66. doi:10.1002/hipo.22807

Petrovich, G. D., Canteras, N. S., & Swanson, L. W. (2001). Combinatorial amygdalar inputs to hippocampal domains and hypothalamic behavior systems. *Brain Res Brain Res Rev, 38*(1-2), 247-289.

Pievani, M., Galluzzi, S., Thompson, P. M., Rasser, P. E., Bonetti, M., & Frisoni, G. B. (2011). APOE4 is associated with greater atrophy of the hippocampal formation in Alzheimer's disease. *Neuroimage, 55*(3), 909-919. doi:10.1016/j.neuroimage.2010.12.081

Plachti, A., Eickhoff, S. B., Hoffstaedter, F., Patil, K. R., Laird, A. R., Fox, P. T., . . . Genon, S. (2019). Multimodal Parcellations and Extensive Behavioral Profiling Tackling the Hippocampus Gradient. *Cereb Cortex*. doi:10.1093/cercor/bhy336

Pluta, J., Yushkevich, P., Das, S., & Wolk, D. (2012). In vivo analysis of hippocampal subfield atrophy in mild cognitive impairment via semi-automatic segmentation of T2-weighted MRI. *J Alzheimers Dis, 31*(1), 85-99. doi:10.3233/jad-2012-111931

Poppenk, J., Evensmoen, H. R., Moscovitch, M., & Nadel, L. (2013). Long-axis specialization of the human hippocampus. *Trends Cogn Sci, 17*(5), 230-240. doi:10.1016/j.tics.2013.03.005

Poppenk, J., & Moscovitch, M. (2011). A hippocampal marker of recollection memory ability among healthy young adults: contributions of posterior and anterior segments. *Neuron, 72*(6), 931-937. doi:10.1016/j.neuron.2011.10.014

Postans, M., Parker, G. D., Lundell, H., Ptito, M., Hamandi, K., Gray, W. P., . . . Winter, M. (2019). Uncovering a Role for the Dorsal Hippocampal Commissure in Recognition Memory. *Cerebral Cortex*. doi:10.1093/cercor/bhz143

Power, J. D., Barnes, K. A., Snyder, A. Z., Schlaggar, B. L., & Petersen, S. E. (2012). Spurious but systematic correlations in functional connectivity MRI networks arise from subject motion. *Neuroimage, 59*(3), 2142-2154. doi:10.1016/j.neuroimage.2011.10.018

Power, J. D., Mitra, A., Laumann, T. O., Snyder, A. Z., Schlaggar, B. L., & Petersen, S. E. (2014). Methods to detect, characterize, and remove motion artifact in resting state fMRI. *Neuroimage, 84*, 320-341. doi:10.1016/j.neuroimage.2013.08.048

Power, J. D., Schlaggar, B. L., & Petersen, S. E. (2015). Recent progress and outstanding issues in motion correction in resting state fMRI. *Neuroimage, 105*, 536-551. doi:10.1016/j.neuroimage.2014.10.044

Price, J. L., Ko, A. I., Wade, M. J., Tsou, S. K., McKeel, D. W., & Morris, J. C. (2001). Neuron number in the entorhinal cortex and CA1 in preclinical Alzheimer disease. *Arch Neurol, 58*(9), 1395-1402. doi:10.1001/archneur.58.9.1395

Prince, S. E., Daselaar, S. M., & Cabeza, R. (2005). Neural correlates of relational memory: successful encoding and retrieval of semantic and perceptual associations. *J Neurosci, 25*(5), 1203-1210. doi:10.1523/jneurosci.2540-04.2005

Pruessner, J. C., Collins, D. L., Pruessner, M., & Evans, A. C. (2001). Age and gender predict volume decline in the anterior and posterior hippocampus in early adulthood. *J Neurosci, 21*(1), 194-200.

Przeździk, I., Faber, M., Fernández, G., Beckmann, C. F., & Haak, K. V. (2019). The functional organisation of the hippocampus along its long axis is gradual and predicts recollection. *Cortex, 119*, 324-335. doi:https://doi.org/10.1016/j.cortex.2019.04.015

Qin, S., Duan, X., Supekar, K., Chen, H., Chen, T., & Menon, V. (2016). Large-scale intrinsic functional network organization along the long axis of the human medial temporal lobe. *Brain Struct Funct, 221*(6), 3237-3258. doi:10.1007/s00429-015-1098-4

Qiu, Y., Li, L., Zhou, T. Y., & Lu, W. (2014). Alzheimer's disease progression model based on integrated biomarkers and clinical measures. *Acta Pharmacol Sin, 35*(9), 1111-1120. doi:10.1038/aps.2014.57

Rajah, M. N., Kromas, M., Han, J. E., & Pruessner, J. C. (2010). Group differences in anterior hippocampal volume and in the retrieval of spatial and temporal context memory in healthy young versus older adults. *Neuropsychologia, 48*(14), 4020-4030. doi:10.1016/j.neuropsychologia.2010.10.010

Raz, N., Ghisletta, P., Rodrigue, K. M., Kennedy, K. M., & Lindenberger, U. (2010). Trajectories of brain aging in middle-aged and older adults: regional and individual differences. *Neuroimage, 51*(2), 501-511. doi:10.1016/j.neuroimage.2010.03.020

Raz, N., Lindenberger, U., Rodrigue, K. M., Kennedy, K. M., Head, D., Williamson, A., . . . Acker, J. D. (2005). Regional brain changes in aging healthy adults: general trends, individual differences and modifiers. *Cereb Cortex, 15*(11), 1676-1689. doi:10.1093/cercor/bhi044

Reid, A. T., Bzdok, D., Langner, R., Fox, P. T., Laird, A. R., Amunts, K., . . . Eickhoff, C. R. (2016). Multimodal connectivity mapping of the human left anterior and posterior lateral prefrontal cortex. *Brain Struct Funct, 221*(5), 2589-2605. doi:10.1007/s00429-015-1060-5

Risold, P. Y., & Swanson, L. W. (1996). Structural evidence for functional domains in the rat hippocampus. *Science, 272*(5267), 1484-1486.

Robinson, J. L., Barron, D. S., Kirby, L. A., Bottenhorn, K. L., Hill, A. C., Murphy, J. E., . . . Fox, P. T. (2015). Neurofunctional topography of the human hippocampus. *Hum Brain Mapp, 36*(12), 5018-5037. doi:10.1002/hbm.22987

Robinson, J. L., Salibi, N., & Deshpande, G. (2016). Functional connectivity of the left and right hippocampi: Evidence for functional lateralization along the long-axis using meta-analytic approaches and ultra-high field functional neuroimaging. *Neuroimage, 135*, 64-78. doi:10.1016/j.neuroimage.2016.04.022

Ronan, T., Qi, Z., & Naegle, K. M. (2016). Avoiding common pitfalls when clustering biological data. *Science Signaling, 9*(432), re6-re6. doi:10.1126/scisignal.aad1932

Rossler, M., Zarski, R., Bohl, J., & Ohm, T. G. (2002). Stage-dependent and sector-specific neuronal loss in hippocampus during Alzheimer's disease. *Acta Neuropathol, 103*(4), 363-369. doi:10.1007/s00401-001-0475-7

Sala-Llonch, R., Bartres-Faz, D., & Junque, C. (2015). Reorganization of brain networks in aging: a review of functional connectivity studies. *Front Psychol, 6*, 663. doi:10.3389/fpsyg.2015.00663

Salami, A., Pudas, S., & Nyberg, L. (2014). Elevated hippocampal resting-state connectivity underlies deficient neurocognitive function in aging. *Proceedings of the National Academy of Sciences, 111*(49), 17654-17659. doi:10.1073/pnas.1410233111

Salami, A., Wahlin, A., Kaboodvand, N., Lundquist, A., & Nyberg, L. (2016). Longitudinal Evidence for Dissociation of Anterior and Posterior MTL Resting-State Connectivity in Aging: Links to Perfusion and Memory. *Cereb Cortex, 26*(10), 3953-3963. doi:10.1093/cercor/bhw233

Salimi-Khorshidi, G., Douaud, G., Beckmann, C. F., Glasser, M. F., Griffanti, L., & Smith, S. M. (2014). Automatic denoising of functional MRI data: combining independent component analysis and hierarchical fusion of classifiers. *Neuroimage, 90*, 449-468. doi:10.1016/j.neuroimage.2013.11.046

Satterthwaite, T. D., Ciric, R., Roalf, D. R., Davatzikos, C., Bassett, D. S., & Wolf, D. H. (2017). Motion artifact in studies of functional connectivity: Characteristics and mitigation strategies. *Hum Brain Mapp*. doi:10.1002/hbm.23665

Satterthwaite, T. D., Elliott, M. A., Gerraty, R. T., Ruparel, K., Loughead, J., Calkins, M. E., . . . Wolf, D. H. (2013). An improved framework for confound regression and filtering for control of motion artifact in the preprocessing of resting-state functional connectivity data. *Neuroimage, 64*, 240-256. doi:10.1016/j.neuroimage.2012.08.052

Schaefer, A., Kong, R., Gordon, E. M., Laumann, T. O., Zuo, X. N., Holmes, A. J., . . . Yeo, B. T. T. (2017). Local-Global Parcellation of the Human Cerebral Cortex from Intrinsic Functional Connectivity MRI. *Cereb Cortex*, 1-20. doi:10.1093/cercor/bhx179

Schlichting, M. L., Mumford, J. A., & Preston, A. R. (2015). Learning-related representational changes reveal dissociable integration and separation signatures in the hippocampus and prefrontal cortex. *Nat Commun, 6*, 8151. doi:10.1038/ncomms9151

Schuff, N., Amend, D. L., Knowlton, R., Norman, D., Fein, G., & Weiner, M. W. (1999). Age-related metabolite changes and volume loss in the hippocampus by magnetic resonance spectroscopy and imaging. *Neurobiol Aging, 20*(3), 279-285. doi:10.1016/s0197-4580(99)00022-6

Scoville, W. B., & Milner, B. (1957). Loss of recent memory after bilateral hippocampal lesions. *Journal of neurology, neurosurgery, and psychiatry, 20*(1), 11-21. doi:10.1136/jnnp.20.1.11

Seeley, W. W., Crawford, R. K., Zhou, J., Miller, B. L., & Greicius, M. D. (2009). Neurodegenerative diseases target large-scale human brain networks. *Neuron, 62*(1), 42-52. doi:10.1016/j.neuron.2009.03.024

Shafto, M. A., Tyler, L. K., Dixon, M., Taylor, J. R., Rowe, J. B., Cusack, R., . . . Matthews, F. E. (2014). The Cambridge Centre for Ageing and Neuroscience (Cam-CAN) study protocol: a cross-sectional, lifespan, multidisciplinary examination of healthy cognitive ageing. *BMC Neurol, 14*, 204. doi:10.1186/s12883-014-0204-1

Shah, P., Bassett, D. S., Wisse, L. E. M., Detre, J. A., Stein, J. M., Yushkevich, P. A., . . . Das, S. R. (2018). Mapping the structural and functional network architecture of the

medial temporal lobe using 7T MRI. *Hum Brain Mapp, 39*(2), 851-865. doi:10.1002/hbm.23887

Shi, F., Liu, B., Zhou, Y., Yu, C., & Jiang, T. (2009). Hippocampal volume and asymmetry in mild cognitive impairment and Alzheimer's disease: Meta-analyses of MRI studies. *Hippocampus, 19*(11), 1055-1064. doi:10.1002/hipo.20573

Small, S. A., Nava, A. S., Perera, G. M., DeLaPaz, R., Mayeux, R., & Stern, Y. (2001). Circuit mechanisms underlying memory encoding and retrieval in the long axis of the hippocampal formation. *Nat Neurosci, 4*(4), 442-449. doi:10.1038/86115

Smith, S. M., Beckmann, C. F., Andersson, J., Auerbach, E. J., Bijsterbosch, J., Douaud, G., . . . Glasser, M. F. (2013). Resting-state fMRI in the Human Connectome Project. *Neuroimage, 80*, 144-168. doi:10.1016/j.neuroimage.2013.05.039

Sowell, E. R., Peterson, B. S., Thompson, P. M., Welcome, S. E., Henkenius, A. L., & Toga, A. W. (2003). Mapping cortical change across the human life span. *Nat Neurosci, 6*(3), 309-315. doi:10.1038/nn1008

Sperling, R. A., Mormino, E. C., Schultz, A. P., Betensky, R. A., Papp, K. V., Amariglio, R. E., . . . Johnson, K. A. (2019). The impact of amyloid-beta and tau on prospective cognitive decline in older individuals. *Ann Neurol, 85*(2), 181-193. doi:10.1002/ana.25395

Spreng, R. N., & Turner, G. R. (2013). Structural covariance of the default network in healthy and pathological aging. *J Neurosci, 33*(38), 15226-15234. doi:10.1523/JNEUROSCI.2261-13.2013

Stark, S. M., Frithsen, A., & Stark, C. E. L. (2019). Age-related alterations in functional connectivity along the longitudinal axis of the hippocampus and its subfields. *bioRxiv*, 577361. doi:10.1101/577361

Stern, Y., Habeck, C., Moeller, J., Scarmeas, N., Anderson, K. E., Hilton, H. J., . . . van Heertum, R. (2005). Brain networks associated with cognitive reserve in healthy young and old adults. *Cereb Cortex, 15*(4), 394-402. doi:10.1093/cercor/bhh142

Strange, B. A., Fletcher, P. C., Henson, R. N., Friston, K. J., & Dolan, R. J. (1999). Segregating the functions of human hippocampus. *Proc Natl Acad Sci U S A, 96*(7), 4034-4039.

Strange, B. A., Witter, M. P., Lein, E. S., & Moser, E. I. (2014). Functional organization of the hippocampal longitudinal axis. *Nat Rev Neurosci, 15*(10), 655-669. doi:10.1038/nrn3785

Strother, S. C., Anderson, J., Hansen, L. K., Kjems, U., Kustra, R., Sidtis, J., . . . Rottenberg, D. (2002). The quantitative evaluation of functional neuroimaging experiments: the NPAIRS data analysis framework. *Neuroimage, 15*(4), 747-771. doi:10.1006/nimg.2001.1034

Sullivan, E. V., Marsh, L., Mathalon, D. H., Lim, K. O., & Pfefferbaum, A. (1995). Age-related decline in MRI volumes of temporal lobe gray matter but not hippocampus. *Neurobiol Aging, 16*(4), 591-606. doi:10.1016/0197-4580(95)00074-o

Sullivan, E. V., Marsh, L., & Pfefferbaum, A. (2005). Preservation of hippocampal volume throughout adulthood in healthy men and women. *Neurobiol Aging, 26*(7), 1093-1098. doi:10.1016/j.neurobiolaging.2004.09.015

Swanson, L. W., & Cowan, W. M. (1977). An autoradiographic study of the organization of the efferent connections of the hippocampal formation in the rat. *J Comp Neurol, 172*(1), 49-84. doi:10.1002/cne.901720104

Ta, A. T., Huang, S. E., Chiu, M. J., Hua, M. S., Tseng, W. Y., Chen, S. H., & Qiu, A. (2012). Age-related vulnerabilities along the hippocampal longitudinal axis. *Hum Brain Mapp, 33*(10), 2415-2427. doi:10.1002/hbm.21364

Taylor, J. R., Williams, N., Cusack, R., Auer, T., Shafto, M. A., Dixon, M., . . . Henson, R. N. (2017). The Cambridge Centre for Ageing and Neuroscience (Cam-CAN) data

repository: Structural and functional MRI, MEG, and cognitive data from a cross-sectional adult lifespan sample. *Neuroimage, 144*(Pt B), 262-269. doi:10.1016/j.neuroimage.2015.09.018

Thal, D. R., Holzer, M., Rub, U., Waldmann, G., Gunzel, S., Zedlick, D., & Schober, R. (2000). Alzheimer-related tau-pathology in the perforant path target zone and in the hippocampal stratum oriens and radiatum correlates with onset and degree of dementia. *Exp Neurol, 163*(1), 98-110. doi:10.1006/exnr.2000.7380

Thirion, B., Varoquaux, G., Dohmatob, E., & Poline, J. B. (2014). Which fMRI clustering gives good brain parcellations? *Front Neurosci, 8*, 167. doi:10.3389/fnins.2014.00167

Treit, S., Steve, T., Gross, D. W., & Beaulieu, C. (2018). High resolution in-vivo diffusion imaging of the human hippocampus. *Neuroimage, 182*, 479-487. doi:10.1016/j.neuroimage.2018.01.034

Ugurbil, K., Xu, J., Auerbach, E. J., Moeller, S., Vu, A. T., Duarte-Carvajalino, J. M., . . . Yacoub, E. (2013). Pushing spatial and temporal resolution for functional and diffusion MRI in the Human Connectome Project. *Neuroimage, 80*, 80-104. doi:10.1016/j.neuroimage.2013.05.012

Van Dijk, K. R., Hedden, T., Venkataraman, A., Evans, K. C., Lazar, S. W., & Buckner, R. L. (2010). Intrinsic functional connectivity as a tool for human connectomics: theory, properties, and optimization. *J Neurophysiol, 103*(1), 297-321. doi:10.1152/jn.00783.2009

Van Dijk, K. R., Sabuncu, M. R., & Buckner, R. L. (2012). The influence of head motion on intrinsic functional connectivity MRI. *Neuroimage, 59*(1), 431-438. doi:10.1016/j.neuroimage.2011.07.044

Van Essen, D. C., & Ugurbil, K. (2012). The future of the human connectome. *Neuroimage, 62*(2), 1299-1310. doi:10.1016/j.neuroimage.2012.01.032

Van Petten, C. (2004). Relationship between hippocampal volume and memory ability in healthy individuals across the lifespan: review and meta-analysis. *Neuropsychologia, 42*(10), 1394-1413. doi:https://doi.org/10.1016/j.neuropsychologia.2004.04.006

van Praag, H., Shubert, T., Zhao, C., & Gage, F. H. (2005). Exercise enhances learning and hippocampal neurogenesis in aged mice. *J Neurosci, 25*(38), 8680-8685. doi:10.1523/jneurosci.1731-05.2005

Vann, S. D., Brown, M. W., Erichsen, J. T., & Aggleton, J. P. (2000). Fos imaging reveals differential patterns of hippocampal and parahippocampal subfield activation in rats in response to different spatial memory tests. *J Neurosci, 20*(7), 2711-2718.

Varikuti, D. P., Genon, S., Sotiras, A., Schwender, H., Hoffstaedter, F., Patil, K. R., . . . Eickhoff, S. B. (2018). Evaluation of non-negative matrix factorization of grey matter in age prediction. *Neuroimage, 173*, 394-410. doi:10.1016/j.neuroimage.2018.03.007

Varikuti, D. P., Hoffstaedter, F., Genon, S., Schwender, H., Reid, A. T., & Eickhoff, S. B. (2017). Resting-state test-retest reliability of a priori defined canonical networks over different preprocessing steps. *Brain Struct Funct, 222*(3), 1447-1468. doi:10.1007/s00429-016-1286-x

Vogel, J. W., La Joie, R., Grothe, M. J., Diaz-Papkovich, A., Doyle, A., Vachon-Presseau, E., . . . Evans, A. C. (2020). A molecular gradient along the longitudinal axis of the human hippocampus informs large-scale behavioral systems. *Nat Commun, 11*(1), 960. doi:10.1038/s41467-020-14518-3

Vos de Wael, R., Larivière, S., Caldairou, B., Hong, S.-J., Margulies, D. S., Jefferies, E., . . . Bernhardt, B. C. (2018). Anatomical and microstructural determinants of

hippocampal subfield functional connectome embedding. *Proceedings of the National Academy of Sciences, 115*(40), 10154. doi:10.1073/pnas.1803667115

Wagner, G., Gussew, A., Kohler, S., de la Cruz, F., Smesny, S., Reichenbach, J. R., & Bar, K. J. (2016). Resting state functional connectivity of the hippocampus along the anterior-posterior axis and its association with glutamatergic metabolism. *Cortex, 81*, 104-117. doi:10.1016/j.cortex.2016.03.022

Walsh, D. M., & Selkoe, D. J. (2007). A beta oligomers - a decade of discovery. *J Neurochem, 101*(5), 1172-1184. doi:10.1111/j.1471-4159.2006.04426.x

Wang, K., Liang, M., Wang, L., Tian, L., Zhang, X., Li, K., & Jiang, T. (2007). Altered functional connectivity in early Alzheimer's disease: a resting-state fMRI study. *Hum Brain Mapp, 28*(10), 967-978. doi:10.1002/hbm.20324

Wang, L., Brier, M. R., Snyder, A. Z., Thomas, J. B., Fagan, A. M., Xiong, C., . . . Ances, B. M. (2013). Cerebrospinal fluid Aβ42, phosphorylated Tau181, and resting-state functional connectivity. *JAMA Neurol, 70*(10), 1242-1248. doi:10.1001/jamaneurol.2013.3253

Wang, L., Miller, J. P., Gado, M. H., McKeel, D. W., Rothermich, M., Miller, M. I., . . . Csernansky, J. G. (2006). Abnormalities of hippocampal surface structure in very mild dementia of the Alzheimer type. *Neuroimage, 30*(1), 52-60. doi:10.1016/j.neuroimage.2005.09.017

Wang, L., Swank, J. S., Glick, I. E., Gado, M. H., Miller, M. I., Morris, J. C., & Csernansky, J. G. (2003). Changes in hippocampal volume and shape across time distinguish dementia of the Alzheimer type from healthy aging. *Neuroimage, 20*(2), 667-682. doi:10.1016/s1053-8119(03)00361-6

Weissenbacher, A., Kasess, C., Gerstl, F., Lanzenberger, R., Moser, E., & Windischberger, C. (2009). Correlations and anticorrelations in resting-state functional connectivity MRI: a quantitative comparison of preprocessing strategies. *Neuroimage, 47*(4), 1408-1416. doi:10.1016/j.neuroimage.2009.05.005

West, M. J., Coleman, P. D., Flood, D. G., & Troncoso, J. C. (1994). Differences in the pattern of hippocampal neuronal loss in normal ageing and Alzheimer's disease. *Lancet, 344*(8925), 769-772. doi:10.1016/s0140-6736(94)92338-8

Wilson, B. A., Baddeley, A. D., & Kapur, N. (1995). Dense amnesia in a professional musician following herpes simplex virus encephalitis. *J Clin Exp Neuropsychol, 17*(5), 668-681. doi:10.1080/01688639508405157

Windischberger, C., Langenberger, H., Sycha, T., Tschernko, E. M., Fuchsjager-Mayerl, G., Schmetterer, L., & Moser, E. (2002). On the origin of respiratory artifacts in BOLD-EPI of the human brain. *Magn Reson Imaging, 20*(8), 575-582.

Wise, R. G., Ide, K., Poulin, M. J., & Tracey, I. (2004). Resting fluctuations in arterial carbon dioxide induce significant low frequency variations in BOLD signal. *Neuroimage, 21*(4), 1652-1664. doi:10.1016/j.neuroimage.2003.11.025

Wisse, L. E., Gerritsen, L., Zwanenburg, J. J., Kuijf, H. J., Luijten, P. R., Biessels, G. J., & Geerlings, M. I. (2012). Subfields of the hippocampal formation at 7 T MRI: in vivo volumetric assessment. *Neuroimage, 61*(4), 1043-1049. doi:10.1016/j.neuroimage.2012.03.023

Yan, C. G., Cheung, B., Kelly, C., Colcombe, S., Craddock, R. C., Di Martino, A., . . . Milham, M. P. (2013). A comprehensive assessment of regional variation in the impact of head micromovements on functional connectomics. *Neuroimage, 76*, 183-201. doi:10.1016/j.neuroimage.2013.03.004

Yang, Z., Wen, W., Jiang, J., Crawford, J. D., Reppermund, S., Levitan, C., . . . Sachdev, P. S. (2016). Age-associated differences on structural brain MRI in nondemented

individuals from 71 to 103 years. *Neurobiol Aging, 40*, 86-97. doi:10.1016/j.neurobiolaging.2016.01.006

Yao, Z., Hu, B., Liang, C., Zhao, L., Jackson, M., & the Alzheimer's Disease Neuroimaging, I. (2012). A Longitudinal Study of Atrophy in Amnestic Mild Cognitive Impairment and Normal Aging Revealed by Cortical Thickness. *PLoS One, 7*(11), e48973. doi:10.1371/journal.pone.0048973

Yarkoni, T., Poldrack, R. A., Nichols, T. E., Van Essen, D. C., & Wager, T. D. (2011). Large-scale automated synthesis of human functional neuroimaging data. *Nature methods, 8*(8), 665-670. doi:10.1038/nmeth.1635

Yassa, M. A., & Stark, C. E. (2011). Pattern separation in the hippocampus. *Trends Neurosci, 34*(10), 515-525. doi:10.1016/j.tins.2011.06.006

Yassa, M. A., Stark, S. M., Bakker, A., Albert, M. S., Gallagher, M., & Stark, C. E. (2010). High-resolution structural and functional MRI of hippocampal CA3 and dentate gyrus in patients with amnestic Mild Cognitive Impairment. *Neuroimage, 51*(3), 1242-1252. doi:10.1016/j.neuroimage.2010.03.040

Yee, Y., Fernandes, D. J., French, L., Ellegood, J., Cahill, L. S., Vousden, D. A., . . . Lerch, J. P. (2017). Structural covariance of brain region volumes is associated with both structural connectivity and transcriptomic similarity. *bioRxiv*. doi:10.1101/183004

Yeo, B. T., Krienen, F. M., Sepulcre, J., Sabuncu, M. R., Lashkari, D., Hollinshead, M., . . . Buckner, R. L. (2011). The organization of the human cerebral cortex estimated by intrinsic functional connectivity. *J Neurophysiol, 106*(3), 1125-1165. doi:10.1152/jn.00338.2011

Zeidman, P., & Maguire, E. A. (2016). Anterior hippocampus: the anatomy of perception, imagination and episodic memory. *Nat Rev Neurosci, 17*(3), 173-182. doi:10.1038/nrn.2015.24

Zeineh, M. M., Holdsworth, S., Skare, S., Atlas, S. W., & Bammer, R. (2012). Ultra-high resolution diffusion tensor imaging of the microscopic pathways of the medial temporal lobe. *Neuroimage, 62*(3), 2065-2082. doi:10.1016/j.neuroimage.2012.05.065

Zeineh, M. M., Palomero-Gallagher, N., Axer, M., Grassel, D., Goubran, M., Wree, A., . . . Zilles, K. (2017). Direct Visualization and Mapping of the Spatial Course of Fiber Tracts at Microscopic Resolution in the Human Hippocampus. *Cereb Cortex, 27*(3), 1779-1794. doi:10.1093/cercor/bhw010

Zhang, X., Mormino, E. C., Sun, N., Sperling, R. A., Sabuncu, M. R., & Yeo, B. T. (2016). Bayesian model reveals latent atrophy factors with dissociable cognitive trajectories in Alzheimer's disease. *Proc Natl Acad Sci U S A, 113*(42), E6535-e6544. doi:10.1073/pnas.1611073113

Ziontz, J., Bilgel, M., Shafer, A. T., Moghekar, A., Elkins, W., Helphey, J., . . . Resnick, S. M. (2019). Tau pathology in cognitively normal older adults: Associations with brain atrophy and cognitive decline. *bioRxiv*, 611186. doi:10.1101/611186

Zonneveld, H. I., Pruim, R. H., Bos, D., Vrooman, H. A., Muetzel, R. L., Hofman, A., . . . Vernooij, M. W. (2019). Patterns of functional connectivity in an aging population: The Rotterdam Study. *Neuroimage, 189*, 432-444. doi:10.1016/j.neuroimage.2019.01.041